CHALMERS
UNIVERSITY OF TECHNOLOGY

Vehicle Speed Estimation During Excessive Tyre Slip Conditions

Master's thesis in Automotive Engineering

Carl Storckenfeldt
Diler Ganatra

DEPARTMENT OF MECHANICS AND MARITIME SCIENCES

CHALMERS UNIVERSITY OF TECHNOLOGY
Gothenburg, Sweden 2021
www.chalmers.se

Master's thesis 2021:18

Vehicle Speed Estimation During Excessive Tyre Slip Conditions

Carl Storckenfeldt
Diler Ganatra

CHALMERS
UNIVERSITY OF TECHNOLOGY

Department of Mechanics and Maritime Sciences
Division of Vehicle Engineering and Autonomous Systems
CHALMERS UNIVERSITY OF TECHNOLOGY
Gothenburg, Sweden 2021

Vehicle Speed Estimation During Excessive Tyre Slip Conditions
Carl Storckenfeldt
Diler Ganatra

Supervisors: Derong Yang, Volvo Cars
Fredrik Broström, Volvo Cars
Martin Hassel, Volvo Cars
Lars Hammarstrand, Department of Electrical Engineering
Examiner: Mats Jonasson, Department of Mechanics and Maritime Sciences

Master's Thesis 2021:18
Department of Mechanics and Maritime Sciences
Division of Vehicle Engineering and Autonomous Systems
Chalmers University of Technology
SE-412 96 Gothenburg
Telephone +46 (0)31 772 1000

Typeset in LaTeX
Printed by Chalmers Reproservice
Gothenburg, Sweden 2021

Vehicle Speed Estimation During Excessive Tyre Slip Conditions
Carl Storckenfeldt, Diler Ganatra
Master's thesis in Automotive Engineering
Department of Mechanics and Maritime Sciences
Chalmers University of Technology

Abstract

Vehicle speed is one of the most important states that needs to be estimated in a vehicle. This quantity is safety critical as it drives a majority of the on-board safety and driver-assistance systems. A normal modern car is equipped with wheel speed sensors, Inertial Measurement Unit (IMU), steering angle sensor and powertrain and brake torque sensors which makes the foundations for the speed estimate. The wheel speed sensors provide a relatively good estimate of the vehicle speed in normal conditions with limited wheel slip. However, in excessive wheel slip conditions the wheels speeds significantly diverge from the true speed of the vehicle. In these situations, no reliable direct measurement of the speed is available and the speed estimate needs to be complemented with e.g. dead reckoning based on accelerometer input. In this thesis, a kinematics based extended Kalman filter (EKF) for longitudinal vehicle speed estimation in excessive all-wheel slip conditions is presented. The filter uses combined vehicle orientation and speed estimation, only considering longitudinal dynamics. The proposed filter utilizes a slip-detection system that detects wheel slip and filters out wheel speed measurements from these slipping wheels. It also has a separate logic for speed estimation in braking on slippery surfaces. Two slip detection approaches are presented. One approach is to assume slip between detection of certain events related to the powertrain torque, wheel acceleration and braking. The other approach makes a decision about slip at every time step. The filter and slip detection systems are tested on real-world driving data recorded from two different all-wheel drive vehicles in excessive slip conditions. The results show that the proposed method provides a better estimate than the reference brake supplier estimate, keeping the estimate within $\pm 4\%$ of the ground truth speed for many cases. Though, none of the slip-detection systems provide flawless slip detection resulting in the filter to sometimes rely on non-representative wheel speed measurements degrading the estimate. It becomes clear that the speed estimation is limited both by the approach of detecting slip and by the limited sensor setup providing no absolute measurement of the speed in excessive all-wheel slip.

Keywords: Vehicle speed estimation, excessive wheel slip, slip detection, dead reckoning, vehicle state estimation, extended Kalman filter

Additional Work

Further analysis is done on how to improve the kinematics based estimation methods and two new approaches are developed. These approaches improve the previous estimation methods. The first approach introduces a modelled GPS speed signal as a secondary speed measurement. The second approach utilizes only the limited sensor suite to develop a new slip detection concept using vehicle dynamic principles. Methods based on these two approaches improve the estimation of vehicle speed as compared to the previous methods for all data logs. The development process, comparison with the previous methods and performance analysis of the new methods and how they improve the estimation are described in **"Vehicle Speed Estimation During Excessive Tyre Slip Using GPS Data and Slip Estimation"** in this thesis work. .

Preface and Acknowledgements

This master's thesis was conducted in the Division of Vehicle Engineering and Autonomous Systems at the Department of Mechanics and Maritime Science at Chalmers University of Technology. This work was done in collaboration with Volvo Cars Corporation's Vehicle Energy and Motion Control Department in Gothenburg, Sweden. The thesis was carried out during the Spring of 2021. Carl studied at the master's program Systems, Control and Mechatronics and Diler as an exchange student at Mobility Engineering. The problem of estimating the vehicle speed in excessive slip conditions is a challenging yet interesting topic and we are grateful to Chalmers as well as Volvo Cars to give us the opportunity to conduct our work on such a topic.

We would like to express immense gratitude to our academic supervisors Mats Jonasson and Lars Hammarstrand for dedicating their time, effort and complete support throughout the thesis. Their expertise, support and guidance has pushed us to work and develop new ideas all through the thesis. Their readiness and expertise to discuss estimation methods for velocity was inspiring.

We would also like to extend a warm thank you to our supervisors at Volvo Cars - Derong Yang, Fredrik Broström and Martin Hassel as well as our manager, Anna Söderlund. We are grateful to them for giving us the opportunity to conduct our Master's Thesis in a challenging yet inspiring topic. Their continued advice, insights from experience, support with data, as well as analysis all throughout the thesis made it possible to for us to develop the thesis smoothly, efficiently and correctly.

We would also like to thank Martin Idegren and Harinath Preetham for indulging in deep discussions, supporting us with additional data, answering our queries and guiding us on the right path during the thesis.

This report would not be complete without thanking Lennart Svensson for his Master's Thesis School lectures along with Lars Hammarstrand. They guided us through every process throughout the thesis, gave us a platform to discuss solutions with other thesis students, get fresh ideas and write a compelling master thesis report.

Lastly, we would like to thank our close friends and family who have been patient, understanding and extremely supportive, which has helped us along the way as we spent countless hours working on the masters thesis.

Carl Storckenfeldt and Diler Ganatra, Gothenburg, June 2021

Individual Contributions

C.S. led the development of the kinematics based approach and implemented it. This includes the filters, signal processing, slip detection concept 2 and the topics mentioned in the method chapter. Both authors developed the slip detection concept 1. D.G. studied the vehicle and tyre dynamic possibilities of estimating speed with a linear tyre model. D.G. was responsible for development of a re-sim environment to evaluate the estimation and slip detection concepts. Both authors contributed to the report manuscript. C.S. took a lead in writing the final manuscript. C.S. has written the method and discussion chapter and a large part of the rest of the report. Both authors have contributed with ideas and insights throughout the report.

D.G. has solely developed and implemented the estimation methods using additional GPS data as well as the vehicle dynamics based slip detection concept 3. This includes studying of true GPS signals and artificially modelling GPS data for use in the estimation process, implementing use of GPS signal in the previously developed Kalman Filter, implementing a new vehicle dynamics based slip estimation process, developing a new slip detection algorithm for acceleration and braking cases, re-developing a leaner re-sim environment in which the performance is studied thus improving the previously developed estimation method. D.G. has also solely written the entirety of the report titled **"Vehicle Speed Estimation During Excessive Tyre Slip Using GPS Data and Slip Estimation"** as part of this thesis document.

Contents

List of Figures

List of Tables

1

Introduction

Recent years have seen a rising influx of vehicles with some degree of autonomous driving (AD) capabilities. Creating such vehicles has given new impetus for better motion control systems, Advanced Driver Assistance Systems (ADAS) and other safety critical functions. To achieve higher levels of AD, it is highly important that these systems work accurately at all times given their significance to vehicle safety. Ensuring the highest standard of accuracy and robustness depends not only on how these systems are built, but also on the fidelity of input data measured by the sensors or being estimated in real time. One key input that must be accurate in every driving scenario and weather condition is the speed of the vehicle. This input drives almost every vehicle system. The vehicle speed is also a safety-critical quantity in that significant speed estimate deviations (outliers) from the true speed can cause systems to make wrong decisions. In turn, this can cause severe hazards for the driver, occupants as well as other drivers or nearby pedestrians.

Modern cars are normally equipped with an on-board sensor suite which includes wheel speed sensors, Inertial Measurement Unit (IMU), steering angle sensor and powertrain and brake torque sensors. These sensors are the foundation for vehicle state estimation. In nominal conditions, without excessive wheel slip, one or several wheel speeds provide a relatively accurate measurement of the true speed of the car. In these cases, the speed estimation can be based on this quantity and be estimated with different approaches as vehicle dynamics modelling or kinematics modelling. In vehicle dynamics modelling, the vehicle is modelled using dynamic equations and relations that have been derived from physics and experimental testing. One example is a tyre model where the propellant force of the car can be estimated using experimental data for how the particular tyre behaves depending on factors like tyre stiffness, slip ratio and road-tyre friction. The force can then be used as a component when estimating the speed of the car. This approach requires a lot of knowledge about parameters specific to the car and the current road-conditions. A kinematics based approach is based purely on the measured signals. This approach still requires modelling of the vehicle to some extent but makes it more simplistic and requires less knowledge about specific parameters.

In normal conditions the speed estimation can be solely based on the wheel speeds however, in slippery low-friction conditions the wheels tend to spin during acceleration and lock during braking. In these situations the wheel speeds do not accurately

represent the true speed of the car. This introduces a big obstacle in vehicle speed estimation as the wheel speeds are the only available absolute speed measurement with the mentioned sensor setup. In these situations, the state-estimation becomes difficult because the information from the sensors are limited and the uncertainties in the estimates increase. A kinematics based approach has the advantage that less parameters and states need to be estimated in these situations. A vehicle dynamics approach depends on many variables and as the uncertainties in some states affect the estimations of others this becomes a problem. The main strategy presented in research for speed estimation in all-wheel excessive slip conditions is to rely on dead-reckoning of the measured or modeled acceleration. However, dead-reckoning is limited by the errors in state estimation and signals and the integrated quantities will drift when the errors are integrated over time. This makes it important to be able to determine what the current state of the wheels are and when they can be trusted for speed estimation to limit the use of dead-reckoning.

As the speed estimation is very important for the on-board vehicle systems and extreme slippery conditions are inevitable, it is important to develop strategies for vehicle speed estimation in these extreme situations with the limited information from the sensors. In this work, the primary focus is to estimate the vehicle speed in the forward direction of an all-wheel driven vehicle in excessive wheel slip conditions. A study has been made on finding indicators of excessive wheel slip. With the knowledge acquired, two wheel selection and slip detection approaches have been set up in combination with a kinematics based approach for estimating the vehicle speed. This thesis work is conducted at Volvo Cars' Vehicle Energy and Motion Control department. Volvo supplied supervision and real-world slippery-condition driving data that has been used for investigating slip and development and testing of the proposed method.

1.1 About the Logged Data Supplied by Volvo

Volvo Cars supplied the thesis work with logged data from two all-wheel drive vehicles. One is a large powerful hybrid vehicle with a combustion engine propelling the front axle and an electric engine propelling the rear axle. The other is a mid-size fully electric vehicle. As the vehicles are all-wheel drive, all wheels are actively subjected to a torque and are likely to spin when the vehicle is accelerating on slippery surfaces. In contrast, a front wheel or rear wheel driven vehicle has one wheel pair that is not propelled which reduces the risk of excessive all-wheel spin. All work presented in this report is developed and tuned for the larger hybrid as this was made available first. The fully electric car was introduced at a late stage of the thesis work. It is mainly used to investigate how the proposed solution worked on a different vehicle with other characteristics and in slightly more extreme conditions to test it's robustness.

The logged data consists of signals from state-of-the-art sensors including wheel speed sensors, 6-Degree of Freedom (DOF) IMU (gyroscope and accelerometer), front wheel steering wheel angle, powertrain torque and brake torque friction esti-

mate. The signals where recorded at 100 Hz. Four redundant IMUs as well as wheel speeds for all four wheel had been recorded. Data from on-board systems as engine Traction Control System (TCS), Anti-lock braking system (ABS) and stability systems had also been recorded. A high accuracy positioning system, Oxford Technical Solutions (OxTS) RT3000 [1], had been used at the point of recording the data. This data is in the thesis used as a ground truth for the states of the vehicle. It includes reference measurements for position, speed (longitudinal and lateral), acceleration (longitudinal, lateral and vertical), orientation (roll, pitch, yaw) of the vehicle and the rate of change of orientation (roll-rate, pitch-rate and yaw-rate).

The brake control system has a stand alone speed estimator provided by the brake manufacturer which has been recorded for both vehicles. Only for the fully electric car, an estimate of the speed from the Volvo lateral state estimation department had been recorded. This estimate is mainly based on the wheel speeds but is complemented with accelerometer measurements to some extent. This estimate is referred to as simplified Volvo estimate throughout the report. Although many signals had been logged including OxTS measurements as reference, parameters like the road-tyre friction and tyre stiffness had not been logged. This might not be possible to do in an easy way, but the authors want to stress that this information is not available. Also, it is not known on a deeper level exactly what the conditions were when the data was logged or how the vehicle was driven. Though, is known that the data has been collected in extreme slippery conditions with aggressive driving with stability systems turned off.

The collected data for both vehicles had been logged while driving on snowy and icy roads with low friction to induce excessive all wheel slip conditions. The data set is majorly composed of straight ahead driving on flat roads, uphill and downhill slopes as well as on a test track. The vehicles are driven aggressively with high accelerations and ABS braking with Electronic Stability Control (ESC) disabled to override the effects of the stability system and let the wheels slip for longer duration. The data logs for the larger hybrid vehicle majorly comprises of low lateral motion and thus low or no body-side-slip. The vehicle has been driven as if was driven on a friction surface but on ice and snow roads with low friction causing the wheels to lose grip and slip. A few runs in the data set also include more aggressive maneuvers where the yaw-rate and lateral acceleration is higher. The data logs for the fully electric car had been logged in a slightly more extreme setting in that the vehicle had been driven on icy roads with changing road inclination and on a handling track which induces high yaw-rate and lateral acceleration. In Appendix A descriptions for each individual log are available.

1.2 Related Research

Vehicle state estimation can be divided into two main categories, model-based and data-driven approaches [2]. Recently, data driven approaches have seen an increase in popularity with the advancements in AI and a variety of different works have been published. The data-driven approaches typically utilise some sort of Artificial

Intelligence (AI), e.g. an artificial neural network, to extract and learn abstract relations and trends from data sets which maybe could not been easily found by a human. The simplified view on this kind of approach is that data from the sensors of a car is fed to a black box with an artificial neural network. The network is then asked to estimate the current state (could be speed) based on the data fed. By using a ground truth the estimate can be scored and this information is then fed back to the network. Assuming that the network is sufficiently structured and that sufficient amount of data is available, the network can learn to estimate the state. It has been shown that a data driven approach can be used to estimate individual states such as side-slip angle [3] and road friction [4] and to complement other methods with e.g. fusion of IMU and GPS signals [5], or dynamically selecting weights in filters used for speed estimation [6]. Thus, this kind of approach shows promising signs of both enabling new methods and complementing existing for state estimation. Some general drawbacks with data driven approaches are possible over-fitting to the data used, how to know how the taught model will behave with data that differs from what it was trained on and that a relatively large and representative data set is needed to make the model general. Mainly because of the uncertainty of how much data would be available in the thesis, this approach was not chosen.

The other main approach for state estimation is model-based approaches. These can be further divided into kinematics based (direct) and vehicle dynamics based approaches (indirect). The difference is that in a kinematics based approach, the measured quantities from the sensors are directly related to the states being estimated whereas in a vehicle dynamics approach the measured quantities are input to experimentally developed mathematical models.

In a vehicle dynamics approach mathematical expressions that describe the transient behavior of the vehicle dynamics are used to estimate the states. These approaches lead to development of vehicle models consisting of force-based equations of motion in tandem with tyre models, that explain it's behaviour based on experimental data. During extreme slip conditions, the dynamics are highly non-linear, making it difficult to model and accurately estimate the sought after state. Some research with limited sensor data similar to the thesis set up provided is cited below.

Work in [7] proposes the use of a simple 3-DOF 1-track model to set up dynamic equations of motion with longitudinal, lateral speeds and yaw rate used as the states for an Adaptive Kalman Filter. It was shown that the filter produces good results for vehicle speed on high and average friction surfaces. However the paper does not talk about wheel slip conditions, very low slip on ice and snow roads. It also assumes availability of non-linear tyre parameters, which is crucial in modelling a tyre in the slipping situation. Use of a bicycle model does not take into account the effects of gravity when driving on a slope or inclined road.

[8] proposes a non-linear tyre model comparable to the Magic Formula along with a nonlinear observer to estimate longitudinal velocity. However, the estimation is based on the fact that there is trustworthy reference wheel speed data available i.e. one wheel is rolling, which defeats the purpose of the thesis work. This model fails

therefore, on low friction surfaces and when all wheels slip, most cases with large slip angles.

[9] uses front/rear axle torque, longitudinal acceleration, pitch rate and wheel rotational velocities in estimating the longitudinal velocity and pitch angle. Again, the work mentioned does not motivate a solution in cases when all wheels are slipping, thus providing no reference wheel speed to trust.

Increased complexity, non-linear dynamics and the inter-related states mean that the small errors in the sensor data heavily affect the estimated states. tyre interactions with the road surface is also difficult to model without experimental data in the non linear range, when it is slipping. Reduced friction, different friction coefficients on each tyre, dynamic changes by the driver, vehicle propulsion are some parameters that largely influence how the vehicle motion is modelled. Research for the vehicle dynamics approach motivates the use of a vehicle and tyre model only during steady state cases or nominal conditions where some or no wheels are slipping on a fairly higher road-tyre friction. In extreme cases however, the results are either not presented or a solution not robust enough to estimate velocity accurately is provided.

Kinematics based approaches are generally more simplistic than vehicle dynamics approaches in that the measured signals are used directly. One of the early and arguably most simplistic methods for estimating the longitudinal speed of a vehicle is to directly convert the angular velocity of the wheels to translational velocity by multiplying with the radius of the wheels. This gives a relatively accurate estimate of the vehicle speed given that the the measurements are accurate, the tyre radius is known and the wheels do not slip severely [10]. In the case of the vehicle turning, each wheel travel with different speeds relative the true speed of the car which in turns depends on where on the car the speed is estimated. Normally this is defined as a point along the center-line of the car, e.g. in the center of gravity or at one of the axles of the vehicle. This speed difference induced by turning can be compensated for using different techniques. [11] presents two approaches that are based on calculating the radius of which the individual wheels are traveling along when turning and utilising the knowledge about the steering angle of the wheels, yaw-rate and body-slip angle to transform the wheel speeds to the equivalent speed at the center of gravity. The steering angle and yaw-rate can easily be measured with available sensors on normal cars but the body-slip normally has to be estimated separately as it directly related to the lateral speed of the car which normally is hard to estimate. This is because the lateral speed needs to be estimated as it is not measurable with standard sensors used in modern cars [12].

Many modern cars are also equipped with wheel speed sensors for each wheel which gives a redundancy in the speed measurement. This is important if a particular wheel speed deviates from the true speed of the car which can happen during e.g. acceleration or braking. Then the speed estimate could be improved if it is based on the most representative wheel or wheels. [13] argue that in acceleration, the slowest wheel should provide the best measurement and vice versa in braking cases. On

the other hand, [14] argue that the second slowest wheel should be used as the best estimate during acceleration. Thus, there's not a unified view of which wheels are the most reliable in different situations.

Furthermore, given a typical modern car, e.g. the vehicles used in this thesis, the wheel speed senors provide the only direct measurement of the speed of the car. This poses a challenge in slippery conditions. In these conditions, the wheels tend to slip severely in acceleration and braking. In the case of excessive all-wheel slip, no accurate speed measurement is available. The main approach that has been presented in literature is to complement the wheel speed sensors with an accelerometer which enables dead-reckoning during events when the wheels cannot be trusted [10], [11], [13], [15]. Due to economical reasons related to the challenges of mass-production, low-cost IMUs with limited consumer-grade performance are normally used in vehicle state applications [2]. This further complicates the speed estimation problem as the limited performance in the sensors only allows for dead-reckoning during short time-periods before the dead-reckoning starts to drift due to the noise and offsets in the measurements [16] [17]. The accelerometer measurements are also contaminated by the gravity component and accelerations induced by centripetal forces from turning of the vehicle [16]. In order to compensate for the gravity the orientation of the car needs to be estimated.

With the limited sensor setup, many challenges arise when the vehicle speed is to be estimated in excessive slip situations. [10] presented a simplistic kinematic based approach for estimating the vehicle speed. Using measurements from wheel speed sensors and longitudinal accelerometer, a fuzzy logic Kalman filter (based on wheel slip estimation) was used to handle situations with wheel slip by trusting the accelerometer in the form of dead reckoning. [15] proposed a similar approach with the addition of an estimation of the accelerometer offset and tyre radius. In excessive slip conditions, the estimate of the vehicle can drift from the true speed of the car and thus the slip estimation might be inaccurate. [11] also proposed a fuzzy-logic based linear Kalman filter approach where the importance of wheel speed correction was stressed. There are also works like [18] where a Rao-Blackwellized particle filters have been used to estimate speed of the vehicle.

In [19] another kinematics based approach with empirical corrections on multi-timescales for estimation of vehicle velocity is proposed. On a longer timescale, the estimated velocities are corrected by two empirical judgements. Firstly, when the yaw rate and steering wheel angle remain around zero for some time, the car is going straight and the lateral velocity can be set to zero. Secondly, when the velocity of each tyre is about the same and the varying rates crosses zero, the slip can be estimated to be zero and thus the longitudinal velocity can be accurately estimated as the product of the tyre radius and average wheel speed. On a short timescale the acceleration bias is recursively estimated.

[13] recognized the importance of minimizing the initial offset before initializing dead reckoning. An excessive slip detection algorithm utilising an estimated max torque limit based on the utilized friction was presented. The proposed method allowed for

early detection of slip. A simple linear Kalman filter with separate road-gradient and vehicle speed estimation was used. The speed estimate was only based on wheel speed sensors and longitudinal accelerometer which was bias compensated with a fixed measured bias value. A best-wheel selection algorithm was also introduced choosing the fastest wheel when breaking and slowest when accelerating. The algorithm was tested in real snow conditions with all wheel slip and showed promising results with estimation errors within 5% during about 5 seconds of excessive wheel slip.

With only wheel speed sensors, IMU, steering wheel angle, powertrain and brake torque available, the options for speed estimation in severe all wheel slip conditions are limited. Still, it constitutes an important challenge in the vehicle industry as the vehicle speed estimate is crucial for many safety-systems. The authors also found that the literature focusing specifically on extreme excessive all-wheel slip situations with the given sensor setup is limited. This thesis continues the work of estimating the vehicle speed particularly in extreme conditions with excessive all-wheel slip. A similar approach to [13] is taken where slipping wheels is tried to be identified and not used in the speed estimate. An investigation of different indicators of slip has been made. The knowledge from the investigation has been used to put together two combined slip-detection and wheel selection concepts. The first slip detection system is based on assuming slip in between certain events. The second slip detection system is based on detecting slip at every time instance mainly based on the characteristics of the error between the speed estimate and the wheel speed measurements. A logic for speed estimation during ABS braking in slippery conditions is also proposed. For relative ease of implementation and good sensor fusion capabilities, an extended Kalman filter (EKF) was set up with a joint estimation of speed and orientation (roll/pitch). Only longitudinal dynamics is considered in the approach. It's also shown that only compensating the bias-offsets in the gyroscopes while the car is standing still and letting the pitch-estimate compensate for the accelerometer bias is a feasible approach for speed estimation. Though, the pitch estimate will in itself be offset relative the true pitch estimate. The proposed methods are tested and compared to the brake manufacturers estimate for the vehicles in real-world extreme excessive all-wheel slip conditions

1.2.1 Other Sensors

This section brings up some alternative ways to estimate speed using other sensors. The main approaches mentioned in literature is utilizing GPS, radar, lidar and cameras.

GPS/GNSS is an existing technique that provides absolute position measurements. INS and GNSS measurements can be fused and provide more accurate estimations of vehicle states as velocity compared to dead reckoning based on IMU data. GPS has been used in a variety of works to estimate speed, wheel slip, body slip, tyre-side slip, tyre radius estimation, tyre stiffness among other states and parameters [20]–[22]. The drawbacks with GPS is, among other things, the risk of the signal being interrupted from surrounding objects as buildings and a slow measurement

frequency relative wheel speed sensors [17].

[23] presents a review of the state-of-the-art visual odometry (VO) techniques (using onboard cameras). It is stated that VO is an inexpensive alternative odometry technique that can be more accurate than conventional techniques as GPS, INS and wheel odometry in certain applications. It is described that the technique has disadvantages as camera exposure problems, problems with finding features in outdoor terrain and scale uncertainty when using monocular vision. Another technique is to use radar to estimate the velocity as proposed by [24]. This alternative approach has the advantage of being more reliable in low visibility scenarios compared to VO. However, the speed estimate from Radars degrades fast if enough points cannot be observed. There has also been experimental approaches using acoustic sensors [25] and chassis vibration [26] to estimate vehicle velocity.

1.3 Objective and Purpose

The purpose of this thesis work is to develop a strategy for estimating the longitudinal speed of a vehicle in excessive wheel slip conditions. This is with a standard sensor suite which includes wheel speed sensors, Inertial Measurement Unit (IMU), steering angle sensor and powertrain and brake torque sensors. The approach chosen is kinematics based with a separate slip-detection system to filter out inaccurate wheel speed measurements during slip. The development and testing of the method-/algorithm will be made on recorded data from real-world driving in extreme slippery conditions.

The main research questions considered are:

- How well can the longitudinal velocity be estimated in all-wheel slip conditions using sensors available on existing production vehicles (including steering wheel angle, IMU, wheel speed sensors, brake signals, powertrain torque)?
- What are the limiting factors in the presented method?
- How could the estimate be further improved on?

The vision is to present a longitudinal speed estimation method/algorithm that can estimate the vehicle speed in all wheel slip conditions over longer time periods, approximately 10 seconds with less than $\pm 4\%$ estimation error relative to the ground truth. As there might be extreme outlier conditions at times, the estimate error should not exceed the $\pm 4\%$ error limit for 99% of the time during excessive slip. The speed should also be estimated without considerable time-delay to provide an online speed estimate feasible in a real-world application. An acceptable outcome would be that the presented method shows promising results during extreme slippery conditions though it may not meet the vision in all conditions.

1.4 Scope and Limitations

The thesis work only focuses on providing an accurate vehicle speed estimate. This is only in the longitudinal direction of the car and lateral dynamics are not considered. Scenarios with high lateral acceleration/velocity or yaw rate are omitted for this purpose. This is done to limit the extent of the work as the complexity of the estimation becomes much higher when including lateral dynamics as e.g. the lateral speed is not measurable with the available sensors. The speed estimation is also only prioritized for normal driving speeds ranging from 10-120 km/h. Speed estimation while reversing with slip is not considered as the data provided did not include such scenarios.

To further limit the scope, online tyre radius estimation and bias compensation for gyroscopes and accelerometers is not considered. This is mainly because most data logs are short and also contain slip right from the starting seconds. This would make such estimations difficult as normally this is done in steady-state situations. Also, scenarios with severe and excessive all-wheel slip over very long time (20+seconds) will not be considered. This is because the approach will be very limited by the sensor performance and maybe requires a different approach.

The hybrid vehicle is equipped with multiple IMU's. Using multiple IMU's can give an improvement in the measurement uncertainty [27] and can also be used to detect failing or deviating IMU's. In this thesis only one IMU is considered. It is assumed that a single IMU can provide reliable measurements under the the short time scales of the data log files. It will also simplify the estimation process. Severe failures would be detected when the estimate is compared with the OxTS reference measurements.

2

Theory

In this chapter basic theory for the methods used is presented. This includes theory about Bayesian filtering, the Kalman filter, sensors and a section about vehicle dynamics and tyres.

2.1 Bayesian Filtering

Assume that the states of a time varying system are to be described. Let the true state-vector for each discrete time step, k, be denoted as $\boldsymbol{x_k}$. The true quantities of the states are hidden for an observer and can only be measured indirectly with noisy measurements $\{\boldsymbol{y_1}, \boldsymbol{y_2}..., \boldsymbol{y_k}\}$. In a filtering sense, the goal is to estimate the unknown state-vector at time k, given the previous measurements. In Bayesian filtering the goal is the same but it is done in a Bayesian statistical way, where the filtering is considered as a statistical inversion problem [28]. In the following sections, the concepts of Bayesian filtering is explained and the Kalman filter equations are presented.

2.1.1 Probabilistic State Space Models

In Bayesian filtering, the time-varying system of interest is described using a probabilistic state space model [28]. This means that the states and measurements are described by probability density distributions that are conditionally dependent on previous states. Such a model consists of a process model, equation (2.1), and a measurement model, equation (2.2).

$$\boldsymbol{x_k} = f_{k-1}(\boldsymbol{x_{k-1}}, \boldsymbol{u_k}, \boldsymbol{q_{k-1}}) \sim p(\boldsymbol{x_k}|\boldsymbol{x_{k-1}}; \boldsymbol{u_k}) \tag{2.1}$$

$$\boldsymbol{y_k} = h_k(\boldsymbol{x_k}, \boldsymbol{u_k}, \boldsymbol{r_k}) \sim p(\boldsymbol{y_k}|\boldsymbol{x_k}; \boldsymbol{u_k}) \tag{2.2}$$

The process model, equation (2.1), describes how the evolution of the states depends on the past states. The main idea with the process model is to make a prediction of how the states will evolve over time to be able to rule out unlikely measurements. The process, f_{k-1}, can be a linear or nonlinear function. It can also take in inputs, $\boldsymbol{u_k}$, from e.g. accurate measurements. $\boldsymbol{q_{k-1}}$ is the process noise vector that describes the stochastic properties of the state propagation. An example of a process model is a train where the the velocity in the next time step can be described by the current velocity plus the acceleration times the time-step size.

The measurement model, equation (2.2), describes the distribution of the measurements given the current state. That is also known as the likelihood function. A measurement model, h_k, can also be linear or non-linear and take in inputs, $\boldsymbol{u_k}$, as well. Here $\boldsymbol{r_k}$ is the measurement noise vector which describes the stochastic properties of the measurements. One example of a measurement model is for a sensor that measures a quantity e.g. angular velocity. The measurement will be contaminated with noise from the sensor that will have some characteristics, e.g. a normal distribution with a noise vector, $\boldsymbol{r_k}$.

In Bayesian filtering the state space model is assumed to be Markovian [28]. For simplicity, the input, $\boldsymbol{u_k}$, is left out in the following sections but the theory still holds. A Markovian state space model has two properties. Firstly, it is assumed that state vector at time k is independent on all states prior to x_{k-1}. The state form what is known as a Markov chain. That is,

$$p(\boldsymbol{x_k}|\boldsymbol{x_{1:k-1}}, \boldsymbol{y_{1:k-1}}) = p(\boldsymbol{x_k}|\boldsymbol{x_{k-1}}). \tag{2.3}$$

Secondly, it is assumed that all measurements are conditionally independent of past measurements and states. That is,

$$p(\boldsymbol{y_k}|\boldsymbol{x_{1:k}}, \boldsymbol{y_{1:k-1}}) = p(\boldsymbol{y_k}|\boldsymbol{x_k}). \tag{2.4}$$

As a result, the noise vectors $\boldsymbol{q_{k-1}}$ and $\boldsymbol{r_k}$ are assumed to be independent of all other noise vectors.

Using a probabilistic graphical model, known as a Bayesian network, it is possible to illustrate the Markov-properties. A Bayesian network is a directed acyclic graph where the states and measurements are represented by vertices and the conditional dependencies are represented by the arcs or arrows [29]. In Figure 2.1 the Markov-properties described in equations (2.3)-(2.4) are visualized.

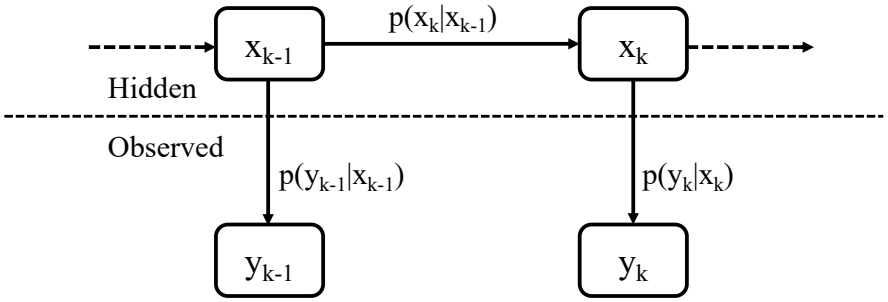

Figure 2.1: Bayesian network illustrating the Markov-properties of a probabilistic state space model. The true state-sequence is hidden from an observer who can only observe the states via noisy measurements y_k. The conditional dependencies of the state and measurement distributions are written beside the corresponding arrow.

2.1.2 Bayesian Filtering Equations

As mentioned in the previous section, the goal with Bayesian filtering is to estimate the unknown state-vector at time k given the previous measurements. This can be

seen as a statistical inversion problem [28]. What is sought for is the conditional distribution $p(\boldsymbol{x_k}|\boldsymbol{y_{1:k}})$ known as the posterior distribution. As pointed out in [28], theoretically the joint posterior distribution for all states, $\boldsymbol{x_{0:T}}$, could be computed using Bayes' rule relating the priors, $p(\boldsymbol{x_{0:T}})$, and likelihoods, $p(\boldsymbol{y_{1:T}}|\boldsymbol{x_{0:T}})$, according to equation (2.5).

$$p(\boldsymbol{x_{0:T}}|\boldsymbol{y_{1:T}}) = \frac{p(\boldsymbol{y_{1:T}}|\boldsymbol{x_{0:T}})p(\boldsymbol{x_{0:T}})}{p(\boldsymbol{y_{1:T}})} \tag{2.5}$$

Based on the Markovian assumption of the state space model, the joint prior distribution of the states and the joint likelihood of the measurements can be derived according to equations (2.6) and (2.7).

$$p(\boldsymbol{x_{0:T}}) = p(\boldsymbol{x_0}) \prod_{k=1}^{T} p(\boldsymbol{x_k}|\boldsymbol{x_{k-1}}) \tag{2.6}$$

$$p(\boldsymbol{y_{1:T}}|\boldsymbol{x_{0:T}}) = \prod_{k=1}^{T} p(\boldsymbol{y_k}|\boldsymbol{x_k}) \tag{2.7}$$

This approach will give a solution to the filtering problem. Though, it is not feasible to do this in a practical sense. As time passes the number of calculations increases with every time step. This makes the approach very computationally heavy.

Fortunately it is possible to express the solution to the filtering problem in an recursive form. This solution is called the Bayesian filtering equations [28]. The approach can be divided into three steps, initialization, prediction and measurement update. The initialization step is to form a prior distribution, $p(\boldsymbol{x_0})$, that is the starting point for the recursion. In the prediction step the Chapman-Kolmogorov equation, equation (2.8), is utilized. It makes it is possible to express the predictive distribution of a state $\boldsymbol{x_k}$ given the process model without adding more computations with each time step.

$$p(\boldsymbol{x_k}|\boldsymbol{y_{1:k-1}}) = \int p(\boldsymbol{x_k}|\boldsymbol{x_{k-1}})p(\boldsymbol{x_{k-1}}|\boldsymbol{y_{1:k-1}})d\boldsymbol{x_{k-1}} \tag{2.8}$$

The last step is the measurement update step in which Bayes' rule is used according to equation (2.9). The normalization factor, $p(\boldsymbol{y_k}|\boldsymbol{y_{1:k-1}})$, can be left out as this is a constant that only will scale the distribution.

$$p(\boldsymbol{x_k}|\boldsymbol{y_{1:k}}) = \frac{p(\boldsymbol{y_k}|\boldsymbol{x_k})p(\boldsymbol{x_k}|\boldsymbol{y_{1:k-1}})}{p(\boldsymbol{y_k}|\boldsymbol{y_{1:k-1}})} \propto p(\boldsymbol{y_k}|\boldsymbol{x_k})p(\boldsymbol{x_k}|\boldsymbol{y_{1:k-1}}) \tag{2.9}$$

The Bayesian filtering equations allows for recursive solving of the posterior distribution without increasing the computational complexity over time. In the case of a

Gaussian distributed posterior, the distribution can be described by its mean, $\hat{\boldsymbol{x}}_{\boldsymbol{k|k}}$, and covariance. The mean, $\hat{\boldsymbol{x}}_{\boldsymbol{k|k}}$, is in that case the state estimate for the given time-step. The filtering steps are summarized in Figure 2.2.

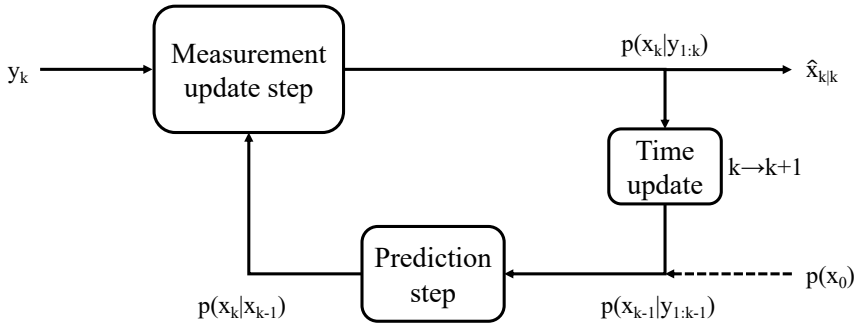

Figure 2.2: Recursive Bayesian filtering illustrated. The recursion is initialized with an prior distribution $P(\boldsymbol{x_0})$. Next, a prediction is made using a process model in the prediction step. The posterior density, $p(\boldsymbol{x_k}|\boldsymbol{y_{1:k}})$, is calculated with the measurement update. The recursion continues in the next time-step but now the posterior density is the last posterior.

2.1.3 Kalman Filter

In previous section the recursive solution for the Bayesian filtering problem was covered. In a linear Gaussian setting, both the process and measurement models are assumed to be linear and all distributions are Gaussian. It turns out that the Kalman filter [30] is the closed form solution to the filtering equations in a linear Gaussian setting [28]. This means that the Kalman filter provides an optimal solution in the Bayesian sense for a discrete linear Gaussian filtering problem. This property in combination with the relative simplicity in setting up the filter makes the Kalman filter widely used in many engineering applications [31]. In the following section the Kalman filter equations are presented. The explicit derivation of the Kalman filter equations is not included in this thesis but can be found in works like [28] and [31].

In a linear Gaussian setting, the state space model can be written as equation (2.10).

$$\begin{aligned} \boldsymbol{x_k} &= \boldsymbol{A_{k-1}}\boldsymbol{x_{k-1}} + \boldsymbol{B_{k-1}}\boldsymbol{u_k} + \boldsymbol{q_{k-1}} \\ \boldsymbol{y_k} &= \boldsymbol{H_k}\boldsymbol{x_k} + \boldsymbol{r_k} \end{aligned} \tag{2.10}$$

Here, $\boldsymbol{A}$ is the state transition matrix, $\boldsymbol{B}$ is the input-matrix and $\boldsymbol{H}$ is the measurement matrix. The additive noise in the process model and measurement model is described by zero-mean Gaussian distributions. That is, $\boldsymbol{q_k} \sim \mathcal{N}(\boldsymbol{0}, \boldsymbol{Q_k})$ and $\boldsymbol{r_k} \sim \mathcal{N}(\boldsymbol{0}, \boldsymbol{R_k})$. As with the filtering equations, the Kalman filter consists of three steps, initialization, prediction and measurement update. All the corresponding distributions are Gaussian, which are fully characterized by its mean and covariance.

Thus, only these moments are needed to be calculated to describe the distributions.

The initial prior distribution of the states is described by the Gaussian distribution $\mathcal{N}(\bar{\boldsymbol{x}}_{\boldsymbol{0}}, \boldsymbol{P}_{\boldsymbol{0|0}})$. The initial mean, $\bar{\boldsymbol{x}}_{\boldsymbol{0}}$, and covariance, $\boldsymbol{P}_{\boldsymbol{0|0}}$, needs to be set with a reasonable guess to get a good starting point for the recursion. The prediction and update distributions are described in equation (2.11).

$$\begin{aligned} p(\boldsymbol{x}_{\boldsymbol{k}}|\boldsymbol{y}_{\boldsymbol{1:k-1}}) &= \mathcal{N}(\boldsymbol{x}_{\boldsymbol{k}}|\hat{\boldsymbol{x}}_{\boldsymbol{k|k-1}}, \boldsymbol{P}_{\boldsymbol{k|k-1}}) \\ p(\boldsymbol{x}_{\boldsymbol{k}}|\boldsymbol{y}_{\boldsymbol{1:k}}) &= \mathcal{N}(\boldsymbol{x}_{\boldsymbol{k}}|\hat{\boldsymbol{x}}_{\boldsymbol{k|k}}, \boldsymbol{P}_{\boldsymbol{k|k}}) \end{aligned} \tag{2.11}$$

In this notation, $\hat{\boldsymbol{x}}_{\boldsymbol{k|k-1}}$ is the prior mean, $\hat{\boldsymbol{x}}_{\boldsymbol{k|k-1}}$ is the predicted mean and $\hat{\boldsymbol{x}}_{\boldsymbol{k|k}}$ is posterior mean. These means represent the states estimations at each filter step. The moments for the prediction distribution are calculated as equation (2.12).

$$\begin{aligned} \hat{\boldsymbol{x}}_{\boldsymbol{k|k-1}} &= \boldsymbol{A}_{\boldsymbol{k-1}}\hat{\boldsymbol{x}}_{\boldsymbol{k-1|k-1}} + \boldsymbol{B}_{\boldsymbol{k-1}}\boldsymbol{u}_{\boldsymbol{k}} \\ \boldsymbol{P}_{\boldsymbol{k|k-1}} &= \boldsymbol{A}_{\boldsymbol{k-1}}\boldsymbol{P}_{\boldsymbol{k-1|k-1}}\boldsymbol{A}_{\boldsymbol{k-1}}^{T} + \boldsymbol{Q}_{\boldsymbol{k-1}} \end{aligned} \tag{2.12}$$

For the update step the calculations are as in equation (2.13).

$$\begin{aligned} \hat{\boldsymbol{x}}_{\boldsymbol{k|k}} &= \hat{\boldsymbol{x}}_{\boldsymbol{k|k-1}} + \boldsymbol{K}_{\boldsymbol{k}}\boldsymbol{v}_{\boldsymbol{k}} \\ \boldsymbol{P}_{\boldsymbol{k|k}} &= \boldsymbol{P}_{\boldsymbol{k|k-1}} - \boldsymbol{K}_{\boldsymbol{k}}\boldsymbol{S}_{\boldsymbol{k}}\boldsymbol{K}_{\boldsymbol{k}}^{T} \\ \boldsymbol{v}_{\boldsymbol{k}} &= \boldsymbol{y}_{\boldsymbol{k}} - \boldsymbol{H}_{\boldsymbol{k}}\hat{\boldsymbol{x}}_{\boldsymbol{k|k-1}} \\ \boldsymbol{S}_{\boldsymbol{k}} &= \boldsymbol{H}_{\boldsymbol{k}}\boldsymbol{P}_{\boldsymbol{k|k-1}}\boldsymbol{H}_{\boldsymbol{k}}^{T} + \boldsymbol{R}_{\boldsymbol{k}} \\ \boldsymbol{K}_{\boldsymbol{k}} &= \boldsymbol{P}_{\boldsymbol{k|k-1}}\boldsymbol{H}_{\boldsymbol{k}}^{T}\boldsymbol{S}_{\boldsymbol{k}}^{\boldsymbol{-1}} \end{aligned} \tag{2.13}$$

It is in the update step that the new information from the measurements is fused with the prediction of process model. $\boldsymbol{v}_{\boldsymbol{k}}$ is called the innovation and describes the difference between what is predicted and observed. The Kalman gain, $\boldsymbol{K}_{\boldsymbol{k}}$, is then calculated based on the covariances (uncertainties) of the prediction and measurements and is used to decide how much to trust the new information.

Based on that the process and measurement models are sufficiently accurate, the key to get a good filtering result is the tuning of the filter. The tuning is made through the covariance matrices $\boldsymbol{Q}_{\boldsymbol{k-1}}$ and $\boldsymbol{R}_{\boldsymbol{k}}$. One strategy is to use previous knowledge about the sensors to tune the measurement noise matrix $\boldsymbol{R}_{\boldsymbol{k}}$ first. This can be based on specifications from the manufacturer or by characterization of the sensor signals in known conditions. Then only the process noise matrix needs to be tuned to get good results. The signal to noise ratio (SNR) describes the characteristics of the response of the filter. A high SNR gives a quicker response to changes in measurements. A lower SNR means that the filter relies more on the predictions.

2.1.4 Extended Kalman Filter

The Kalman filter, presented in previous section, is bound to linear Gaussian process and measurement models. In the case of non-linear process and measurement models, the Kalman filter cannot be directly applied. The extended Kalman filter (EKF) is a modified version of the linear Kalman filter that works for non-linear models [28]. It builds on the same principles as the linear Kalman filter but instead non-linear models are linearized to approximate the linear case. In the following section the EKF equations are presented.

Let the process and measurement models be described by two non-linear functions, $\boldsymbol{f}$ and $\boldsymbol{h}$. Assuming that the functions are not too non-linear, the functions can locally be represented by a first order Taylor expansion. In the EKF, the functions are linearized around the corresponding mean according to equation (2.14) where $\boldsymbol{F}$ and $\boldsymbol{H}$ are the Jacobians of the functions.

$$\begin{aligned}\boldsymbol{x_k} &= \boldsymbol{f}(\boldsymbol{x_{k-1}}, \boldsymbol{u_k}) + \boldsymbol{q_{k-1}} \approx \boldsymbol{f}(\hat{\boldsymbol{x}}_{\boldsymbol{k-1|k-1}}, \boldsymbol{u_k}) + \boldsymbol{F}(\hat{\boldsymbol{x}}_{\boldsymbol{k-1|k-1}}, \boldsymbol{u_k})(\boldsymbol{x_{k-1}} - \hat{\boldsymbol{x}}_{\boldsymbol{k-1|k-1}}) + \boldsymbol{q_{k-1}} \\ \boldsymbol{y_k} &= \boldsymbol{h}(\boldsymbol{x_k}) + \boldsymbol{r_k} \approx \boldsymbol{h}(\hat{\boldsymbol{x}}_{\boldsymbol{k|k-1}}) + \boldsymbol{H}(\hat{\boldsymbol{x}}_{\boldsymbol{k|k-1}})(\boldsymbol{x_k} - \hat{\boldsymbol{x}}_{\boldsymbol{k|k-1}}) + \boldsymbol{r_k}\end{aligned} \tag{2.14}$$

As with the Kalman filter, the filtering consists of the same three steps, initialization, prediction and measurement update. The initialization is done as with the regular Kalman filter as described in section 2.1.3. The prediction and posterior distribution is still expressed by equation (2.11). Though, the moments are calculated with a slight modifacation as described in [28].

The moments for the the prediction distribution is calculated as equation (2.15).

$$\begin{aligned}\hat{\boldsymbol{x}}_{\boldsymbol{k|k-1}} &= \boldsymbol{f}(\hat{\boldsymbol{x}}_{\boldsymbol{k-1|k-1}}, \boldsymbol{u_k}) \\ \boldsymbol{P_{k|k-1}} &= \boldsymbol{F}(\hat{\boldsymbol{x}}_{\boldsymbol{k-1|k-1}}, \boldsymbol{u_k})\boldsymbol{P_{k-1|k-1}}\boldsymbol{F}(\hat{\boldsymbol{x}}_{\boldsymbol{k-1|k-1}}, \boldsymbol{u_k})^T + \boldsymbol{Q_{k-1}}\end{aligned} \tag{2.15}$$

For the posterior distribution, the calculations are as equation (2.16).

$$\begin{aligned}\hat{\boldsymbol{x}}_{\boldsymbol{k|k}} &= \hat{\boldsymbol{x}}_{\boldsymbol{k|k-1}} + \boldsymbol{K_k}\boldsymbol{v_k} \\ \boldsymbol{P_{k|k}} &= \boldsymbol{P_{k|k-1}} - \boldsymbol{K_k}\boldsymbol{S_k}\boldsymbol{K_k^T} \\ \boldsymbol{v_k} &= \boldsymbol{y_k} - \boldsymbol{H_k}(\hat{\boldsymbol{x}}_{\boldsymbol{k|k-1}})\hat{\boldsymbol{x}}_{\boldsymbol{k|k-1}} \\ \boldsymbol{S_k} &= \boldsymbol{H_k}(\hat{\boldsymbol{x}}_{\boldsymbol{k|k-1}})\boldsymbol{P_{k|k-1}}\boldsymbol{H_k}(\hat{\boldsymbol{x}}_{\boldsymbol{k|k-1}})^T + \boldsymbol{R_k} \\ \boldsymbol{K_k} &= \boldsymbol{P_{k|k-1}}\boldsymbol{H_k}(\hat{\boldsymbol{x}}_{\boldsymbol{k|k-1}})^T\boldsymbol{S_k^{-1}}\end{aligned} \tag{2.16}$$

EKF is one of several approaches for filtering in a non-linear setting. The Unscented Kalman filter and particle filter are two other examples mentioned in [28]. Compared to those approaches, EKF is a relatively computationally efficient alternative. As long as the models are not too non-linear the EKF performs well as it approximates the optimality of the linear Kalman filter. Though, it should be clear that it is not an optimal solution in the same sense as the Kalman filter is in a linear Gaussian setting.

2.2 Sensors

In this section, a brief overview of the main sensors used in this work is presented.

2.2.1 Inertial Measurement Unit

An inertial measurement unit (IMU) is a device that measures acceleration, angular velocity and sometimes the magnetic field. This is done using a combination of accelerometers, gyroscopes and sometimes magnetometers. There are many applications of IMUs, ranging from inertial navigation to use in consumer electronics. Early IMU systems used in aerospace in the 1950's used mechanical gyroscopes and could weigh up to 1200kg [32]. Modern IMUs fit inside a phone and weighs only a few grams. In the following section, a short introduction to accelerometers, gyroscopes, different types of IMUs is made.

An accelerometer measures proper acceleration, which means that the acceleration is measured relative free-fall. In free fall the accelerometer will measure 0 m/s^2. At rest on the surface of the earth it will measure the gravity acceleration g. It can also be subject to measuring additional accelerations caused by e.g. centripetal acceleration. A single accelerometer measure the acceleration along a one axis. By combining several accelerometers it is possible to measure the direction and magnitude of the acceleration.

Gyroscopes are devices that measure the rate of change of orientation. Historically, gyroscopes were mechanical devices that contained a spinning disc on an axis mounted to freely move in any direction [32]. When moved, the rotating axis will induce a counter moment and remain it's orientation. The gyroscope can either be used to define a certain direction in the inertial frame or be used in a strap-down configuration where it is mounted to e.g. a vehicle and measure the angular velocities of the body. Today there exist several types of gyroscopes with different accuracy, weights and prices. The performance is normally described by the amount of orientation error that accumulates over time expressed in degrees per hour. Sometimes the performance is referred to as bias stability or the bias drift. On the higher end, ring-laser and fiber-optic gyroscopes can typically achieve drift of 1°/hour with a cost per unit around 10000 USD [16]. Whereas on the lower end micro electro mechanical systems (MEMS) provide a smaller and more affordable solution that achieve a typical drift of 70°/hour with a price of around 100 USD [16].

2.2.2 Sensor Noise

All sensors are affected by errors and biases. Although there exists very accurate sensors, the performance of a sensor needs to be weighted to the cost and what is needed for the application at hand. Especially in consumer products where the margins might be low. One example of the difference between consumer grade and military grade gyroscopes is in the bias stability over time. A military grade gyroscope can have a bias drift of less than 0.00002 deg per hour while consumer

grade could be as high as 0.01-0.2 deg per second [32]. The military grade sensor outperforms the consumer grade sensor but the precision might not be needed in let's say a phone where maybe it is enough to know if there's rotation or not.

[32] explain that a signal measured by a sensor, x_m, can be related to the true signal, x, by a scale factor, s, an offset or bias, b, and a random noise, ϵ, according to equation (2.17).

$$x_m = sx + b + \epsilon \tag{2.17}$$

These parameters and additional specifications and tolerances of a sensor are normally made available by the manufacturer. The properties of e.g. the bias can also be experimentally determined. In an MEMS IMU the scale factor, s, and bias, b, varies with time and temperature. The scale error is usually not the biggest problem in practice, it is the bias which makes the biggest impact, at least in applications where the signals are integrated [32]. For example, if an angle was to be calculated from a gyroscope signal with a constant bias of 0.2/s. Then the angle estimate will drift linearly and have a 12 degrees error after one minute.

The biases of a sensor can be accounted for in several ways. One way is to put the device in a stationary position with known orientation right before use. During this time, it is known that the IMU is not moving and it is possible to measure what the gyroscope offsets are [32]. The accelerometer offsets could also be determined if the gravity was accounted for. As the offsets vary with time this approach is fairly limited for use over longer times. An alternative approach would be to estimate the biases online. This could be done using e.g. a Kalman filter where the biases are described as slowly changing states [33].

2.2.3 Wheel Speed Sensors

Wheel speed sensors are a type of tachometers that are used in the automotive industry. The working principle is that a disc with a number of cutouts is mounted to the axle/wheel. By counting the number of ticks per time unit it is possible to determine the angular velocity of the wheel. The translational velocity can then be calculated by multiplying the angular velocity with the radius of the wheel. The sensor has the advantage of measuring the velocity in the plane of the road, thus not being affected by road inclination and banking. In nominal conditions where the wheel is not slipping, wheel speed encoders give accurate estimates of the velocity assuming that the tyre radius is known accurately. If a vehicle are equipped with several wheel speed sensor there is also a redundancy in the measurement.

However, wheel speed encoders are prone to errors. The tyre radius may differ from it's nominal value when driving which can cause an error in the radius of up to 5%. The sensor can at times make corrupt readings and therefore give outlier observations as 0 speed. The angular speed is also measured in the direction of the wheel. That is, when the car is turning, the measured velocities will have an

offset compared to the true speed and needs to be corrected for. Likewise, if the tyre slips or skids the speed measurement will be offset. Lastly, in low speeds the measurements is not very accurate as the gaps between each "tick" is too far to get accurate estimation of the speed. [10].

2.2.4 Steering Wheel Angle Sensor

Steering wheel angle gives a measurement of the wheel angles i.e. in which direction the steered wheels are pointing. It is an important quantity in assessing vehicle dynamics and motion. In most cases, optical sensors are used that work on the hall effect principle. The sensor is mounted in the steering column.

Steering angle sensors can either be analog or digital. When the steering angle changes,the sensor generates a signal whose resolution is calibrated such that the maximum voltage generated relates to 360° turn of the steering wheel. The sensors are also calibrated such that they give positive or negative voltage based on the direction of turning. Digital sensors produce a signal that indicates the angle of steering. The steering angle measurements can be easily related to the wheel angles via a set of mechanical connection equations.

In a steering module, multiple sensors used for redundancy, accuracy and safety since this sensor is a part of the stability program which is safety critical. The output of the two sensors gives accurate reading on the steering and thus wheel angle, how fast the angle is changing as well as can be used to cross check the values produced on both outputs.

2.2.5 Powertrain Torque

Powertrain torque sensors are used to measure the applied torque from the engine to the wheels to propel the vehicle. Torque sensors are categorized as using angular displacement as measurement or a transducer mounted on the drive shaft. The angular displacement method measures the torsion angle between the point where the sensor is placed and the end of that shaft. It needs a longer shaft to work which reduces its use in automotive powertrains. Transducers are more widely used in the automotive industry for torque sensing. Transducers can be based on strain gauges, Software Acoustic Waves using ultrasonic pulse propagation, or using magneto-electric properties of a ferromagnetic substance.

For most cases, the accuracy of the torque sensor depends on temperature and prolonged exposure to vibrations. Torque sensors are subjected to lot of relative movements in the driveline, engine braking, dynamic driving that induce mechanical and signal noise in the measurements. All these parameters increase it's intensity and effects on the torque measurement as speed increases.

2.2.6 Brake Friction Torque

Applied braking torque can either be measured by using piezoelectric sensors mounted in the brake calipers or by pressure sensors in the brake lines. The transferred brake torque that eventually works to stop the vehicle is not directly measured, but estimated based on the friction between the brake pads and the disc. The brake friction torque data is calibrated and translated with high accuracy for different working temperatures and speeds after rigorous testing. For most vehicle OEMs, brake sensors are tightly integrated and calibrated by the brake supplier.

2.3 Tyres Dynamics

Tyres are the only part of the vehicle that are in contact with the road and play a pivotal role in generating forces necessary to provide motion. They are generally made from rubber compounds that interact with the road surface to provide tractive, braking or turning forces as well as produce grip. Tyres are also responsible for carrying the weight of the vehicle. They dictate the way power produced from the powertrain unit is "put down" on the road to accelerate or brake the vehicle as well as generate lateral forces through the steering mechanism to provide manoeuvrability and controllability to the vehicle.

Tyres used throughout this thesis and for explanation in the report are pneumatic tyres made from a rubber compound used widely in every passenger vehicle. The wheel is defined as the hub and rim assembly on top of which the tyre sits.

The wheels that are actively provided driving torque from the powertrain are called driven wheels. The wheels not connected to any active drive axle are non-driven wheels. For eg. on a Front-Wheel-Drive car, the driven wheels are the front wheels.

2.3.1 Producing Grip

Here is a simplified explanation of grip produced by the tyre to help the reader visualize. The knowledge of exactly how the grip is generated is beyond the scope of the thesis however the reader is directed to [34] for in depth explanation.

Imagine a tyre on a flat road that is carrying a certain vertical load and connected to a drive axle. The area of the tyre that is contact with the road surface is called a contact patch which is produced due to the elasticity of the tyre and the subjected vertical load. We now apply a propulsion torque on the axle that will make the tyre roll on the surface. As the tyre starts rolling, the treads come in contact with the road, press against it on the contact patch and release contact as they move long, creating adhesion between the tyre and road. This happens continuously at low and high speeds through every rotation producing grip that keeps the tyres in contact with the road. The deformation and contact patch formation can be seen in figure 2.3.

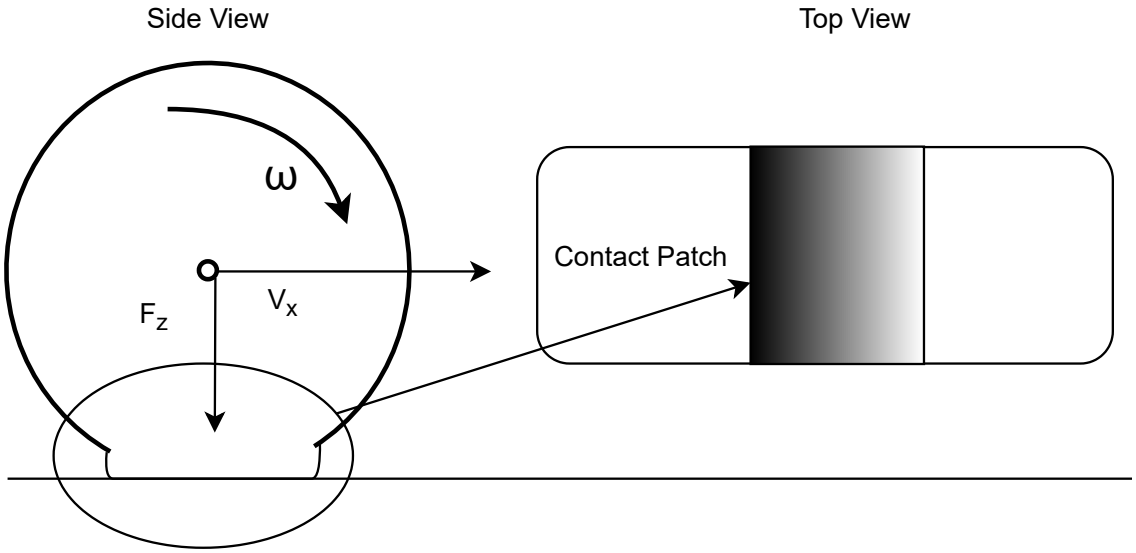

Figure 2.3: Deformation and Contact Patch of the Tyre

2.3.2 Brush Tyre Model

A brush tyre model is used to understand the interactions of the tyre and road and explain how forces are generated. The model consists of a row of elastic bristles that touch the road plane, and can deflect in a direction parallel to the road surface. These bristles are called tread elements as seen in figure 2.4a. The tail of the tread is attached to the rim body upon which the tyre sits. The head of the tread is in contact with the road surface and produces the adhesion or grip. For further detailed reading the, reader is directed to [34].

2.3.3 Effective Rolling Radius

Assume a loaded tyre moving with angular velocity ω on a flat surface in figure 2.4b. The unloaded radius of the tyre is R_0. The point A on the tyre is the point under compression just before the contact patch, which has a radius of R_a also known as reduced radius. Point B is just after the contact patch begins which has a radius called the effective radius, R_e. It is this radius that gives the tangential/peripheral velocity of the tyre. Next, at point C is the loaded radius R_h. Point D is again the effective radius as it is just about to leave the contact patch and point E is just after it leaves the contact patch.

The changing radius between point A and B is R_1, between B and D is R_2 and between D and E is R_3. The velocity of motion or longitudinal velocity of the wheel is given as $V_x = R_e.\omega$. However, the tangential velocity is actually changing at each point on the tyre. It can be seen from the figure 2.4b that the radius $R_0 > R_a > R_e > R_h$. This means that $(R_1 = R_3) > R_2$.

Thus within every region, the tangential velocity differs from the longitudinal velocity.

Region $A \rightarrow B$

$$V_t = R_1.\omega > V_x \tag{2.18}$$

Region $B \rightarrow D$

$$V_t = R_2.\omega < V_x \tag{2.19}$$

Region $D \rightarrow E$

$$V_t = R_3.\omega > V_x \tag{2.20}$$

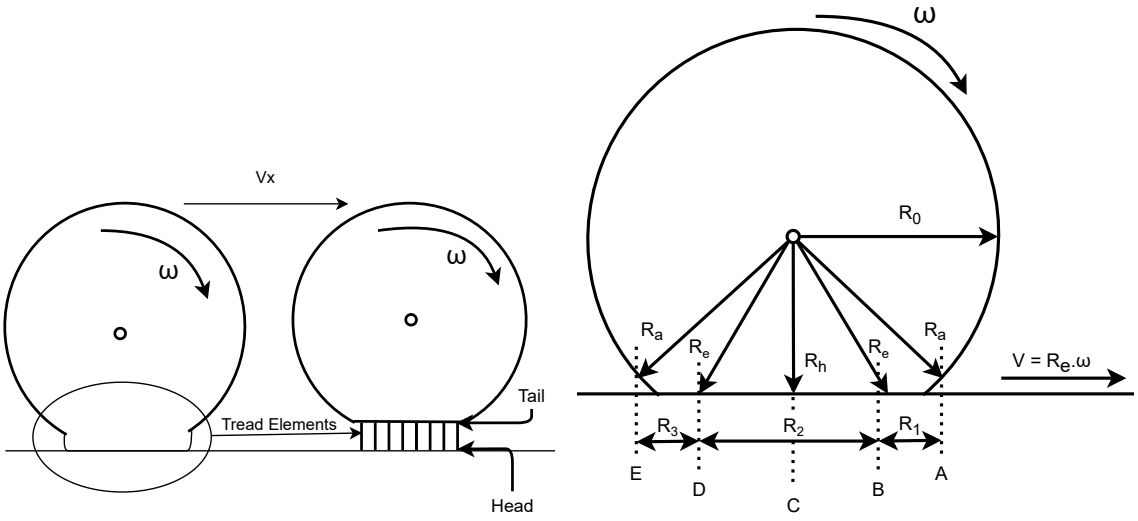

(a) Brush Tyre Model with tread elements

(b) Changes in effective rolling radius that affect translation speed

Figure 2.4: Brush Tyre Model and Effective Radius

2.3.4 Longitudinal Force

Longitudinal Force is generated by the tyre through it's interaction with the road via adhesion or grip, and from the torque provided through the drive axle. These forces provide acceleration or braking to the vehicle.

To better explain these forces, it is best to use the brush tyre model depiction in figure 2.5 and the equations 2.18,2.19 and 2.20. The explanation below is simplified to understand slipping phenomenon. This is based on works in CHAPTER III [34],[35] to which the reader can refer for detailed understanding and explanations.

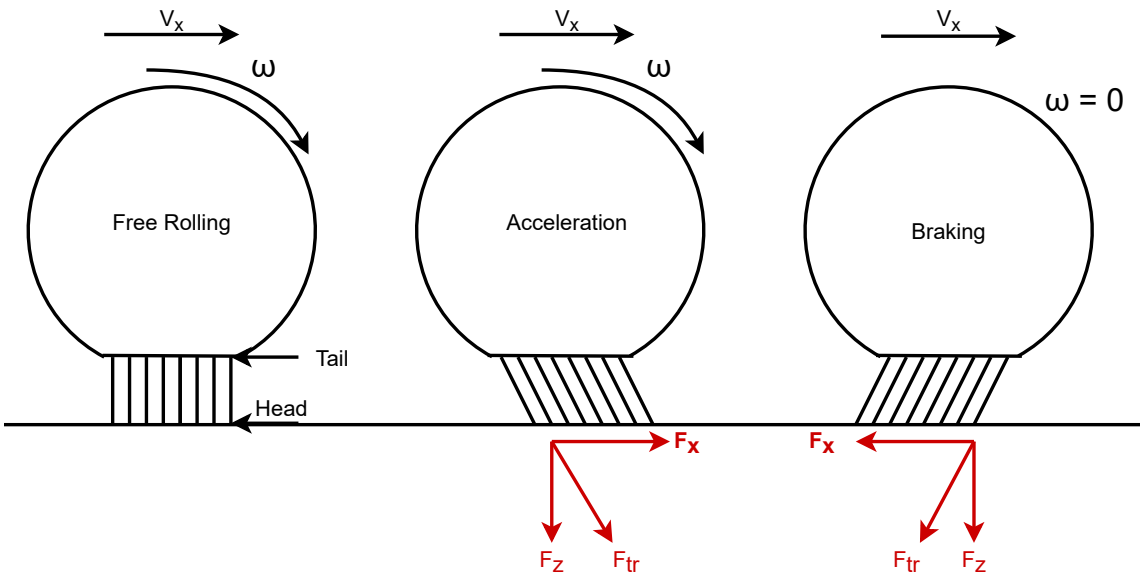

Figure 2.5: Longitudinal Force generated in different scenarios - Free Rolling , Acceleration and Braking

Free Rolling

Let us assume a loaded, free rolling tyre i.e. no torque or force is applied to it. The contact patch in this case is theoretically just a point in 2-D or a line in 3-D consideration. The tread tail and head move with the same velocity. Thus the longitudinal velocity of the vehicle and tangential velocity of the tyre is the same $V_x = V_t$. This means that there is no relative movement between the tail and head and thus no tangential forces are generated.

Acceleration

When positive torque is applied to the wheel, the tyre deforms as seen for acceleration in figure 2.5. The adhesion between the tread head and the road surface holds the tread where it initially enters the contact patch. The tail, connected to the rim, is subjected to varying tangential velocities V_t as discussed in section 2.3.3 due to applied torque and the effective rolling radius, given by equations 2.18,2.19 and 2.20. The head is subjected to the longitudinal velocity of motion V_x, which is the forward velocity of the vehicle. While there is enough adhesion for the tread head to remain attached to the road, a difference in velocities between the tread tail and head creates a tension F_{tr} in the tread elements which when resolved, gives longitudinal force F_x. This is the tractive force that propels the car forward.

Braking

When maximum brake torque is applied such that it locks the wheel and thus it skids along the road surface. The tyre deforms again as seen for the braking case in figure 2.5. However this time, the tangential speed of the tyre $\omega = 0$ and thus $V_t = 0$. Now, the tail connected to the rim has no velocity. However the head is subjected to the velocity V_x with which it was moving along the ground. This difference in velocities causes a tension force in the opposite direction within the tread elements

such that the head is behind the tail. Resolving with force gives the braking force $-F_x$ that helps to brake the vehicle.

2.3.5 Longitudinal Slip

We know that a difference in the longitudinal velocity and tangential velocity of the tyre, as the tread sticks to the road, generates a force to propel or brake the vehicle. This difference in velocities causes a relative motion between the tread head and tail thus giving rise to a phenomenon called slip. Slip velocity is defined as the difference between the longitudinal velocity of the tyre and the tangential velocity of the tyre. This velocity when normalized by the longitudinal velocity gives the slip ratio [35].

$$S_x = \frac{(V_x - R_e\omega)}{R_e\omega} \quad \text{in Acceleration} \qquad S_x = \frac{(V_x - R_e\omega)}{V_x} \quad \text{in Braking} \tag{2.21}$$

This forms an important physical relation that tyres produce slip when the tyres have grip to stick to the road surface, which then generates the tractive or braking forces.

Free Rolling
In free-rolling conditions, there is no relative motion or velocity between the tread head and the tail. Thus the slip ratio $S_x = 0$ and no force is generated, $F_x = 0$.

Acceleration
In acceleration, the $V_x < V_t$, which means that the slip ratio S_x is positive and a propulsion force F_x is generated.

Braking
In extreme braking when the wheels lock, the $V_t = 0$ which means that the slip ratio $S_x = -1$ and braking force $-F_x$ is generated.

2.4 Parameters that affect Grip and Slip

As mentioned in 2.3.5, slip produced when there is adhesion or grip between road and tyre, that holds the tread head in contact, creates a difference between the longitudinal velocity of the vehicle and tangential velocity of the tyre. This produces the tractive or braking force. This means that grip plays a major role in generating slip that produces longitudinal force. Grip is basically the road surface holding on to the tread head through friction or adhesion . The friction or adhesion between the road surface and the tyre is a function of the interaction of the two surfaces. This also dictates the magnitude of maximum slip ratio and force generated, as well as how much torque can be applied to the wheel before grip is lost. However, the two most important ones are - vertical loading on the tyre and the road-tyre friction that are discussed next.

2.4.1 Effect of Vertical Loading

Effects of different vertical loads on the tyre can be seen in figure 2.6. For a load of 1000 N on a tyre, the longitudinal force is lowest. This means that the amount of deformation and tension in the tread is only enough to produce such low forces before the tyre starts losing grip. The longitudinal force values increase with the load on the tyre. The increase is initially linear as torque is applied, till the tyre develops maximum friction or grip. At that peak point, it produces maximum traction or braking force for a slip ratio. Beyond this peak as the applied torque and slip ratio increase, the grip and longitudinal force decreases. This means that the tyre's contribution to the longitudinal motion keeps reducing. The longitudinal force drops down to the kinetic friction force that makes the wheel spin without contributing to vehicle propulsion. It is important to note that this decrease does not instantly make the tyre visibly spin or lock up. However, the tyre visibly spinning or locking up is an indication that the torque applied to the tyre way too high for it to catch any grip on the road.

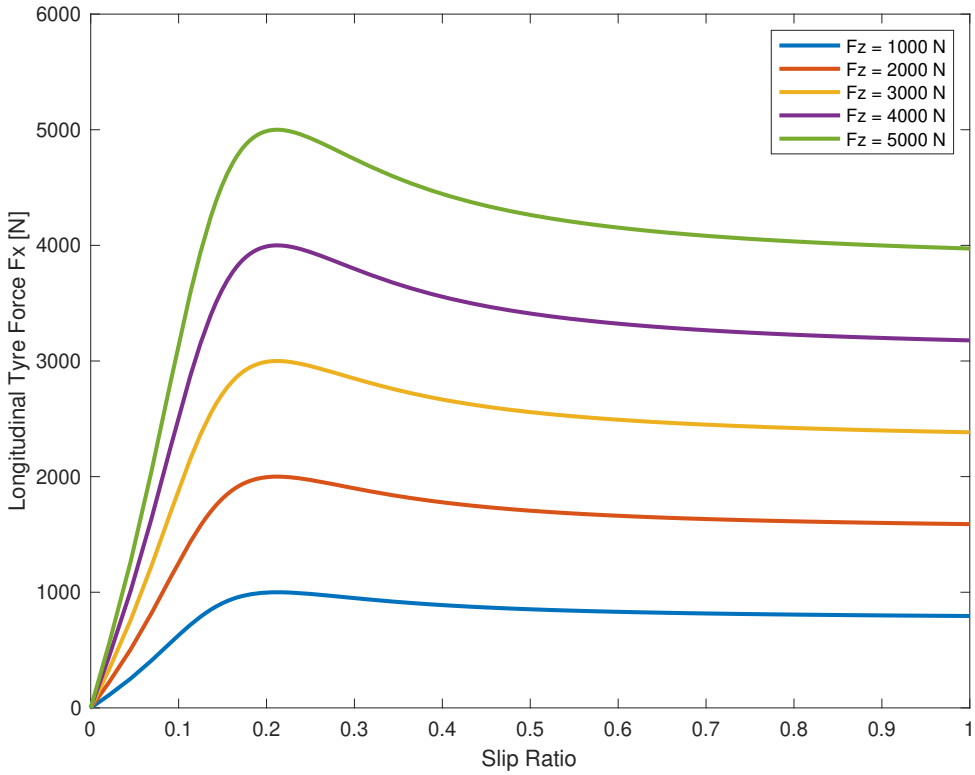

Figure 2.6: Longitudinal Force vs Slip Ratio for different vertical loads on a dry asphalt road

2.4.2 Effect of Road-Tyre Friction

The effect of road tyre friction can be observed in figure 2.7 for a constant load. For a tyre rolling on ice, the friction coefficient is usually around 0.15 while on dry asphalt

it is around 0.8. Looking at the figure 2.7, one can observe that the longitudinal force generated by the tyre is higher when the friction coefficient is higher.

First we consider the tyre rolling on dry asphalt. As the engine torque applied to the tyre, slip is generated through difference in tangential and longitudinal velocity. As the amount of torque increases, slip increases and the amount of longitudinal force increases linearly as the tread elements are subjected to more and more tension. This increase happens up until the peak static friction is reached. This is the point where maximum force is generated at a slip ratio. Beyond this point i.e. when the engine torque provided to the tyre crosses the friction limit, the tyre starts slipping more and more till they start spinning in place and do not contribute to the vehicle motion.

For a tyre rolling on ice, the longitudinal forces generated are much smaller since there is not enough friction to hold the tread head to the ground and can be easily overcome by low engine applied torque. The longitudinal force peaks out at 250 N and at a slip ratio of 0.03 or 3%. When compared to dry asphalt, the longitudinal peaks out at 3000 N and achieves a higher slip ratio at 0.2 or 20% before losing grip and inducing wheel spin. Given such a low threshold for inducing spinning condition on ice means that the tyres are bound to spin under acceleration or braking in normal as well as extreme driving maneuvers.

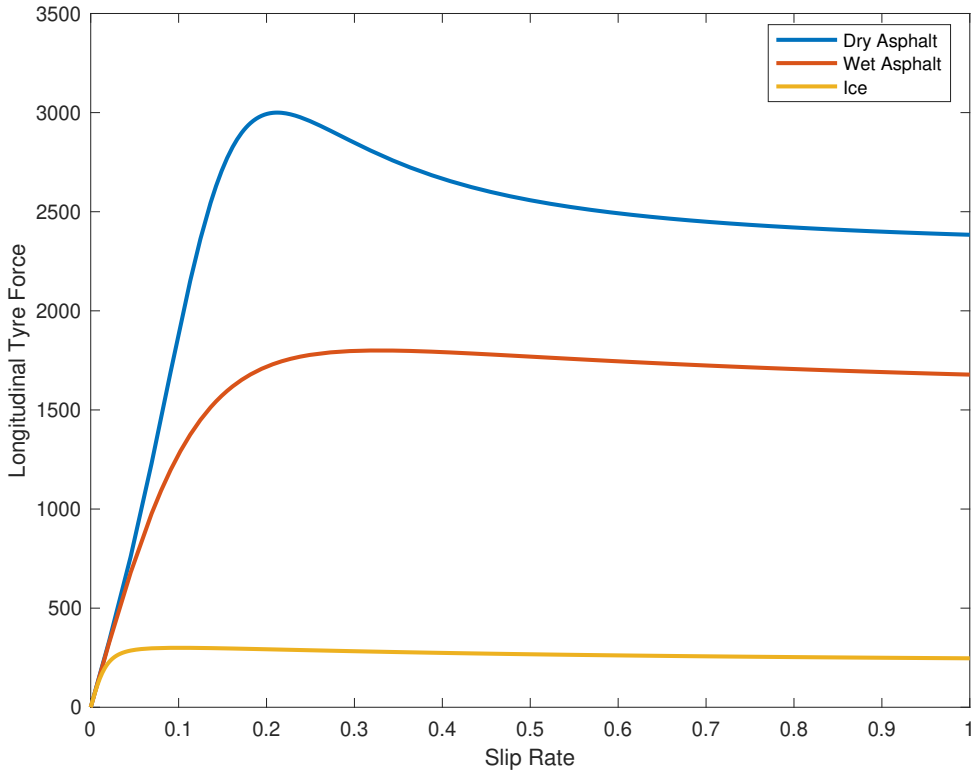

Figure 2.7: Longitudinal Force vs Slip Ratio for different road surfaces at constant load

2.5 Modelling Tyre Behaviour

Modelling tyre behaviour is difficult based on it's characteristics as the parameters mentioned above and others, change dynamically in real time, affecting how the tyre reacts, how the slip is generated and thus how much force is produced.

2.5.1 Non Linear Tyre Model

The most widely used model is the non linear tyre model called the Magic Formula Tyre Model developed by Hans B. Pacejka [34]. In this model, the tyre characteristics are modelled into an equation that fits the curve of experimental data points. Data generated from testing a tyre on a test rig, with different loads, friction, slip and speed gives data points that are used for curve fitting using the equation :

$$F_x = D.\sin\left(C.\arctan\left(Bx - E(Bx - \arctan\left(Bx\right))\right)\right).F_z \tag{2.22}$$

where, B is the stiffness factor that decides the initial slope for the tyre curve, where to force and slip increase linearly, C is the shape factor of the curve, D is the peak value of the tyre curve and E models the effect of friction, deciding where the peak value of force occurs.

Advantages of using magic formula tyre models are that they base the tyre curve on experimental data, providing sufficiently accurate behaviour, both in linear and non linear range. Modelling of the non-linear range helps in determining how peak force is achieved and how the tyres react when the grip is lost i.e. just after the peak as the slip increases and wheel spin situations occur. However, the accuracy of the curve is limited by the availability and accuracy of the experimental data itself. Each coefficient mentioned above depends on factors such as wheel load, temperature, pressure, camber and slip, which need to be accurately analysed and recorded during testing.

2.5.2 Linear Tyre Model

A simpler way of modeling tyre characteristics is by using a tanh tyre model given by the equation 2.23. It accurately represents the linear range, where there is slip in the presence of grip and force increases linearly. It depicts peak longitudinal force but does not represent the non linear range accurately, which is the region of most uncertainty since the tyre loses grip and starts to spin. In fact, the model peaks out the force and makes it constant as slip increases beyond this peak, depicting that there is no reduction in force, but a constant peak force propelling or braking the vehicle. Less complexity and less data requirements are some plus points of using this model, however it does not accurately represent wheel slip and spin cases. It also requires the coefficient of friction and slip to get longitudinal force. As calculation of slip depends on velocity which is what needs to be estimated, using the tanh model does not help.

$$F_x = \mu F_z \tanh\left(\frac{C_x.S_x}{\mu F_z}\right) \tag{2.23}$$

where μ is the coefficient of friction and C_x is the longitudinal stiffness of the tyre, which is also the slope of the tyre plot.

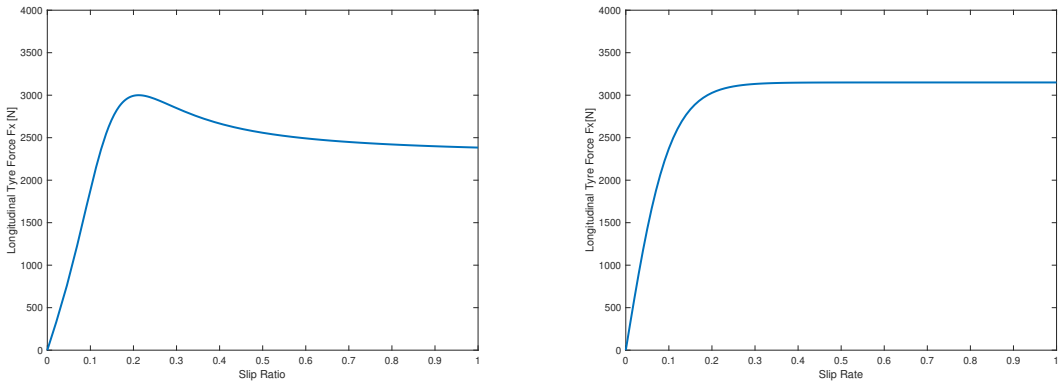

(a) Non Linear Tyre Model **(b)** Linear tanh Tyre Model

Figure 2.8: Non Linear and Linear Tyre model curves for Longitudinal Force vs Slip Ratio

2.5.3 Load Transfer

Load transfer is an unavoidable phenomenon that occurs during vehicle motion. The weight distribution of the car changes dynamically in acceleration, braking and turning, inducing two kinds of load transfer - geometric and elastic. Calculating elastic load transfer requires a lot of spring-damper stiffness data. Geometric load transfer about the centre of gravity can be calculated in a very simple way by considering rigid axles using the equation:

$$\begin{aligned}
F_{z,FL} &= \frac{m \cdot g \cdot b}{2l} - \frac{m \cdot a_x \cdot h}{l} - \frac{m \cdot a_y \cdot h}{t_w} \\
F_{z,FR} &= \frac{m \cdot g \cdot b}{2l} - \frac{m \cdot a_x \cdot h}{l} + \frac{m \cdot a_y \cdot h}{t_w} \\
F_{z,RL} &= \frac{m \cdot g \cdot a}{2l} + \frac{m \cdot a_x \cdot h}{l} - \frac{m \cdot a_y \cdot h}{t_w} \\
F_{z,RR} &= \frac{m \cdot g \cdot a}{2l} + \frac{m \cdot a_x \cdot h}{l} + \frac{m \cdot a_y \cdot h}{t_w}
\end{aligned} \tag{2.24}$$

where,
m = mass of the vehicle
g = acceleration due to gravity
a = distance from front axle to centre of gravity

b = distance from rear axle to centre of gravity
l = wheel base
t_w = track width
a_x = longitudinal acceleration
a_y = lateral acceleration
h = distance of centre gravity from the ground

2.6 Challenges using Tyre Dynamics for Velocity Estimation

The biggest challenge is to accurately represent tyre behaviour, especially in the non linear region which is the central to velocity estimation for this thesis. A non linear magic formula based tyre model accurately represents the non-linear range where the wheels are spinning but, unavailability of experimental data makes this unfeasible to model. Using the data available, a linear tyre model was feasible, which accurately represents wheel speed in nominal or no spin conditions in the linear range. But in the spin condition, the tanh model caps the longitudinal force at the peak value, depicting that even after the tyre has lost grip, the longitudinal force produced is the maximum possible and is actively contributing to the motion of the vehicle. This incorrectly biases the calculated force and the slip ratio. The slip ratio, having slip velocity, which is basically the difference between wheel speed and vehicle speed, then cannot be used to compensate and estimate vehicle velocity.

Another way of compensating for slip ratio or slip velocity could be by using these set of connected equations

$$\begin{aligned} S_x &= \frac{(V_x - r\omega)}{r\omega} \quad \text{in Acceleration} \\ S_x &= \frac{(V_x - r\omega)}{V_x} \quad \text{in Braking} \\ F_x &= C_x.S_x \\ T &= R_e.F_x \end{aligned} \tag{2.25}$$

where,
S_x = Slip Ratio
R_e = Effective radius of tyre
F_x = longitudinal Force
T = Rotational Torque applied on the wheel
C_x = Longitudinal Stiffness of the Tyre
Merging equation 2.25 gives a slip compensation term that can be used to calculate actual speed of the vehicle as

$$V_x = r\omega\left(1 - \frac{T}{r.C_x}\right) \tag{2.26}$$

where $(1 - \frac{T}{r.C_x})$ is the slip compensation term. However, a lack of accurate power-train torque values and longitudinal stiffness but most importantly, the wheel speed values under slip or spin conditions skew the slip compensation velocity and thus the final velocity estimation.

The road-tyre friction cannot be measured directly and thus also needs to be estimated. An experimental tyre model such as the non-linear magic formula tyre model can be fitted for different coefficients of friction however, it requires a lot of testing data which was not available. In real-world driving, each tyre might be subjected to different coefficients of friction. Couple this with varying amount of load on each tyre on an AWD car means that the value of applied torque that induces wheel spin is different on each wheel and thus each wheel has a different slip ratio at a given time. This kind of modelling is difficult given the limited quantity and accuracy of tyre data from testing. A study and analysis of velocity estimation using a feasible linear tyre model was conducted but produced bad results, especially in extreme slip or spinning conditions, which is the main part of the thesis objective.

3

Method

In this chapter, the approach for speed estimation is presented in detail. First, an overview of the approach is given in section 3.1. In the following sections, the different components of the speed estimation is presented. This includes the modelling of the vehicle, sensor characteristics, filter setup, investigation of ways of detecting slip, slip detection and wheel selection concepts and speed estimation strategy during braking.

3.1 Overview of the Speed Estimation Approach

In Figure 3.1 an overview of the structure of the speed estimation is presented. The speed estimation is based on an extended Kalman filter which consists of a prediction step and an update step. In the prediction step the speed for the current time step is predicted using a process model which takes inputs from the IMU. In the update step the wheel speed measurements, which are the only absolute measurement of the vehicle speed, are used to update the speed estimate. The modelling of the vehicle and the Kalman Filter is explained in detail in section 3.2 and 3.4. The main idea with the speed estimation approach is to use a slip-detection system that decides which wheels are slipping and should not be used to update the speed estimate in the update step. An investigation of different ways of detecting slip is presented in section 3.5. Based on this investigation, two slip-detection and wheel selection concepts are set up and presented in section 3.6. An additional speed estimation strategy specific for when the vehicle is braking is presented in section 3.7. As the data is pre-recorded a for-loop is used to loop-through the data in the files. This also allows for pre-processing of the data and setting initial values for the estimation beforehand.

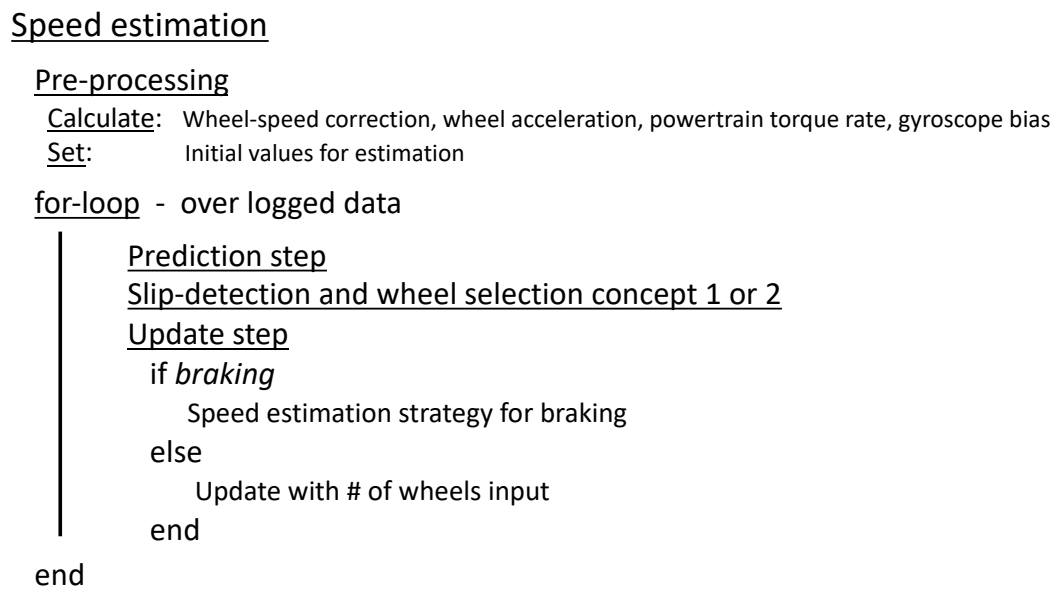

Figure 3.1: Overview of speed estimation approach

3.1.1 Pre-Processing

In the pre-processing step, the wheel accelerations and powertrain torque rates, wheel speed measurement correction and gyroscope bias is calculated. This is mainly because the data is pre-recorded and this can be made beforehand to reduce the amount of computations needed in each for-loop. The wheel accelerations and powertrain torque rates are calculated in a simplified manner by low-pass-filtering the numerical derivative calculated by the finite difference of the quantities. These quantities are later utilised by the slip-detection concepts. The wheel speed corrections, which are explained in detail in section 3.2.5, are made to compensate for different speeds of the wheels induced by turning of the vehicle. As the vehicle is standing still in the beginning of each file, the gyroscope bias can be calculated. This is done before the speed estimation is made and this is further explained in section 3.4.5.

3.1.2 Comment on Speed Estimation

If no slip is detected, all wheel speed measurements are fed to the update step of the Kalman filter. Otherwise a varying number of wheel speed measurements are fed to the filter by the slip-detection and wheel selection concept used. Depending on if the car is accelerating or decelerating, the fastest or slowest wheel is assigned a larger measurement covariance to bias the estimate towards the more likely wheels. If no wheels are input then dead-reckoning is performed which means that the speed estimation at this time is completely based on the integration of the gravity compensated accelerometer readings. The gravity compensation is further explained in section 3.2. The speed estimation uses a specific strategy when the vehicle is braking. This is further explained in section 3.7.

3.2 Modelling of Vehicle

In the following section the modelling of the vehicle is described. This includes definitions of coordinate frames, how the orientation of the vehicle is described, kinematic relations and correction of wheel speed measurements.

3.2.1 Defining Coordinate Frames

In this thesis, two coordinate frames are defined. The inertial coordinate frame (X, Y, Z) and the vehicle coordinate frame (x, y, z). Both frames follow the right hand rule convention. The inertial frame is aligned with the Earth such that the Z-axis is pointing up parallel with the gravity and X-axis and Y-axis are parallel with the sea level. The vehicle coordinate frame is fixed with the vehicle body and centered in the center of gravity (CoG) with the x-axis pointing in the forward direction of the car and z-axis up as in Figure 3.2. In this thesis, it is the longitudinal component of the speed at the center of gravity that is estimated. That is the quantity of the v_x component relative the inertial frame. The lateral speed component, v_y and thus the side slip angle, β is assumed to be negligible. The rotation around each coordinate axis is described by Euler roll, pitch and yaw angles which is further explained in section 3.2.2.

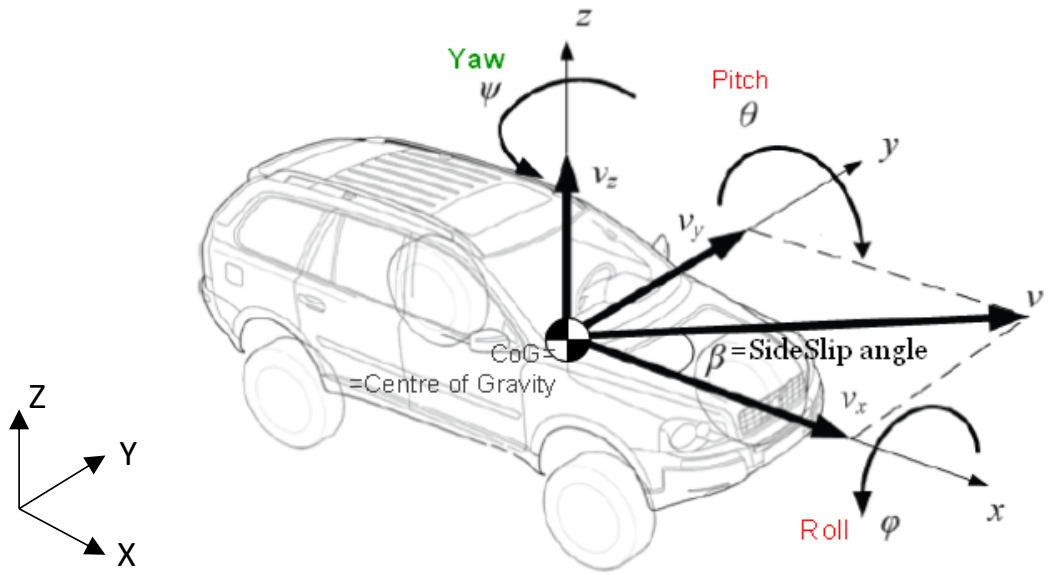

Figure 3.2: Schematic sketch of the coordinate frames and vehicle.

3.2.2 Describing the Orientation of a Rigid Body

There exists different ways to describe the orientation of a rigid body in relation to a fixed orthogonal reference coordinate frame. One commonly used method in vehicle modelling is Euler angles [32]. According to Euler's rotation theorem, any

rotation of a three dimensional orthogonal coordinate system can be described by sequence of three consecutive rotations about different coordinate axles where no consecutive rotation is made about the same axle. There are 12 possible consecutive rotations which can be divided into two groups. One is proper Euler angles where the rotations are made around two axes (e.g. ZYZ), and the other is Cardan angles (also known as Tait-Bryan angles) where the rotations are made around each axle (e.g. ZYX). The angles describing the rotation about the axes x, y, z are usually notated φ, θ, and ψ respectively. Following, the elementary rotation matrices around each axis are introduced.

$$\begin{aligned}
\boldsymbol{R_x}(\varphi) &= \begin{bmatrix} 1 & 0 & 0 \\ 0 & \cos(\varphi) & -\sin(\varphi) \\ 0 & \sin(\varphi) & \cos(\varphi) \end{bmatrix} \\
\boldsymbol{R_y}(\theta) &= \begin{bmatrix} \cos(\theta) & 0 & \sin(\theta) \\ 0 & 1 & 0 \\ -\sin(\theta) & 0 & \cos(\theta) \end{bmatrix} \\
\boldsymbol{R_z}(\psi) &= \begin{bmatrix} \cos(\psi) & -\sin(\psi) & 0 \\ \sin(\psi) & \cos(\psi) & 0 \\ 0 & 0 & 1 \end{bmatrix}
\end{aligned} \tag{3.1}$$

In this thesis the Euler angles convention ZYX (also known as roll-pitch-yaw angles XYZ) is used to represent the orientation of the car. During acceleration, braking and cornering, the suspension of the car compresses and induces chassis roll and pitch angles. The road inclination and bank angle is not separated from the chassis roll and pitch and pitch angle in this thesis. As the orientation estimate is only used for compensation of the gravity vector in accelerometer this simplification should not affect the speed estimation. The Euler angles roll, φ, pitch, θ, and yaw, ψ, are expressed relative a non-moving inertial coordinate frame which is fixed in the center of gravity of the car and has parallel axes with the sea-level and gravity vector. See Figure 3.2 for notation. The two coordinate frames are related by a rotation matrix, $\boldsymbol{R}$, according to,

$$\boldsymbol{X_{body}} = \boldsymbol{R}^T \boldsymbol{X_{inertial}} = \boldsymbol{R_z}^T \boldsymbol{R_y}^T \boldsymbol{R_x}^T \boldsymbol{X_{inertial}}, \tag{3.2}$$

where a vector in the inertial frame can be expressed in the body frame by multiplication of the rotation matrix described by equation (3.3). Note that c and s are used as abbreviations of cos and sin in this equation.

$$\boldsymbol{R}^T = \begin{bmatrix} c(\theta)\,c(\psi) & c(\theta)\,s(\psi) & -s(\theta) \\ c(\psi)\,s(\theta)\,s(\varphi) - c(\varphi)\,s(\psi) & c(\varphi)\,c(\psi) + s(\theta)\,s(\varphi)\,s(\psi) & c(\theta)\,s(\varphi) \\ s(\varphi)\,s(\psi) + c(\varphi)\,c(\psi)\,s(\theta) & c(\varphi)\,s(\theta)\,s(\psi) - c(\psi)\,s(\varphi) & c(\theta)\,c(\varphi) \end{bmatrix} \tag{3.3}$$

It is noted that Euler angles suffer from what is known as gimbal lock. In a physical gyroscope this means that two of the gimbals align and thus one degree of freedom is lost. The same apply for Euler angles and the orientation cannot be completely determined at that point. According to [32] the gimbal lock for ZYX Euler angles occur at $\theta = \pm(2k+1)\frac{\pi}{2}$, where k is an integer. In this thesis it is assumed that the vehicle will not be rotated by 90 degrees in pitch. Therefore gimbal lock should not be a problem for the intended use.

3.2.3 Relating Gyroscope Measurements and Euler Angular Rates

The gyroscopes measure the angular velocities, $\omega_{x,y,z}$, in the vehicle coordinate frame. This is not the same velocities as the Euler angular rates. Utilizing the conjugate Euler angle rates matrix, $\boldsymbol{E}'$, it is possible to relate angular velocities expressed in the fixed vehicle coordinate frame to the Euler angular rates [36]. The conjugate Euler angle rates matrix is defined as,

$$\begin{aligned}\boldsymbol{E}' &= \begin{bmatrix} \begin{bmatrix} 1 \\ 0 \\ 0 \end{bmatrix}, & \boldsymbol{R_x^T} \begin{bmatrix} 0 \\ 1 \\ 0 \end{bmatrix}, & \boldsymbol{R_x^T R_y^T} \begin{bmatrix} 0 \\ 0 \\ 1 \end{bmatrix} \end{bmatrix} \\ &= \begin{bmatrix} 1 & 0 & -\sin(\theta) \\ 0 & \cos(\varphi) & \cos(\theta)\sin(\varphi) \\ 0 & -\sin(\varphi) & \cos(\theta)\cos(\varphi) \end{bmatrix}.\end{aligned} \tag{3.4}$$

By inverting the conjugate Euler angle rates matrix it is possible to express the Euler angular rates in terms of the vehicle coordinate frame fixed angular velocities measured by the gyroscopes according to,

$$\begin{aligned}\begin{bmatrix} \dot{\varphi} \\ \dot{\theta} \\ \dot{\psi} \end{bmatrix} &= \begin{bmatrix} 1 & 0 & -\sin(\theta) \\ 0 & \cos(\varphi) & \cos(\theta)\sin(\varphi) \\ 0 & -\sin(\varphi) & \cos(\theta)\cos(\varphi) \end{bmatrix}^{-1} \begin{bmatrix} \omega_x \\ \omega_y \\ \omega_z \end{bmatrix} \\ &= \begin{bmatrix} 1 & \sin(\varphi)\tan(\theta) & \cos(\varphi)\tan(\theta) \\ 0 & \cos(\varphi) & -\sin(\varphi) \\ 0 & \frac{\sin(\varphi)}{\cos(\theta)} & \frac{\cos(\varphi)}{\cos(\theta)} \end{bmatrix} \begin{bmatrix} \omega_x \\ \omega_y \\ \omega_z \end{bmatrix}.\end{aligned} \tag{3.5}$$

3.2.4 Modeling Acceleration of a Car

A vehicle experiences accelerations in longitudinal (x), lateral (y) and vertical (z) directions when driving. The on board IMU measures these accelerations. As mentioned in section 2.2.1, the accelerometer does not solely measure the linear acceleration of the car, e.g. $\dot{v}_x$, but is also affected by other accelerations. Similar to [16], [37] and [38] it is assumed that the measured acceleration can be modelled as in equation (3.6).

$$\boldsymbol{a_{meas}} = \dot{\boldsymbol{v}} + \boldsymbol{\omega} \times \boldsymbol{v} + \boldsymbol{g} = \begin{bmatrix} \dot{v}_x \\ \dot{v}_y \\ \dot{v}_z \end{bmatrix} + \begin{bmatrix} \omega_z v_y - \omega_y v_z \\ \omega_x v_z - \omega_z v_x \\ \omega_y v_x - \omega_x v_y \end{bmatrix} + g \begin{bmatrix} -\sin\theta \\ \cos\theta \sin\varphi \\ \cos\theta \cos\varphi \end{bmatrix} \tag{3.6}$$

The accelerations are divided into three components, linear acceleration, centripetal acceleration and gravitational acceleration. The linear acceleration is related to how fast the car is accelerating in the inertial frame denoted as $\dot{\boldsymbol{v}}$. The centripetal acceleration is induced when the car is moving and rotating at the same time. Finally, the gravity component is measured as well, e.g. when turning hard. In the inertial frame the gravity is only acting in the z-direction. As the IMU is mounted to the car, it will have the same orientation as the vehicle coordinate frame. Thus, the gravity component measured by the accelerometer in each direction can be found using the last column in the rotation matrix in equation (3.3).

For practical reasons it is seldom possible to mount the IMU at the absolute center of gravity [39]. This will introduce an additional acceleration component because of the lever arm from the center of gravity offset [38]. In this thesis it is assumed that the IMU is placed in the exact CoG of the vehicle and that the IMU is perfectly aligned with the vehicle coordinate frame. Thus the CoG-offset component is neglected. It is also assumed that the offset will cause a relatively small error in comparison with wheel slip and orientation estimation error. The correction used in [39], also utilizes the derivative of the gyroscope measurements which will introduce noise.

3.2.5 Compensating Wheel Speeds

As mentioned in section 2.2, a wheel speed sensor measures the angular velocity of a wheel. This quantity differs from the longitudinal speed at the CoG of the car which should be estimated. Therefore, these measurements need to be processed such that they can be used as observations for this state. The processing used in this thesis consists of two steps. First the wheel speeds are multiplied with the wheel radius to obtain the translational velocity in the direction of the wheel. Secondly, each individual wheel speed measurement has to be transformed to the center of gravity. For simplicity the tyre-radius is assumed to be constant. This is because the data files used are rather short, contain all-wheel slip from the beginning of the logs and that no external absolute velocity measurements signals as GPS are available which makes it hard to estimate the tyre radius.

The CoG-transformation can be made in several ways. A simplistic technique presented in [11] is used in this thesis. It is based on the assumption that if the distance from the vehicle CoG to the instantaneous center of motion is sufficiently large compared to the distance between the CoG and each wheel, then the differential curve radii can be assumed to be parallel. The transformation then uses the differential curve radii, yaw-rate, body slip angle and steering angle to correct the wheel speeds measurements according to equation (3.7). In this equation, V_{FL} is the corrected front left (FL) wheel speed measurement, $V_{\omega,FL}$ is the angular wheel speed measurement for the front left (FL) tyre multiplied with the tyre radius, b_f and b_r is the front and rear track width, l_f and l_r the distance between the CoG and the front and rear axle and δ_W the steering wheel angle. The reader is referred to [11] for the full derivation of the wheel speed compensation.

$$
\begin{aligned}
V_{FL} &= (V_{\omega,FL} + \dot{\psi}(\frac{b_f}{2} - l_f\beta))\cos(\delta_W - \beta) \\
V_{FR} &= (V_{\omega,FR} - \dot{\psi}(\frac{b_f}{2} + l_f\beta))\cos(\delta_W - \beta) \\
V_{RL} &= (V_{\omega,RL} + \dot{\psi}(\frac{b_r}{2} + l_r\beta))\cos(\beta) \\
V_{RR} &= (V_{\omega,RR} - \dot{\psi}(\frac{b_r}{2} - l_r\beta))\cos(\beta)
\end{aligned}
\tag{3.7}
$$

Furthermore, as it is assumed that the lateral velocity is low, it is assumed that the body slip angle, β, is negligible. Also, for large steering angles, it has been decided to set a max-limit on the steering angle compensation to 11 degrees. For angles larger than 11 degrees the compensation is limited to the compensation for 11 degrees. The specific angle of 11 degrees does not have a great importance. This modification has been done with the idea that it is better to have a measurement related to the rotational equivalent wheel speed than to have a very distorted wheel speed measurement for large steering angles. E.g. if the car is turning sharply, the $\cos(\delta_W)$ would be very small causing the front wheel speed measurements to be overcompensated.

In Figure 3.3 the transformation of the wheel speeds are showcased. Figure 3.3a show that the non-transformed wheel speeds are differing with roughly 4% from the reference speed when the car is turning in this example. Figure 3.3b show that the wheel speeds follow the reference speed much closer after transformation. Hence showing the importance of the wheel speed correction.

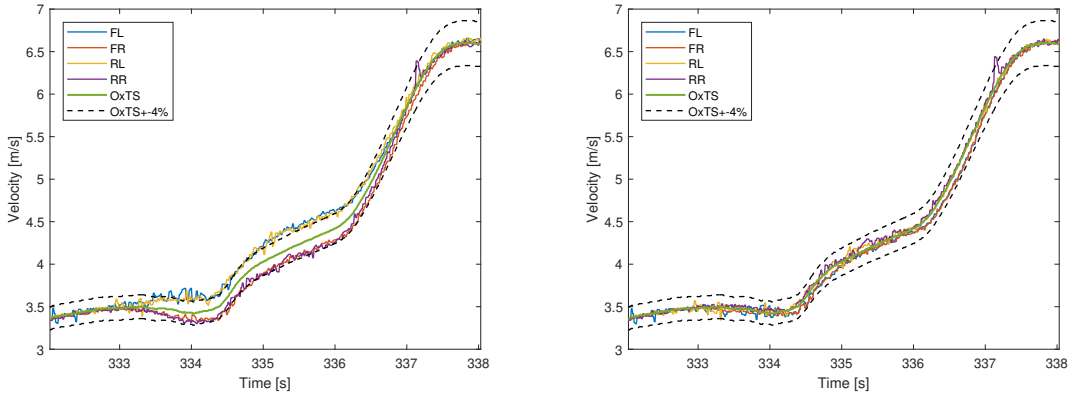

(a) Wheel speed measurements multiplied with wheel radius and OxTS measurement.

(b) Corrected and transformed wheel speed measurements and OxTS measurement.

Figure 3.3: Wheel speed measurements multiplied with wheel radius and corrected and transformed wheel speed measurements compared to reference OxTS velocity.

3.3 Sensor Characteristics

In this section the characteristics in the signals are analysed. Using data from nominal conditions (without wheel spin) and when the car is standing still, the noise characteristics of the signals can be determined. The main signals used for estimating the velocity and orientation of the car is the longitudinal accelerometer, the gyroscopes and the corrected wheel speed measurements. Each of these signals are analysed in the following subsections. Note that the lateral and vertical accelerometer is not included in this section. This is because these measurements are not used in the speed estimation which is further explained in 3.4.

3.3.1 Gyroscope and Longitudinal Accelerometer

The IMU signals were analysed for a couple of data log files when the car was standing still. Everything mentioned in this section is related to the hybrid vehicle. This is to remove all noise induced by the dynamics of the motion of the car. The files looked at are from the same sensors but from different days. This is to get a better understanding about the sensors. In the first file (case 1), the car was standing still for roughly 6 seconds before a test run. In the second file (case 2) the car was standing still for roughly 5 seconds after a test run. The variance and mean of the signals were calculated for these samples and are found in Table 3.1. As the data is logged at 100 Hz, this corresponds to roughly 500-600 data points. This is assumed to be enough to get an idea of what the characteristics in the noise is but this short time samples does not give an idea of how the sensor bias changes over time. As mentioned in section 2.2, the bias in MEMS IMU sensors vary with time and temperature. Though, most of the data logs provided were short roughly one-minute scenarios. It is assumed that the drift of the sensor bias is not severe in this short amount of time.

Table 3.1: Mean and variance for longitudinal accelerometer and gyroscopes for two cases when the vehicle was standing still.

	Case 1				Case 2			
	a_x	ω_x	ω_y	ω_z	a_x	ω_x	ω_y	ω_z
Mean	-0.87	8.67e-5	-0.32e-2	0.52e-2	-5.28e-2	8.13e-5	-0.34e-2	0.52e-2
Variance	2.32e-4	5.33e-7	6.83e-7	1.10e-6	5.31e-4	5.28e-7	9.24e7	1.11e-6

As the car is standing still, the gyroscope should be zero-mean if there are no biases. As can be seen in Table 3.1 and Figure 3.4a the signals are not zero mean. The non-zero mean for the gyroscopes indicate that there are biases in the order of up to 1e-2 for these sensors. However for the accelerometer it is not possible to distinguish any bias from the gravity component if the true orientation is not known. Using the reference pitch estimate from the OxTS it is possible to compensate for the gravity component. The OxTS measurement delivers a pitch angle measurement with an accuracy of 0.05° for one standard deviation [1]. The pitch angle was in case 1 0.066

rad and case 2 -0.0177 rad. If this is factored in, the accelerometer bias in the two cases are -0.2203 and -0.2262.

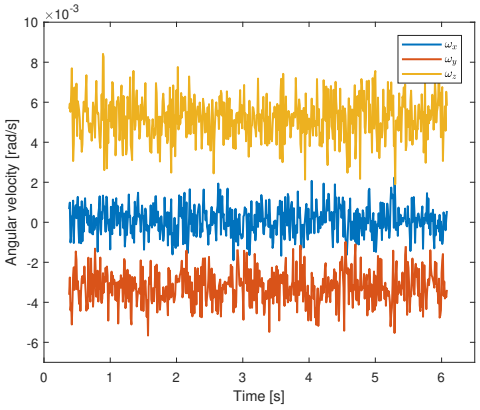

(a) Gyroscope measurements in case 1 from stationary vehicle.

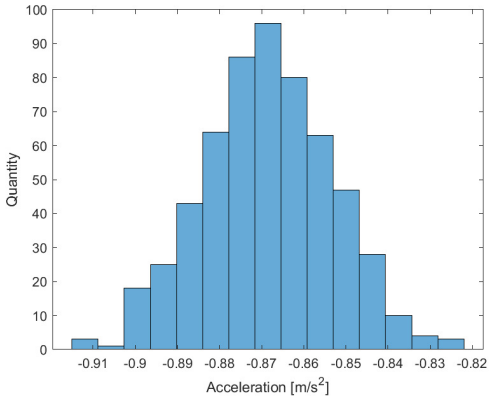

(b) Histogram of longitudinal accelerometer readings from case 1. The histogram includes roughly 500 data points.

Figure 3.4: Gyroscope measurements and histogram of longitudinal accelerometer measurements in case 1.

The noise in the of the IMU signals seems to be pretty accurately described as Gaussian. This is illustrated in Figure 3.4b where the accelerometer readings are plotted in a histogram indicating a bell-curve. Summarizing Table 3.1, the variance of the noise for the gyroscopes are in the order of 1e-6 and around 1e-3 for the accelerometer. It is observed that the biases (mean) and variances change slightly with time but the change between these two cases from different days are relatively small.

3.3.2 CoG Translated Wheel Speed Measurements

The wheel speed sensor measure the angular velocity of the wheel. As described in section 3.2.5, these measurements are translated to the CoG to represent the longitudinal speed of the vehicle. Only the corrected signal is later used in the filter. Therefore it is motivated to analyse the corrected signal. The main attribute of interest is the variance of signal in nominal conditions. This is the conditions when the wheel is not slipping and the measurements can be used to update the speed of the car.

When the car is standing still, the wheel speed sensors does not produce a noise as with the IMU. Instead a constant 0 is output as a consequence of the tachometer. This makes the characterization slightly trickier. The variance of the wheel speed signal was evaluated using two techniques. First, a short section of a nominal log file where the speed is constant was used to calculate the variance of each individual wheels. As the data logs was very sparse on this data, only very short sections was found as can be seen in Figure 3.5a. Secondly, the difference between the corrected

wheel speeds and the reference velocity was used to calculate the variance of the signal. The idea is that during nominal conditions, the wheel speed measurements should relatively accurately measure the true speed which in this case is represented by the OxTS measurement. In Figure 3.5b a histogram for the residual between the corrected wheel speed and the OxTS measurement is plotted for roughly 20 seconds of data corresponding to 2000 data points. The distribution is well represented by a Gaussian distribution as indicated with the red bell-curve.

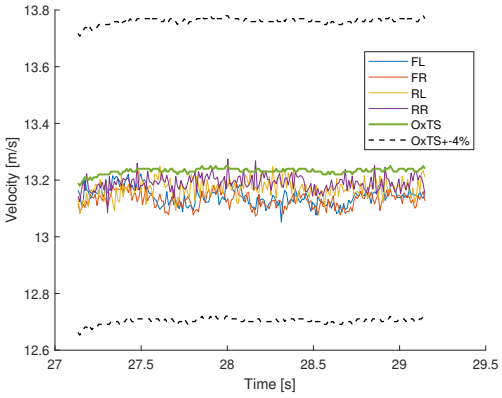

(a) Corrected wheel speed measurements and OxTS measurement during constant speed.

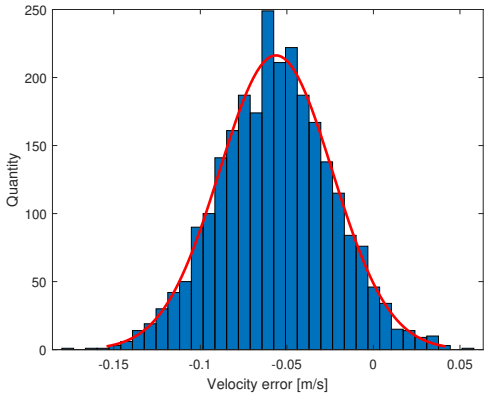

(b) Histogram of velocity error between measured speed and OxTS. The red curve show that a normal distribution is a good fit for the noise.

Figure 3.5: Corrected wheel speed measurements and histogram of residual of corrected wheel speed and reference OxTS velocity.

The variance was calculated for all four wheels using both techniques. The result, presented in Table 3.2, points at that the variance in the corrected wheel speed measurements is in the order of 1e-3.

Table 3.2: Variance of corrected wheel speed measurements in nominal conditions using two different techniques.

	Technique 1				Technique 2			
	FL	FR	RL	RR	FL	FR	RL	RR
Variance	0.95e-3	0.66e-3	1.03e-3	0.69e-3	1.12e-3	1.11e-3	0.74e-3	1.11e-3

3.4 Filter Base

The filter is the backbone of the velocity estimation. In this tool, the motion of the vehicle is modelled and measurements from wheel speed sensors and IMU are fused in order to produce an estimate of the states. An extended Kalman filter (EKF) was used for this purpose. In the following section the kinematic equations used in the

filter are described. Then three variations of the filter with slight variations of the states are set up. The three variations are set up and tested to see if there are any indication that some state combinations produce significantly better estimate.

In this thesis, the goal is to estimate the longitudinal speed, mainly in cases with low lateral acceleration and velocity. This allows for simplifications in the modelling of the vehicle. It is assumed that the lateral acceleration/velocity and vertical acceleration/velocity are low. Therefore these states are disregarded in the filter. The lateral and vertical velocities are also challenging to estimate in this case as they are not directly measured. By reducing the number of states, the filter also gets computationally lighter and has fewer parameters to tune. Though, only modeling the longitudinal dynamics will have an impact of the filter performance in conditions where the assumptions do not hold.

In the accelerometer model presented in equation (3.6), only the equation that describes the longitudinal acceleration, a_x, will be considered. Furthermore the centripetal force will be excluded from this model as the components $\omega_x v_z$, $\omega_z v_y$ are assumed to be negligible. The Euler pitch angle, θ, which includes both the road inclination and chassis pitch angle, needs to be estimated to compensate for the gravity component. Thus, at least v_x and θ needs to be a state in the filter. The gyroscope measures the angular rate of change of the vehicle orientation which is related to the Euler angular rates according to equation (3.5). The change in orientation (Euler angles) can be obtained by integrating the Euler angle rates. This information is then used in the filters to achieve a better estimate the orientation of the vehicle.

As a result of the Euler angular rate translation, it can be seen in equation (3.8) that the Euler pitch-rate is dependent on the Euler roll angle and that the Euler roll-rate is dependent on both Euler pitch and roll angle. As the Euler pitch-rate depends on both the Euler roll and pitch angle, the Euler roll angle should also be included as a state. Alternatively, it could be argued that the Euler roll angle for the most part is small in low lateral acceleration scenarios and that $\sin(\theta) \sim 0$ for small angles. Then the Euler roll angle could be assumed to be fixed to 0 and removed as a state. The kinematics of the vehicle can thus be summarized with the following equations.

$$\begin{aligned} \dot{v}_x &= a_x + g\sin(\theta) \\ \dot{\varphi} &= \omega_x + \sin(\varphi)\tan(\theta)\omega_y + \cos(\varphi)\tan(\theta)\omega_z \\ \dot{\theta} &= \cos(\varphi)\omega_y - \sin(\varphi)\omega_z \end{aligned} \tag{3.8}$$

As described in section 3.2.5, the wheel speed measurements are pre-processed before they are input to the filters. This processing consists of converting the angular velocity to linear velocity and transforming the speeds to the center of gravity. The transformed quantity is then treated as a direct measurement of the longitudinal speed.

The filter can be set up in many configurations varying the states, inputs and mea-

surements. Based on the equations in 3.8 three filters were set up and tested to see if there are any indications of which states need to be modelled. The filters were for simplicity named by the states they use. That is V_xP, V_xRP and $V_x\dot{V}_xP$. All filters have joint orientation and speed estimation combined. This is because the states are related and it is assumed that combining the estimations will have positive effects on the estimate as there will be cross-correlation that adjust the estimates. Specifically, this means that the Euler pitch angle will partly be estimated based on the integration of the Euler pitch rate, partly corrected in the gravity compensation equation which is related to the speed and acceleration. Alternatively, the orientation and velocity estimation could be done separately in two filters. The kinematic equations (3.8) are discretized using the forward Euler method.

3.4.1 Filter V_xP

In this filter only the longitudinal velocity, v_x, and the Euler pitch angle, θ, is considered as states. The Euler roll angle, φ, is assumed to be small and is neglected. The acceleration is not modelled as a state but is together with the pitch-rate input to the filter in the prediction step. This limits the filtering of the acceleration measurement but reduces the delay in the measurement as the measurement update is not lagging one step behind. The noise of the gravity corrected acceleration measurement is assumed to be white and zero mean which would cancel out when integrated over time. The process model equations for filter V_xP is presented in equation (3.9) and the Jacobian in equation (3.10).

$$\begin{aligned} v_{xk+1} &= v_{xk} + T_s\left(a_{xk+1} + g\sin(\theta_k)\right) \\ \theta_{k+1} &= \theta_k + T_s\omega_{y_{k+1}} \end{aligned} \tag{3.9}$$

$$\boldsymbol{F} = \begin{bmatrix} 1 & T_s g\cos(\theta_k) \\ 0 & 1 \end{bmatrix} \tag{3.10}$$

The wheel speed measurements are used in the measurement update. As this is considered a direct measurement of the longitudinal speed the update is linear. The measurement matrix for one wheel measurement, $\boldsymbol{H}$, is presented in equation (3.11). If several measurements of the wheel speeds are used, multiple measurement matrices can be stacked on top of each other.

$$\boldsymbol{H} = \begin{bmatrix} 1 & 0 \end{bmatrix} \tag{3.11}$$

3.4.2 Filter V_xRP

The filter V_xRP differ from V_xP in that the roll angle, φ, is included as a state. As the lateral velocity and acceleration is not modelled, the idea is that the roll angle can be used to compensate the pitch estimate for lateral dynamics. This should improve the estimate as these dynamics are modelled. Though, the Euler roll angle is not directly measured or directly related to the velocity as with the pitch angle.

This might be make the estimate offset at times which in turn would have an effect on the other states. The process model equations for the filter are presented in equation (3.12) and the Jacobian in equation (3.13).

$$\begin{aligned} v_{xk+1} &= v_{xk} + T_s\left(a_{xk+1} + g\sin(\theta_k)\right) \\ \varphi_{k+1} &= \varphi_k + T_s\left(\omega_{xk+1} + \sin(\varphi_k)\tan(\theta_k)\omega_{y_{k+1}} + \cos(\varphi_k)\tan(\theta_k)\omega_{zk+1}\right) \\ \theta_{k+1} &= \theta_k + T_s\left(\cos(\varphi_k)\omega_{y_{k+1}} - \sin(\varphi)\omega_{zk+1}\right) \end{aligned} \tag{3.12}$$

$$\boldsymbol{F} = \begin{bmatrix} 1 & 0 & T_s g\cos(\theta_k) \\ 0 & T_s\left(\omega_{y_{k+1}}\cos(\varphi_k)\tan(\theta_k) - \omega_{zk+1}\tan(\theta_k)\sin(\varphi_k)\right) + 1 & T_s\frac{\left(\omega_{zk+1}\cos(\varphi_k) + \omega_{y_{k+1}}\sin(\varphi_k)\right)}{\cos(\theta_k)^2} \\ 0 & -T_s\left(\omega_{zk+1}\cos(\varphi_k) + \omega_{y_{k+1}}\sin(\varphi_k)\right) & 1 \end{bmatrix} \tag{3.13}$$

As for the filter V_xP, the measurement model is linear and the measurement matrix for one wheel speed measurement is described by equation (3.14).

$$\boldsymbol{H} = \begin{bmatrix} 1 & 0 & 0 \end{bmatrix} \tag{3.14}$$

3.4.3 Filter $V_x\dot{V}_xP$

The third filter, $V_x\dot{V}_xP$, disregards the roll motion but models the linear acceleration, $\dot{v}_x$, as a state. In this configuration, the acceleration, a_x, is not input in the prediction step but is instead used as a measurement in the update step. In the prediction step the acceleration is modelled as a slowly varying Gaussian process. With this setup, the acceleration measurement will be filtered before it is integrated in the prediction step. Depending on the tuning of the filter, the filtering properties of the Kalman filter will make the linear acceleration state have a slight lag as it is filtered. Compared to the other filters this might affect velocity estimation during dead-reckoning as the acceleration is not input directly in the prediction step and runs with a slight delay. The process model equations are described in equation (3.15) and the prediction step is in fact linear for this filter. The state transition matrix, $\boldsymbol{A}$, is presented in equation (3.16).

$$\begin{aligned} v_{x_{k+1}} &= v_{x_k} + T_s\dot{v}_{x_k} \\ \dot{v}_{k+1} &= \dot{v}_{xk} \\ \theta_{k+1} &= \theta_k + T_s\omega_{y_{k+1}} \end{aligned} \tag{3.15}$$

$$\boldsymbol{A} = \begin{bmatrix} 1 & T_s & 0 \\ 0 & 1 & 0 \\ 0 & 0 & 1 \end{bmatrix} \tag{3.16}$$

The measurement update for this filter is non-linear with the measurement model equations presented in equation (3.17).

$$\begin{aligned} v_{whlk+1} &= v_{xk} \\ a_{xk+1} &= \dot{v}_{xk} - g\sin(\theta_k) \end{aligned} \tag{3.17}$$

The Jacobian for a single wheel speed measurement and accelerometer update is presented in equation (3.18). Based on the number of wheel speed measurements, the first row in the matrix can be repeated accordingly.

$$\boldsymbol{H} = \begin{bmatrix} 1 & 0 & 0 \\ 0 & 1 & -g\cos(\theta_k), \end{bmatrix} \tag{3.18}$$

3.4.4 Filter Tuning and Initial Conditions

A Kalman filter is tuned with the process and measurement noise covariance matrices Q and R. As mentioned in section 2.1.3, a high signal to noise ratio, $\frac{|Q|}{|R|}$, will make the filter respond quickly to changes in the measurements and a low signal to noise ratio will make the filter respond slower to changes in the measurements. The process noise matrix Q is not known and has to be tuned. The tuning is mainly made such that the speed estimate does not respond too quickly to noise or abrupt changes in the wheel speed measurements which frequently happens when driving on a slippery surface. First the measurement noise covariance, R, for the wheel speed measurements for all filters is tuned according to the measured variance in the corrected wheel speed signal presented in section 3.3.2 (roughly $1e-3$). Then process noise covariance, Q, was by trial and error tuned to a value of $6e-6$. This yields a low signal to noise ratio and the estimated speed is smoother than the wheel speed measurements but still follows the wheels speeds. The process noise covariance for the pitch and roll states are set to a low value ($1e-8$) as the input gyroscope measurements are integrated and were known to have a low variance from the measurements in section 3.3. For the $V_x\dot{V}_xP$ filter, the tuning of the noise covariance for all states is kept the same as the V_xP filter. However, the measurement covariance for the a_x has been set to achieve a slight low pass filtering effect which differ from the other filters where the accelerometer readings are input directly to the process model.

The initial prior state values for the filters has been set as the first wheel speed measurement (and first accelerometer value for $V_x\dot{V}_xP$ filter) and 0 for the orientation states. The initial prior state covariance has been set to the process noise covariance but with 10-100 times larger values. This is to describe that the initial values are uncertain and to let the filter converge to the measurements initially.

3.4.5 Handling of Offset-Biases

As mentioned in section 3.3, both gyroscope and accelerometer sensors are contaminated by a slowly varying offset bias. The online bias estimation problem is out of scope for this thesis as mentioned in section 1.4. Though, if the biases are not considered, the integration of the offset signals will introduce errors in the estimations

and greatly reduce the dead-reckoning capabilities. In this thesis a simplified bias estimation method is used where only the gyroscope bias is directly compensated for.

In the beginning of the data-log files, the vehicle is standing still for a few seconds. As a part of the pre-processing step, the mean of the gyroscope measurements are calculated for the time that the car is standing still. As the vehicle is still, it is assumed that the gyroscope measurements should be zero mean. If not, the mean is a direct measurement of the offset-bias. The calculated mean is then used to compensate all gyroscope measurements for the rest of the file. This bias estimation is only accurate for a short time-period as the offset-bias is changing with time and temperature. Though, the data log-files used are short and only contain roughly one minute of data each. Therefore it is assumed that the constant bias-estimation is a good approximation of the offset-bias. The bias estimation is also done for each log-file individually.

The longitudinal accelerometer used in the Kalman filter is also contaminated by an offset-bias. This bias is not directly compensated for as with the gyroscope. The offset-bias and the gravity-component in the accelerometer readings are not distinguishable unless the Euler pitch angle is known. Thus, the mean of the measured accelerometer does not represent what the sensor bias is. As the longitudinal acceleration is gravity compensated in the filter solely using the Euler pitch angle and that the speed and pitch-orientation estimation is made jointly, the accelerometer offset will be included in the Euler pitch-estimate according to equation (3.19).

$$\dot{v}_x = a_x + g\sin(\theta_{true}) + Bias \sim a_x + g\sin(\theta_{true} + \theta_{bias}) \sim a_x + g\sin(\theta_{est}) \quad (3.19)$$

This works because firstly the joint estimation of Euler pitch and velocity introduces cross-correlations in the Kalman gain thus making the wheel speed update influence the Euler pitch angle estimate, secondly the gyroscopes are bias compensated such that the integration of the Euler pitch and roll rates does not drift as fast as when not compensated. The filter needs some time with updates before the Euler pitch angle estimate converges to the offset angle estimate that includes the accelerometer bias. This means that the Euler pitch estimate is offset and does not accurately describe the true pitch angle, but it is only used for compensation of the longitudinal accelerometer in the filter. It is only the longitudinal speed that is the quantity of interest to accurately estimate. With this setup, the offset-bias of the accelerometer is indirectly compensated for which improves the dead-reckoning capabilities.

3.4.6 About Dead-Reckoning

Assuming that all wheels slip severely, the wheel speed measurements cannot be trusted and speed estimate needs to be entirely based on dead-reckoning. In these situations, the accuracy in the speed estimate is highly dependent on the dead-reckoning process which in turn is dependent on several factors. The main factors

are the initial offsets in the state estimates and the errors in the quantities that are being integrated. In the case of dead-reckoning, the speed estimate is based on the gravity-compensated accelerometer measurements where the gravity compensation is in turn based on the Euler pitch estimate which during dead-reckoning completely relies on dead-reckoning of the gyroscope measurements. The chain of the dependent states are apparent.

Assuming that the fixed gyroscope compensation is valid, i.e. that the initial bias has not drifted, and that the vehicle is in nominal conditions where the Euler pitch has converged to an angle which includes the accelerometer bias as mentioned in section 3.4.5, then the current state estimates are good for providing dead-reckoning performance. However, if the filter is fed wheel speed measurements from a slipping tyre, the state estimates will soon degrade. An initial offset in the speed estimate is not the main concern with the current filter setup (unless it is very large). This is because when dead-reckoning, the danger is that an offset occurs in the integrated quantity, i.e. the error in the corrected acceleration. The initial speed offset can limit how long the dead-reckoning can be sustained before the process drifts outside a certain error limit. However, the offset in the integrated acceleration builds up an additive speed error where the speed in the error build up, i.e. the drift-rate, depends on how large the offset is. Thus, to achieve a good dead-reckoning process, the initial detection of slip becomes crucial.

3.4.7 Comment on Acceleration Estimate

In section 3.5 it is mentioned that the difference between the wheel acceleration and vehicle acceleration is used as an indicator of slip. In section 3.1 it is mentioned that a weight is assigned to the fastest or slowest wheel speed measurement based on if the vehicle is accelerating or decelerating. However, as the acceleration is not a state in two of the filters presented, the acceleration is not an available quantity. The linear vehicle acceleration is therefore calculated in an alternative way. As the wheel acceleration and vehicle acceleration is compared, the quantities should have the same phase such that there's not a delay in between the signals. The wheel acceleration is calculated by low-pass-filtering the numerical derivative of the wheel speed measurements. Therefore, the vehicle acceleration is calculated by low-pass-filtering the accelerometer measurements and then gravity-compensating this with the calculated Euler pitch estimate.

3.5 Ways to Detect Positive Slip

In order to make a slip detection system it is important to be able to accurately distinguish whether the wheels are slipping or free-rolling. Therefore an investigation has been made to identify and break down different indicators of slip using the available signals. Practically, it turns out that it is a hard problem to deterministically detect slip. The difficulties do not only lie in detecting the initial slipping of the wheel but also being able to track the continuous slipping over time and when the wheels come back to free rolling. In the search for indicators of slip, the goal

of keeping the speed estimate within ±4% of the true speed has shaped the investigative process. E.g. with this condition, trusting a wheel that is slipping with one or two percent would not be needed to be detected as slip as the measurement is within the limits but the wheel is still slipping.

If we start by breaking down what's happening with the wheel. The wheel itself has a direction of heading, angular speed, angular acceleration and higher order angular dynamics. Slip can be defined as when there is a speed difference between the linear speed of the wheel and the vehicles speed relative the ground at the road-tyre contact point. If the linear speed of the wheel is higher than the car, the tyre spins (positive slip), and if it is lower the tyre might lock (negative slip). At the point of slip the friction between the tyre and ground surface cannot hold the force applied to the tyre which can be either powertrain or brake torque. In Figure 3.6a a simplified model of the wheel is illustrated with the mentioned quantities marked. In the following sections different indicators of positive slip that were identified and investigated are presented and discussed. This quantity is only used in acceleration comparison and to determine if the vehicle is accelerating or decelerating.

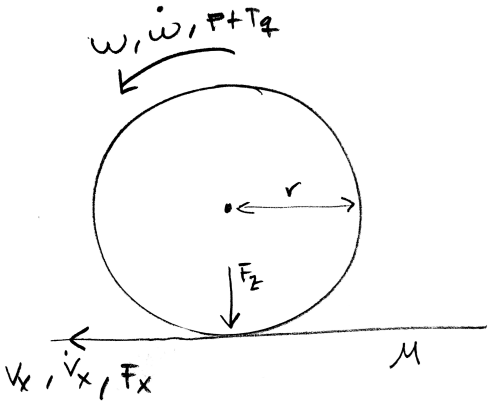

(a) Simple model of a wheel.

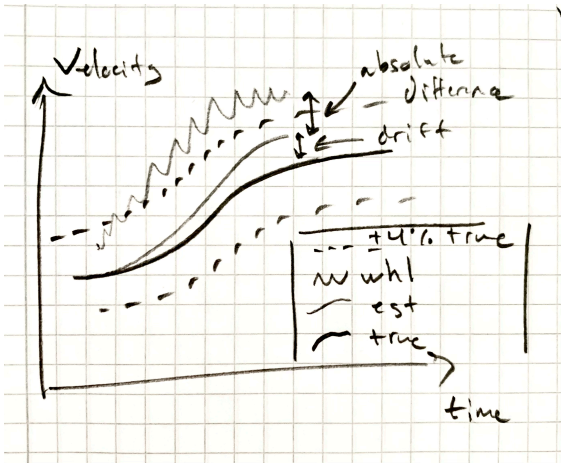

(b) Example of drift and speed difference between slipping wheel and drifted estimated speed.

Figure 3.6: Simple model of wheel (a) and example of drifted speed estimate in slip scenario (b).

3.5.1 Wheel Speed

The wheel speed measurement on its own is not sufficient to detect if the wheel slips. E.g. the measurement 10 m/s doesn't provide enough information to tell if the wheel is slipping. However, if the true speed of the car is known it is possible to calculate the absolute difference or the relative difference between the wheel speed and true speed, also known as the slip ratio. Theoretically, the slip ratio could be used to accurately determine how much the wheel is slipping. The problem lies in that the true speed is not known and is estimated online. The wheel speed and

speed estimate comparison is highly dependent on that the current speed estimation is accurately representing the true speed of the car. This is something that is hard to guarantee in severe all-wheel slip conditions.

As mentioned in the section 3.4.6 the dead-reckoning process is mainly affected by the initial offsets of the states and the errors in the states that are integrated. In the case of good initial slip detection and a relatively short slip the dead-reckoning process should provide a good estimate of the speed. Then the difference between wheel speed and estimated speed should be fairly accurate. If the speed estimate on the other hand has drifted from the true speed (e.g. by late slip detection or drift in dead-reckoning), the slip ratio will not be accurately representing how much the wheel is slipping. This is illustrated in Figure 3.6b.

For example, if the current estimate has drifted to 3% slower than the true speed and the current wheel speed measurement is 2% faster than the true speed. The difference in terms of true speed would be 5% and slightly higher compared to the current estimate. In this case it would be hard to know that the wheel speed measurement has a better estimate than the current estimation. Another example is when the estimate drift to 3% above the true speed and the wheels slip by 5%. Now the difference is only 2% in terms of the true speed, but the wheel speed measurement is outside the 4% limit. This makes it very hard to tell whether the measurement is good or not when compared to the current estimate.

Another point in regards of using the speed difference or slip ratio as a hard threshold is that it might lead to a critical flaw. Assume that a threshold is set such that the difference between the current estimate and the wheel speed measurement needs to be within a certain limit in order for the filter to trust the wheel speed measurement. If the estimate by some reason drifts far enough, the criteria would never be fulfilled and thus an infinite loop is created where no wheel is trusted and the estimate drift further away.

3.5.2 Wheel Acceleration

The wheel acceleration can be used on its own to detect slip. By using knowledge about the physical limitations of the vehicle it is possible to rule out unreasonable measurements of the car. E.g. if a car cannot accelerate/decelerate with more than $\pm$ 1g then the tyre can be assumed slipping if it has higher acceleration. A problem with a threshold like this is that it is fairly limited to extreme slip situations where the wheel rapidly looses traction. This is not always the case as the wheel might slowly lose traction and increase the slip. Instead, if the longitudinal acceleration of the vehicle is known, a threshold could be set to relate the acceleration of the car and the wheels. This way, it is possible to more accurately detect when the wheels slip as the acceleration limit can be set with a narrower limit. This threshold would activate faster than the one relating to the max theoretical acceleration as the current acceleration is known.

It's important to emphasize that depending on the tuning of the acceleration difference threshold, the threshold might activate even though the wheel is not slipping. It could be that the current acceleration of the wheel is momentarily higher than the car because of noise in the measurements or that the wheel for a short time accelerates faster than the car because it previously was slower for some reason. Though, the acceleration difference threshold does give an indication that the wheel speed is changing relative the vehicle speed which is an early indication of that wheel might be slipping. Therefore it might be advantageous to have a relatively low threshold such that indications of slip can be detected early.

Another problem with using acceleration as a slip detection is that in a slip-situation, the wheel is not accelerating at all times. Initially in an slip-event the acceleration might be high, but after some time the wheel speed tends to "hover" above the true speed but it is still slipping, see Figure 3.7a. Around this point, the acceleration is rather low and might coincide with the acceleration of the car, making the threshold inactive illustrated in Figure 3.7b. Therefore it is hard to track the wheel slip only based on this threshold.

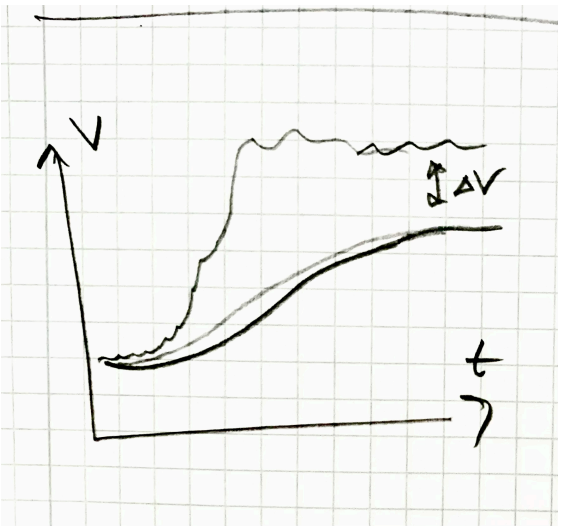

(a) Example of acceleration scenario, velocity plot. The wheel speed (upper graph) increases faster (higher acceleration) than the true speed (lower graph). After some time the speed difference is constant meaning that the wheel is still slipping but the acceleration difference is low.

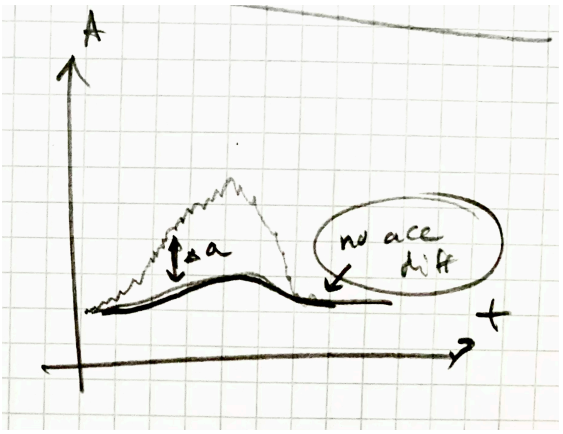

(b) Example of acceleration scenario, acceleration plot. The wheel speed (upper graph) increases faster (higher acceleration) than the true speed (lower graph). After some time the speed difference is constant meaning that the wheel is still slipping but the acceleration difference is low.

Figure 3.7: Example of wheel slip with initial acceleration difference between wheel and vehicle and which ends with a constant offset-slip.

Theoretically, higher order of wheel angular dynamics could be used to determine the state of the wheel. The second derivative of the velocity could e.g. be used to detect when the acceleration is increasing and decreasing. This information might be tricky to accurately calculate as the wheel speeds are rather noisy and derivation of the higher dynamic quantities introduces noise. The derivatives could for example be estimated by modelling the wheel as a higher order Taylor expansion in a Kalman filter. Though this was not further investigated in this thesis.

3.5.3 Powertrain Torque

The data logs from the test cars included powertrain torque signals for front and rear axle. These signals provide information about how the wheels are propelled and can also indicate when certain events as slip occur. The characteristics in torque signals from combustion and electric engines differ. An electric engine has a quicker torque response in comparison to a combustion engine. This is a result of the internal inertia of the engine and lag in the combustion. In the following section two ways of utilizing the powertrain torque for detection of slip are presented.

Max Torque Estimation

At the point of excessive all wheel slip, all tyres are saturated meaning that the tyres utilize all available friction. According to equation (3.20), the propelling force of the vehicle, F_x, is equal to the normal force for all wheels, F_z, times the friction μ. Thus, the maximum utilized friction for the car or the average friction for each wheel can be calculated according to equation (3.21) where M is the total weight of the vehicle.

$$F_x = M\dot{v}_x \leq Mg\mu = F_z\mu \tag{3.20}$$

$$\mu = \frac{a_x}{g} \tag{3.21}$$

As described in [13], the maximum utilized friction estimate can be used to estimate the theoretical maximum torque that can be applied for the rear axle which in turns can be compared to the measured powertrain torque. This can then be used indicate when the wheel is likely to slip as more torque is applied than can be supported by the friction. The the theoretical maximum torque can be estimated with the max utilized friction estimate, the axle load and the wheel radius according to equation (3.22). The longitudinal load transfer needs to be included in the axle load.

$$T_{max} = F_{z,axle}\mu r_{wheel}, \tag{3.22}$$

When testing this criteria, it was found that the indicator is somewhat inconsistent for the larger hybrid vehicle. In cases with clear severe excessive slip, as shown in Figure 3.8b, the criteria could provide a good indication that the wheels are slipping as the applied powertrain torque exceeds the estimated max torque. In other cases when not all wheels are slipping at the same time, the criteria was sometimes activated, sometimes it did not. Theoretically, if the friction was known for each wheel the criteria could be used on individual level by taking the current load transfer into account. Though, as the powertrain torque is provided per axle, in this thesis the criteria was only looked at per axle.

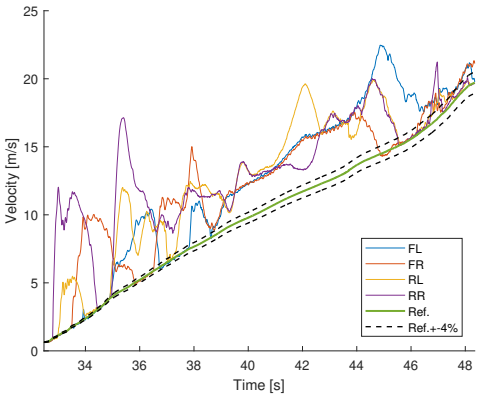

(a) Wheel speeds and reference speed in an excessive all wheel slip scenario.

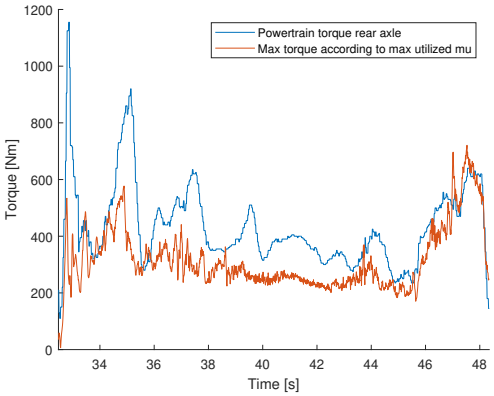

(b) Example where applied powertrain torque on rear axle exceeds the estimated max torque.

Figure 3.8: Example of max powertrain torque estimation criteria.

Powertrain Torque Rate

When investigating the powertrain torque signals it was found that before the wheels slipped, the torque tended to increase rapidly. This can alternatively be expressed as that before the wheel slip the powertrain torque rate tended to be high. In Figure 3.9 the phenomenon is shown. It is believed that when the tyre starts to slip, the torque applied exceeds what can be sustained by the friction. The torque peaks were found to align well with when slip occurred for the hybrid vehicle data logs. However, it could be that the peaks are a result of how the vehicle was driven and that the peaks actually is a result of that the throttle was increased rapidly to induce slip.

It was also found that when the wheels was in slip and the powertrain torque rate was very low, i.e. the torque dropped fast, the wheels tended to return to free-rolling. This phenomena is also showed in Figure 3.9. It is believed that when the torque drops fast, the wheels are not propelled as much by the engine and thus the wheels should be allowed to come back to free-rolling. It could also be that some system activates when the throttle is let go.

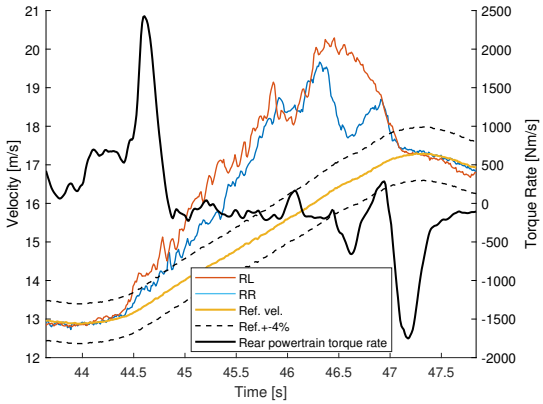

Figure 3.9: Rear powertrain torque rate for an excessive wheel slip example. A clear peak is visible in beginning of the slip-event and a dip is visible in the end of the slip-event.

However, the torque-rate indicator is prone to errors in that for example the torque rate could be high when the vehicle accelerates hard in nominal conditions even though the wheels does not slip. This could be ruled out by combining this criteria with another criteria as for example looking at the wheel acceleration as mentioned earlier. Also, in the case of the wheels returning from slip while the torque is not significantly dropped the rapid torque drop criteria would not detect that the wheels are back.

3.5.4 Relating Wheel Speeds and Estimate Over Time

Variance of Residual of Estimated Speed and Wheel Speeds

It was found that based on the characteristics of the difference between the estimated speed and the measured speed it is possible to get indications on whether the wheels are slipping or not. When a wheel is not slipping it provides relatively accurate measurements of the true speed in terms of noise and absolute speed, assuming that the radius is known and that the wheel speeds are corrected for turning of the vehicle. However when slipping, the measurements gets noisier and drift away from the true speed. By observing the speed difference between the true speed and the measured wheel speed over time it is possible to see how much the error is changing. As the exact amount of drift in the current speed estimate at a given point is not known, the absolute and relative speed difference might not give a good indication if the wheel is slipping or not, as mentioned in section 3.5.1. Therefore a measurement of how much the speed difference is changing is to calculate the variance of the error for some past time instances. When the wheel is not slipping, the variance is low and when the wheel is slipping the variance is higher as the wheel speed measurement is nosier and the speed is changing. This principle was found to be applicable to the estimated speed as well. This is because the filter is tuned such that the estimated speed is to a large extent is based on the integration of accelerometer making the estimate not quickly respond to the noise in the wheel speed measurements, as

explained in section 3.4.4. In Figure 3.10 an example of this is shown.

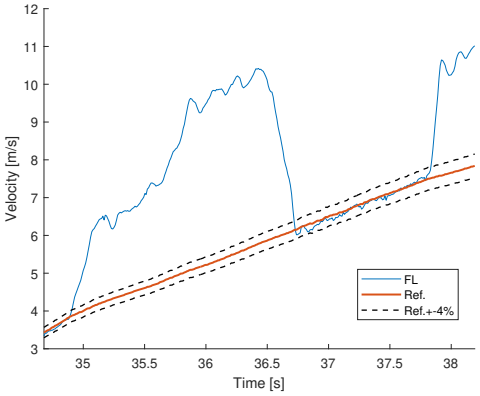

(a) Example of slipping front left wheel and reference speed. Prior to 35 seconds and around second 37, it can be seen that the wheel is not slipping.

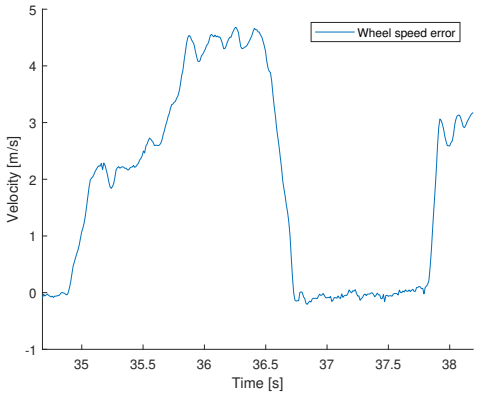

(b) Speed difference between the true speed and wheel speed.

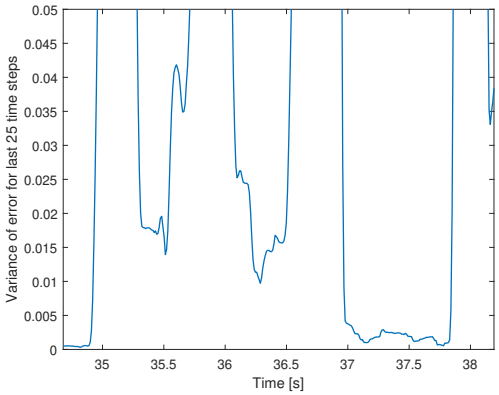

(c) Variance of the speed difference. It can be seen that the variance is lower before 35 seconds and around 37 seconds when the wheel is not slipping.

Figure 3.10: Example of how the variance of the speed difference can be used to indicate slip.

This indicator of slip might as well as the previous presented indicators fail to detect slip at times. Depending on how the residual evolves over time the criteria might falsely deactivate. For example situations where the wheel speeds slowly drift away from the true speed, the error variance could be low. Or if the wheels slip with a constant velocity offset to the true speed, then the error variance could also be low. The size of the interval for the residual plays a role for how the indicator detects slip. A short interval would make the indicator be able to detect when the variance is low faster with an increased risk of the variance being low for the short amount of data. Conversely, a long interval would make the unnecessarily response slow. However, these flaws could possibly be corrected for by additional slip indicators.

Variance Between Wheel Speed Measurements

Another indicator of slip was found looking at the the differences of the individual wheel speed measurements. In nominal conditions the wheel speed measurements provide similar measurements that are closely related to the true speed. When one or several wheels are slipping, the difference between the wheel speed measurements for the given time becomes relatively large. By looking at how the variance of the wheel speed measurements evolve over time it is possible to identify when all wheels are back at traction. In Figure 3.11 an example is shown. In the beginning and end of the example, the wheels are not slipping. At those points the variance between all wheel speed measurements are relatively low for some time. If the variance is observed to be low for some time interval, the wheels can be assumed to be not slipping. Theoretically, if all wheels slip with the same amount and with relatively low noise for a certain time instance this criteria could fail. Therefore the variance threshold should be set low and should be needed to be fulfilled for a certain amount of time before assuming that the wheels are back.

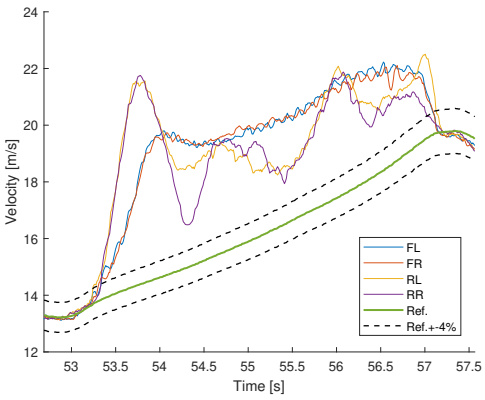

(a) Wheel speed measurements during slip and reference speed.

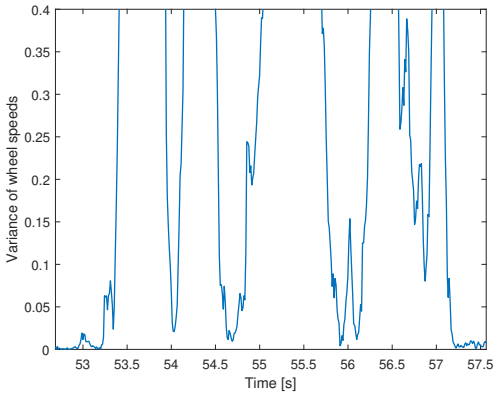

(b) Variance between the speed measurements. It can be seen that the variance between the wheel speeds is low when the wheels are not slipping.

Figure 3.11: Example of variance between the wheel speeds during slip.

3.5.5 Vehicle System Signals

In the data-log files, flags from the vehicles safety systems as TCS, ABS and yaw-stability programs was included. The flags indicate when different systems are active. The main flag that was found useful was the engine TCS for the front and rear engine. Though, it was not enough to solely rely on the flag for slip detection in that it was only activated for severe slip and that the activation of the flag was slow compared to other slip indicators mentioned in this section. In general the delay in activation was roughly up to one second when the vehicle experienced slip in acceleration. It is believed to be a result of that the system has to first detect slip and then activate before it can send out the flag which is then logged. The main

application for the TCS signal was found to be an alternative view of the current state of the vehicle. If the TCS is activated, probably the wheels are slipping.

3.5.6 Summary of Ways to Detect Slip

To summarize, several different indicators of slip were investigated and presented, see point-list below. When analysing the indicators one by one it becomes apparent that it is hard to find a single indicator or threshold that solely can be used to detect whether a wheel is slipping or not. Therefore several indicators need to be combined and assumptions to be made in order to successfully detect and isolate the wheels during a slip-event. One way of looking at this is to divide the slip-event into three stages, identification of initial slip, continuous tracking of the slip and identification of when the wheels come back. In section 3.6 two concepts for estimating the speed and detecting slip are presented. These concepts utilize the indicators presented in this chapter and uses some further logic and assumptions to identify slipping wheels.

- Slip ratio
- Wheel acceleration
- Acceleration difference between wheel and vehicle
- Max torque estimation
- Powertrain torque rate
- Variance of residual of estimated speed and wheel speeds
- Variance between wheel speed measurements
- Vehicle system flags (Engine TCS)

3.6 Slip Detection and Wheel Selection Concepts

A slip detection system could be set up in very many ways combining different methods, logic and indicators of slip. Based on the different indicators of slip discussed in section 3.5, two concepts for detecting slip and selecting which wheels to feed the filter with have been constructed. The two concepts presented in this section are two possible ways of how a slip detection system could be set up. The concepts are specifically made for detecting positive slip. Concept 1 was developed first out of the two. It is based on assuming slip between certain events occurring. Concept 2 is instead completely based on detecting slip at every time instance and does not lock a slip assumption based on different events.

3.6.1 Concept 1

Concept 1 has been developed with the idea of detecting slip individually on each wheel and then feeding the wheel speed measurements related to all wheels that are not detected to slip to the filter. The concept is based on deterministically assuming that a wheel is slipping in between certain slip-indicators are activated. In section 3.5 different indicators of slip were discussed and presented. It was observed that a high powertrain torque rate (sudden increase increase of torque) could be seen as an indicator of slip. With slip detection concept 1 this is assumed to be true and set as the base principle for detection of slip. Though, as the powertrain torque is supplied per axle this indicator is not enough to determine on each wheel individually whether it is slipping or not. Therefore the torque rate indicator is complemented with the indicator that monitors the difference between wheel and vehicle acceleration. With this combination of indicators it is possible to detect the initialization of a slip-event for individual wheels. When both indicators are activated within a short time-period of 0.2 seconds, a slip-flag is raised for the particular wheel. The slip flag indicates that the wheel is slipping. When the flag is raised, it can only be cleared by a set of slip-release events when the engine TCS system is not activated. Slip is also assumed if the TCS activates but the slip-flag is not activated. As mentioned in section 3.5, the TCS-flag in the logs are raised with a delay and this slip-flag activation is used a back-up if slip is not successfully detected for some reason.

The slip-release events are defined as the following events:

- High powertrain torque decrease rate
- Low torque and acceleration difference between wheel and car
- After hard braking

The first and main slip-release event is based on when a high powertrain torque decrease rate is observed. As mentioned in section 3.5 it was observed that when the powertrain torque is subject to a sudden decrease (a high decrease rate) the wheels tended to come back to free-rolling after a short delay. This was used as one of the slip-release events. When slip is released, the trust in the wheel speed measurement is faded in with a linear change of the measurement noise covariance. This is to get a smoother switch from dead-reckoning and to the trust in the wheel speed measurements.

If there was no high torque decrease rate, the slip flag would not be decreased. Therefore a second slip-release event is added to complement the first. When the powertrain torque for the axle in question is low for a certain time and the difference between the wheel acceleration and vehicle acceleration is low, it is assumed that the wheel is not slipping anymore. This is because when a low amount of torque is applied the wheel it is less likely that the wheel is slipping. To make this criteria more accurate it is combined with the acceleration difference indicator. Thus, the slip is not released if the acceleration between the car and wheel still is large.

The last slip-release-event is based on an assumption that after braking, the wheels should not be positively slipping. As the slip-detection is active at all times, it could also be activated during braking. As mentioned in section 3.1, the speed estimation strategy specifically used when braking does not depend on which wheels the slip-detection system determine as slipping. This means that any slip activation during braking doesn't affect the speed estimation. The strategy specific for braking is explain in detailed in section 3.7. However, when the vehicle has been braking for at least one second it is assumed that the wheels should not be affected by excessive slip. Thus, the slip flag is released after such an event.

During long accelerations in slippery conditions, it was found that after initially slipping, the rear wheels tended to regain traction during the acceleration when higher speed was reached. In many cases the slip flag was initially locked but remained locked throughout the acceleration as none of the slip-release-event occurred. This is partially because the torque was not dropped during the acceleration and if it was dropped the TCS might hinder the slip-release. Also, the torque level is generally not low during acceleration. To make use of the rear-wheels that regained traction, a logic was set up to detect this. The logic is set such that if there is no engine TCS activated and that the wheel have the slip flag activated for 3 seconds or more and that the acceleration difference between the wheel and vehicle is low and that the slip ratio is less than 6% then the wheel speed measurement on the particular wheel is updated with even if the slip flag is raised.

Additionally, a safety feature was added to ensure that the estimate does not drift positively by an uncontrolled amount in the case that the dead-reckoning process would fail for some reason. If the estimated speed is more than 1 m/s faster wheel speed, during all wheel slip, the slowest wheel is set to be trusted. This is supposed to work as an upper limit for the speed estimation such that the estimated speed does not provide a considerably faster speed than the slipping wheels if something in the dead-reckoning process fails.

All tuning of the thresholds was made with trial and error for some data files from the hybrid vehicle. The threshold for the front and rear powertrain torque rate for the activation of the slip flag is set to 650 Nm/s and 950 Nm/s respectively. The powertrain torque rate for the slip-release is set to -950 Nm/s and -750 Nm/s for the front and rear respectively. The levels are set differently for the the front and rear axle as they were found to have different characteristics. The threshold for the wheel and car acceleration difference was to $0.8 m/s^2$. The low-torque limit is set to 150 Nm for 0.5 seconds. At the same time as the acceleration difference is below the 0.8 for same time.

3.6.2 Concept 2

Slip detection and wheel selection concept 2 was developed after concept 1 was developed. This concept does not include any slip-lock assumptions as with concept 1. Instead the slip detection is made individually for every wheel in every time step. This allows for a more dynamic slip detection that theoretically can pick out short

sections where the wheels are not slipping and update the speed of the estimate with the detected non-slipping wheels. The main idea of the concept is to provide all wheel speed measurements to the filter if no slip is detected and if any wheel is detected slipping only the slowest of the non slipping wheels is fed to the filter. Only the slowest wheel is used to test if this is a good approach or not.

As discussed in section 3.5, during slip the acceleration of the wheels differ from the acceleration of the car. The speed of the wheels also differ from the true speed of the car which makes the variance of residual between the two larger. It's also known that during severe slip, the wheel speeds are much faster than the true vehicle speed. The slip detection of concept 2 is based on these observations. The following three indicators of slip, which are discussed individually in section 3.5, are combined in order to form a way of detecting slip throughout a slip-event.

- Variance of residual of estimated speed and wheel speeds
- High acceleration difference between wheel and car
- Slip ratio

The indicators are set up to complement one another. If any of these indicators are triggered, the wheel in question is seen as slipping. The variance of the residual indicator is the main indicator in this concept. As long as the estimated speed follows the "shape" of the true speed of the car (there's almost always an offset between the estimated speed and true speed), this indicator can detect slip of a wheel as long as the wheel speed is changing sufficiently much relative the estimated speed. The acceleration indicator can detect when the wheel is accelerating differently relative the vehicle. Thus, this indicator can complement the variance-indicator in order to correctly detect the initial identification of slip. The slip ratio is added to keep track of the relative speed error of each wheel. In the case of a wheel spinning up but then following the speed of the car with a constant offset, which was found common, then the slip ratio can be used to rule out wheel speed measurements with unreasonable high slip ratio.

When positive slip is detected on one or more wheels, the vehicle is assumed to be in a slip-situation. In these situations it is decided that only the slowest non slipping and non braking wheel should be trusted. The reason for why only the slowest wheel is trusted is because in a slip-situation, the wheels tend to be faster than the car. Thus, the slowest wheel should be the most representative speed measurement. The reason for why braking wheels are excluded is because it was found that individual wheels were braked at times which made the measurements relatively slow and sometimes not very reliable. Thus, it is tried to avoid these too slow measurements.

In the case of dead-reckoning, the estimate is sensitive to noise and offsets in the states as this can cause the estimate to drift. This will affect the estimate and also how well the indicators work. Especially the slip-ratio and the variance of the

residual indicator might be sensitive to an inaccurate speed estimation. E.g. if the dead-reckoning drifts positively for some reason, the slip-ratio might be locked indefinitely. In order to avoid indefinite-slip lock, two additional features where added. Firstly, the indicator presented in section 3.5 which monitor the variance in-between the individual wheel speed measurements over a time-period was added. The idea is that if the variance between the wheel speed measurements are very low for a certain time, it is very likely that the wheels are stable and are not slipping. When this is detected, any slip detection by the earlier mentioned indicators are overruled and it is assumed that all wheels are free-rolling. Secondly, in the case that the estimated speed is for a consecutive time period faster than any of the wheel speed measurements during an all wheel slip sequence, the slip-detection for the slowest wheel is released. This is added as a safety feature such that if something goes wrong in the dead-reckoning process the estimate does not drift away to infinity.

All tuning of the thresholds was made with trial and error. The threshold for the variance of the residual is set to 0.005 (m^2/s^2) and is calculated for the residual of the previous 0.25 seconds. The variance threshold is set relatively low and should only allow the slip-detection to trust the wheels if the residual is changing relatively little. The time interval for which the variance is calculated is important in that it determines how fast the criteria can detect slip and free-rolling. A longer interval would mean that the residual would need to be low for a relatively long time before no slip is decided. This would make it rather slow in detecting when wheels are back. On the other hand, a too short interval would make it relatively easy to indicate that the wheels are back. In turns this could make the criteria indicate no slip too fast when the wheel actually is slipping. The threshold for the wheel acceleration difference indicator is set to $0.8m/s^2$ as with concept 1. The threshold for the slip-ratio indicator was set such that slip was detected if the wheel speed measurements differed by the max of either 0.5 m/s from the current estimated speed or 4% from the estimated speed. This was because when traveling at slow speeds, naturally the relative error becomes rather large. Furthermore, the threshold for the variance in between the wheel speed measurements is set to 0.01 and the variance needs to be consecutively below this value for 0.2 seconds for the indicator to activate. The threshold of the when the estimate is faster any wheel speed was set such that it activated when the estimate is consecutively faster than any of the wheels by 1 m/s for 0.1 seconds when all wheel slips.

3.7 Speed Estimation Strategy in Braking

When braking, the wheels speeds tend to be slower than the true speed of the car. Though, unless the wheels are braked aggressively the wheels speeds still represents the true speed of the car relatively accurately as can be seen in Figure 3.12a. In hard braking the wheels tend to lock for a short amount of time. This is happens as the applied brake force exceeds the road-tyre friction. All modern cars utilizes ABS-systems when braking heavy. These systems build on the idea of keeping the tyre at the friction limit to maximize the braking force that can be applied. The ABS works in cycles where the wheel is braked until it locks and then for one or

several wheels the brake force is reduced such that the wheel momentarily comes back to free-rolling. This is so that the ABS system can update what the current speed is and make decisions on how much brake force should be applied. The ABS-cycles becomes very clear when observing the wheel speed measurements during heavy braking as shown in Figure 3.12b.

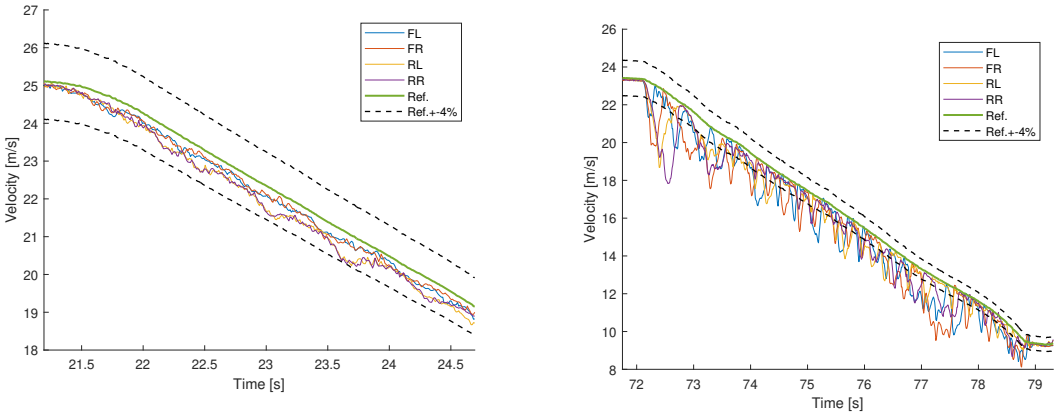

(a) Normal braking, the wheel speeds are slightly slower than the reference speed of the car.

(b) ABS-braking, the ABS-cycles are visible in the plot.

Figure 3.12: Examples of wheel speeds in normal and ABS braking

When estimating the speed of a vehicle, unreliable and faulty wheel speed measurements should be avoided. With the knowledge that the wheel speeds tend to be slower and lock when braking it was decided that a separate logic for the update step should be used in braking conditions. To successfully do this it is needed to define how to detect that the car is braking. It turned out that defining when a vehicle is braking and decelerating is not very easy. Sometimes individual wheels are braked when the car is driving to counter act slip and stabilize the car. Therefore one wheel braking is not enough to determine that the car is braking. It was found that when in slippery conditions, the amount of brake torque applied before the wheel was locked varied a lot. Sometimes a relatively low amount of brake torque could make the wheel lock. Furthermore, it was found that at the time the acceleration changed sign to negative, some wheels where already locked. With this in mind it was decided that when three or more wheels are braking (brake-torque measurement), the car is defined as actively braking.

Utilizing the knowledge that the wheel speeds tend to be slower than the true speed of the car and that the wheels tend to lock, the main idea when estimating the speed in braking is to try to keep the estimate at the peaks of the wheel speed measurements. The brake-update-logic is divided into two parts. First, when three or more wheels are detected braking, dead-reckoning is performed for 0.25 seconds. This is to not perform any measurement updates if the wheels where initially locked. This also makes it so that if there is no long braking-section the fastest wheel does not need to be updated with. Secondly, it is determined if the fastest wheel speed is

faster or slower than the current predicted speed. If the fastest wheel speed is faster than the prediction, the measurement is assigned a lower measurement covariance to make the filter trust the measurement more and bring the estimate "up" to what likely is the true speed of a free-rolling wheel. However, if the fastest wheel speed is slower than the current estimate, the measurement covariance is set higher such that the measurement is not trusted as much. This is because it is believed that the wheel is locking.

4

Results

In this chapter, the performance of the proposed filters and slip detection concepts are evaluated for the data logs from the two vehicles. First the evaluation process is described in section 4.1. Then the partition of the data and the evaluation parameters are defined in section 4.2 and 4.3. Finally, the results for the hybrid and fully electric vehicle is presented in section 4.4 and 4.5. In these sections, both quantitative tables of the performance metrics and examples and comparisons between the different filters and brake manufacturer estimate are made.

4.1 Process of Evaluating Performance

Initially, only the data logs from the hybrid vehicle were available. At a later stage of the thesis the data logs from the fully electric vehicle were made available. Therefore the evaluation for these data sets are split into two separate sections. The evaluation of the filter and slip detection combinations as well as the brake manufacturer and simplified Volvo estimates (which are based on the wheel speed sensors only) is made in two parts. In the first part of the evaluation, the estimates from the filter and slip detection combinations for the data logs is generated. Then the statistical parameters described in section 4.3 are calculated for the complete data and specifically for the sections of the data where the vehicle is experiencing positive slip and braking. The partition of the data is explained in detail in section 4.2. The statistical parameters includes metrics as the RMSE, standard deviation and the percentage of time the estimate is within the error of $\pm 4\%$ for each file. All performance numbers are put in a consolidated table to provide an overview and comparison of each method. The second part of the evaluation is to bring up examples from different logs and to analyse how the different slip-detection concepts perform and why they struggle at times. In both parts of the evaluation, the proposed filters and slip detection concepts are compared with the brake manufacturer and simplified Volvo estimate (only available for the fully electric vehicle).

As mentioned in section 3.4, three filter variations called V_xP, V_xRP and $V_x\dot{V}_xP$ were set up to investigate any indications that show if one set of states makes a better speed estimate. The filters were evaluated with slip-detection concept 1. As the slip-detection depends on the estimate and the estimate depends on the slip detection, the performance of the estimate does not only represent the filters but also how the

combination of the filters and slip detection works. This makes the performance result for each individual filter slightly ambiguous. Without anticipating events, the three filter combinations performs very similar. Therefore slip-detection concept 2 was only evaluated with the V_xRP filter as it solved most amount of the data log files out of the three filters, based on the results of the hybrid testing for the filters and slip detection concept 1. This is further discussed in section 4.4.1.

4.2 Data Description

The data for this thesis is provided by Volvo Cars from their winter testing for autonomous drive development. All data logs are recorded while driving on extremely icy and snow-packed roads with very low friction, including various maneuvers. Detailed explanation of the logged data is provided in section 1.1. In Appendix A descriptions of each individual logs are available.

4.2.1 Data Selection

To evaluate the performance of longitudinal velocity estimation methods, data logs with very high lateral motion and velocity are excluded. Also, data logs that have next to, or no wheel slip i.e. data logs where the wheel speeds can be sufficiently trusted to keep estimated velocity within the desired ±4% of the reference speed are omitted. Lastly, all performance evaluation for each data log is done for velocities above 10 km/h defined by the thesis scope in section 1.4.

4.2.2 Data Categorization

To evaluate the performance of the filter and slip detection concept in different driving scenarios, each data was categorized into three different cases. As explained above, all cases are defined for speeds above 10 km/h. These three cases are used to partition the data logs such that all data, only data in slipping or braking can be looked at separately. This way, the performance of the estimated speed can be analysed for the different parts of files separately, making it easier to see where the filter and slip detection concepts struggles.

- **Complete data:** This includes the complete driving data set from start to finish.

- **Slipping in acceleration:** Also called "spinning", this case includes the times where the wheels are slipping e.g. while the car is accelerating. To pick out these cases from the data, a slip scenario flag is created which canopies this scenario as seen in figure 4.1a. The flag switches ON 1 second before at least one wheel spins 4% faster than the reference velocity. This is done to include the beginning of slipping. The flag stays ON as long as the condition above is true and no brake torque is applied at any time.

  While the slip flag is ON, if all wheels are back i.e. less than 4% faster and

at most 1% slower than the reference velocity for 1 full second, the flag turns OFF. Allowing the wheel speed to drop to 1% slower than reference is done to avoid false flag OFF due to Electronic Stability Program (ESP) activating the brakes. Further, this 1-second delay is to allow the wheel speeds to stabilize and get back close to the reference velocity. Also, the flag will instantly turn OFF if the speeds are more than 1% slower as compared to the reference velocity or a brake torque is actively applied on 3 or more wheels.

- **Braking :** This case includes all the braking scenarios in the data. The braking scenarios consist of situations ranging from no wheel lock to all-wheel lock situations. A Brake Flag that canopies this scenario in the data observed in figure 4.1b. A driving scenario is labelled as braking if a brake torque is applied to three or more wheels. This is done to avoid false detection of braking case due to ESP interventions. The short drop in the flag between 25 and 30 seconds disregards coasting or engine braking scenario i.e. when the brake is not actively applied by the driver.

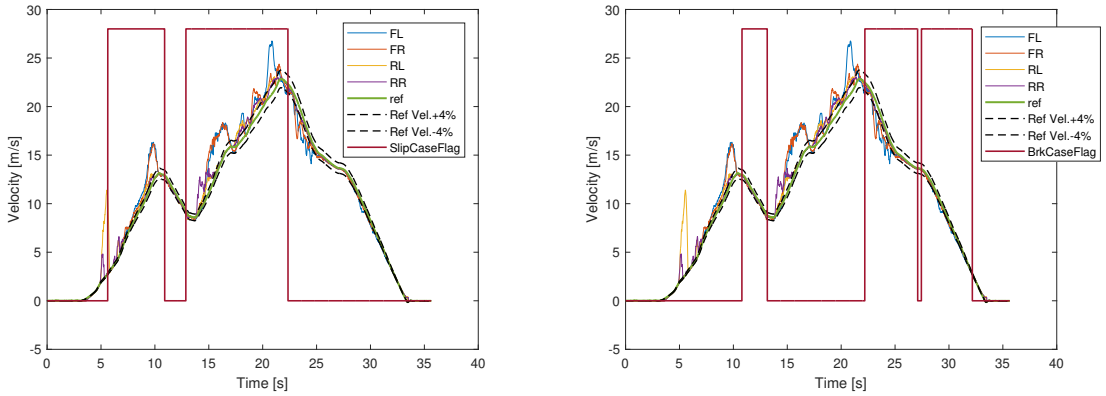

(a) Slipping in Acceleration Scenario **(b)** Braking Scenario

Figure 4.1: Data Categorized into 2 different scenarios for evaluation

4.3 Performance evaluation parameters

The performance of the estimation methods is evaluated upon reviewing a few statistical parameters for each data log in each scenario 4.2.2.

4.3.1 Amount of data log solved

This parameter gives an overall idea of how good the estimation is by looking at the amount of time it keeps the velocity within a defined accuracy range. It is defined as

$$Solved = \frac{T_{work}}{T_{tot}} \times 100 \quad \% \tag{4.1}$$

where $T_{working}$ is the amount of time the estimation is within the desired $\pm 4\%$ of the reference velocity V_{xref} and T_{tot} is the total time of the data log.

4.3.2 Root-Mean-Squared Error

Root Mean Squared Errors (RMSE) basically is the standard deviation of the estimation errors. It tells how well the estimation is concentrated around the reference or how far away the estimation errors are spread out from the reference. This parameter has been calculated to evaluate the accuracy of these estimation methods. Two kinds of RMSE were calculated which are explained subsequently.

The RMSE in absolute sense depicts the RMSE of estimation in the units of the estimated variable, which is m/s for velocity. It is calculated as :

$$RMSE = \sqrt{\frac{1}{N}\sum_{i=1}^{N}(Vx_{Ref,i} - Vx_{Est,i})^2} \tag{4.2}$$

where N is the number of data points of observed reference velocity.

RMS Relative Error or RMSRE is a parameter that helps in comparing errors produced in each estimation, however they are highly sensitive when velocities are slower. It is calculated as

$$RMSRE = \sqrt{\frac{1}{N}\sum_{i=1}^{N}\left(\frac{Vx_{Ref,i} - Vx_{Est,i}}{Vx_{Ref,i}}\right)^2} \tag{4.3}$$

where $\frac{Vx_{Ref} - Vx_{Est}}{Vx_{Ref}}$ is the relative error between the estimated and reference velocity.

4.3.3 Peak errors

Peak errors are calculated to find the peak deviation in how much slower or faster the estimated velocity is compared to the ground truth in all scenarios.

Peak Absolute Errors
Maximum absolute error gives the largest deviation in m/s between the estimated and ground truth velocity.

$$e_{max,abs} = max(Vx_{Est} - Vx_{Ref}) \tag{4.4}$$

A positive $e_{max,abs}$ depicts that the estimate is faster than the ground truth and the number gives the magnitude of how much faster it is in m/s. A negative value depicts that the estimate is never faster than the reference.

When the estimated velocity is slower, the minimum absolute error gives the largest deviation value in m/s between the estimated and ground truth velocity.

$$e_{min,abs} = min(Vx_{Est} - Vx_{Ref}) \tag{4.5}$$

A negative $e_{min,abs}$ depicts that the estimated velocity is slower than the reference velocity, while the number gives the magnitude of how much slower it is in m/s. A positive value depicts that the estimate is never slower than the reference.

Peak Relative Errors
Relative error indicates the error between the estimation and reference in %, however they are highly sensitive at lower speeds. Maximum relative error gives the relative error at the time when maximum error as defined above is reached i.e. greatest relative difference between estimated and reference velocity, when estimated velocity is faster.

$$e_{max,rel} = max\left(\frac{Vx_{Est} - Vx_{Ref}}{Vx_{Ref}}\right) \tag{4.6}$$

Minimum Relative Error indicates the relative error between the estimation and reference at the time when the minimum error as defined above is reached i.e. greatest relative difference between estimated and reference velocity when estimated velocity is slower.

$$e_{min,rel} = min\left(\frac{Vx_{Est} - Vx_{Ref}}{Vx_{Ref}}\right) \tag{4.7}$$

Standard Deviation

$$StdDev = \sqrt{\frac{1}{N}\sum_{i=1}^{N}\left(Vx_{Est} - Vx_{Ref}\right)^2} \tag{4.8}$$

4.4 Results for Hybrid Car

4.4.1 Complete Data

The amount of data solved i.e. the amount of time the estimated velocity is within ±4% of reference velocity for each estimation method and the brake manufacturer's estimate is consolidated in Table 4.1. The cell color ranges from green indicating most of the data log is solved, to red indicating less amount of data log is solved. This on its own does not represent how good the estimate is, but it gives an idea of how well the method performs on average. A complementary consolidated table of averaged statistic parameters for each estimation method can be seen in 4.2. Here, the five estimations are compared among each other with green being the best and red being the worst performing. The main purpose of these parameters is to give some insight on the accuracy of each method. It is important to note that this are average errors over fifteen data logs which might be skewed by some outlier estimate in some data log.

Table 4.1: Filter performance in terms of share of estimated speed within the ±4% of reference speed for hybrid car: Complete data

COMPLETE DATA					
	Vx-R-P with CONCEPT 1	Vx-P with CONCEPT 1	Vx-P-VxDOT with CONCEPT 1	Vx-R-P with CONCEPT 2	BRAKE MANUFACTURER
Data Logs	Solved [%]	Solved [%]	Solved [%]	Solved [%]	Solved [%]
HY - 1	89.26	88.70	88.47	89.58	74.63
HY - 2	84.25	86.93	87.08	92.77	71.78
HY - 3	98.17	97.37	97.61	97.13	84.42
HY - 4	97.82	98.08	98.16	97.99	75.58
HY - 5	96.24	96.24	91.76	97.13	43.01
HY - 6	49.90	40.15	25.81	66.16	19.50
HY - 7	96.86	96.91	96.97	95.91	94.75
HY - 8	94.06	94.06	93.99	94.16	46.26
HY - 9	90.18	83.59	83.76	87.59	66.95
HY - 10	88.08	88.35	88.50	84.45	60.92
HY - 11	88.69	88.69	88.69	87.80	65.15
HY - 12	99.13	99.11	98.98	99.08	77.10
HY - 13	99.73	99.79	99.79	99.79	98.05
HY - 14	99.57	99.57	99.55	100.00	99.63
HY - 15	99.94	99.95	99.96	99.94	99.79
Average	**91.46**	**90.50**	**89.27**	**92.63**	**71.83**

By observing the percentage of the data files solved in Table 4.1, it is clear that the proposed filters and slip detection systems solve a lot more of the data logs. This of course is only with respect to the estimate being within the ±4%. It is also clear that none of the combinations solve all data logs within this limit which means that the estimate deviates more than 4% from the reference at times. Only looking at this parameter, the performance of the three filters with concept 1 are similar. This is partly because the evaluation is ambiguous as both the filters and slip detection depends on one another.

Table 4.2: Average statistic parameters over every driving data for Hybrid car : Complete Data

COMPLETE DATA : Average of each statistic parameter						
Stat Parameters	Unit	Vx-R-P with CONCEPT 1	Vx-P with CONCEPT 1	Vx-P-VxDOT with CONCEPT 1	Vx-R-P with CONCEPT 2	BRAKE MANUFACTURER
Solved	[%]	**91.46**	**90.50**	**89.27**	**92.63**	**71.83**
Absolute RMSE	[m/s]	0.29	0.29	0.30	0.28	0.86
Max Absolute Error	[m/s]	0.52	0.52	0.54	0.44	2.46
Min Absolute Error	[m/s]	-1.01	-0.99	-0.99	-1.11	-1.73
Relative RMSE	[%]	2.14	2.19	2.23	2.06	9.80
Max Relative Error	[%]	4.49	4.33	4.59	4.02	36.92
Min Relative Error	[%]	-6.27	-6.00	-6.07	-6.67	-10.78
Standard Deviation	[m/s]	0.26	0.26	0.26	0.25	0.74

It can also be seen in Table 4.2 that, the average performance metrics for the three filters in combination with slip detection concept 1 are similar. However, on average, the filter combination V_xRP solves slightly more amount of the data files than the other filters. As no obvious performance difference was found between the filters when tested with slip detection concept 1, it was decided to only evaluate slip detection concept 2 with filter V_xRP.

In Table 4.2 the average performance metrics for the filters and brake manufacturer estimates are presented. It can be observed that all of the filters greatly improve in all the metrics. The greatest improvements are made in reducing the peak estimation errors as a result of the slip-detection concepts. This also improves the standard deviation and RMSE significantly. What can also be observed is that the combination V_xRP and concept 2 is the best performing on average for all metrics except the mean absolute error. This might have an explanation in that concept 2 only relies on the slowest non-slipping wheel when in slip. Though, the difference in mean minimum absolute error compared to the best performing is still rather low, being roughly 0.11 m/s.

4.4.2 Slip Scenario Data

In Table 4.3 the share for when the speed estimate is within the ±4% estimation error for the slipping partition of each data file is presented. The average of the statistical parameters for the same intervals is presented in Table 4.4. Only considering the positive slip sections of the estimates, the results are similar as when considering all data. It is noted that the estimates for the filter and slip detection concept combinations are within the error limit for more of the files when only considering the slipping partition. It is also noted that the combination V_xRP and concept 2 is the best performing with respect to all parameters except the average minimum errors.

For log files HY-2, HY-6 and HY-9, it is observed that the share for when the speed estimate within the ±4% estimation error is particularly low. HY-2 is a challenging log file as the vehicle was deliberately attempted to drift. In HY-6, slip-detection concept 1 incorrectly detects slip at a low speed when the speed is offset, similarly as shown in the example in section 4.4.4. The dead-reckoning then keeps the estimate just outside the ±4% error limit. Finally, in log file HY-9 it is observed that the dead-reckoning of the IMU data differs from the reference speed, see example in section 4.4.6. This causes the dead-reckoning process to drift relative to the reference speed. However, when dead-reckoning the reference acceleration from the OxTS, the estimate still drifts relative the reference speed. The speed estimate drift in this file is one of the reasons for the large minimum error for the filters in comparison to the brake manufacturer estimate seen in Table 4.4.

Table 4.3: Filter performance in terms of share of estimated speed within the ±4% of reference speed for hybrid car: Slipping in acceleration scenarios

SLIPPING IN ACCELERATION SCENARIOS					
	Vx-R-P with CONCEPT 1	Vx-P with CONCEPT 1	Vx-P-VxDOT with CONCEPT 1	Vx-R-P with CONCEPT 2	BRAKE MANUFACTURER
Data Logs	Solved [%]	Solved [%]	Solved [%]	Solved [%]	Solved [%]
HY - 1	100.00	100.00	100.00	100.00	76.32
HY - 2	72.87	77.48	77.74	87.54	48.26
HY - 3	95.44	93.81	94.24	93.26	59.63
HY - 4	100.00	100.00	100.00	100.00	65.75
HY - 5	95.49	95.49	90.13	96.57	26.15
HY - 6	66.00	65.20	34.80	99.20	13.43
HY - 7	91.28	91.42	91.57	91.35	85.41
HY - 8	100.00	100.00	100.00	100.00	31.88
HY - 9	84.46	70.51	70.74	79.29	34.93
HY - 10	100.00	100.00	100.00	94.43	65.66
HY - 11	100.00	100.00	100.00	100.00	72.86
HY - 12	100.00	100.00	100.00	100.00	71.35
HY - 13	100.00	100.00	100.00	100.00	93.34
HY - 14	99.22	99.22	99.17	100.00	95.33
HY - 15	100.00	100.00	100.00	100.00	96.34
Average	**93.65**	**92.88**	**90.56**	**96.11**	**62.44**

Table 4.4: Average statistic parameters over every driving data for Hyrbid car : Slipping in acceleration scenarios

SLIPPING IN ACCELERATION SCENARIOS : Average of each statistic parameter						
Stat Parameters	Unit	Vx-R-P with CONCEPT 1	Vx-P with CONCEPT 1	Vx-P-VxDOT with CONCEPT 1	Vx-R-P with CONCEPT 2	BRAKE MANUFACTURER
Solved	[%]	**93.65**	**92.88**	**90.56**	**96.11**	**62.44**
Absolute RMSE	[m/s]	0.22	0.23	0.24	0.19	0.91
Max Absolute Error	[m/s]	0.50	0.50	0.53	0.44	2.50
Min Absolute Error	[m/s]	-0.34	-0.36	-0.36	-0.47	-0.14
Relative RMSE	[%]	1.76	1.82	1.94	1.50	11.03
Max Relative Error	[%]	3.49	4.33	3.94	3.23	35.80
Min Relative Error	[%]	-2.84	-2.83	-3.01	-3.90	-0.48
Standard Deviation	[m/s]	0.17	0.18	0.18	0.16	0.61

4.4.3 Brake Scenario Data

In Table 4.5 the share for when the speed estimate is within the ±4% estimation error for the braking partition of each data file is presented. The average of the statistical parameters for the same intervals are presented in Table 4.6. For this partition of the data the same trend with the estimates being generally better than the brake manufacturer is observed. All filters and slip concept combinations have the same speed estimation strategy for braking. It can be seen that they perform similarly with slight variations. This can be explained by the fact that the estimates are differently offset in the beginning of the braking scenarios because of the different

slip-detection concepts. However, it can be seen in Table 4.6 that the combination V_xRP and concept 2 is not the best performing estimate in terms of the share of data solved within the error limit or with respect to the different statistical parameters. Though, the statistical metrics are similar between the four filters. The files with a low share of the speed estimate inside the error limit normally includes severe wheel lock situations. This causes the speed estimate to be too slow due to the measurement updates as explained in section 3.7.

Table 4.5: Filter performance in terms of share of estimated speed within the ±4% of reference speed for hybrid car: Braking with and without locking up scenarios

ALL BRAKING SCENARIOS WITH AND WITHOUT LOCKING					
	Vx-R-P with CONCEPT 1	Vx-P with CONCEPT 1	Vx-P-VxDOT with CONCEPT 1	Vx-R-P with CONCEPT 2	BRAKE MANUFACTURER
Data Logs	Solved [%]	Solved [%]	Solved [%]	Solved [%]	Solved [%]
HY - 1	72.64	71.23	70.64	73.47	62.15
HY - 2	100.00	100.00	100.00	97.83	100.00
HY - 3	100.00	99.11	99.56	96.97	99.04
HY - 4	91.65	92.64	92.96	92.31	46.97
HY - 5	100.00	100.00	100.00	100.00	82.50
HY - 6	38.54	21.53	21.88	39.24	24.31
HY - 7	100.00	100.00	100.00	94.23	100.00
HY - 8	84.29	84.29	84.11	84.55	68.48
HY - 9	95.38	96.31	96.42	95.38	97.08
HY - 10	63.52	64.34	64.82	63.99	44.04
HY - 11	65.81	65.81	65.81	65.90	58.16
HY - 12	97.02	96.94	96.51	96.85	84.34
HY - 13	97.75	97.83	97.92	97.79	80.12
HY - 14	100.00	100.00	100.00	100.00	97.92
HY - 15	99.36	99.39	99.51	99.36	99.56
Average	**87.06**	**85.96**	**86.01**	**86.52**	**76.31**

Table 4.6: Average statistic parameters over every driving data for Hybrid car : Braking with and without locking up scenarios

ALL BRAKING SCENARIOS WITH AND WITHOUT LOCKING : Average of each statistic parameter						
Stat Parameters	Unit	Vx-R-P with CONCEPT 1	Vx-P with CONCEPT 1	Vx-P-VxDOT with CONCEPT 1	Vx-R-P with CONCEPT 2	BRAKE MANUFACTURER
Solved	[%]	87.06	85.96	86.01	86.52	76.31
Absolute RMSE	[m/s]	0.37	0.36	0.36	0.38	0.58
Max Absolute Error	[m/s]	0.07	0.06	0.06	0.08	0.48
Min Absolute Error	[m/s]	-0.94	-0.90	-0.89	-1.02	-1.73
Relative RMSE	[%]	2.61	2.62	2.60	2.65	4.34
Max Relative Error	[%]	2.41	0.33	2.56	2.75	4.24
Min Relative Error	[%]	-5.76	-5.37	-5.35	-6.18	-10.78
Standard Deviation	[m/s]	0.23	0.22	0.22	0.25	0.43

4.4.4 Example of When Both Concepts Work in Hill Scenario (HY-5)

In Figure 4.2a the reference velocity, wheel velocity, brake manufacturer estimate and estimated velocity for an all-wheel slip scenario is shown (HY-5). The vehicle was driven up a hill with a slippery surface. The traction was lost at a low velocity. Both concepts detect slip and initiate dead-reckoning at this point. What can be seen in Figure 4.2b is that the wheel speed measurements never converged to the true speed before they start to slip. This means that the dead-reckoning starts with a slight speed offset.

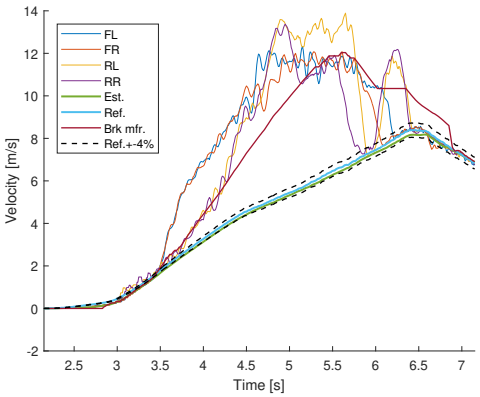

(a) Estimated velocity, brake manufacturer estimate, wheel speeds, and reference velocity for all wheel slip case in hill.

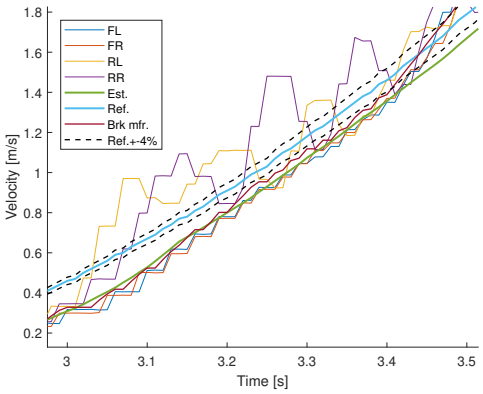

(b) Zoomed in figure in the beginning showing that the wheels do not converge to the true speed before slipping and showing that the estimated speed (green) is outside the ±4% limits in the beginning.

Figure 4.2: Plots of speed estimate for concept 2 in all-wheel slip example from data log file HY-5.

As can be seen in Figure 4.3a and 4.3b, both concepts perform very similar and the estimates do not drift much in particularly. This is because the orientation estimate was sufficiently accurate estimated such that the gravity bias in the accelerometer could be corrected for. Another factor is that as the speed increases the ±4% relative error will span a greater absolute error which partly explains why the relative error starts outside the ±4% relative error line in the error figures. Initially, the orientation is not known and therefore set to 0 degrees for both pitch and roll angles. What can be seen in Figure 4.4a is that the Euler pitch angle converges within the first second of data. As the Euler pitch estimate includes the accelerometer offset the Euler pitch estimate is offset. Throughout the scenario it can be seen that the offset is relatively constant. It can also be observed that the Euler roll estimate initially is offset and does not converge as seen with the Euler pitch estimate.

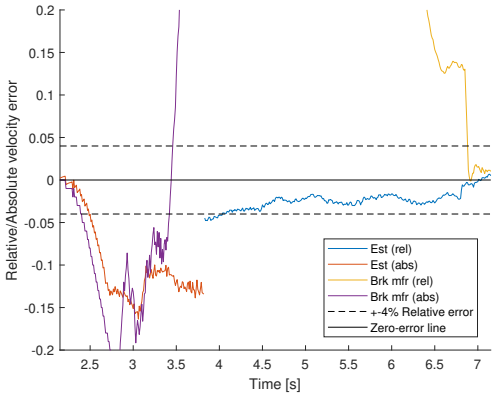

(a) Relative and absolute error for brake manufacturer and concept 1 estimate

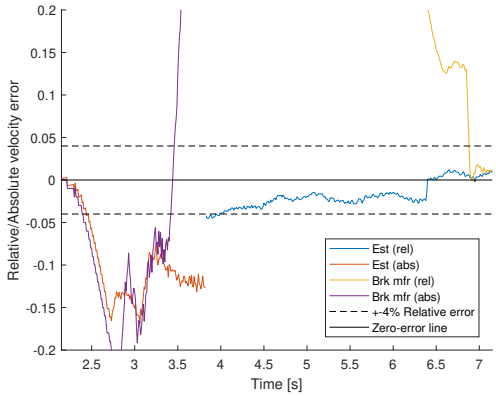

(b) Relative and absolute error for brake manufacturer and concept 2 estimate

Figure 4.3: Plots of speed estimate error for concept 1 and 2 in all-wheel slip example from data log file HY-5.

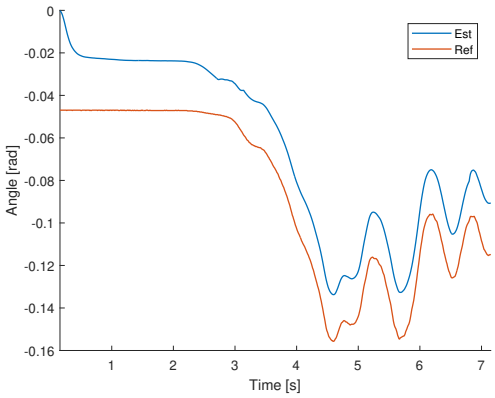

(a) Euler pitch estimate for hill scenario. Initial convergence of pitch estimate occur within first second of the data. It is visible that the there's and pitch-angle offset which is explained by that the accelerometer bias is not corrected for.

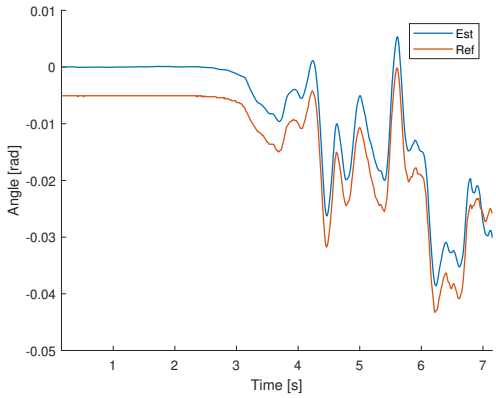

(b) Euler roll estimate for hill scenario. The estimate follow the shape of the reference but includes an offset. This offset does not converge as for the pitch estimate as the pitch is based on the integration of the gyroscope.

Figure 4.4: Euler pitch and roll estimate for the example.

Using the reference pitch angle, it is possible to check if the offset in the Euler pitch estimate is reasonable. As the car is standing still in the beginning of the scenario, the linear acceleration and velocity is zero. By calculating the mean of the measured acceleration for the time the car is still and subtracting the gravity component based on the reference pitch angle, the accelerometer bias can be calculated, see equation (4.9). This is with the assumption that the reference pitch angle is accurate.

$$\text{Bias} \sim a_x + g\sin(\theta_{ref}) \tag{4.9}$$

The bias can also be calculated using the difference in the Euler pitch estimate and the reference pitch, see equation (4.10). The accelerometer bias estimate for the accelerometer based method is 0.2336 and 0.2296 with the angle difference method. This means that the difference in the bias estimation is roughly 0.0039 m/s^2 for the initial stationary section of the data. The accuracy of the bias estimation will vary with time.

$$\text{Bias} \sim g(\sin(\theta_{ref}) - \sin(\theta_{ref} + \theta_{bias})) \sim g(\sin(\theta_{ref}) - \sin(\theta_{est})) \tag{4.10}$$

4.4.5 Examples of Speed Estimation Strategy in Braking

This is an example of how the brake logic works. In Figure 4.5a it can be seen that the speed estimate follows the reference relatively close but slowly drifts away towards the wheel speeds. This is because the wheel speed measurements are trusted with a larger measurement noise covariance when the speed estimate is faster than the fastest wheel. Over time the estimate slowly converges to the wheel speeds. Though, when the speed estimate is slower than the fastest wheel speed measurement, the covariance is decreased and the speed estimate gets "slingshot" up towards the true speed. An alternative approach would be to dead-reckon throughout the braking-sequence. This is demonstrated in Figure 4.5b. What can be seen in this Figure is that the speed estimate drifts in the positive direction and the estimate surpasses the upper 4% error limit. This positive-drift is limited with the proposed brake logic. At second 27 in Figure 4.5b the dead-reckoning process has been active for roughly 5 seconds and at this point the magnitude of positive error in the speed estimate is larger than the magnitude of negative error in the proposed method.

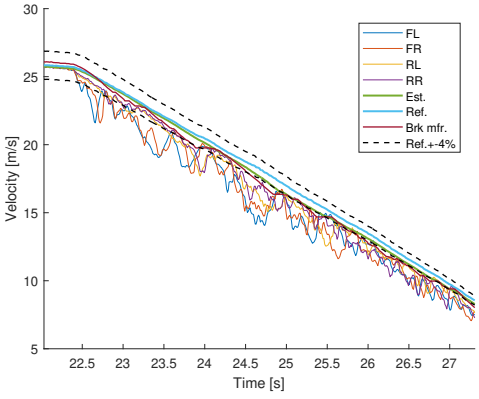

(a) Example of speed estimation strategy when ABS braking.

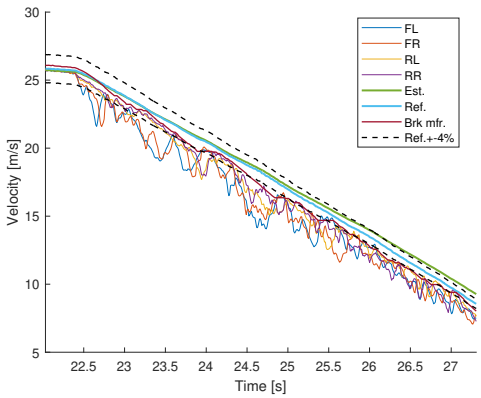

(b) Example of pure dead-reckoning instead of brake logic. Figure shows that the estimate drifts outside the ±4% error limit at around 26 seconds.

Figure 4.5: Example of speed estimation strategy in ABS braking.

In Figure 4.6a, an example of a nominal braking case is shown. The speed estimate then remains at the fastest wheels. The fastest wheel speeds are well within the 4% limit. However, in Figure 4.6b, an example of the brake logic working in an extreme wheel-lock situation in data log HY-6 is shown. The wheel speeds remain well below the reference speed of the car for roughly 2 seconds, without any wheel speeds getting close to the reference speed in an ABS-cycle. This causes the estimate to slowly drift from the true speed. Though, at around 11.5 seconds, an ABS-cycle peak occurs and the estimate now updates with a lower covariance causing it to slingshot back towards the true speed. The speed estimate is well outside the 4%-limit for most of the shown interval but it is closer to the reference speed than the brake manufacturer for the most part.

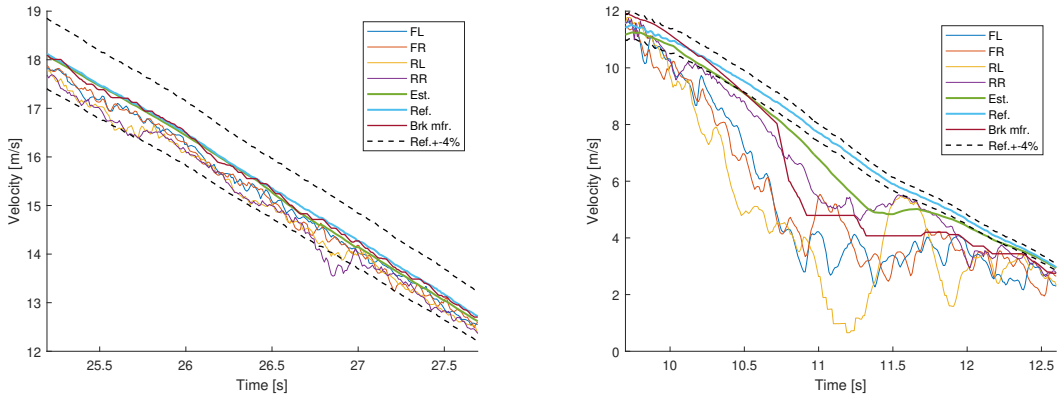

(a) Example of speed estimation strategy in nominal braking.

(b) Example of speed estimation strategy in extreme wheel lock situation.

Figure 4.6: Example of speed estimation strategy in normal and extreme braking.

4.4.6 Example When Dead-Reckoning Fails (HY-9)

This is an example from data log file HY-9 when the dead-reckoning process seems to not work. In Figure 4.7a a section of the log file is shown where the vehicle first is ABS-braking and then accelerating hard such that all wheels slip. Both slip detection concepts detect that the wheels are slipping and force the filter to dead-reckon. However, the estimate is observed to drift considerably in comparison to the reference speed. This is surprising because the dead-reckoning earlier in the log file was working without considerable drift. It is even more surprising that when dead-reckoning the reference accelerometer measurement from the OxTS, the speed estimate also drifts relative the reference speed measurement of the OxTS. In Figure 4.7b the speed estimate from the dead-reckoning of the filter, dead-reckoning of the reference OxTS accelerometer measurements and dead-reckoning of the raw longitudinal accelerometer that is not bias or gravity compensated is shown. The dead-reckoning processes are started at the same time from the same initial velocity before the acceleration starts. It can be seen that the speed estimate from the dead-reckoning of the raw IMU is the closest to the reference speed. It is not known if it is the IMUs that fail specifically after braking or if the reference speed estimate is

unreliable at this point.

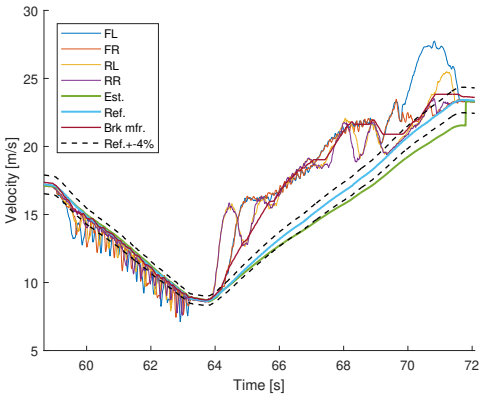

(a) Example where dead-reckoning unexpectedly fails.

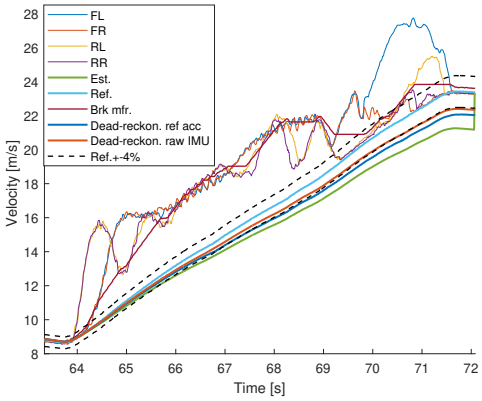

(b) Dead-reckoning comparison for the specific time interval. All dead-reckoning speed estimates, including the reference accelerometer, differ from the reference speed.

Figure 4.7: Example where dead-reckoning fails in data log HY-9 and comparison of dead-reckoning of different measurements.

4.4.7 Example of When Gyroscope is Not Bias-Compensated

This is an example of how the dead-reckoning performance reduces if the gyroscope is not compensated for the offset-bias. In Figure 4.8a the speed estimate using concept 2 for data log file HY-12 is shown. Both concepts solves the absolute majority of the log file except a short section in the braking section as shown in Figure 4.8b. In Figure 4.8c the speed estimate for the same log file is shown when the filter is forced to dead-reckon from the 5 second mark without gyroscope bias-compensation. The dead-reckoning is forced for 30 seconds to showcase how much the dead-reckoning process drifts without any bias-correction. The speed estimate exceeds 4% error limit within the first few seconds of the dead-reckoning and differ by roughly 15 m/s after 30 seconds. The bias of the pitch-rate gyroscope was measured in the beginning of the log file when the car was standing still to 0.0028. In Figure 4.8d the Euler pitch estimate is observed to be linearly drifting. It is also observed that the Euler pitch angle estimate rapidly change when the dead-reckoning is ended. This is a result of the combined pitch and speed estimation. It may be questionable to allow these abrupt changes in the estimate.

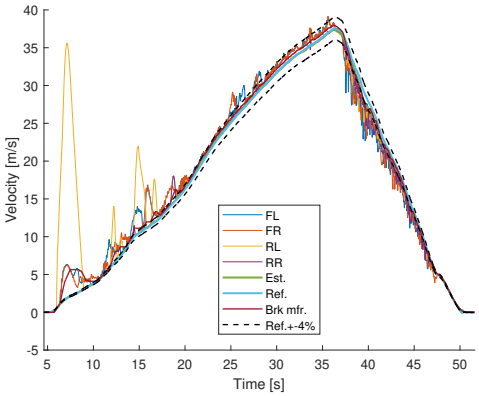

(a) Speed estimate, wheel speeds and reference speed for log file HY-12.

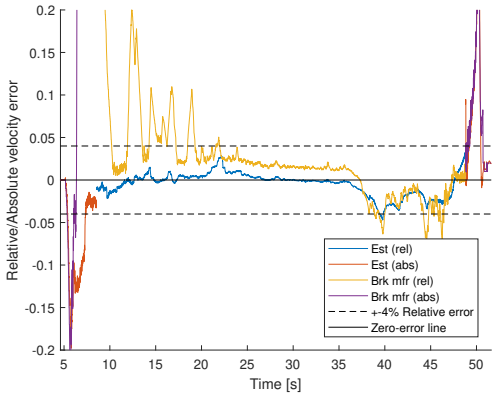

(b) Error plot for concept 2 for log file HY-12.

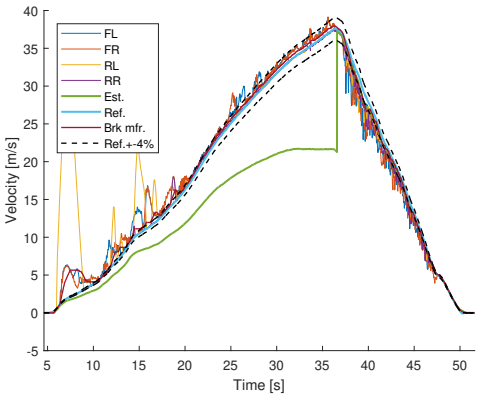

(c) Example of 30 seconds of dead-reckoning without any bias compensation.

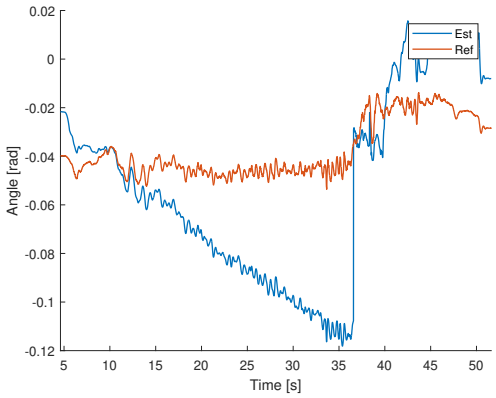

(d) Euler pitch estimate drifts during the dead-reckoning without gyroscope compensation.

Figure 4.8: Example of the impact of not bias-compensating the gyroscopes.

4.5 Fully Electric Car

During the final weeks of the thesis, a new set of driving data from a fully electric car was provided for testing of the speed estimation method. The two slip-detection concepts have not been developed or tuned for these data logs. As mentioned in section 1.1, these data logs contains slightly more challenging scenarios in that they are collected from the lateral stability department. The logs both contains scenarios with slipping in hills causing the vehicle to decelerate and slip scenarios where the wheel slip is right on the 4% error limit. The evaluation of these data logs was made in the same way as for the hybrid. First the share of data within the error limit and the average statistical parameters for the filter and slip detection concepts in different partitions of the data is presented. Then some examples are given. However, as only some of the data logs contained braking scenarios, the specific evaluation for the braking partition of the data is left out. In these data logs an on-board speed estimate from Volvo beyond the brake manufacturer was available.

This estimate is for the most part only based on the wheel speed measurements and is labeled as simple Volvo.

4.5.1 Complete Data

In Table 4.7 and Table 4.8, the share for when the speed estimate within the ±4% estimation error for the whole data files and the average of the statistical parameters for the same intervals are presented. It can be seen in Table 4.7 that the filter and slip detection concepts do not perform significantly better than the wheel-based-methods for the log files. Slip detection concept 2 still produces an estimate with on average the most share of the estimate within the error limit. Observing the average statistical parameters in Table 4.8 it becomes clear that concept 1 performs the worst out of the estimates. This solely comes down to that the slip-detection criteria fails to activate at several points, see section 4.5.4 for example. It turns out that the torque-rate characteristic found and tuned specifically for the hybrid car does not perform as well for the fully electric car. However, it also becomes clear that concept 2 on average performs the best out of the estimates even though the estimate is not kept within the error limit for all files.

Table 4.7: Filter performance in terms of share of estimated speed within the ±4% of reference speed for fully electric car: Complete data

COMPLETE DATA						
	Vx-R-P with CONCEPT 1	Vx-P with CONCEPT 1	Vx-P-VxDOT with CONCEPT 1	Vx-R-P with CONCEPT 2	SIMPLE VOLVO ESTIMATE	BRAKE MANUFACTURER
Data Logs	Solved [%]	Solved [%]	Solved [%]	Solved [%]	Solved [%]	Solved [%]
FE-1	92.07	92.95	94.93	94.10	94.97	84.06
FE-2	70.23	70.19	70.19	91.69	87.51	83.52
FE-3	52.23	52.23	52.23	67.06	57.76	56.28
FE-4	97.30	97.27	97.20	100.00	96.01	97.36
FE-5	96.70	97.35	97.28	100.00	99.46	99.57
FE-6	94.12	94.39	94.30	97.52	96.41	97.58
FE-7	93.96	93.15	92.99	95.49	96.64	96.97
FE-8	89.08	89.08	89.08	70.70	62.71	75.50
FE-9	82.36	82.32	82.36	95.62	82.02	88.24
FE-10	85.32	85.32	86.47	74.53	81.44	80.72
Average	85.34	85.42	85.70	88.67	85.49	85.98

Table 4.8: Average statistic parameters over every driving data for Fully electric car : Complete data

COMPLETE DATA : Average of each statistic parameter							
Stat Parameters	Unit	Vx-R-P with CONCEPT 1	Vx-P with CONCEPT 1	Vx-P-VxDOT with CONCEPT 1	Vx-R-P with CONCEPT 2	SIMPLE VOLVO ESTIMATE	BRAKE MANUFACTURER
Solved	[%]	85.34	85.42	85.70	88.67	85.49	85.98
Absolute RMSE	[m/s]	0.66	0.65	0.65	0.23	0.47	0.47
Max Absolute Error	[m/s]	1.92	1.87	1.88	0.62	1.81	1.59
Min Absolute Error	[m/s]	-0.35	-0.32	-0.31	-0.40	-0.55	-0.64
Relative RMSE	[%]	10.51	10.29	10.29	2.56	6.35	5.93
Max Relative Error	[%]	31.29	30.84	30.87	6.65	21.45	19.03
Min Relative Error	[%]	-4.70	-4.24	-4.26	-6.13	-6.35	-7.73
Standard Deviation	[m/s]	0.57	0.56	0.56	0.21	0.42	0.42

4.5.2 Slip Scenario Data

In Table 4.9 the share for when the speed estimate within the ±4% estimation error for the slipping partition of each data file is presented. It is observed that all estimates struggle to keep the estimate withing the error limit and that the performance in regards to this metric seems to be sporadic between the log files. Concept 2 again solves the most amount of the data. Concept 1 on the other hand is not performing well in regards to this, though this again comes down to the failing of the torque-rate criteria. When looking at the average of the statistical parameters for the same intervals presented in Table 4.10, it becomes clear that concept 2 on average is the best estimate out of the six compared. Concept 2 does not seem to be very far from the true speed on average with an RMSE of 0.23 m/s, a max absolute error of 0.62 m/s and a standard deviation of 0.21 m/s. Only observing the share for when the speed estimate is within the ±4% estimation error gives a slightly skewed view of the performance. E.g. in section 4.5.4 an example from log-file FE-3 shows that concept 2 detects slip slightly late for one occasion causing the speed estimate to be offset just outside the 4% error limit. This makes the solved percent only show up as 67% in Table 4.9. However, the speed error is limited to about 6% in this estimate compared to the roughly 100% error from the other estimates.

Table 4.9: Filter performance in terms of share of estimated speed within the ±4% of reference speed for fully electric car: Slipping in acceleration scenarios

SLIPPING IN ACCELERATION SCENARIOS						
	Vx-R-P with CONCEPT 1	Vx-P with CONCEPT 1	Vx-P-VxDOT with CONCEPT 1	Vx-R-P with CONCEPT 2	SIMPLE VOLVO ESTIMATE	BRAKE MANUFACTURER
Data Logs	Solved [%]	Solved [%]	Solved [%]	Solved [%]	Solved [%]	Solved [%]
FE-1	89.51	90.67	93.29	92.19	93.28	74.48
FE-2	51.30	51.24	51.24	86.40	79.58	69.05
FE-3	36.86	36.86	36.86	56.47	44.18	37.34
FE-4	90.62	90.50	90.27	100.00	86.04	90.85
FE-5	93.47	94.76	94.63	100.00	98.88	97.65
FE-6	73.62	74.82	74.45	88.88	83.73	81.65
FE-7	87.92	82.64	82.16	88.30	90.73	88.99
FE-8	89.80	89.80	89.80	64.92	57.68	68.77
FE-9	72.64	72.57	72.64	94.89	74.56	77.46
FE-10	100.00	100.00	100.00	56.03	65.52	60.54
Average	78.57	78.39	78.53	82.81	77.42	74.68

Table 4.10: Average statistic parameters over every driving data for fully electric car : Slipping in acceleration scenarios

SLIPPING IN ACCELERATION SCENARIOS : Average of each statistic parameter							
Stat Parameters	Unit	Vx-R-P with CONCEPT 1	Vx-P with CONCEPT 1	Vx-P-VxDOT with CONCEPT 1	Vx-R-P with CONCEPT 2	SIMPLE VOLVO ESTIMATE	BRAKE MANUFACTURER
Solved	[%]	78.57	78.39	78.53	82.81	77.42	74.68
Absolute RMSE	[m/s]	0.78	0.77	0.77	0.29	0.55	0.50
Max Absolute Error	[m/s]	1.91	1.87	1.87	0.62	1.81	1.59
Min Absolute Error	[m/s]	-0.11	-0.10	-0.10	-0.15	-0.12	-0.22
Relative RMSE	[%]	12.20	11.96	11.98	3.13	7.42	6.72
Max Relative Error	[%]	31.29	30.84	30.87	6.65	21.45	19.03
Min Relative Error	[%]	-1.50	-1.53	-1.59	-2.64	-1.50	-3.89
Standard Deviation	[m/s]	0.57	0.56	0.56	0.17	0.40	0.42

4.5.3 Example with Deceleration While Slipping in 20% Hill (FE-1)

In this example from data log file FE-1, the vehicle slips while driving on a road with a 20% incline causing the vehicle to decelerate, see Figure 4.9a. Both slip-detection concepts detect slip, though concept 1 does detect slip slightly later than concept 2 causing the estimate to be just outside the 4% limit when the dead-reckoning starts as can be seen in Figure 4.10a and 4.10b. In the end of the log at around 14 seconds, it can be seen in Figure 4.9b that the speed estimate for concept 2 deviates from the true speed even though the wheels does not slip severely at that point. This is because the vehicle at that point is yawing by 0.7 rad per second as can be seen in Figure 4.11b. As the filters only consider longitudinal dynamics and that the slip-detection concept 2 relies on comparing the acceleration of the wheel with the acceleration with the car for slip detection, all wheels are determined to be slipping at around second 14. This makes the filter to rely on dead-reckoning of the yaw-rate contaminated acceleration which in turns causes the dead-reckoning to drift as can be seen in Figure 4.11a.

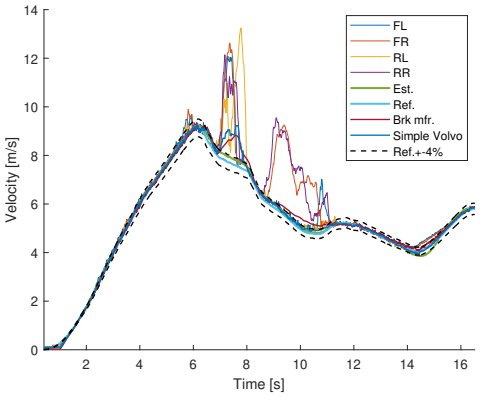

(a) Wheel speed, reference speed and estimated speed plot for concept 2.

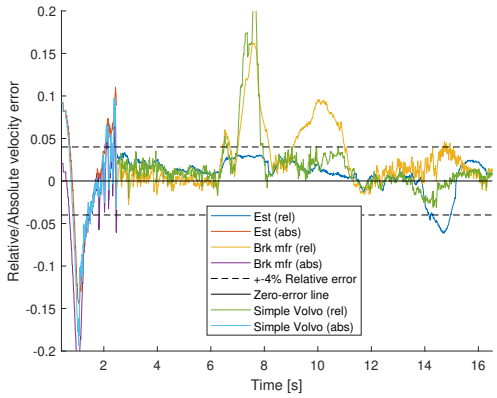

(b) Error plot for concept 2.

Figure 4.9: Speed and error plot for concept 2 in all-wheel slip scenario with deceleration in hill.

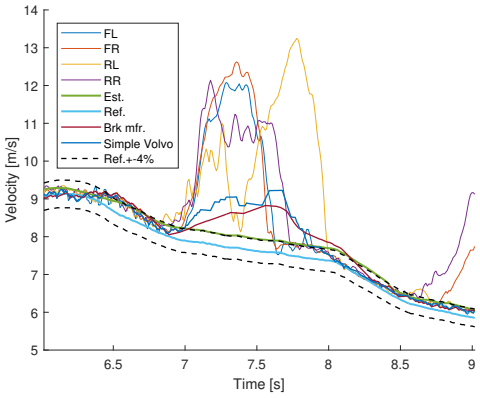

(a) Wheel speed, reference speed and estimated speed plot for concept 1 zoomed in at first wheel slip peak.

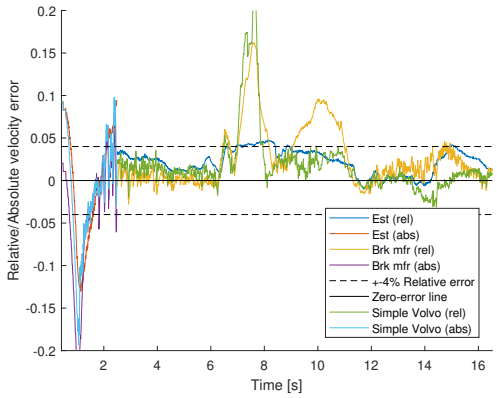

(b) Error plot for concept 1.

Figure 4.10: Speed and error plot for concept 1 in all-wheel slip scenario with deceleration in hill.

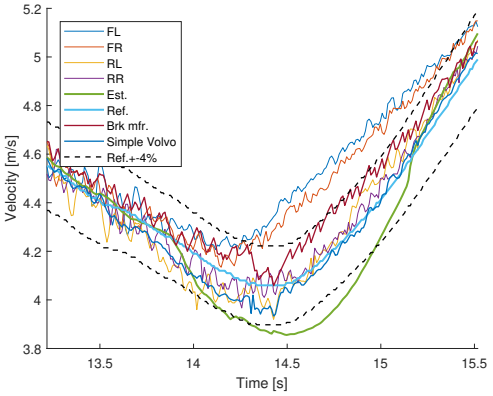

(a) Zoomed in speed estimate plot for concept 2 at the point of heavy yawing.

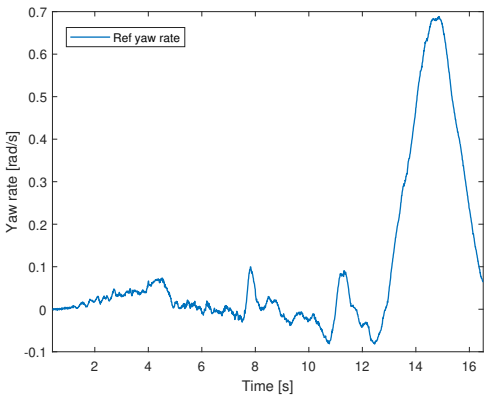

(b) Yaw rate for the data log FE-1.

Figure 4.11: Zoomed in speed and yaw-rate plot for data log FE-1.

4.5.4 Example of Tip of the Throttle on Ice-Road (FE-3)

This example is from data log FE-3 where the vehicle is driven on an ice-road and the driver tips the throttle such that the wheels experience excessive slip two times after one another. As can be seen in Figure 4.12a, slip-detection concept 1 fails to activate and the speed estimate follows the slipping wheels. The slip detection was not activated because the torque did not increase sufficiently fast, i.e. the torque-rate is not high enough as shown in Figure 4.12b. However, slip-detection concept 2 successfully activates during the first slip event and activates with a slight delay during the second slip event. This causes a slight initial offset and drift in the speed

estimate as can be seen in Figure 4.13b. With slip-detection concept 2, the speed estimate is better than both brake manufacturer and the simplified Volvo estimate as seen in Figure 4.13a. However, the estimate is outside the error limit of 4% for the second all-wheel slip event.

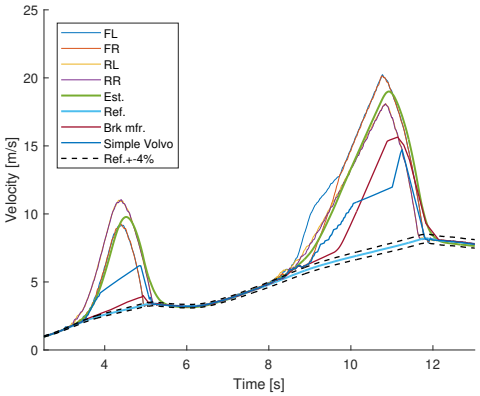

(a) Concept 1 fails to detect slip and speed estimate is based on wheel speeds.

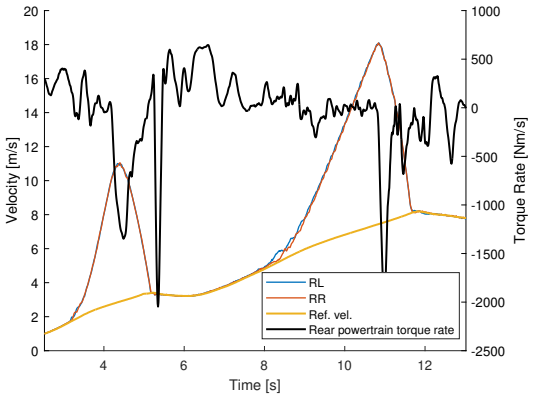

(b) Rear axle powertrain torque rate showing no distinctive spikes above the thresholds before slip.

Figure 4.12: Example of tip of the throttle on ice for slip detection concept 1 (FE-3)

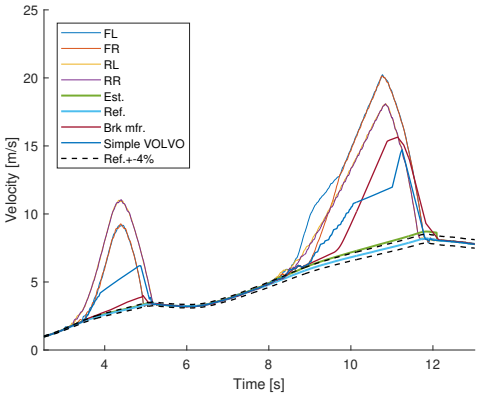

(a) Concept 2 successfully detects slip in the first slip. During the second slip, the slip is detected with a slight delay causing an offset and drift in the estimate.

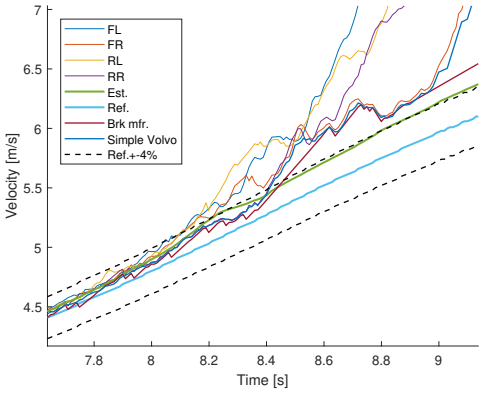

(b) Zoomed in view of the start of the second slip. The wheel speeds slowly drift away from the true speed before slipping severely fooling the slip-detection system.

Figure 4.13: Example of tip of the throttle on ice for slip detection concept 2 (FE-3)

4.5.5 Example Where Concept 2 Struggles

In this example, the vehicle is accelerating and the wheels are subject to severe excessive slip. Slip-detection concept 1 successfully detects the slip and locks the

slip-detection for the whole slip event which can be seen in Figure 4.14a. Concept 2 on the other hand struggles to detect that the wheels are still slipping at around 14 seconds where the wheels almost regain some traction and slip with about 4%, see Figure 4.14b. Since the estimate has a slight speed offset initially, the wheel speeds are within the slip-ratio-constraint for slip-detection concept 2 and since the residual between the wheel speed and estimate is relatively constant at this point the system faulty trusts the wheels at this point. This causes the estimate to be offset severely before the slip-detection again detects slip and dead-reckoning starts. When the wheels comes back to free rolling at around 15.5 seconds, the speed estimate is "too far away" from the wheel speeds and the wheels are falsely determined as slipping by the slip-ratio criteria. Though, as can be seen in the figure, the estimate soon regains trust in the wheels as the criteria that monitors the variance of the speeds detect that the wheel speeds has been close for some time and thus must be free-rolling.

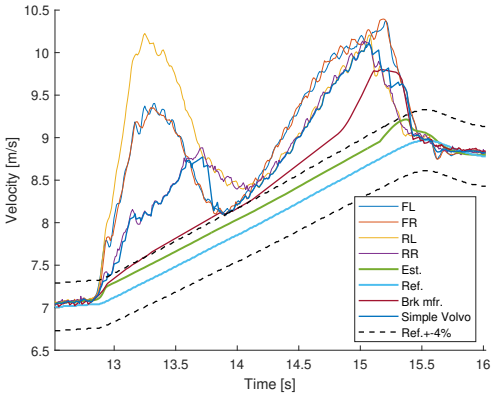

(a) Concept 1 successfully detects slip and dead-reckons throughout the slip-event in this example.

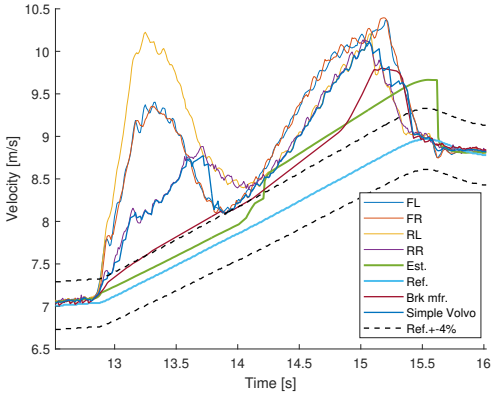

(b) Concept 2 struggles as the wheels comes back and rolls with a relatively constant error fooling the system to trust the wheels.

Figure 4.14: Example where concept 2 struggles to detect slip but concept 1 successfully detects slip.

In Figure 4.15 an additional representative example for when concept 2 struggles to detect slip. What happens in this case is that the wheels slowly slips and the speeds slowly drift from the true speed of the vehicle. Also, the noises in the measurements are not particularly high. This makes none of the criteria for detecting slip to activate which in turns makes the estimate to be based on the wheel speeds. This is a common problem in several of the log files for the hybrid vehicle.

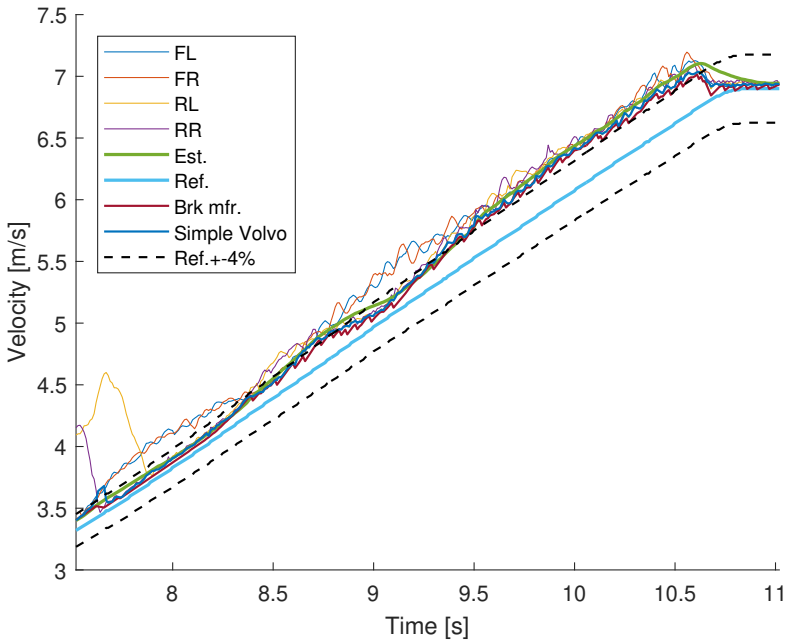

Figure 4.15: Example of slip at 4% border with slow initiation. It is shown that slip-detection concept 2 does not detect the wheel slip and the estimate is based on the slipping wheels outside the error limit.

5

Discussion

During excessive wheel slip, the wheel speed measurements do not accurately represent the true speed of the car. In this thesis a simplistic kinematics based approach for estimating the longitudinal vehicle speed during excessive slip conditions was taken. There are two main ideas with the approach. Firstly, the filter is kinematics based and only considers the longitudinal velocity, acceleration and orientation (pitch and roll) in order to limit the dependencies on different states as e.g. the road friction which is difficult to accurately determine in slippery conditions. Secondly, a slip-detection system is used to deterministically detect and filter out wheel speed measurements from wheels that experience excessive slip in order to limit the influence from the distorted measurement on the estimated speed. Additionally, a specific strategy for speed estimation during braking is complementing the slip-detection system. With this relatively simplistic approach the results show that the speed can be estimated within the vision error limit of $\pm 4\%$ relative the true speed during both excessive positive and negative slip. However, it is hard to specify how well the speed can be estimated with the approach as the speed estimate cannot be robustly kept withing the error limit for all data log files. The presented method does on the other hand provide a better speed estimate than the brake manufacturer estimate in terms of the average share of speed estimate within the error limit and that it considerably reduces the RMSE, standard deviation and peak errors for the data logs for both cars (except slip detection concept 1 for the fully electric vehicle where the detection does not align well).

5.1 The Limiting Factors in the Presented Method

There are three main limitations with the method. Firstly, the slip detection concepts do not cover for all situations and cannot always detect slip correctly. Secondly, during excessive all wheel slip the estimate is entirely based on dead-reckoning which is a delicate process sensitive for errors. Thirdly, the presented speed estimation strategy during braking is struggling with extreme braking scenarios where the wheels are locking or are heavily reduced in speed. These points are further discussed in the following subsections.

5.1.1 The Difficulties With Slip Detection

On a high level, the problem with slip detection is how to define what is an acceptable amount of slip, how to detect slip and how to track slip throughout a slip-event (from initiation of slip to when the wheels comes back). The only measurement of the true speed is from the wheels which are slipping with a varying amount at all times. With the sensor setup the speed estimate needs to be based on the wheel speeds which will make the estimate slightly offset from the true speed at most times. As the speed is set to be estimated within an error limit, some wheel slip can be tolerated. How much slip that can be tolerated is a balancing act, trusting a slipping wheel will cause the speed estimate to be offset relative the true speed by some amount but the estimate will not drift as it would if based completely on dead-reckoning. Letting the estimate be offset on the other hand can reduce the dead-reckoning capabilities as the estimate is already offset which limits how much the dead-reckoning process can drift before the estimate degrades.

In this thesis one of the main ideas is to limit the influence of wheels that are excessively slipping as the speed measurements at this point are not representing the true speed. Therefore excessive slip has to be identified. Theoretically, the slip-ratio tells how much the wheel is slipping. The problem is that the true speed is not known and that the estimated speed most times will be slightly offset and also drift during dead-reckoning such that the slip-ratio may not be very accurate at all times. Instead of using the slip ratio, an investigation of how to detect slip using the provided signals (mainly wheel speeds, accelerometer and powertrain torque) was made. Ideally, an indicator of slip should be able to detect slip throughout a complete slip-event and do so without being influenced by what the current state estimates are. In the investigation it was not found indicators like this. It was only found indicators of slip that can detect slip for parts of a slip event. E.g. the acceleration difference between wheel and vehicle is high initially during slip but not necessarily during a complete slip event. The indicators studied are also based on relating the measurements to the estimated quantities as it allows to detect slip more accurately. This makes it harder to tune and study the indicators as the estimated states are influenced by when slip is detected which depends on what the estimated quantities are. It was also found necessarily to combine different indicators of slip such that they can constitute a slip-detection concept that can detect excessive slip throughout a slip event.

The two presented slip detection concepts are based on different principles. Slip detection system 1 is based on assuming slip in between certain slip indicating events occur. This way, the tracking of slip during a slip-event is to some extent left out as only the initialisation and end of slip has to be defined. Slip detection 2 on the other hand is based on detecting slip in every time step. Both concepts were developed using the data from the hybrid vehicle and in the results it is clear that both systems perform well for the hybrid vehicle. This is best observed in the Tables that only consider the positive acceleration partitions of the data logs (Tables 4.3 and 4.4). Both concepts outperforms the brake manufacturer estimate and concept 2 has slightly better performance than concept 1 for the hybrid vehicle. The results

for the fully electric vehicle data logs shows that none of the slip detection concepts consistently perform better than the brake manufacturer or the simplified Volvo estimate in terms of share of estimate within the 4% error limit. Slip-detection concept 1 is notably the worst performing out of the estimates with large deviations from the reference speed. This can be explained with that the powertrain torque-rate criteria, which is the foundation for the slip-detection concept 1, did not work well for the fully electric vehicle. Concept 2 on the other hand shows that on average the RMSE, standard deviation and peak errors are lower than the other methods. The two concepts will be discussed separately in more detail but first some common problems will be discussed.

None of the slip detection concepts are perfect and even though they work with different principles they have some common problems which can explain some of the performance issues. First of all, the excessive slip detection is not necessarily related to a specific amount of slip. This is because the true speed is not known and that the detection is based on deterministic thresholds that has been tuned based on the data logs from the hybrid vehicle. A related problem to this is that none of the concepts can detect when all wheels are slowly slipping. This is because it is hard to detect. An example of this can be found in section 4.5.5. As the slip is slow, there is no clear indicator of slip as e.g. the acceleration difference is low, the torque-rate is not high and the variance of the residual between the estimated speed and wheel speeds is low. In turn, the wheels are trusted and the speed gets offset, sometimes outside the 4% error limit. This phenomena was not observed to be as frequent in the hybrid vehicle data logs as it was in the fully electric data logs. Another problem is that the excessive slip detection happens with a slight delay as the slip needs happen before it can be detected. For the most part this is not a crucial problem though it introduces a slight offset in the estimate. Slip detection in low speeds is also a challenging problem. This is partly because it was found that the wheel speed measurements does not provide an accurate estimate of the vehicle speed in low speeds. Partly because estimate will be offset if slip is detected at low speeds as the wheels are trusted in low speeds. This will cause the dead-reckoning to start outside the 4% error limit even though the estimate might not be far from the true speed in absolute terms.

In slip detection concept 1 a lot of pressure is put on that the identification of the initialisation of slip and when the wheels comes back can is accurate. To do this, a combination of powertrain torque-rate, acceleration difference between wheel and vehicle and torque level was used. For the hybrid vehicle, the concept was found to work relatively well. The speed estimate is better than the brake manufacturer estimate and compares well with concept 2 but it performs just slightly worse. However, it was found that the powertrain torque-rate criteria developed for the hybrid vehicle did not translate well for the fully electric vehicle data logs causing the concept to fail considerably to detect slip and the estimate to be very degraded. One example of this is shown in section 4.5.4 where there was no powertrain torque-peak before slip on an ice road. This raises the question if the powertrain torque rate slip indicator either is specifically working for the hybrid vehicle or if it is specifically related to how the vehicle was driven in these data logs. This could be an example

of over-fitting a slip indicator. Furthermore, the concept is limited to only detecting slip when there is a combination of high powertrain torque-rate and acceleration difference, which might not always be the case as a wheel could be slipping even though there is not a particular spike in the powertrain torque level. It has also been observed that the torque decrease rate criteria does not always align well with that the wheels are coming back. This is e.g. when the torque level is reduced fast to a lower level but not completely shut off. It can also be problematic to clear the slip-assumption in certain conditions as when the car is accelerating aggressively for a long time as none of the defined free-rolling assumption events occurs. To summarize this concept, the particular criteria used for detecting if the wheels are slipping and when the wheels come back might not be optimal, but this concept showed in several instances, e.g. in section 4.5.5, that locking the slip assumption might be a better approach compared to trying to detect slip in every step at some points.

Slip-detection concept 2 on the other hand, detects slip at every time step. This instead puts pressure on that the slip-detection is done correctly in each time-step but it reduces the risk of completely missing detection of obvious slip as with concept 1. Concept 2 proved to be working better and to be more general in it's formulation than concept 1 as it performed better for both the hybrid vehicle and the fully electric vehicle data log. Though it was found to be struggling with slip-detection particularly in two grey-zones. The first grey-zone is when the wheels are slowly slipping. This problem was discussed earlier in this section. In these situations it might be needed to use some sort of delay in the estimate and compare dead-reckoning from one point in time to the current estimate in order to detect the slow slip. This could be further researched. The second grey-zone is when the estimate has drifted slightly but still is within the error limit and a wheel comes back from severe slip but still slips with an offset outside the error limit. This is shown in an example in section 4.5.5. At the point when the wheels slip with a relatively constant offset relative to the estimated speed, the acceleration and variance in the speed error is low. The concept then completely relies on the slip-ratio, however, this is not the true slip-ratio as the estimate has drifted slightly causing the slip-detection to falsely assume that the wheel is not slipping. It was not found a easy solution to this problem. In this concept it was also tested to only rely on the slowest wheel when slip is detected. This is because theoretically the slowest wheel should best represent the true speed in acceleration. However, it was found that when the vehicle is turning relatively sharp during slip, the speed measurements from the steering wheels can be overcompensated by the presented wheel correction method which can cause the corrected measurements to be too slow. If the slowest wheel speed is then trusted the speed estimate can get degraded. This is believed to be the reason for why concept 2 has the largest minimum speed error during acceleration slip.

5.1.2 Dead-Reckoning Process

During all wheel slip, the speed estimate is completely based on dead-reckoning with the presented method. This is what makes the estimate perform well during all wheel slip scenarios. Purely basing the speed estimate on the dead-reckoning process might be questionable, at least over longer periods of time. This is because the dead-reckoning process is susceptible for many points of errors as sensor biases, the gravity compensation which requires an accurate Euler pitch estimate as well that the initial speed offset plays a role. Unless all of these causes of errors are sufficiently dealt with, the process is not very accurate over time because of the error build up during integration. Model inaccuracies is also a factor as for example shown in section 4.5.3 where the dead-reckoning with a high yaw rate causes the estimate to drift considerably. However, situations with lateral dynamics was not within the scope, but it is clear that it has to be considered for those situations. To limit the risk of positive drift caused by some error in the dead-reckoning process, both presented slip-detection concepts have a logic that makes the filter trust the slowest wheel if the estimate is faster than any of the slipping wheels by 1 m/s. This is to set an upper limit of how much the estimate can differ from the true speed. However, a lower limit in the case of negative drift was not formulated because it is hard to set a limit of how much slower the estimated speed can be as it is hard to know how much the wheels slips.

5.1.3 Speed Estimation Strategy in Braking

A separate strategy for speed estimation in braking was developed, see section 3.7 for full explanation. This is mainly because it was found that the slip-behaviour in braking differs from the behaviour in positive slip and also that the slip is slightly more consistent with the ABS is working. Furthermore, it was decided to define braking as if three or more wheels are experiencing any brake torque. This might generally be a questionable definition, but as it was found that the wheels could lock with low amounts of brake torque due to the low road friction and that the brake friction torque estimates can show up to 50% errors it was found to be a reasonable definition. This is only used as a way to switch logic in the speed estimation strategy. The errors in the brake friction torque estimate partly comes down to if the disks are contaminated with e.g. water. Purely electronically actuated brakes could perhaps be give a better more accurate estimate of the braking torque. If this information was available, maybe a more sophisticated brake-definition could be formulated.

The results show that the speed estimation strategy for braking in nominal braking cases works well. This is because the fastest wheel speed measurement is trusted and this is normally close to the reference speed during normal braking. In more extreme braking when the ABS activates the strategy works in many cases. Though, the strategy is based on that the speed peaks for each wheel during the ABS-cycles are within the $\pm 4\%$ error limit. In the case of a severe speed reduction because of braking on slippery surfaces or locking the wheels, the speed estimate will many times drift outside the error limit if the wheel speed peaks are not within the limit. An example of this is shown in section 4.4.5. The reason for the drift is that the

wheels are trusted with a high uncertainty even though they are slower than the estimate (and true speed). An improvement here would be to further extend the strategy to for example dynamically reduce the trust in the wheels even further if it was detected that the wheel speed deviation from the estimated speed is particularly fast or large in the beginning of the braking. Then the initial dead-reckoning that is in the presented strategy could be extended. An alternative approach would be to completely rely on dead-reckoning during braking. This was tested and it was found that the dead-reckoning for many files tended to drift outside the error limit as shown in Figure 4.5b. Therefore it was decided that it is better to do updates with the wheel speed measurements at all times as it proved to work except for the extreme lock-cases. However, this makes share of when the estimated speed is within the error limit to be reduced in many cases as can be seen in e.g. Table 4.5.

5.2 Which Driving Scenarios Does the Estimation Work For?

A clear answer was not found for which scenarios the slip-detection concepts works best. The different slip detection concepts were not developed with specific scenarios in mind except that only longitudinal dynamics were considered in the process model. Most of the data logs used are fairly similar in that they consists of heavy acceleration starting from stand still and then either braking followed by more acceleration or braking to stand still. There are also several logs with some amount of turning while driving on e.g. an ice-track and also logs with attempts of drifting the vehicle.

One part in answering this is how to define when the estimation is working. One way is to only look at when the estimate is within the 4 % error limit. By looking at the positive slip partition and the braking partition of the data logs it can be seen that for some logs the estimate is kept within the error limit at all times. When looking at the descriptions of the logs (see Appendix A) it is not clear that the concepts only work for some particular scenario. Both concepts work for various cases of hard acceleration, calm driving and also driving with some turning and maneuvers. It is however clear that none of the methods works well with the drifting data logs as the high lateral dynamics has a large influence. It is also clear from some examples shown in the result section that the estimation can work well for most of a log until a particular problem is ran into. One example is in section 4.5.3 where concept 2 solves the challenging slip scenario in uphill where the vehicle is also decelerating because of the slip but in the end the concept fails to keep the speed within the limit when the vehicle is experiencing heavy yawing (lateral dynamics). Similarly, concept 1 for the same case also solves the particular case but the estimate is just outside the 4% error limit as slip is detected with a slight delay. Even though the speed estimate is not within the vision error limit, the error in the estimate is much lower than compared to the brake manufacturer.

Another part of the answer is basically that it is more a question of which scenarios

align with the slip-detection concepts the best and where the systems have gaps in the logic. If the slipping wheels are not successfully filtered out the speed estimate will degrade. As mentioned, the main limitations of the method is that the slip detection concepts does not cover all scenarios or cannot always detect slip correctly at all times, that the dead-reckoning might fail or drift and that the speed estimation strategy in braking does not keep the estimate within the error limit during extreme braking with wheels locking. These limitation are discussed in greater detail in section 5.1. Generally the method for speed estimation strategy works best in scenarios with straight line driving or with some turning and with relatively clear slip-events which means that the excessive slip happens quite abruptly such that it is easy to detect for the systems. Also, normal and hard braking is working fine but when the fastest wheel is much slower than the true speed the estimate will eventually degrade during braking. To summarize when the estimation method does not work well this is when the slip happens at a very low speed, when the slip is slow, when it is high lateral dynamics, when the torque is going on and off which makes it hard for concept 1 to detect slip and finally for concept 2 when the estimate has drifted and the speed is right outside the error limit.

5.3 Different Filters

Initially, three different filters were set up with slight variations of the states to see if there were any indications that one filter was performing significantly better. All filters consider the longitudinal speed and Euler pitch angle with the variations that filter V_xRP includes the Euler roll angle and that filter $V_x\dot{V}_xP$ includes the acceleration as a state. When testing the filters in combination with the slip detection concept 1, no significant difference was observed. As can be seen in Table 4.1 the performance of the filter and slip detection combinations are very similar. However, this testing is slightly ambiguous as it is not only the performance of the particular filter that is evaluated. It is the combination of how the filter and the slip-detection logic performs.

Out of the three filters, V_xRP keeps the speed estimate within the error limit for the most amount of the data logs for the hybrid car. A reason for this could be that this filter was used to develop the slip-detection concept 1. It might also be that taking the roll motion into consideration, the Euler pitch estimate gets slightly affected in the integration of the gyroscopes while turning or if the road is banking. Therefore this filter was chosen as the filter to compare the two slip detection concepts with. One thing that speaks against using this particular filter is that the Euler roll estimate is purely based on the integration of the gyroscopes which over time will make it drift. However this was not found to be a problem in this work as the gyroscope was bias-compensated and that the time periods the filter was running are relatively short. It was also found that the filter variations was hard to study in the excessive slip condition data and that it seemed to make a small impact on the estimation results. Therefore this particular investigation was not focused on.

5.4 About Offset Compensation

The gyroscope offset compensation was not made in a practically feasible way as a car might go for long time without stopping. In this time the biases would have changed so much that the initial offset would be inaccurate and the dead-reckoning capabilities would have reduced. Drift is a big problem and this needs to be further looked into in an real-world implementation. Additionally, this was not a part of the scope. However it was shown that only compensating the gyroscopes when standing still, the dead-reckoning performance with the used sensors was good and the accelerometer bias could be included in the Euler pitch-estimate, see section 3.4.5. In turn, the Euler pitch estimate is not very accurate as it is offset. Since the speed estimate is accurate, this could be used in a separate filter to estimate the true orientation in a similar manner. Also, it is questionable if this approach would work if equations relating several accelerometers would have been used in the process model. This is because the Euler pitch would then be related to the errors of several accelerometers and it is unclear if it would be possible to distinguish the different offsets in the different accelerometers.

5.5 Pointing out error in filter V_xRP

Late in the thesis it was realized that the filter V_xRP had a problem with stability of the covariance calculation. In certain combinations of states and inputs, the covariance was calculated with negative values. This was not detected as the filter seemed to perform well compared to the other filters as can be seen in Table 4.2. The reason for the negative covariance is not completely understood. In the following example it is described how the filter is more or less guaranteed to get negative values in the first step of prediction.

The covariance in the prediction step is calculated according to equation (5.1) where $\boldsymbol{F}$ is the Jacobian of the process model, $\boldsymbol{P}$ is the initial covariance and $\boldsymbol{Q}$ is the process noise.

$$\boldsymbol{P} = \boldsymbol{F}\boldsymbol{P}\boldsymbol{F}^T + \boldsymbol{Q} \tag{5.1}$$

In the initial step of the filtering, both $\boldsymbol{P}$ and $\boldsymbol{Q}$ are diagonal matrices. Let $\boldsymbol{P}$ be described as equation (5.2) where a, b, c are positive values.

$$\boldsymbol{P} = \begin{bmatrix} a & 0 & 0 \\ 0 & b & 0 \\ 0 & 0 & c \end{bmatrix} \tag{5.2}$$

In the simplified initial case when both Euler roll and pitch angles are assumed to be 0 the expression $\boldsymbol{F}\boldsymbol{P}\boldsymbol{F}^T$ have the following explicit expression.

$$\boldsymbol{F}\boldsymbol{P}\boldsymbol{F}^T = \begin{bmatrix} cT_s{}^2g^2 + a & \boldsymbol{T_s^2\,\omega_z\,c\,g} & T_s\,c\,g \\ \boldsymbol{T_s^2\,\omega_z\,c\,g} & cT_s{}^2\omega_z{}^2 + b & \boldsymbol{-T_s\,\omega_z\,(b-c)} \\ T_s\,c\,g & \boldsymbol{-T_s\,\omega_z\,(b-c)} & bT_s{}^2\omega_z{}^2 + c \end{bmatrix} \tag{5.3}$$

It can be seen in equation (5.3) that the elements marked in bold may be negative. This happens if either ω_z is negative or if ω_z is positive and $b < c$. The covariance matrix $\boldsymbol{P}$ should not be able to take negative values. This means that the filtering concept is fundamentally flawed. Negative covariance have no physical meaning. The filter flaw does an impact on the calculation of the Kalman filter gain matrix which in turns affect how the state estimates are updated with the wheel speed measurements. Though, the negative values in the covariance matrix did not seem to affect the estimate notably in a negative way. This could be because the Kalman gain is not used during dead-reckoning, as the IMU signals are directly input to the filter in the dead-reckoning step. Thus, the covariance matrix does not affect the estimate during these sequences.

The root of the problem was not further investigated. The authors believe that the problem perhaps could originate from either a linearization of a too non-linear function or that too many states involved in the Euler roll-equation are directly input in the prediction step. The solution might be to include other states and equations relating the different states in the filter or to simply put all IMU signals as measurements in the Kalman filter.

5.6 Future works

In this section, a summary of interesting future research topics are presented.

Introducing Additional Measurement of the Speed

If the main interest is to estimate the speed with the highest possible accuracy and robustness the authors think that introducing an alternative measurement of the speed would greatly improve the chances of providing a more robust estimate. This could be done by introducing other sensors as radars, cameras and GPS for example. This would increase the computational complexity. It would also introduce a problem of which of the methods should be trusted. The different methods mentioned also has its own flaws and specific use cases that has to be considered. For example, the GPS might have problems with the reception and cameras problem with exposure. The main idea however, is that by combining more sensor data, especially with alternative measurements of the speed, it is far less likely that all sensors fail at the same time.

Another possibility is to study if using several dead-reckoning processes from different IMUs could improve the speed estimation. At least errors in particular IMUs could possibly be detected.

Speed Estimation With Time-Delay or Improving the Speed Estimate by Going Back in Time.

As the detection with the current proposed methods tend to be slightly delayed, see beginning of examples in Figure 4.14, there will be a slight offset in the speed estimate as the wheels are trusted in the initiation of the slip. One thing that was

tested but was not included in the final version is to use this knowledge to further improve the estimate. With the current approach dead-reckoning is used to estimate the speed when all-wheel slip is detected. If the estimate prior to the all-wheel slip was good without an speed offset relative the true speed, then the idea is that it would be better to start the dead-reckoning from this point instead. This would eliminate the initial speed offset and any possible Euler pitch angle errors induced from the slight delay in the detection of the slipping wheel.

The reason this was not included in the proposed method is that it was not found a way to always be able to know if the speed estimate in every time step is close to the true speed of the car. It could be that the slip detection system does not detect any slip but the wheels currently are slipping with some percent. Then further increasing the dead-reckoning time by initiation a dead-reckoning from an earlier time could possibly decrease the amount of time the dead-reckoning can be made before it starts to drift outside the limit.

Alternatively a separate estimate with a time delay could be investigated. By introducing a time-delay it is believed that it would be possible to make better estimates about what the true speed is as more information is available. However, this introduces a time-delay in the estimate as well. Therefore this might not be feasible as the only speed estimate as a lot of systems is depending on what the speed is. Though, in situations with on-off slip that is hard to detect it might be a better option than an online estimation.

Developing a Way to Accurately Describe the Uncertainty in the Speed Estimate

With the current filter, the calculated covariance does not represent the accuracy or uncertainty of the speed estimate very well during dead-reckoning. What is meant is that the true speed can be outside the 3-σ region from the estimated speed. If this uncertainties were trusted by some system faulty decisions could be made. The authors believe it would be a good future work to try to accurately describe the uncertainty in the speed estimate.

Analysing the Effects of Feedback When the Estimate is Used in the Vehicle

Another interesting aspect that is left out in this thesis is to consider the feedback effects that occurs when the speed estimate is used by the systems in the vehicle. This could introduce unexpected challenges.

Investigating Dynamic Thresholds and Criteria for Detection of Slip

In the presented approach, all thresholds and conditions are fixed. It was shown to be a big challenge to set up different threshold that can cover all situations. Therefore an alternative way would be to introduce dynamically changing thresholds for determining slip. The threshold could perhaps be changing depending on speed or yawing. It could also be investigated how an approach that is based on dynamically

determining and changing uncertainties in the signals would affect the estimate. This might be advantageous in the mentioned grey-zones where the wheels are slipping slowly or are just around the error limit.

Also, the dynamics of tyres in slip conditions depends on load which also changes dynamically during driving. A correlation was looked at but it had very little linear dependency to fit the tyre dynamics curve and determine maximum torque or slip. It's effect over each tyre in different conditions could also be investigated further.

Use Machine Learning for Detection of Slip

Perhaps machine learning could be used in different ways to improve speed estimation. As it was found that it is hard to define and track when a wheel is slipping by hand, the authors believe that it could be possible to train a neural network, or similar, for the classification problem of deciding slip based on different input signals. This would allow for abstract patterns and rules in the data that a human finds it hard to detect.

Reversing and Lateral Dynamics Scenarios

Both reversing scenarios and scenarios with high lateral dynamics were not studied in this thesis. However, these scenarios are important to consider. The authors believe that a similar approach as presented in this thesis could be used in the reversing cases but, the low-speed cases might be a challenge as the wheel speed encoders does not provide an accurate measurement in low speeds. Also, for scenarios with high lateral dynamics, this needs to be considered in the process model.

Take Advantage of the Powertrain Torque and Friction Estimation

One slip indicator that was tested but not used in the final version of the slip-detection concepts is the max-torque estimation criteria presented in [13]. The presented version of the threshold is limited to all-wheel slip conditions as it is only at these times the utilized friction can be directly estimated with linear acceleration. It is also limited to axle-wise slip indication and will only indicate slip if torque is actively applied. The authors believe that this criteria would be more relevant if the individual wheel friction was estimated and if the powertrain torque was provided for individual wheel enabling for individual max torque estimation at all times. However, in winter road-conditions, the road-tyre-friction changes momentarily and also at an individual tyre level. Therefore this might not be very feasible. Alternatively, the torque level could probably be taken advantage of in a better way than presented in this thesis. This needs to be further investigated.

Study of Larger Data Set of Slip and Testing in CarMaker

If an approach similar to the one presented in this thesis is taken, the authors believe it is necessarily to study a larger data set with more examples of different types of slip. This is to try to identify different outlier scenarios and different types of slip

such that the logic is set up with a better understanding of what can happen. This could also be combined with a slip-detection indicator development and testing. If this had been to a further extent in this thesis, maybe it would have been detected earlier that the powertrain torque rate criteria only worked well for the hybrid vehicle data. Furthermore, if a large amount of data logs are not available, simulators like CarMaker could be used to set up different scenarios for testing and evaluating of the speed estimation strategy.

6

Conclusion

The presented approach for estimating speed in excessive all-wheel slip conditions proved successful in many situations and shows that it is possible to estimate the speed in line with the vision of keeping the estimate within ±4% of the reference speed. It was shown that both of the presented slip detection concepts can provide a good filtering out of the slipping wheel speed measurements. Particularly for the hybrid car where both methods perform considerably better than the brake-manufacturer estimate. It was also shown that only compensating the gyroscope bias when the car is standing still and letting the Euler pitch-estimate be offset with an amount corresponding to the accelerometer bias is a feasible approach to allow for accurate dead-reckoning of the accelerometer. Though, this only works for a limited time as the sensor biases drift over time. The online bias estimation problem needs to be considered in an real-world application.

However, the results show that the presented approach is not robust in keeping the estimate within the vision of ±4% of the reference speed. This mainly is a result of the complete reliance in the proposed slip detection system, which cannot detect slip for all situations. The difficulties in detecting slip partly lies in that it is hard to formulate a way of detecting slip throughout a slip-event, partly that many indicators of slip depend on the estimated quantities as the speed. This creates a circle dependency. It was found that the torque-rate criteria used in slip detection concept 1 did not work well for the fully electric car. The slip detection concept 2 on the other hand showed a more general functionality.

Furthermore, at the point of all wheel slip, the speed estimate is purely based on the dead-reckoning of the IMU signals. This process is in turns susceptible for errors in several ways, including sensor biases, gravity and model inaccuracies. The dead-reckoning on the other hand is what makes it possible to provide a good estimate of the speed during excessive slip but the process is limited by how well the states and biases are estimated. With the limitations mentioned it is hard to determine how well the speed can be estimated in such conditions. Though it was not studied in this work, the authors are convinced that utilising other sensors as radar, GPS or another sensor that can provide an absolute measurement of the speed of the vehicle independently of if the wheels slip would greatly improve the accuracy and robustness in the speed estimate in excessive all-wheel slip conditions.

Bibliography

[1] O. T. S. Ltd, *User manual rt3000 v3 and rt500 models*, English, version Revision: 200804, OxTS, 2020.

[2] X. Jin, G. Yin, and N. Chen, "Advanced estimation techniques for vehicle system dynamic state: A survey," *Sensors (Switzerland)*, vol. 19, no. 19, pp. 1–26, 2019, ISSN: 14248220. DOI: 10.3390/s19194289.

[3] S. Melzi and E. Sabbioni, "On the vehicle sideslip angle estimation through neural networks: Numerical and experimental results," *Mechanical Systems and Signal Processing*, vol. 25, no. 6, pp. 2005–2019, 2011, ISSN: 08883270. DOI: 10.1016/j.ymssp.2010.10.015. [Online]. Available: http://dx.doi.org/10.1016/j.ymssp.2010.10.015.

[4] S. Song, K. Min, J. Park, H. Kim, and K. Huh, "Estimating the Maximum Road Friction Coefficient with Uncertainty Using Deep Learning," *IEEE Conference on Intelligent Transportation Systems, Proceedings, ITSC*, vol. 2018-Novem, pp. 3156–3161, 2018. DOI: 10.1109/ITSC.2018.8569965.

[5] K. Saadeddin, M. F. Abdel-Hafez, M. A. Jaradat, and M. A. Jarrah, "Performance enhancement of low-cost, high-accuracy, state estimation for vehicle collision prevention system using ANFIS," *Mechanical Systems and Signal Processing*, vol. 41, no. 1-2, pp. 239–253, 2013, ISSN: 08883270. DOI: 10.1016/j.ymssp.2013.06.013. [Online]. Available: http://dx.doi.org/10.1016/j.ymssp.2013.06.013.

[6] J. H. Kim and S. W. Yoon, "Dual Deep Neural Network Based Adaptive Filter for Estimating Absolute Longitudinal Speed of Vehicles," *IEEE Access*, vol. 8, pp. 214 616–214 624, 2020, ISSN: 21693536. DOI: 10.1109/ACCESS.2020.3040733.

[7] L. Chu, Y. Shi, Y. Zhang, H. Liu, and M. Xu, "Vehicle lateral and longitudinal velocity estimation based on adaptive kalman filter," *ICACTE 2010 - 2010 3rd International Conference on Advanced Computer Theory and Engineering, Proceedings*, vol. 3, pp. 325–329, 2010. DOI: 10.1109/ICACTE.2010.5579565.

[8] H. F. Grip, L. Imsland, T. A. Johansen, J. C. Kalkkuhl, and A. Suissa, "Estimation of road inclination and bank angle in automotive vehicles," *Proceedings of the American Control Conference*, pp. 426–432, 2009, ISSN: 07431619. DOI: 10.1109/ACC.2009.5159912.

[9] T. Gustafsson and M. Jonasson, "Method and system for determining friction between the ground and a tire of a vehicle," EP3 309 024 A1, Apr. 2018.

[10] K. Kobayashi, K. Watanabe, and C. Science, "Estimation of Absolute Vehicle," no. June, pp. 1–5, 1995.

[11] U. Kiencke and L. Nielsen, *Automotive Control Systems For Engine, Driveline, and Vehicle*. Berlin Heidelberg: Springer, 2005.

[12] J. Farrelly and P. Wellstead, "Estimation of vehicle lateral velocity," *IEEE Conference on Control Applications - Proceedings*, pp. 552–557, 1996. DOI: 10.1109/cca.1996.558920.

[13] M. Klomp, Y. Gao, and F. Bruzelius, "Longitudinal velocity and road slope estimation in hybrid electric vehicles employing early detection of excessive wheel slip," *Vehicle System Dynamics*, vol. 52, no. SUPPL. 1, pp. 172–188, 2014, ISSN: 17445159. DOI: 10.1080/00423114.2014.887737. [Online]. Available: https://doi.org/10.1080/00423114.2014.887737.

[14] A. W. Barrowman and C. R. Aron, "Slip or loss of traction detector using the third dervative of rotational speed difference," US8,831,853B1, Sep. 2014.

[15] C. K. Song, M. Uchanski, and J. K. Hedrick, "Vehicle speed estimation using accelerometer and wheel speed measurements," *SAE Technical Papers*, no. March, 2002, ISSN: 26883627. DOI: 10.4271/2002-01-2229.

[16] H. Ahmed and M. Tahir, "Accurate Attitude Estimation of a Moving Land Vehicle Using Low-Cost MEMS IMU Sensors," *IEEE Transactions on Intelligent Transportation Systems*, vol. 18, no. 7, pp. 1723–1739, 2017, ISSN: 15249050. DOI: 10.1109/TITS.2016.2627536.

[17] K. Tin Leung, J. F. Whidborne, D. Purdy, and A. Dunoyer, "A review of ground vehicle dynamic state estimations utilising GPS/INS," *Vehicle System Dynamics*, vol. 49, no. 1-2, pp. 29–58, 2011, ISSN: 00423114. DOI: 10.1080/00423110903406649.

[18] K. Berntorp, "Particle filter for combined wheel-slip and vehicle-motion estimation," *Proceedings of the American Control Conference*, vol. 2015-July, pp. 5414–5419, 2015, ISSN: 07431619. DOI: 10.1109/ACC.2015.7172186.

[19] J. Lv, H. He, W. Liu, Y. Chen, and F. Sun, "Vehicle velocity estimation fusion with kinematic integral and empirical correction on multi-timescales," *Energies*, vol. 12, no. 7, 2019, ISSN: 19961073. DOI: 10.3390/en12071242.

[20] D. M. Bevly, J. C. Gerdes, and C. Wilson, "The Use of GPS Based Velocity Measurements for Measurement of Sideslip and Wheel Slip," *Vehicle System Dynamics*, vol. 38, no. 2, pp. 127–147, 2002, ISSN: 00423114. DOI: 10.1076/vesd.38.2.127.5619.

[21] S. L. Miller, B. Youngberg, A. Millie, P. Schweizer, and C. Gerdes, "Calculating longitudinal wheel slip and tire parameters using GPS velocity," *Proceedings of the American Control Conference*, vol. 3, pp. 1800–1805, 2001, ISSN: 07431619. DOI: 10.1109/acc.2001.945995.

[22] X. Ding, Z. Wang, L. Zhang, and C. Wang, "Longitudinal Vehicle Speed Estimation for Four-Wheel-Independently-Actuated Electric Vehicles Based on Multi-Sensor Fusion," *IEEE Transactions on Vehicular Technology*, vol. 69, no. 11, pp. 12 797–12 806, 2020, ISSN: 19399359. DOI: 10.1109/TVT.2020.3026106.

[23] M. O. Aqel, M. H. Marhaban, M. I. Saripan, and N. B. Ismail, "Review of visual odometry: types, approaches, challenges, and applications," *SpringerPlus*, vol. 5, no. 1, 2016, ISSN: 21931801. DOI: 10.1186/s40064-016-3573-7.

[24] R. Ghabcheloo and S. Siddiqui, "Complete Odometry Estimation of a Vehicle Using Single Automotive Radar and a Gyroscope," *MED 2018 - 26th Mediterranean Conference on Control and Automation*, pp. 855–860, 2018. DOI: 10.1109/MED.2018.8442474.

[25] V. Cevher, R. Chellappa, and J. H. Mcclellan, "Acoustic Wave Patterns," vol. 57, no. 1, pp. 30–47, 2009.

[26] M. Lindfors, G. Hendeby, F. Gustafsson, and R. Karlsson, "Vehicle speed tracking using chassis vibrations," *IEEE Intelligent Vehicles Symposium, Proceedings*, vol. 2016-Augus, no. Iv, pp. 214–219, 2016. DOI: 10.1109/IVS.2016.7535388.

[27] I. Skog, J.-O. Nilsson, and P. Händel, "An open-source multi inertial measurement unit (mimu) platform," in *2014 International Symposium on Inertial Sensors and Systems (ISISS)*, 2014, pp. 1–4. DOI: 10.1109/ISISS.2014.6782523.

[28] S. Särkka, *Bayesian Filtering and Smoothing*. Cambridge: Cambridge University Press, 2013.

[29] I. Ben-Gal, "Bayesian networks," in *Encyclopedia of Statistics in Quality and Reliability*. American Cancer Society, 2008, ISBN: 9780470061572. DOI: https://doi.org/10.1002/9780470061572.eqr089. eprint: https://onlinelibrary.wiley.com/doi/pdf/10.1002/9780470061572.eqr089. [Online]. Available: https://onlinelibrary.wiley.com/doi/abs/10.1002/9780470061572.eqr089.

[30] R. E. Kalman, "A New Approach to Linear Filtering and Prediction Problems.," *Transactions of the ASME, Journal of Basic Engineering*, vol. 82(1), pp. 35–45, 1960. DOI: https://doi.org/10.1115/1.3662552.

[31] P. Zarchan and H. Musoff, *Fundamentals of kalman filtering : A practical approach*. American Institute of Aeronautics and Astronautics, 2000, ISBN: 9781600867187.

[32] P. Corke, *Robotics, Vision and Control*. Springer, Cham, 2017, ISBN: 978-3-319-54412-0. DOI: https://doi-org.proxy.lib.chalmers.se/10.1007/978-3-319-54413-7.

[33] V. M. Tereshkov, "A simple observer for gyro and accelerometer biases in land navigation systems," *Journal of Navigation*, vol. 68, no. 4, pp. 635–645, 2015, ISSN: 14697785. DOI: 10.1017/S0373463315000016.

[34] H. B. Pacejka, *Tyre and Vehicle Dynamics*. 2012. DOI: 10.1016/B978-0-08-097016-5.00002-4.

[35] R. Rajamani, *Lateral Vehicle Dynamics and Control*. 2016, pp. 135–181, ISBN: 9781461414322. DOI: 10.1002/9781118380000.ch5.

[36] J. Diebel, *Representing attitude: Euler angles, unit quaternions, and rotation vectors*, 2006.

[37] M. Jonasson, Å. Rogenfelt, C. Lanfelt, J. Fredriksson, and M. Hassel, "Inertial Navigation and Position Uncertainty during a Blind Safe Stop of an

Autonomous Vehicle," *IEEE Transactions on Vehicular Technology*, vol. 69, no. 5, pp. 4788–4802, 2020, ISSN: 19399359. DOI: 10.1109/TVT.2020.2971667.

[38] L. Xiong, X. Xia, Y. Lu, W. Liu, L. Gao, S. Song, Y. Han, and Z. Yu, "IMU-based automated vehicle slip angle and attitude estimation aided by vehicle dynamics," *Sensors (Switzerland)*, vol. 19, no. 8, 2019, ISSN: 14248220. DOI: 10.3390/s19081930.

[39] C. Lanfelt and Å. Rogenfelt, *Dead reckoning during safe stop of autonomous vehicles*, 2017.

A

Appendix 1

Table A.1: Description of data logs for hybrid vehicle. All logs are from low-friction conditions in winter driving.

Data Log	Description
HY1	Straight acceleration and ABS braking without ESC, main ice track.
HY2	Attempts to drift without ESC, main ice track.
HY3	Half a lap on main ice track without ESC.
HY4	Without ESC high acceleration, constant speed, deceleration, main ice track.
HY5	Spin in uphill, road from main ice track.
HY6	Spin in downhill, road from main ice track.
HY7	More aggressive driving (some drifting) on circular track, anti-clockwise, ESC off.
HY8	Acceleration without ESC on ice track.
HY9	Acceleration deceleration and various maneuvers also without ESC, partly ice.
HY10	Dito with ESC.
HY11	Dito with ESC.
HY12	Acceleration and deceleration with ESC but "traction control temporarily unavailable".
HY13	Calm driving around main track for offset compensating, then platform safe stop.
HY14	AD driving on main track, manual intervention.
HY15	AD driving on main track, manual intervention, reactivation of AD.

Table A.2: Description of data logs for fully electric vehicle. All logs are from low-friction conditions in winter driving.

Data Log	Description
FE1	Slip in 20% hill incline
FE2	Hills with varying incline (±15%)
FE3	Throttle tip on ice road
FE4	Throttle tip on snow road
FE5	Handling track calm
FE6	Handling track calm
FE7	Handling track calm
FE8	Throttle tip and braking
FE9	Hills with varying incline
FE10	Straight acceleration and braking

DEPARTMENT OF MECHANICS AND MARITIME SCIENCES
CHALMERS UNIVERSITY OF TECHNOLOGY
Gothenburg, Sweden 2021
www.chalmers.se

CHALMERS
UNIVERSITY OF TECHNOLOGY

CHALMERS
UNIVERSITY OF TECHNOLOGY

Vehicle Speed Estimation During Excessive Tyre Slip Using GPS Data and Slip Estimation

Developing two approaches - one with modelled GPS data and one with vehicle dynamics based slip-detection

Master's thesis in Automotive Engineering

DILER GANATRA

DEPARTMENT OF MECHANICS AND MARITIME SCIENCES

CHALMERS UNIVERSITY OF TECHNOLOGY
Gothenburg, Sweden 2021
www.chalmers.se

MASTER'S THESIS IN AUTOMOTIVE ENGINEERING

Vehicle Speed Estimation During Excessive Tyre Slip Using GPS Data and Slip Estimation

Developing two approaches - one with modelled GPS data and one with vehicle dynamics based slip-detection

DILER GANATRA

Department of Mechanics and Maritime Sciences
Division of Vehicle Engineering and Autonomous Systems
CHALMERS UNIVERSITY OF TECHNOLOGY

Göteborg, Sweden 2021

Vehicle Speed Estimation During Excessive Tyre Slip Using GPS Data and Slip Estimation
Developing two approaches - one with modelled GPS data and one with vehicle dynamics based slip-detection
DILER GANATRA

Master's thesis 2021:18
Department of Mechanics and Maritime Sciences
Division of Vehicle Engineering and Autonomous Systems
Chalmers University of Technology
SE-412 96 Göteborg
Sweden
Telephone: +46 (0)31-772 1000

Industrial Supervisors at Volvo Cars

Derong Yang, Fredrik Broström, Martin Hassel

University Examiner and Supervisor

Mats Jonasson, Department of Mechanical Engineering and Maritime Sciences

Cover:
A vehicle driven on icy roads,representing the scenarios in which the project is set for vehicle speed estimation.
Creative commons from Unsplash

Chalmers Reproservice
Göteborg, Sweden 2021

Vehicle Speed Estimation During Excessive Tyre Slip Using GPS Data and Slip Estimation
Developing two approaches - one with modelled GPS data and one with vehicle dynamics based slip-detection
Master's thesis in Automotive Engineering
DILER GANATRA
Department of Mechanics and Maritime Sciences
Division of Vehicle Engineering and Autonomous Systems
Chalmers University of Technology

Abstract

With the advent of autonomous driving cars, the data fed to the autonomous brain is of utmost importance with vehicle speed being one of the more crucial data. Vehicle speed can be estimated with a standard sensor suite equipped in a modern car that includes IMU, wheel speed sensors, steering angle sensor, powertrain and brake torque. When the wheels slip excessively however, they can not be used to represent the true speed of the vehicle and thus the onus falls on dead-reckoning of the IMU. In the precursor thesis work, vehicle speed estimation during excessive wheel slip was based on a kinematics approach designed with an Extended Kalman Filter. To detect the slipping wheels and filter them out from the input, two slip detection concepts were developed. The first approach used static thresholds for slip indicators such as torque rate and wheel-car acceleration difference. However, since the thresholds to detect slip were static, it was highly prone to missing or incorrectly assuming slip on wheel. The second approach was prone to missing slipping wheels when slip would increase slowly. The work in this project now is based on improving these methods by two different ways and analyzing the improvement in the estimate. The first approach is to introduce a GPS speed signal as another measurement of speed to trust in case all wheels slip and their speeds can't be used. This reduces the burden on dead-reckoning at all times. The second approach utilizes the limited sensor suite to develop a new slip detection concept that is dynamic and that estimates the slip ratio at each time instant. The development and testing is done a large AWD hybrid for which excessive wheel slipping data from real-world driving is logged and provided. The results are promising in terms of improvement. Both approaches improve the speed estimation when compared to the previous method as well as the brake manufacturer Volvo's wheel speed based simple estimate. It keeps an even larger share of the data log's speed estimate within ±4% error limit. The new methods are better on average over all data logs as well as individual data logs however it does not solve all data logs 100% of the time. The speed estimation methods in this case also provide a comparison analysis from the previous methods.

Keywords: Vehicle speed estimation, wheel slip estimation, GPS speed, slip detection, slip ratio, vehicle state estimation, extended Kalman filter, vehicle dynamics

Preface

This continuation of thesis work development was conducted at Chalmers University of Technology's Vehicle Engineering and Automation Systems department. This work was done in collaboration with Volvo Cars Corporation's Vehicle Energy and Motion Control department in Göteborg, Sweden. The work was carried out during the Summer of 2021. The problem of improving velocity estimations developed in the thesis was an interesting challenge. I would like to thank Chalmers as well as Volvo Cars for giving me the opportunity to work on this topic.

Acknowledgements

Firstly, I would like to thank my academic examiner and mentor Mats Jonasson for his dedicated support, time and wealth of knowledge shared during this work. His expertise in this field and readiness to guide me during crucial stages of the work was truly helpful.

I would like to extend my gratitude to my industrial supervisors at Volvo Cars - Derong Yang, Fredrik Broström and Martin Hassel for their continued support throughout this work, giving insights and advice from experience as well as expertise in this field.

It was a great experience to be working on such an interesting topic at Volvo Cars and I am grateful to be able to learn from the best in the industry. Thank you for putting your trust in me and believing in me all throughout this work.

Finally, I would like to thank my friends and family without whom this work would never have come to fruition. I would like to express immense gratitude to my parents who have been understanding, patient and supportive during this thesis work to make working on this much easier and comfortable.

Contents

List of Figures

List of Tables

1 Introduction

The modern fleet of vehicles comes equipped with various degrees of Autonomous Driving (AD) systems and Advanced Driver Assistance Systems (ADAS). Running these systems in vehicles calls for better and more robust control systems. Most of the AD and ADAS systems safeguard are safety-critical to vehicle, occupant and pedestrian safety alike; making the systems that control it, equally important. Thus, the information fed to these systems from estimated states and sensors must be accurate at all times. Vehicle speed is one of the most important inputs to these systems, making it a critical quantity that needs to be known accurately in all situations. Any significant deviation in the estimated vehicle speed from the true speed can compromise the functionality of the systems and hinder their ability to make the correct decisions.

A standard sensor suite on a modern car includes an Inertial Measurement Unit (IMU), sensors that measure wheel speeds, steering wheel angle, powertrain torques and brake torques. This data, along with a vehicle motion model form the basis of vehicle speed estimation. Driving on high grip surfaces with no or low tyre slip, wheel speed sensors can be trusted to give vehicle speed measurements very close to the true speed. However, while driving on slippery surfaces like snow or ice with low friction, the wheel speeds start spinning in acceleration and lock under braking scenarios. Here, the wheel speed measurements are far off from the true speed of the vehicle and cannot be used to estimate vehicle speed.

From the research carried out during the thesis work [1], it was found that during all-wheel slip conditions, the solution is to rely on dead reckoning the acceleration from the IMU. However, this is not a viable solution for longer duration of slip as the IMU is susceptible to drift due to the integration of errors. This makes it important to know the current state of the wheels and when they can be trusted to help limit the use of dead reckoning. The thesis work [1] thus focused on developing two slip detection concepts - one utilizing slip indicating parameters and the other using wheel speed variances. These concepts were used in combination with a kinematic based vehicle motion model for estimating the forward velocity of a vehicle being driven in extreme all-wheel slip inducing conditions.

The lack of direct, on-board speed measurement sensors is one of the limitations for vehicle speed estimation methods developed in [1]. Wheel speeds are the only direct measurement of speed which, in all-wheel slip conditions cannot be trusted. Another limitation lies in the slip detection concepts. The first slip detection concept utilizes two parameters with static thresholds to indicate slip. A static threshold means that it does not change with dynamic conditions road conditions and driving maneuvers, which means that the thresholds don't hold in all cases. So, a change in any of those would mean that wheel slip could be missed or incorrectly assumed. The second slip detection concept uses variances in errors generated by the difference between wheel speed and estimated speed. This concept is susceptible to incorrect slip detection when wheel slip increases slowly or when the wheel variance falls but not below the error limit, making the concept incorrectly assume slip. Also, the slip ratio calculation used in this concept uses the estimated speed which does not always give an accurate value.

Now, this continued development of precursor thesis work [1] focuses on developing two new speed estimation methods that improve upon the previous ones. The first limitation is tackled by introducing a secondary measurement of speed - a modelled GPS speed signal that is used along with the previously developed slip detection concept. Using the same slip detection concepts help to keep the number of variables in the method low, and help to understand how improvements in speed estimation can be made just by introducing a new speed measurement. The limitations in the slip detection concepts are tackled with a completely new, dynamic slip detection and wheel selection strategy without using the modelled GPS speed signal. The modelled GPS speed is not used to keep the number of variables in the method low, which helps in understanding the true improvement over the previous methods. The kinematics model from the thesis work is used for its lower complexity and requirement than a vehicle dynamic model. This work is carried out at Volvo Cars' Vehicle Energy and Motion Control department who also provided real-world driving data.

1.1 Related Research

During the precursor thesis work [1] , an intensive research on various ways developed to estimate velocity was carried out. Section 1.2 from the thesis report [1] talks in detail about the relevant research papers and it's contribution to the vehicle speed estimation methods. It talks about the various kinematics and dynamic

models, use of different sensor setups as well as different sensors. Research based on using GPS speed data, visual odometry as well as RADAR and LiDAR is also presented. The reader is referred to [1] for more information.

INS and GNSS measurements can be fused and provide more accurate estimations of vehicle states as velocity compared to dead reckoning of IMU. The drawbacks with GPS is, among other things, the risk of the signal being interrupted from surrounding objects as buildings and slow update frequency [2].

GPS can also be used to improve the estimation of other vehicle states. [3] showed the feasibility of estimating wheel slip, body slip and tyre side slip angle using GPS vehicle velocity measurements. The wheel slip was estimated by comparing the GPS velocity to the wheel speed sensors which also allows for tyre radius estimation. Vehicle side slip angle was measured as the difference between vehicle heading (integration of gyro or dual antenna GPS) and direction of travel from GPS. tyre slip angle was measured as the difference between tyre direction translated from the GPS velocity and the tyre longitudinal axis relative the car.

[4] further demonstrated how GPS measurements can enable estimation of longitudinal stiffness of the tyres. This in combination with the effective tyre radius and wheel speed can be used to completely specify the linear part (low amount of slip) of the force-slip curves referred to as "the Magic formula" [5].

[6] present an enabling multi-sensor fusion-based estimation of longitudinal speed for a four wheel drive EV. The sensors used are GPS in tandem with Beidou Navigation Positioning (GPS-BD) module, and a low-cost IMU. The consequence of gravity/road inclination in the acceleration signal is compensated for by combing the wheel speed sensor and the GPS-BD information. A multi-sensor fusion-based estimation method is implemented "by employing three virtual sensors which generate three longitudinal vehicle speed tracks based on multiple sensor signals". The results show promising estimations of vehicle speed under low friction surfaces, sloped roads, hard acceleration and braking conditions. The method shows good robustness and real-time performance.

[7] proposed a solution that uses a single band antenna that measure the carrier phase outputs tightly integrated with IMU and wheel speed sensors. Real world testing indicated that the technique could make the error growth slow enough for accurate position estimation for about 10 seconds.

These solutions require accurate GPS measurements of position and velocity from real world driving which are not available in the data logs received during the previous work. However, some data logs from highway driving on asphalt roads on the E6 route which included a few tunnels were later provided for this work. The GPS speed measurement was logged for these files, which provided the basis to model a similar GPS speed signal with added noise and update frequency from reference velocity measured by the OxTS for all the excessive slip data logs supplied for development. This modelled GPS speed is used as a secondary speed measurement to the kinematic based Extended Kalman Filter(EKF) for vehicle speed estimation when all wheels are detected to be slipping. These studies below give an idea of how the GPS speed standard deviations and mean errors should behave and help in assessing the errors in the GPS speed measurements provided.

Error differences between a tracking point GNSS and a doppler shift GNSS module are explained in [8]. A GNSS module tracking satellites that uses doppler shift phenomenon to estimate the moving speed of a target satellite has an error of 0.238 km/h for speeds upto 1800 km/h. An increase in Position Dilution of Precision values as it loses connection to satellites that help to estimate velocity due to weather leads to marginal increase in average errors (0.254 km/h for speeds upto 1800 km/h).

The errors of a GPS speeds based on doppler shift is also shown to be significantly low for vehicles driven on vegetative and uneven lands in [9]. Their study shows that the errors in speed output from a GPS module mounted on a vehicle driven at steady state speeds between 3 and 9 mph have a maximum error of only 0.08 mph over different surfaces. However, the GPS module suffers from speed errors in dynamic driving conditions such as acceleration and deceleration mainly due to it's update frequency being too slow at 4 Hz. In acceleration, the maximum speed error in acceleration at 1 m/s^2 was 2.7 mph. The peak error was higher for deceleration of 1 m/s^2 at 4 mph.

[10] compared five different GPS devices attached to a vehicle driven on highway roads. It was found that a GPS module calculating speed using doppler effect at an update frequency of 1 Hz has fairly low errors at constant speeds of 50 to 70 km/h. The peak error at very low speed of 3 km/h was 1 km/h. During rapid acceleration, the standard deviation of error was roughly 5 km/h at 50 km/h, while during rapid decelerations from 50 to 0 km/h, the standard deviation was upto 10 km/h.

[11] compared 4 GPS modules based on costs. The cheapest GPS module was a 1 Hz receiver costing $ 75. This was attached to a hatchback car and driven around the roads of Melbourne including city driving amidst high rise buildings, tunnels, highway driving, under passes and over passes. At relatively good Horizontal Dilution of Precision (HDOP) <= 1, the standard deviation of speed error was 0.7 km/h ranging up to 4.4 km/h at higher HDOPs. It also states that HDOP is an industry standard value to determine if the GPS data is accurate or not.

[12] compared GPS modules with frequencies of 1 Hz, 5 Hz and 7 Hz. It was found that at extremely low constant speeds of 2 mph for 1 Hz GPS, the mean error was 0.08mph while it increased in acceleration and deceleration cases. In acceleration, it was found that the GPS speed was always slower than the reference and in braking, faster than the reference due to latency and low update frequency.

Estimation of longitudinal velocity of the vehicle is based on two fuzzy logic controllers in [13]. Wheel speed sensors are used with one fuzzy logic control to estimate the speed. The wheel speed sensor output is translated and a dynamic tyre radius change factor is introduced. This is used to calculate the slip ratio based on the slowest wheel speed sensor data and the speed estimate. The fuzzy logic controller then decides the confidence given to each wheel speed measurement like a slip detection system and estimates the speed. The accelerometer data is integrated to gain a second speed estimate. The second fuzzy logic controller takes both these speed estimates as input and using a weight factor, decides which estimate to trust.

[14] develops a slip detection and slip ratio estimator for a small single-seat, fully electric vehicle with motors in each wheel. This is used to estimate velocity and for slip control. They estimate wheel slip ratio based on differentiating the slip ratio equation. Then, this estimated slip ratio is used as an input to the wheel slip indicator that detects whether the wheels are slipping using a recursive least squares method. Along with this, torque thresholds and acceleration thresholds are set as another indicator of slip. [15] uses a similar technique to estimate the slip ratio. Their work estimates slip ratio based on a differentiating the equation of slip ratio, utilizing different tyre parameters, torque inputs and wheel speeds for an autonomous 4 Wheel Drive electric race car. Instead of using other indicators of slip, they use this slip ratio as a state in a kalman filter. The equation for slip ratio estimation studied in this paper and the torque thresholds and acceleration thresholds from **thesis** and [14] create the foundation for the developed method in this work.

1.2 Objective and Purpose

The primary objective of this work is to improve upon the previously developed vehicle speed estimation methods in excessive all - wheel slip conditions via different approaches and analyze it's performance gains.[1]. The focus is on utilizing two different strategies. The first strategy is to introduce a modelled GPS speed signal to be used as a secondary speed measurement in all wheel slip conditions. This is used in combination with slip detection Concept 2 with a modified kinematics-based V_xRP filter (which is the best performing combination, [1]) for vehicle speed estimation. The second strategy is to develop a new slip detection system with braking logic, only by using the available on-board sensors - IMU, wheel speeds, steering angle, powertrain and brake torque sensors. The new system is more dynamic and capable of estimating slip at each time-step. This system is used with the V_xRP filter. The development and testing of these approaches will be done on real-world driving data provided by Volvo for the large AWD hybrid vehicle.

The vision set during the thesis work is the same for this complementary work as well. The vision of this work is to develop longitudinal velocity estimation methods that can estimate the speed of the vehicle in extreme, all-wheel slip conditions especially. The goal is to achieve estimation errors that are less than $\pm 4\%$ of the ground truth for 99% of the time, avoiding extreme outliers. The speed estimation method should also be feasible enough in the real-world to use on-board with low latency / lag estimates. The speed should also be estimated without considerable time-delay to provide an online speed estimate.

The two methods developed in this work are based on the analysis carried out during the precursor thesis work and the future work suggestions to improve the estimation method. The purpose of this work is now to develop the two methods. Since these methods were expected to make the speed estimation better, an acceptable outcome would be that the two new methods perform better than the previous methods overall in all conditions ranging from nominal to extreme slip, even though it might not work for some data logs or cases at all times.

1.3 Scope and limitations

The scope and limitations of this work rests majorly upon the same limitations set during the thesis work apart from a few limitations in the new methods developed.

This continued development to the precursor thesis work focuses on developing vehicle speed estimation method/s that is accurate and better than the ones developed in [1]. The vehicle speed is only considered in the longitudinal direction while lateral dynamics are ignored, along with data logs containing scenarios with high lateral motion of the vehicle. The speed estimation is done for speeds ranging between 10 and 120 km/h. Reversing scenarios are also omitted. Online estimations of tyre radius, tyre stiffness and bias/offsets of the IMU are not considered. Data logs that contain all-wheel slip for greater than 20 seconds are also ignored. The hybrid vehicle data logs had multiple IMUs, however it is assumed that just one IMU is enough to give accurate data about the vehicle's accelerations and orientation rates. GPS speed signal is modelled based on literature review and the data available. New data has not been collected for extreme slip cases with a GPS module. Comparison of the new methods is done only with V_xRP filter with Concept 2 among the previously developed methods since it was the best performing filter-concept combination.

2 Theory

In this chapter, the background knowledge and theory applied in the vehicle speed estimation is very briefly listed and explained. This includes an explanation of Bayesian filtering, kalman filters, sensors and tyre dynamics. For in depth knowledge about the theory of these topics, the reader is referred to the previous thesis work Chapter 2 [1].

2.1 Bayesian Filtering and Kalman Filters

Bayesian Filtering is a fundamental technique used for estimating the states of time-varying system where the true quantity of the state at time k is denoted as $\boldsymbol{x_k}$. The true quantity however is unknown to an outside observer, who can only measure these states via noisy outputs from the sensors in the system denoted as $\{\boldsymbol{y_1}, \boldsymbol{y_2}..., \boldsymbol{y_k}\}$. The end goal is to filter out this noise in the measurements and arrive at the true state quantity at time k, given the previous measurements and the evolution of the system defined via a dynamic state space model. Thus the main goal of any filtering algorithm, including Bayesian filtering is to model the believed state quantity on the previous state, noisy observations, and any control input to the system. Bayesian filtering does this using a mathematical approach for conditional probability or a statistical inversion problem [16].

2.1.1 Probabilistic State Space Models

In Bayesian filtering, the time-varying system of interest is described using a probabilistic state space model [16]. The goal is here to estimate the distributions of the states given the measurements from the sensors. The estimation of the state is divided into two parts. One is the process model, equation (2.1) that predicts the next state via a dynamic equation, based on the actions done upon the system and the previous state. The measurement model, equation (2.2) defines how the observation or sensor output affects the next state.

$$\boldsymbol{x_k} = f_{k-1}(\boldsymbol{x_{k-1}}, \boldsymbol{u_k}, \boldsymbol{q_{k-1}}) \sim p(\boldsymbol{x_k}|\boldsymbol{x_{k-1}}; \boldsymbol{u_k}) \tag{2.1}$$

$$\boldsymbol{y_k} = h_k(\boldsymbol{x_k}, \boldsymbol{u_k}, \boldsymbol{r_k}) \sim p(\boldsymbol{y_k}|\boldsymbol{x_k}; \boldsymbol{u_k}) \tag{2.2}$$

To understand how these equations work together for recursive state estimation, how a Hidden Markovian Model describes the filtering process and the final set of equations for Bayesian filtering with a flow model, the reader is directed to the precursor thesis work [1].

2.1.2 Kalman Filter

Bayesian Filtering is fundamental tool for recursive state estimation and filtering solutions. Kalman Filter is special case of Bayesian filtering where the process or dynamic model and the measurement or sensor model are linear Gaussian. A Kalman filter in a way works by making the predictions and the observations linear about their mean values and all distributions are Gaussian. The Kalman filter [17] can also be defined as a closed form solution to the bayesian filtering equations where the process and measurement models are linear Gaussian [16]. The Kalman filter's ability to provide optimal solutions using the fundamentals of Bayesian filtering makes it a popular choice in state estimation problems [18]. Below are the equations that constitute a Kalman filter. It's derivations can be found in [16] and [18].

A linear Gaussian state space model can be depicted as (2.3).

$$\begin{aligned} \boldsymbol{x_k} &= \boldsymbol{A_{k-1}}\boldsymbol{x_{k-1}} + \boldsymbol{B_{k-1}}\boldsymbol{u_k} + \boldsymbol{q_{k-1}} \\ \boldsymbol{y_k} &= \boldsymbol{H_k}\boldsymbol{x_k} + \boldsymbol{r_k} \end{aligned} \tag{2.3}$$

Where, $\boldsymbol{A}$ is the state transition matrix that defines the dynamic evolution of the states, $\boldsymbol{B}$ is the control input matrix while $\boldsymbol{H}$ is the measurement matrix that describes how the sensor outputs relate to the states. The noise in both models is designed to be zero-mean Gaussian distributed.

To understand these equations and how they constitute a Kalman Filter's prediction and update steps, as well as an explanation excerpt from the precursor thesis work [1] explains how these equations are utilized together to form a linear kalman filter.

2.1.3 Extended Kalman Filter

The Kalman filter described above is mainly used for linear systems (process and measurement models). To estimate the states of a non-linear system, some changes need to made. The extended Kalman filter (EKF) is a modified version of the linear Kalman filter that works for non-linear models [16]. The fundamental principles remain the same, however the non-linear system is linearized to an "approximately" linear system. This however only works if the system as a whole is non-linear but is still locally linear, allowing the system to be approximated via a Taylor expansion series of order 1. Also, unlike a linear kalman filter, the output of an EKF is not the true value but a Taylor Series approximation of the value.

A time varying system (process and measurement model), defined by non linear functions f and h is first linearized about it's mean amd given by the equation (2.4) where $\boldsymbol{F}$ and $\boldsymbol{H}$ are the Jacobian transformations of the functions non-linear functions. .

$$\begin{aligned} \boldsymbol{x_k} &= \boldsymbol{f}(\boldsymbol{x_{k-1}}, \boldsymbol{u_k}) + \boldsymbol{q_{k-1}} \approx \boldsymbol{f}(\hat{\boldsymbol{x}}_{\boldsymbol{k-1|k-1}}, \boldsymbol{u_k}) + \boldsymbol{F}(\hat{\boldsymbol{x}}_{\boldsymbol{k-1|k-1}}, \boldsymbol{u_k})(\boldsymbol{x_{k-1}} - \hat{\boldsymbol{x}}_{\boldsymbol{k-1|k-1}}) + \boldsymbol{q_{k-1}} \\ \boldsymbol{y_k} &= \boldsymbol{h}(\boldsymbol{x_k}) + \boldsymbol{r_k} \approx \boldsymbol{h}(\hat{\boldsymbol{x}}_{\boldsymbol{k|k-1}}) + \boldsymbol{H}(\hat{\boldsymbol{x}}_{\boldsymbol{k|k-1}})(\boldsymbol{x_k} - \hat{\boldsymbol{x}}_{\boldsymbol{k|k-1}}) + \boldsymbol{r_k} \end{aligned} \tag{2.4}$$

To understand more about the process model and measurement update steps that combine to form the EKF, the reader is guided to the previous thesis work [1].

2.2 Sensors

A short overview of the sensors that were used to log the data used in this work is presented below. For further details about the sensor's working and errors, the reader is referred to the previous thesis work [1].

2.2.1 Inertial Measurement Unit

An Inertial Measurement Unit or IMU for short, is a module that is used to measure the accelerations and angular rates of a body. IMU in itself contains accelerometers, gyroscopes and in some cases, a magnetometer. An accelerometer is a sensor that measures accelerations. Each accelerometer measures acceleration along one direction, so three accelerometers aligned in X,Y and Z direction can be used together to measure the body's longitudinal, lateral and vertical accelerations. A gyroscope is device that measures rate of orientation of a body i.e. for a car, it's yaw, roll and pitch rate. The device is mounted around a rotation axis which when changes it's orientation, induces a moment in the opposite direction which allows it to maintain it's own orientation. This counter moment can be used to gives angular rates of a body.

2.2.2 Wheel Speed Sensors

A wheel speed sensor is in essence a tachometer. The working principle is based a rotary encoder. The sensor is attached to the drive axle connecting the wheels which has a disc with cutouts or "teeth". The number of teeth it passes through are recorded. This number when divided by a unit time quantity gives the angular speed of the wheel. The advantage of these sensors is that it the measurements are not biased or affected by road surface, banks or inclinations. The wheels speeds however can give erroneous readings while turning as the the speed is measured for wheels spinning in the plane parallel to the ground, or at low speeds when the distance between the "teeth" is too much (or it's resolution is too less). [19].

2.2.3 Steering Wheel Angle Sensor

A steering wheel angle sensor outputs the wheel angle. This angle is the direction in which the front wheels (usually steered) are pointing. The sensor is based on hall effect for eg: optical sensors mounted on the steering axis. Since these sensors are safety critical to know the motion and dynamics of the car at each time, there are usually multiple steering wheel angle sensors for redundancy and accuracy.

2.2.4 Powertrain Torque

Torque sensors measure the torque that is applied from the driveline to the wheel used to the drive the vehicle. The sensors could either use angular displacements or transducers that work as a strain gauge, use Software

Acoustic Waves or a few other techniques. However, using these sensors is tricky due to packaging constraints in the complex powertrain design. Torque is also often estimated using other sensors such as fuel and air flow rate sensor, engaged gears and others. The accuracy however may vary due to the subjected temperature and vibrations and large relative motions in the powertrain. This may induce a lot of errors and noise in the outputs.

2.2.5 Brake Friction Torque

Brake torque can be measured at the brake disc as a friction torque using piezoelectric sensors. These sensors are attached in brake calipers. The output of the sensor is not the actual braking torque, but the estimated torque since the friction of the disc is a dynamic quantity that changes with temperature and other things on it's surface like oil, water and snow. Another way is to mount pressure sensors in the brake lines to measure the hydraulic pressure and use it along with a wheel and powertrain model to estimate the brake torque applied at the wheels.

2.3 Tyres

Tyres of a vehicle are responsible to generate the forces to propel the car in the desired direction. Understanding how the tyres behave and influence the vehicle's dynamic motions and interpreting the sensor outputs is highly important since the tyre is like a black box with a large number of hidden variables. To understand the thesis work, such in-depth analysis and study is not required. A simple explanation of tyre dynamics is presented below. For more detailed explanations, the reader is directed to [20].

The wheels that are actively provided driving torque from the powertrain are called driven wheels. The wheels not connected to any active drive axle are non-driven wheels. For eg. on a Front-Wheel-Drive car, the driven wheels are the front wheels. An overview of how grip is produces, a brush tyre model to explain how a tyre generates forces, the longitudinal force and the effective rolling radius is presented in the precursor thesis work [1].

2.3.1 The Longitudinal Tyre Slip

The difference between the tyre's longitudinal and tangential velocity is produced as the tyre stretches and compresses when in contact with the road surfaces and produces grip. This induces a phenomenon called "slipping". Slip velocity is defined as the difference between the longitudinal velocity of the tyre and the tangential velocity of the tyre. This velocity when normalized by the longitudinal velocity gives the slip ratio [21].

The equation below describes the slip ratio as [20].

$$S_x = \frac{(R_e \cdot \omega - V_x)}{R_e \cdot \omega} \quad \text{in Acceleration} \qquad S_x = \frac{(R_e \cdot \omega - V_x)}{V_x} \quad \text{in Braking} \tag{2.5}$$

The following excerpt from thesis work [1] defines the slip ratio for different driving conditions.

This forms an important physical relation that tyres produce slip when the tyres have grip to stick to the road surface, which then generates the tractive or braking forces.

Free Rolling
In free-rolling conditions, there is no relative motion or velocity between the tread head and the tail. Thus the slip ratio $S_x = 0$ and no force is generated, $F_x = 0$.

Acceleration
The slip ratio S_x is positive and a propulsion force F_x is generated.

Braking
In extreme braking when the wheels lock, the tangential velocity of the wheel is zero since it is not rotating. This means that the slip ratio $S_x = -1$ and braking force $-F_x$ is generated.

2.4 Parameters that affect Grip and Slip

Two very important factors that affect how slip and grip is produced are the vertical load on the tyre and the road-tyre friction coefficient. To explain briefly, as vertical load increases, the maximum possible longitudinal tyre force increases, but the increase is however marginal as the load is increased further. This can be observed in figure 2.1a made using a non-linear magic tyre formula model from [22]. Peak longitudinal force produced increases as well as the vertical load on the tyre increases. Once the peak force is reached, then any additional torque applied leads to a decrease in longitudinal force and thus grip. The longitudinal force drops down to the kinetic friction force that makes the wheel spin without contributing to vehicle propulsion. It is important to note that this decrease does not instantly make the tyre visibly spin or lock up. However, the tyre visibly spinning or locking up is an indication that the torque applied to the tyre way too high for it to catch any grip on the road [1].

Next, as road-tyre friction, the maximum generated longitudinal force increases, keeping the grip between the tyre and the road. As it crosses it's maximum longitudinal force value, the grip reduces and the tyre starts slipping and eventually free-spinning, producing no grip. For eg: a tyre rolling on asphalt will be able to

generate more longitudinal force before losing grip than a tyre rolling on ice. For in depth explanation, the reader is guided to previous thesis work [1]. This phenomenon can be observed in figure 2.1b where the tyre is subjected to a load of 3000 N. The coefficient of friction for dry asphalt is 0.8, for wet asphalt is 0.3 and for ice is 0.15. The curves are governed by the same magic tyre formula used in the previous explanation from [22].

When a tyre rolls on an icy surface with coefficient of friction of approximately 0.15, the longitudinal forces the tyre is able to generate are very low when compared to dry asphalt (friction coefficient of 0.8). This is because under low friction conditions, the grip produced by the sliding of the tyre contact patch. Thus even a small engine applied torque can be enough to make the wheel roll freely or start spinning in-placed.

The longitudinal force peaks out at 250 N and at a slip ratio of 0.03 or 3%. When compared to dry asphalt, the longitudinal peaks out at 3000 N and achieves a higher slip ratio at 0.2 or 20% before losing grip and inducing wheel spin. Given such a low threshold for inducing spinning condition on ice means that the tyres are bound to spin under acceleration or braking in normal as well as extreme driving maneuvers. [1]

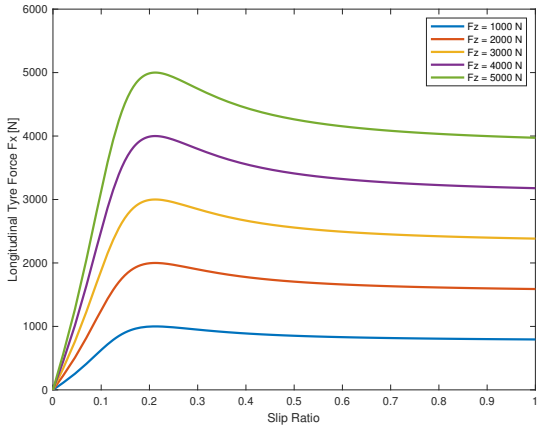

(a) *Longitudinal Force vs Slip Ratio for different vertical loads on a dry asphalt road [1]*

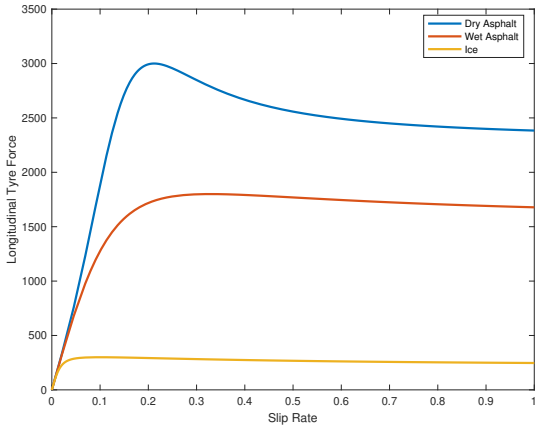

(b) *Longitudinal Force vs Slip Ratio for different road surfaces at constant load [1]*

Figure 2.1: *Parameters that affect longitudinal slip*

2.5 Load Transfer or Vertical Load on the Tyre

Load transfer is something that must occur during dynamic vehicle motion guided by the law of physics. The car's weight shifts under longitudinal and lateral accelerations. This leads to load transfer via two different ways - geometric and elastic. Geometric load transfer about the centre of gravity can be calculated in a very simple way by considering rigid axles. Calculating elastic load transfer requires suspension, damper and anti-roll bar data which was not available during this work. Thus only the geometric load transfer was considered using the equation:

$$\begin{aligned} F_{z,FL} &= \frac{m \cdot g \cdot b}{2l} - \frac{m \cdot a_x \cdot h}{l} - \frac{m \cdot a_y \cdot h}{t_w} \\ F_{z,FR} &= \frac{m \cdot g \cdot b}{2l} - \frac{m \cdot a_x \cdot h}{l} + \frac{m \cdot a_y \cdot h}{t_w} \\ F_{z,RL} &= \frac{m \cdot g \cdot a}{2l} + \frac{m \cdot a_x \cdot h}{l} - \frac{m \cdot a_y \cdot h}{t_w} \\ F_{z,RR} &= \frac{m \cdot g \cdot a}{2l} + \frac{m \cdot a_x \cdot h}{l} + \frac{m \cdot a_y \cdot h}{t_w} \end{aligned} \tag{2.6}$$

where,
m = mass of the vehicle
g = acceleration due to gravity
a = distance from front axle to centre of gravity
b = distance from rear axle to centre of gravity
l = wheel base
t_w = track width
a_x = longitudinal acceleration
a_y = lateral acceleration
h = distance of centre gravity from the ground

A dynamic vertical loading plays a major role in determining the amount of peak longitudinal force and thus slip ratio without spinning that can be produced by the tyre driven on a given road-surface. Thus it is important to know the weight on each wheel while the car is in motion to understand how much the tyre might slip.

3 Previous Work

This chapter lists down and explains briefly, the developments done during the precursor thesis work that are good to know to understand the work done in this continued development. This includes wheel speeds translation to centre of gravity, overview of pre-processing of data, filter base, V_xRP filter, slip detection concepts along with the strategy in braking. For in-depth detail about these parts, as well as information on sensor characteristics, kinematics modelling, filter tuning and slip indicators, the reader is referred to the precursor thesis work [1]

3.1 Pre-Processing

Parameters such as torque rates, wheel speeds, offset biases in the gyroscopes and wheel accelerations are computed during pre-preocessing. Since the data required to compute these parameters is pre-recorded, calculating them before entering the main estimation process helps to reduce complexity and time for each iteration in the for-loop. The wheel acceleration and torque rate is calculated by first low pass filtering the wheel speed and torque to reduce noise errors that arise when a numerical differential is taken to compute the required parameters. Online gyroscope bias computation is not included in the thesis work, thus while the car is at stand still at the beginning of the data log, the gyroscope offset is computed.

In almost data logs, the vehicle starts from a stand-still, allowing for gyroscope offset bias to be calculated. Then, the initial values of the states , the inputs to the filter and the tuning parameters of the filter are set. For more details on calculating these parameters and setting initial values for the filters, the reader is directed to the precursor thesis work chapter 3 [1].

3.1.1 Translating wheel speeds to CoG

The wheel speed sensor outputs the rotational or angular speed of the wheel, however the wheel's longitudinal velocity is needed to be used as a measurement of vehicle speed. To do this, the angular speed is multiplied by the radius of the wheel (which is assumed to be constant) to get the tangential speed of the wheel, and then translated to the centre of gravity (CoG). The equation used to translate the tangential speed of the wheel is from [23] and is given by equation 3.1.

$$\begin{aligned} V_{FL} &= (V_{\omega,FL} + \dot{\psi}(\frac{b_f}{2} - l_f\beta))\cos(\delta_W - \beta) \\ V_{FR} &= (V_{\omega,FR} - \dot{\psi}(\frac{b_f}{2} + l_f\beta))\cos(\delta_W - \beta) \\ V_{RL} &= (V_{\omega,RL} + \dot{\psi}(\frac{b_r}{2} + l_r\beta))\cos(\beta) \\ V_{RR} &= (V_{\omega,RR} - \dot{\psi}(\frac{b_r}{2} - l_r\beta))\cos(\beta) \end{aligned} \tag{3.1}$$

where, $V_{\omega,FL}$ is the tangential speed of the wheel, $\dot{\psi}$ is the yaw rate of the vehicle, b_f and b_r are the front and rear track-width of the vehicle respectively, l_f and l_r are the distance from the front and rear axle respectively to the CoG, β is the body slip angle and δ_W is the steering angle at the wheel or wheel angle. Since lateral dynamics are not within the scope of the thesis, the body side slip is neglected. The steering angle is also capped at 11 degrees to avoid noisy and over-estimated wheel speeds at CoG with high steering angles.

3.2 Setting up a kinematics-based filter

A kalman filter is a tool used for estimation of vehicle speed using a process model that defines how the speed evolves dynamically at each time step, as well as a measurement model that uses the sensor output to update the prediction made by the process model. An Extended Kalman Filter (EKF) is set up for this purpose. Since lateral and vertical dynamics of the vehicle are not considered, they are ignored from state equations. The most important states considered are - the longitudinal speed V_x since it needs to be estimated, and the Euler pitch of the vehicle θ used for compensation of gravity in accelerometer output. Also, from Euler angle translations,

Euler pitch and Euler roll are inter-dependent on each other, requiring Euler roll to also be a state. To read more about the equations and the acceleration and Euler models, the reader is directed to [1].

The kinematic equations of the vehicle are shown in equation 3.2.

$$\begin{aligned} \dot{v}_x &= a_x + g\sin(\theta) \\ \dot{\varphi} &= \omega_x + \sin(\varphi)\tan(\theta)\omega_y + \cos(\varphi)\tan(\theta)\omega_z \\ \dot{\theta} &= \cos(\varphi)\omega_y - \sin(\varphi)\omega_z \end{aligned} \tag{3.2}$$

where $\omega_{x,y,z}$ are the angular rates measured by the gyroscope in the vehicle co-ordinate frame, θ is the vehicle Euler pitch angle, φ is the Euler roll angle, V_x is the speed of the vehicle and g is the acceleration due to gravity.

3.2.1 Filter V_xRP

This filter has three states which are V_x longitudinal velocity, φ roll and θ pitch. The process model is presented in equation 4.3 and the Jacobian is given in equation 4.4.

$$\begin{aligned} v_{x\,k+1} &= v_{x\,k} + T_s\left(a_{x\,k+1} + g\sin(\theta_k)\right) \\ \varphi_{k+1} &= \varphi_k + T_s\left(\omega_{x\,k+1} + \sin(\varphi_k)\tan(\theta_k)\omega_{y\,k+1} + \cos(\varphi_k)\tan(\theta_k)\omega_{z\,k+1}\right) \\ \theta_{k+1} &= \theta_k + T_s\left(\cos(\varphi_k)\omega_{y\,k+1} - \sin(\varphi)\omega_{z\,k+1}\right) \end{aligned} \tag{3.3}$$

$$\boldsymbol{F} = \begin{bmatrix} 1 & 0 & T_s g\cos(\theta_k) \\ 0 & T_s\left(\omega_{y\,k+1}\cos(\varphi_k)\tan(\theta_k) - \omega_{z\,k+1}\tan(\theta_k)\sin(\varphi_k)\right) + 1 & T_s\frac{\left(\omega_{z\,k+1}\cos(\varphi_k) + \omega_{y\,k+1}\sin(\varphi_k)\right)}{\cos(\theta_k)^2} \\ 0 & -T_s\left(\omega_{z\,k+1}\cos(\varphi_k) + \omega_{y\,k+1}\sin(\varphi_k)\right) & 1 \end{bmatrix} \tag{3.4}$$

The measurement model is linear i.e. it has a direct speed measurement which are the wheel speeds. Thus the matrix for each wheel speed measurement is given in equation 4.5.

$$\boldsymbol{H} = \begin{bmatrix} 1 & 0 & 0 \end{bmatrix} \tag{3.5}$$

3.3 Slip Detection

3.3.1 Concept 1

This concept uses slip indicators such as torque rate and difference between wheel acceleration and vehicle acceleration to determine if a wheel is slipping or not. It determines this based on when these slip indicators are active. A torque rate indicator along with an indicator to look at difference between wheel and vehicle acceleration makes it possible to identify slip on each individual wheel. A wheel is said to slip if both indicators have crossed a set threshold within 0.2s or if the traction control system (TCS) in the vehicle is on. Upon this condition being true, a slip flag is activated. It is held active until the indicators cross a threshold that indicates that the wheels have stopped slipping or when the TCS on-board turns off.

The slip flag deactivates if:

- High decrease in powertrain torque rate
  AND
- Low difference between wheel-car acceleration and wheel acceleration for a specified amount of time
  AND
- Engine TCS is OFF

- Or if hard braking begins. This is to avoid activating slip flags during braking since they are not as accurate as expected.

The slip flag activates if :

- High increase in powertrain torque rate
  AND
- High wheel-car acceleration difference and wheel acceleration for a specified amount of time
  OR
- Engine TCS is ON OR
- During initial acceleration motion from stand still in the beginning.

The slip flag activation torque rate threshold is 650 Nm/s for the front and 950 Nm/s for the rear. For slip flag deactivation, the torque rates are -950 Nm/s and -750 Nm/s for the front and rear respectively. The wheel and car acceleration difference threshold is $0.8m/s^2$. A torque of 150 Nm for 0.5 seconds as well as a wheel-car acceleration difference of less than 0.8 m/s^2 is set to deactivate the flag.

Using torque rates as thresholds, especially when static poses some problems because they for one a rate of increase and thus sensitive at lower torques since a small increase would lead to a higher torque rate being computed and triggering slip the slip flag. To avoid this, the second slip indicator that monitors wheel-car acceleration difference is used.

3.3.2 Concept 2

This concept is not based purely on slip indicators and detects slip at each time step rather than triggering based on thresholds This concept does not lock the slip flag between two events but rather checks for slip at each time step. If no wheels are slipping, all of them are fed to the filter as measurement, however the wheels are slipping, then the filter is fed only the speed of the slowest wheel out of the non-slipping ones. The three indicators used for slip detection in this concept are :

- Variance of difference of estimated speed and wheel speeds
- Wheel acceleration compared to vehicle acceleration
- Slip ratio

The variance threshold for error activation of slip flag is 0.005 calculated over 0.25s. The threshold for wheel-car acceleration difference is $0.8m/s^2$. The threshold for the slip-ratio indicator calculated between the estimated speed and wheel speed activates slip if the wheel speeds differ by 0.5 m/s or more from the current estimated speed or 4% from the estimated speed. The threshold for the variance between the wheel speed measurements when below 0.01 for continuous 0.2 seconds deactivates the slip flag. The slip flag would also drop if the wheel speeds are faster than the estimated speed by 1 m/s for 0.1 seconds.

3.3.3 Braking Logic

ABS braking does not help concept 1 or concept 2 to detect slip and the only strategy is to use pure dead-reckoning as soon as braking begins except for some side cases. The vehicle is said to be actively braking if three or more wheels are actively supplied brake torque. When this condition is detected, dead-reckoning is done for 0.25s. Then, a checks is made to see if any wheel is faster than the predicted speed. If that is true then the measurement is fed to the filter with low covariance or higher trust. If the fastest wheel speed is slower than the predicted speed, they are not trusted or given a high covariance.

4 Method

This chapter delves into the newly developed vehicle speed estimation methods in the continued work to support the precursor thesis. The reader is advised to read through chapter 3 in the precursor thesis [1] as some work such as the filter design, the slip detection concepts, sensor characteristics and sensor offset compensation are adopted from there.

4.1 Logged Data

The data is supplied by Volvo Cars from real world driving on icy and snowy roads. The data logs from the large all-wheel drive (AWD) vehicle is used for this work and development. The data logs from a second, mid-sized all electric AWD vehicle are not used. The large vehicle is a hybrid, with it's front axle driven by an Internal Combustion Engine (ICE) and it's rear axle driven by one electric motor. The data logs consist of data from a 6 Degree of Freedom (DOF) IMU, wheel speeds, steering wheel angle, powertrain and brake torque sensors, system flags like Anti-Lock Braking (ABS) and Traction Control System (TCS). As for ground truth measurements, Oxford Technical Solutions' (OxTS) RT3000 is used. This sensor records the vehicle position, longitudinal and lateral velocity, longitudinal, lateral and vertical acceleration, the orientation - roll, pitch, yaw as well as it's rate(velocity) at an update frequency of 100 Hz. As for the driving maneuvers, the vehicle is driven aggressively on straight roads, banks, uphill and downhill slopes with high accelerations. In some data logs, small lateral motions are also induced while driving on a test track. Harsh braking scenarios are also included with ABS braking and ESC disabled to induce longer and sustained all-wheel slip situations. For more detailed information on the driving maneuvers, conditions, and sensors used to log the data, the reader is guided to the precursor thesis work.[1]

In addition to this data, Volvo Cars also provided real world driving data from the AWD large hybrid that logged speed and Position Dilution of Precision (PDOP) values from on-board GPS module and a ground truth measurement of speed. The GPS module. The vehicle was driven on the E6 highway route, including two tunnels. The vehicle speed peaked at 130 km/h and the GPS PDOP values ranged from 0 to 22. The vehicle was driven relatively straight forward on the highway without any excessive slip or extreme maneuvers.

4.2 Approach 1 : Using GPS Speed

A standard sensor suite contains only wheel speeds as a direct measurement of vehicle speed. When the wheels slip excessively, mostly in snowy and icy road conditions, these speeds are far away from the true speed of the vehicle. In such situations , the previous speed estimation methods relied purely on dead-reckoning which in turn, relied on the slip detection concepts to accurately detect slip and start dead-reckoning from a position where the wheel speeds were accurate. This was done to avoid an early onset of integral drift errors in the speed estimation. However, the slip detection concepts had limitations, inducing errors in velocity estimation due to dead-reckoning.

From the related research done during the precursor thesis as well as analysing the limitations of the developed methods, it was found that having a secondary measurement of speed would avoid the reliance on pure dead reckoning when all wheels are detected to slip. Even if the slip detection concept falsely detects all-wheel slip, a secondary speed measurement would avoid the early onset of integral drift errors as the dead-reckoning process would begin at a point where wheel speeds are truly indicative of the vehicle's speed. A second speed measurement would also help correct the dead-reckoned estimate if it drifts away between two secondary measurement updates. Most modern vehicles come with a standard GPS module which outputs the velocity of the vehicle. This can be used a secondary measurement only when all wheels are detected to slip. This is because, when the wheels are not slipping, the wheel speed sensor measurements accurately represent the true speed of the vehicle.

4.2.1 Error Characteristics of GPS Speed Signal

GPS speed was not logged in the excessive slip data received from real world driving. So, a speed signal with characteristics similar to an actual GPS speed signal is modelled from the ground truth (OxTS) speed signal for the excessive wheel slip data. To understand the GPS signal and it's errors characteristics, two new data logs were provided with GPS speed and the ground truth measurement for speed. To model any signal, it is important to understand it's error and noise characteristics along with the parameters that affect it. This is needed to model the noise that will be added to the ground truth signal.

From the data received, it was observed that the errors in GPS speed are normally distributed with high density peaks at mean error as seen in figure 4.1b. The errors were normally distributed but were not zero-mean, mostly due to a constant offset error between the GPS speed and the ground truth measurement. The error is calculated as $V_{xgps} - V_{xref}$. The skewed concentration of errors towards the negative side in figure 4.1b suggests that the GPS speed is slower than the ground truth. It was also found that there were a few parameters that affected the GPS speed errors, especially the mean and standard deviation of errors. The observations are explained in the following sections.

Constant Offset Between GPS and ground truth measurement

From the data provided, it was first observed that there is a constant offset between the two speed signals. The GPS speed signal indicates a slower velocity than the ground truth which could be due to the dynamic radius estimation used in the ground truth signal. This offset would not likely occur when compared to the OxTS, thus constant is first corrected and then the study of the parameters is done. The constant offset in this case was found to be very small, approximately 0.88 m/s at a constant speed of 34 m/s and can be observed in figure 4.1a.

The constant offset is uncharacteristic of a GPS module and occurs due to the ground truth signal bias towards a faster speed. Thus constant error is eliminated before studying the error characteristics. It is eliminated by computing the mean error from the data log and adding it to the GPS speed measurement. The final speed signals are shown in figures 4.2a and 4.2b.

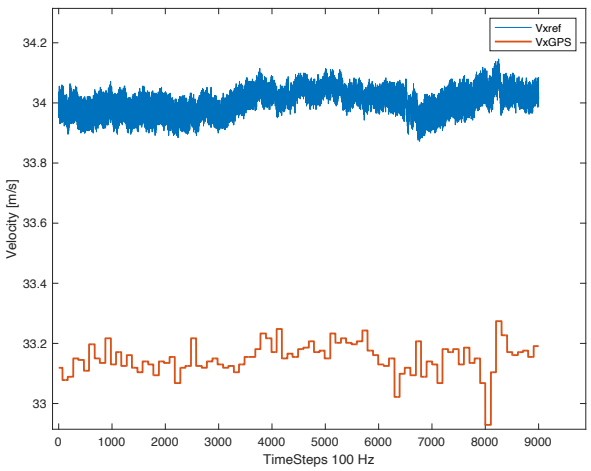

(a) *Constant offset between GPS speed and reference speed*

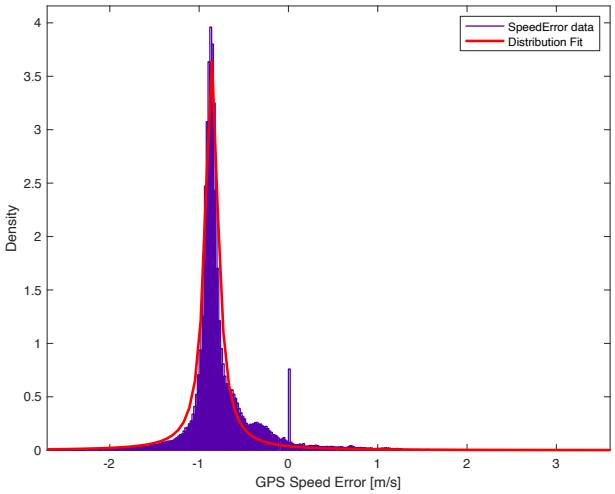

(b) *Distribution of GPS speed errors*

Figure 4.1: *Constant Offset*

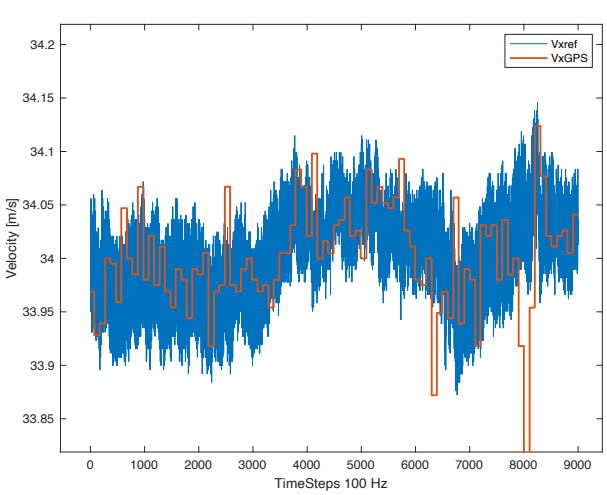

(a) *Speed signals after eliminating constant offset*

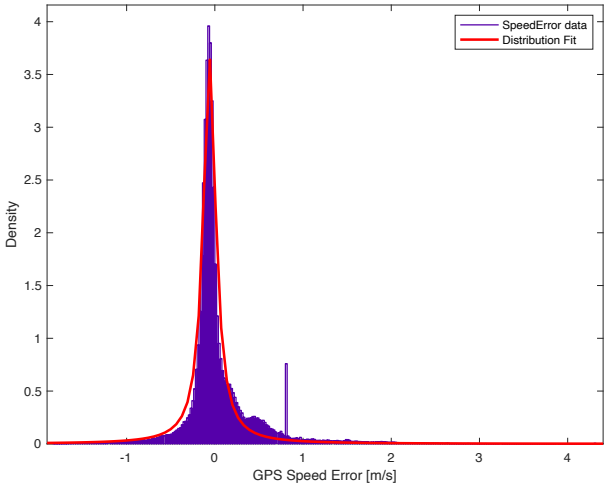

(b) *Distribution of GPS speed errors after constant offset elimination*

Figure 4.2: *Without Constant Offset*

Update Frequency

The most significant factor that causes the GPS speed error is the GPS module's update frequency. GPS update frequency lies between 1 and 100 Hz. The GPS module from the data log had on average, a 1 Hz update frequency. The GPS receiver gets a new speed update at a frequency of 1 Hz or every 1 second via communications from different satellites. However, the other signals in the vehicle such as the wheel speed sensors, IMU, torque sensors, steering angle sensor and the OxTS update at 100 Hz or every 0.01 second. This discrepancy leads to an error in the speed measurement received from the GPS. This is because while the speed measurement is updating continuously every 0.01 second, The GPS speed measurement is held constant at the previously logged speed until a new measurement is received. This results in a signal that looks like a staircase function with an update every 1 second. Figures 4.3a and 4.3b shows how the signal looks in constant speed and acceleration cases.

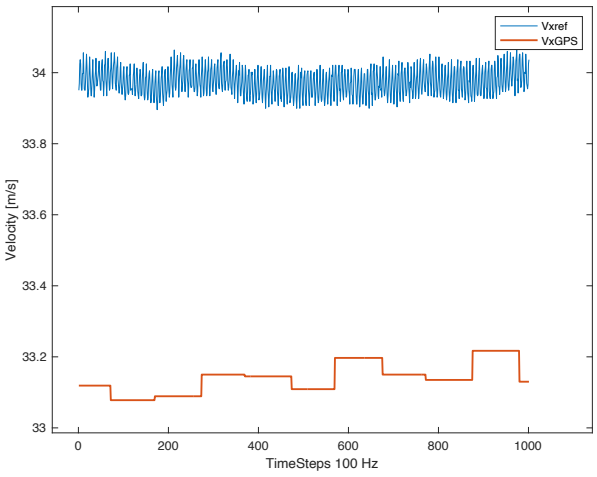

(a) *GPS signal during constant speed*

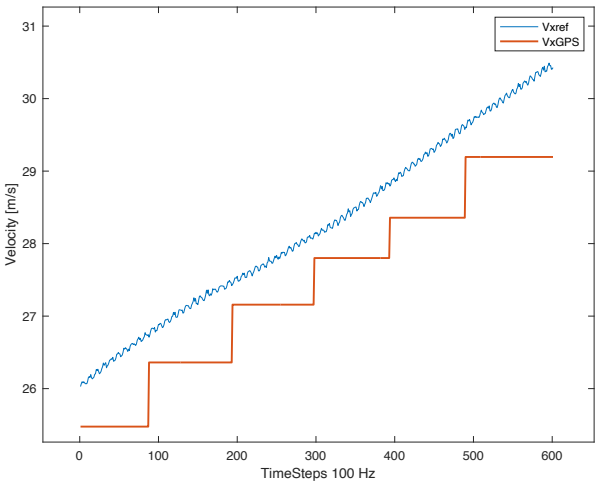

(b) *GPS signal during acceleration*

Figure 4.3: *GPS speed signal updates at 1 Hz or every 1 second and follows a staircase curve*

The update frequency discrepancy does not have a huge effect when the speeds are relatively constant. However, it's effect is pronounced when the vehicle is subjected to any acceleration or braking, even as low as 0.5 m/s^2.

Once a speed measurement is received, the GPS updates the speed signal. This measurement received at that instant might be fairly accurate. Then, that speed measurement is held constant until a new measurement arrives i.e. for 1 second. If the vehicle is accelerating or decelerating, then in the 1 second gap between the two GPS speed updates, the GPS speed signal will deviate from the true vehicle speed largely, generating big errors. The higher the acceleration or deceleration, the larger the error.

Position Dilution Of Precision

Position Dilution of Precision (PDOP) value is an output generated by the GPS module. The value indicates the positional accuracy of the GPS. This is based on how many satellites the GPS is connected to while estimating position.

PDOP	**Significance**
0	No Satellites Connected
1 to 5	Excellent Accuracy
6 to 10	Good Accuracy
Above 10	Bad Accuracy

The given data contains PDOP values ranging from 0 to 22. It is easy to think that a higher PDOP value would indicate bad GPS accuracy however, that is only in the case of position and not the speed signal. The speed of the vehicle is computed using Doppler Effect phenomenon that is seldom affected by the PDOP values. It was observed for the given data that the PDOP values had no effect on the errors of the GPS speed. This was verified using the Pearson Correlation Coefficient, which came to -0.0058, indicating that any relation between an increase in GPS speed error due to increased PDOP value is insignificant. The p-value was 0.0011 (which is < 0.005), suggesting that the above hypothesis is true.

Speed

The GPS speed has a linear relation with the speed of the vehicle. The GPS speed error is observed to reduce as the speed increases. This can be observed in figure 4.4, which plots mean speed errors against the speed recorded by the GPS. However, this decrease in error at higher speeds is because of the way the vehicle is driven in the data log. The vehicle is accelerated up to a high speed and then kept constant at these high speeds. Thus a condition where large accelerations are produced at high speeds is unavailable in the data. Also, the constant speed sections appear only at higher speeds in the provided data logs. Thus even if 4.4 shows a linear correlation between speed and GPS speed error, this parameter is not used solely to model the error characteristics of the GPS signal.

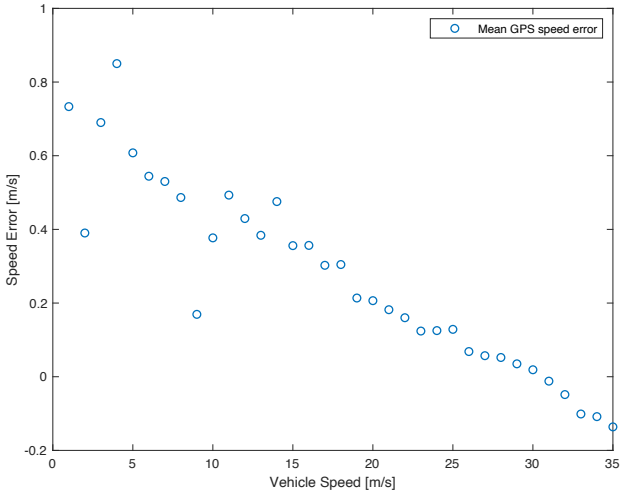

Figure 4.4: *Trend of mean GPS speed error for different vehicle speeds*

Acceleration and Deceleration

The GPS speed error caused due to it's low update frequency is not the same in acceleration and deceleration scenarios, and it varies with speed as well. This means that acceleration and deceleration influences the errors seen in 4.4. It was observed that the errors increase in the negative direction with vehicle acceleration. The increase is in the negative direction because the GPS update lags behind the ground truth due to it's lower update frequency and the error gets larger as the acceleration increases. While the GPS holds the previous speed measurement, the true speed of the car increases, increasing the errors generated between the GPS signal and ground truth. This can be observed in 4.5a. IT can also be seen that the GPS speed signal always shows slower speed measurement in acceleration conditions since it lags behind due to it's low update frequency. The mean speed errors for different acceleration levels are shown in figure 4.5b.

The braking case can be explained similarly. As the braking or deceleration of the vehicle increases, the lower update frequency of the GPS leads to increasing errors. Figure 4.6a shows the effect of low update frequency during braking. As the speed of the vehicle drops rapidly with increasing deceleration, the GPS update lags behind and outputs a measurement faster than the speed of the vehicle. From figure 4.6b it can be observed that as the vehicle decelerates more, the GPS speed error increases linearly.

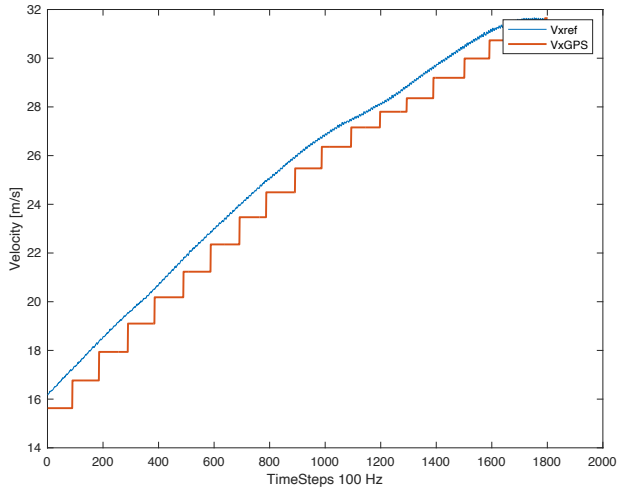

(a) *GPS speed signal during acceleration*

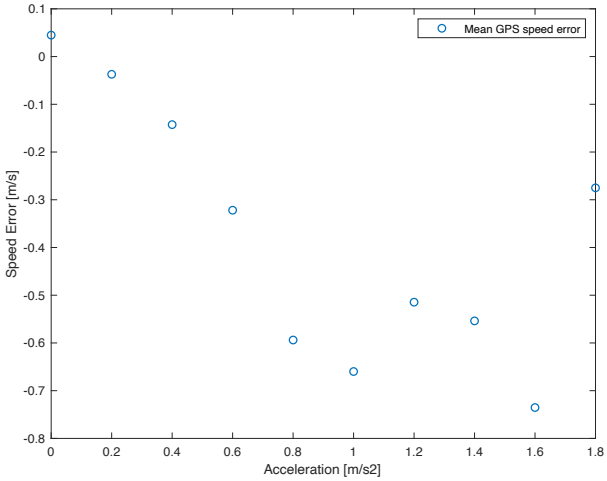

(b) *Mean GPS speed error during acceleration*

Figure 4.5: *GPS speed signal and speed error during acceleration*

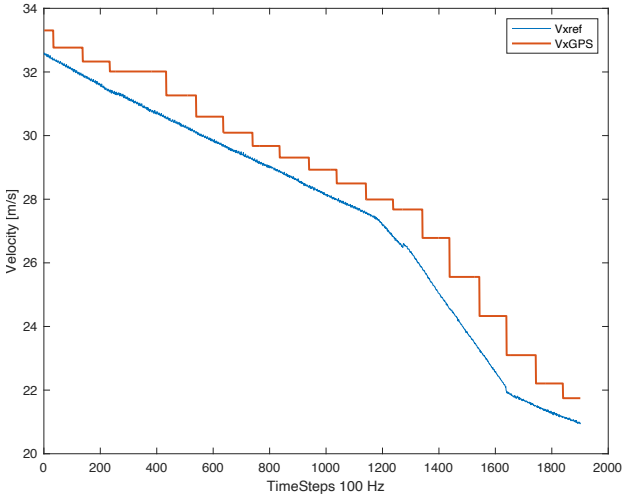

(a) *GPS speed signal during braking*

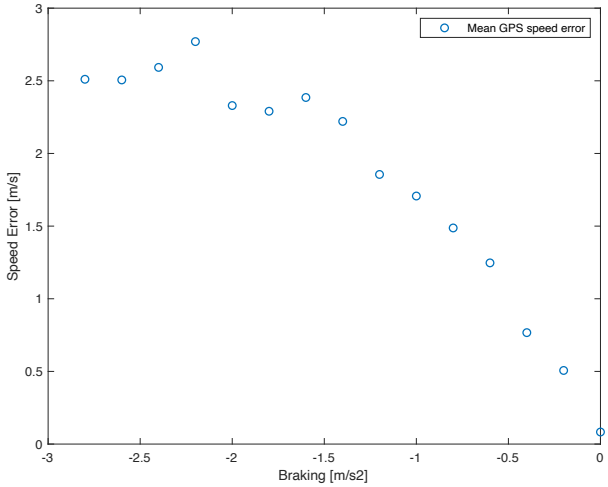

(b) *Mean GPS speed error during braking*

Figure 4.6: *GPS speed signal and speed error during braking*

To understand the how acceleration, deceleration and speed affect the GPS speed errors, a contour plot is generated as seen in figure 4.7. It is observed that the errors due to acceleration do not depend on speed while the errors during braking do. The errors are fairly constant throughout accelerations, with similar means and standard deviations. The errors in braking however are different such that at lower speeds, the mean errors and standard deviations are much larger, and then taper off to smaller errors and narrower standard deviations as speed increases.

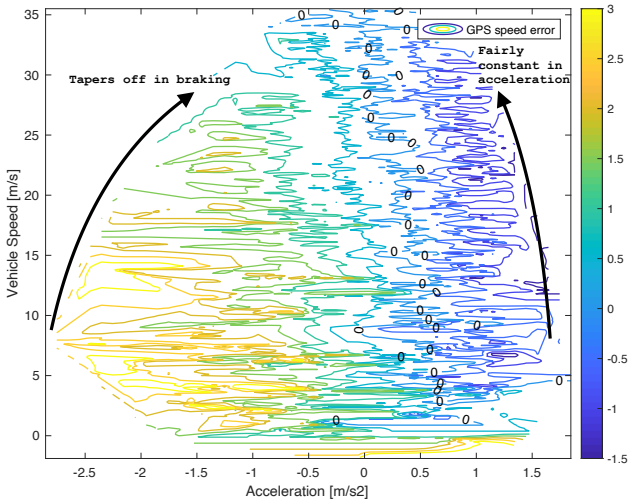

Figure 4.7: *Effect of accelerations, deceleration and speed on GPS speed error*

4.2.2 Limitations

The error characteristics found are based on vary scarce data available. The data is for the same vehicle however, but driven on asphalt roads without excessive slip. Any effects of the environment such as cities and dense trees, weather and cloud cover and numerous tunnels, underpasses, overpasses were not included since the data log did not contain such driving scenarios. New, more recent GPS modules generate a Velocity Dilution of Precision (VDOP) number indicating how accurate the speed signal is at each time. This data was not available in the data logs. The data logs provided are also limited; 2 runs of 45 to 60 minutes of highway driving passing through only 2 short tunnels.

4.2.3 Modelling GPS Speed

The process of modelling GPS speed is in general adding noise based on how the GPS speed errors vary as defined in the table for standard deviations and mean of errors. Here is a step-by-step approach of how the speed is modelled.

Adding Gaussian Noise

The errors in GPS speed are normally distributed as observed in 4.1b and after the constant offset elimination in figure 4.2b with high peaks. Since the modelled GPS speed will be based on the OxTS measurement, the OxTS speed signal is contaminated with this noise based on the speed and accelerations of the vehicle. The noise is added as in the equation 4.1.

$$V_{xGPS} = V_{xref} + \mu_{error} + \sigma_{error} \cdot Z_{0,1} \tag{4.1}$$

$$Noise = \mu_{error} + \sigma_{error} \cdot Z_{0,1} \tag{4.2}$$

where μ_{error} and σ_{error} is the mean and standard deviation of the GPS speed error respectively while $Z_{0,1}$ is a random number vector that carries values between 0 and 1 and has a length equal to the that of the V_{xref} array. In this way, a normally distributed noise about mean μ_{error} and standard deviation σ_{error} is added to the OxTS speed signal.

Scenario	Acceleration / Deceleration [m/s2]	Speed [m/s]	Mean Error [m/s]	Standard Deviation [m/s]
Constant Speed	0	-	0	0.02
Acceleration	0 to 1.5	-	-0.01	0.30
	greater than 1.5	-	-0.8	0.32
Braking	0 to 1.5	0 to 15	0.9	0.65
	greater than 1.5	0 to 15	2	0.58
	0 to 1.5	greater than 15	0.6	0.3
	greater than 1.5	greater than 15	1.6	0.4

Table 4.1: Mean and Standard Deviations of the noise added for different scenarios in the data log

This noise is modelled and added based on different categories or scenarios such as acceleration and braking with speed thresholds since these parameters affect the errors generated in GPS signal as discussed in section 4.2.1. The table 4.1 below shows the different scenarios and the mean and standard deviation of errors in them, which are used in equation 4.1 for modelling GPS speed signal.

As seen in figure 4.7, the errors generated in acceleration cases are on dependent on the level of acceleration and not the speed of the vehicle. Thus, in acceleration scenarios, the noise is added based on the level of acceleration. However, for braking cases, the errors depend on both level of deceleration and the vehicle speed, which is why noise added in braking depends on both these parameters. For constant speeds, the error very small and thus the standard deviation is very small, almost negligible. It is important to note that these values have been extracted from the two data logs provided with GPS signals. More GPS data, especially in different environments and extreme driving maneuvers is necessary to do a thorough analysis of GPS speed signal errors.

Data Sampling

As mentioned earlier, a GPS module has an update frequency of 1 Hz. The OxTS speed signal V_{xref} has an update frequency of 100 Hz. So, after adding the noise, V_{xref} is down-sampled to 1 Hz. After down-sampling, just as in a GPS speed signal, the speed value are connected together or "up-sampled" back to 100 Hz using a staircase function which holds the previous speed value constant until the next measurement update is received. After adding the noise and sampling V_{xref} signal, the modelled GPS velocity looks like a staircase function similar to an actual GPS signal with an update frequency of 1 Hz, as seen in figure 4.8.

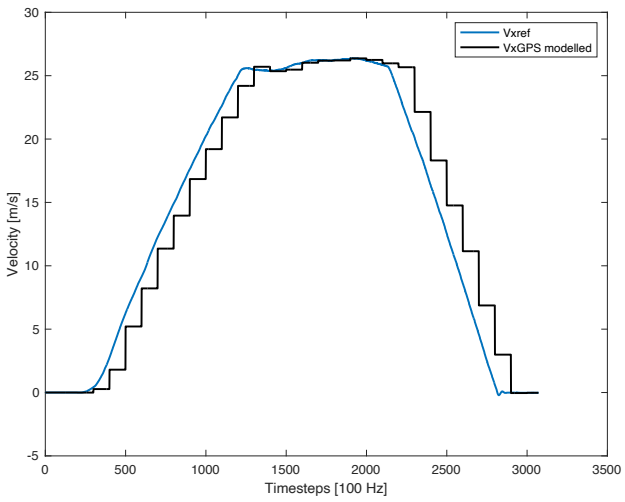

Figure 4.8: *Modelled GPS Speed signal with the ground truth signal* V_{xref}

4.2.4 Adding GPS Speed as a Measurement

To incorporate GPS speed as a measurement, some changes are made to the V_xRP filter from the previous thesis work [1]

Filter V_xRP, GPS

This filter uses GPS speed as measurement update when all wheels are detected to slip. The states of this filter are the same as in the V_xRP filter and thus the process model of the kinematic based EKF remains the same [1]. The states in this filter are the vehicle speed v_x, vehicle roll φ_k and vehicle pitch θ_k. The process model equations 4.3 and their jacobian are given in equation 4.4.

$$\begin{aligned} v_{x\,k+1} &= v_{x\,k} + T_s\left(a_{x\,k+1} + g\sin(\theta_k)\right) \\ \varphi_{k+1} &= \varphi_k + T_s\left(\omega_{x\,k+1} + \sin(\varphi_k)\tan(\theta_k)\omega_{y\,k+1} + \cos(\varphi_k)\tan(\theta_k)\omega_{z\,k+1}\right) \\ \theta_{k+1} &= \theta_k + T_s\left(\cos(\varphi_k)\omega_{y\,k+1} - \sin(\varphi)\omega_{z\,k+1}\right) \end{aligned} \tag{4.3}$$

$$\boldsymbol{F} = \begin{bmatrix} 1 & 0 & T_s g\cos(\theta_k) \\ 0 & T_s\left(\omega_{y\,k+1}\cos(\varphi_k)\tan(\theta_k) - \omega_{z\,k+1}\tan(\theta_k)\sin(\varphi_k)\right) + 1 & T_s\frac{\left(\omega_{z\,k+1}\cos(\varphi_k) + \omega_{y\,k+1}\sin(\varphi_k)\right)}{\cos(\theta_k)^2} \\ 0 & -T_s\left(\omega_{z\,k+1}\cos(\varphi_k) + \omega_{y\,k+1}\sin(\varphi_k)\right) & 1 \end{bmatrix} \tag{4.4}$$

The output or measurement matrix H is given as 4.5. H matrix has three terms, one for each state input. However ,the only measurement in this model is the speed measurement. Primarily, it comes from the wheel sensors. Unless all wheels are slipping, the non-slipping wheels are fed to the kalman filter as a speed measurement.

However, a change happens in the update step while dead-reckoning i.e. when all wheels are detected to slip. In these situations, wheel speeds can't be trusted and fed to the system. Since the GPS Speed signal is a speed measurement i.e. the measurement of the first state V_x, the GPS speed signal replaces the wheel speed sensor as measurement to the system and updates using this signal.

Since GPS speed is only used in all-wheel slip cases, the GPS speed signal is not permanently added to the measurement matrix.

$$\boldsymbol{H} = \begin{bmatrix} 1 & 0 & 0 \end{bmatrix} \tag{4.5}$$

4.2.5 Speed Estimation

It is important to note that the GPS speed is only used when all wheels are detected to slip. This is done because the wheel speeds, when not slipping are a very accurate measurement of the true speed of the vehicle. GPS speed is a secondary measurement that is used to help and guide the dead reckoned velocity such that it stays within the desired 4% error limit.

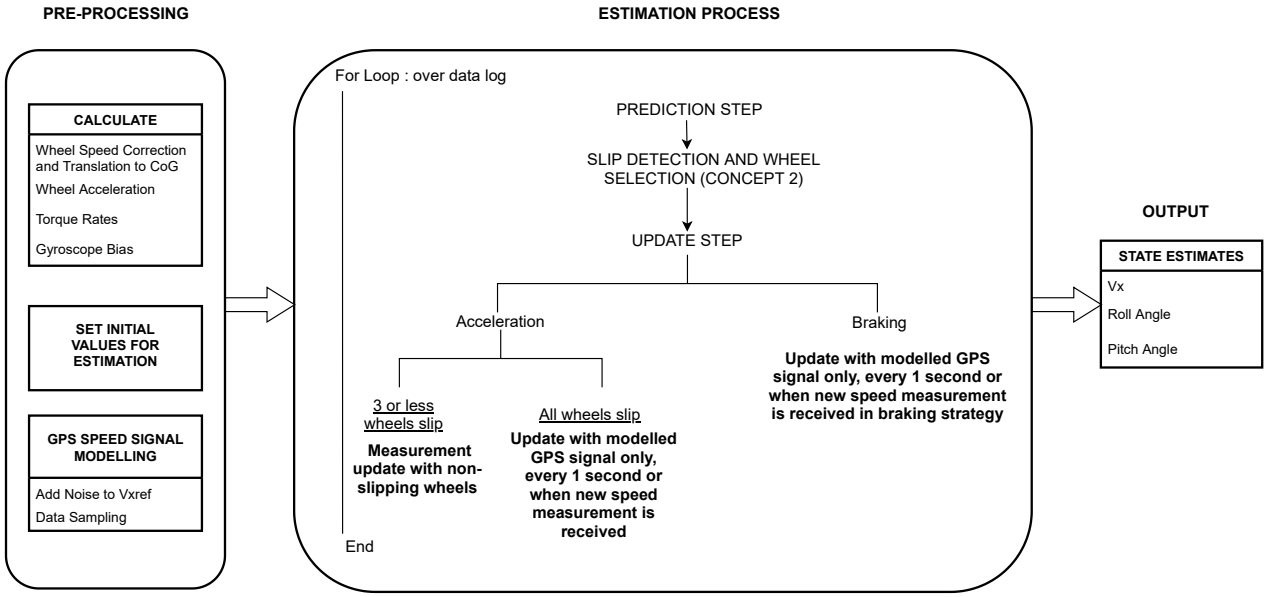

Figure 4.9: *Overview of estimation process for approach 1 : GPS Speed*

Pre-processing

The pre-processing block in figure 4.9 involves first, the calculation of necessary variables and parameters such as the translated wheel speeds, wheel acceleration, torque rates and gyroscope bias. Since the data required is pre-recorded, calculating these variables ahead of the processing step helps to reduce complexity and time for each iteration in the for-loop. The wheel acceleration and torque rates are calculated using the finite difference between two time steps and low-pass filtering. The wheel speed corrections and translation to CoG are made using the equation 3.1. The reader is directed to [23] for detailed explanation of this equation.

The final step in pre-processing is the GPS speeds signal modelling. As explained in section 4.2.3, the GPS speed is modelled by adding noise and then sampling the ground truth measurement signal. Again. this is done before hand since the data is pre-recorded and it helps to reduce complexity and time in each iteration of the estimation process.

Estimation Process

The pre-processed variables and parameters are fed to a for-loop that contains a kinematics based EKF, slip detection and wheel selection concept along with a braking strategy. The prediction step remains the same as in previous thesis work [1]. Concept 2 as explained in section 3.3.2 is used to detect which wheels are slipping. Concept 2 is used since it was the best performing method from the precursor thesis [1].

Acceleration

Then, if during acceleration, the slip detection concept detects slip on 3 or less wheels, the wheel that is not slipping is fed to the kalman filter as a measurement. The only time GPS speed is used is when all four wheels are detected to slip. In such cases, the GPS speed is fed as a measurement to the system during the update step. The GPS speed however, is only fed to the system at the instant it updates i.e. every 1 second a new measurement of speed is fed to the filter. This is done to avoid the errors caused due to update frequency and the constant speed that is held until the next measurement is received, as explained in section 4.2.1. This update helps reduce the drifting of the speed estimate by updating with a speed measurement and avoids the need to rely on dead-reckoning continuously for longer duration of slip. The GPS speed is also only update if the PDOP value between 1 and 5. It is important to note that even though it is mentioned that PDOP value does not affect the performance of the GPS speed error in the given data logs, it is the only measure of GPS accuracy in the data log. Hence, to avoids any unnecessary errors that could be caused due to loss or drop of communication with the satellites, a PDOP threshold is used.

Braking

The precursor braking strategy relied heavily on dead reckoning at all times due to the slip detection concept not being able to accurately detect slip in braking cases, which made the estimate drift away often, reducing it's performance. Having a secondary measurement of speed during braking helps to take off the burden from pure dead-reckoning. So, when the vehicle begins to brake, irrespective of the number of wheels locking or slipping, the estimate is updated with a GPS speed measurement every 1 second (again, to avoid the large errors due to update frequency and constant measurements held between the update). This helps guide the dead-reckoning. It also helps to start dead reckoning at a more accurate position, thus also reducing chance of drifting.

When a wheel is slower than the predicted speed in acceleration

In such cases, if the predicted speed of the vehicle is greater than or equal to 100 km/h, then a wheel speed that is slower than the predicted speed by 4 km/h is trusted. For speeds less than 100 km/h, a wheel speed slower than the predicted speed by 2 km/h is trusted.

About using GPS Speed

The GPS speed in this method is purely used a guide or alternative to dead reckoning. This is done to see the improvements that could be made in the performance of the previous methods [1]. This is why, the only way GPS is used is when all wheels are detected to be slipping during acceleration. Since the GPS speed here is modelled and not a true signal, the use of this to calculate slip ratio and use it to compensate the wheel speed measurements would not be a well developed solution. So, for slip detection, it was deemed best to make a new concept using the original sensor setup. This is explained in the subsequent section.

Why Slip Detection Concept 2 Is Used

The modelled GPS Speed signal is a secondary measurement that is fed to the $V_X RP, GPS$ EKF when all wheels are detected to slip. This is done to only use the speeds when the wheels cannot be trusted. This is because when the wheels are not slipping and can be trusted, they give a very accurate measurement of the vehicle speed. Hence, to know when all wheels are slipping and thus feed the GPS speed measurement, a slip detection is essential. For this purpose, slip detection concept 2 is used, which was the best performing method in the precursor thesis work [1]. Another benefit of using a slip detection concept whose performance analysis and numbers are known is that the performance of Approach 1 will give the possible improvements in the previously developed method and evaluate the gains possible by adding a secondary measurement of speed. It keeps the variables for comparison low and makes it better to analyse it's true potential. However, some place could be skewed by the slip detection concept's misjudgment of slip conditions, the overall gain can be clearly understood and the shortcomings of pure dead reckoning could also be analysed.

4.3 Approach 2 : Slip Detection Concept 3

This section explains the new slip detection concept developed based on calculating the slip ratio at every time instant. The slip ratio is calculated using data from the standard sensor setup only - wheel speeds, torques, steering angle sensor and IMU.

4.3.1 Why dynamic slip detection

A dynamic slip detection method is necessary to know exactly and accurately which wheels to trust and at which time instant. Having a more dynamic slip detection method, that would change with driving conditions and maneuvers as well as include all dynamic motion generating parameters such as torque, acceleration, load transfer, that would encompass the vehicle's predicted behavior based on it's motion dynamics would help in understanding slip and even predict the actual slip ratio.

Concept 1 uses certain slip indicators, such as powertrain torque rate and a comparison between wheel and vehicle acceleration to determine which wheel is slipping. Thresholds are set for these two slip indicators. The concept assumes slip between events that were triggered by these thresholds being crossed. One limitation with this concept is the static nature of the thresholds. The thresholds are pre-determined from observing

the data logs provided and they do not change with any other dynamic parameter. That means, the concept does not take into account the the velocity, the driving maneuver or the road conditions, which eventually leads to less robustness and incorrect speed estimates. As for concept 2, even though the slip detection is done dynamically at each time step, the vehicle dynamics and motion are a missing factor. The concept is also prone to missing slowly increasing slip events and would lead to incorrect speed estimations. One aspect of concept 2 uses calculated slip ratio from the estimated speed to detect if the wheels are slipping. This sometimes fails to detect slip if the estimated speed has drifted up slightly and a wheel, that was previously slipping with a higher slip ratio, drops down to a lower slip ratio, but is still outside the 4% slip limit. An incorrectly deactivated slip flag would make the estimate trust that wheel and generate errors.

4.3.2 The Slip Ratio Equation

The slip detection concept begins with estimating the slip ratio at each time instant. The equation is based on the works of [15]. First, the slip ratio is defined from [24] and [15] as equation 4.6 where R_e is the effective rolling radius of the tyre, ω is the rotational speed of the wheel and V_x is the speed of the car in longitudinal direction.

$$S_x = \frac{R_e \cdot \omega - V_x}{R_e \cdot \omega} \quad \text{in Acceleration} \qquad S_x = \frac{R_e \cdot \omega - V_x}{V_x} \quad \text{in Braking} \tag{4.6}$$

Differentiating equation 4.6 for acceleration with respect to time gives the non-linear wheel dynamics equation for slip at every time instance. The time differential is given by equation 4.7.

$$\dot{S_x} = \frac{R_e \dot{\omega} V_x}{R_e^2 \omega^2} - \frac{R_e \omega \dot{V_x}}{R_e^2 \omega^2} \tag{4.7}$$

Next, the torque applied to the vehicle is computed as the sum of the torque that overcomes the rotational inertia of the vehicle and propels the wheels. This is given by equation 4.8

$$I_w \cdot \dot{\omega} = T_q - R_e \cdot F_x \tag{4.8}$$

Also in the linear range, the driving force F_x is given as

$$F_x = C_x \cdot S_x \tag{4.9}$$

Re-arranging the terms and substituting the value of $\dot{\omega}$ in the first term of the equation 4.7, and the value of F_x in the second term gives the equation

$$\dot{S_x} = \frac{T_q \cdot R_e}{V_x \cdot I_w} - \frac{C_x \cdot S_x \cdot R_e^2}{V_x \cdot I_w} - \frac{R_e \omega \dot{V_x}}{R_e^2 \omega^2} \tag{4.10}$$

V_x is the vehicle speed given by the translational wheel speed which for this equation, since only longitudinal dynamics are needed, is assumed to be simply

$$V_x = R_e \cdot \omega \tag{4.11}$$

Also, another constituent relation to note is that the acceleration of the vehicle is simply the time derivative of the velocity V_x

$$a_x = \dot{V_x} \tag{4.12}$$

Now, substituting equations 4.11 and 4.12 in equation 4.10, the time derivative of slip ratio can be written as

$$\dot{S_x} = \frac{T_q \cdot R_e}{V_x \cdot I_w} - \frac{F_x \cdot R_e^2}{V_x \cdot I_w} - \frac{a_x}{V_x} \tag{4.13}$$

The last term in equation 4.13 can also be re-written by using the slip equation 4.6 thus giving the wheel dynamics equation

$$\dot{S_x} = \left(\frac{C_x \cdot R_e^2}{V_x \cdot I_w} - \frac{a_x}{V_x}\right) \cdot S_x + \left(\frac{T_q \cdot R_e}{V_x \cdot I_w} - \frac{a_x}{V_x}\right) \tag{4.14}$$

The equation can be cut split into two different elements based on the dynamic parameters as seen in equation 4.16.

$$E_{Sx} = \left(\frac{C_x \cdot R_e^2}{V_x \cdot I_w} - \frac{a_x}{V_x}\right) \tag{4.15}$$

$$E_{Tq} = \left(\frac{T_q \cdot R_e}{V_x \cdot I_w} - \frac{a_x}{V_x}\right) \tag{4.16}$$

The slip ratio estimation equation in continuous time is given by equation 4.17.

$$\dot{S_x} = W \cdot [\cdot E_{Sx} \cdot S_x + \cdot E_{tq}] \tag{4.17}$$

Converting equation 4.17 to discrete where k is the time instant and T_s is the sampling time is given by equation 4.18.

$$S_{x,k+1} = W \cdot [(E_{Sx,k} + 1) \cdot S_{x,k} + E_{Tq,k}] \cdot T_s \tag{4.18}$$

where, k is the time instant, S_x is the slip ratio,C_x is the longitudinal stiffness of the tyre, I_w is the rotational inertia of the wheel assembly, a_x is the acceleration of the vehicle, V_x is the tangential velocity of the wheels, T_q is the torque applied to the wheels, W is the constant gain parameter or linear factor and E_{Sx} and E_{Tq} are the terms of the equation divided based on the parameter that affects it; slip and torque based elements respectively.

This equation is used to estimate the slip ratio for each wheel without using the speed of the car which we need to estimate but rather with the wheel speed translated to CoG. This eliminates the circular dependency between the slip ratio calculation and speed estimation. The equation contains dynamic, static and tuning terms that not only make the slip detection dynamic, but also tune it based on the vehicle being driven and tyres used. We now look at each component and understand how it affects slip.

4.3.3 Dynamic Parameters

The equation contains some parameters that change in every time step, making the slip ratio calculation more dynamic. Here we discuss the parameters.

Acceleration

Acceleration of the vehicle plays an important role to determine if the wheels will slip or not. The relation between slip and acceleration is positive, which means that as acceleration increases due to the torque applied at the wheels, the wheels will slip more and the slip ratio increases. This phenomenon occurs to produce grip and thus propelling force, irrespective of the road-tyre friction coefficient. It will only affect what peak force and grip is and at what slip ratio it occurs as seen in figure 2.1b. The friction coefficient in this case is assumed to be constant in this case.

Torque

Similar to acceleration, torque also has a positive relation to slip. As the torque applied to the wheels increases, more propelling force is produced at the contact patch and the slip ratio increases.

Velocity

The slip ratio equation has a velocity term which affects slip and makes the equation non-linear. In this case, the slip ratio calculation evolves with the velocity of the wheels translated to the centre of gravity V_x. This velocity is used to take in to consideration even the small steering angles in the data log, as well as the yaw rate from the equation 3.1. Using wheel speed instead of the vehicle speed eliminates any circular dependency that could have occurred if the estimated velocity itself would have been used.

4.3.4 Static Parameters

The static parameters, mainly of the tyres, also play an important role in slip ratio calculation. These parameters are based on the size and construction of the tyre and wheel assembly. In reality, these parameters will also change dynamically, but for the scope of thesis and the data available, they are considered to be static.

Tyre longitudinal stiffness

The longitudinal stiffness of the tyre is defined as the slope of the the tyre force-slip curve from 2.1a. A stiffer tyre produces peak propelling force as well as lose grip beyond the peak at relatively lower slip ratio. So, the longitudinal tyre stiffness guides how the new slip ratio will depend on the previous slip ratio as seen in equation 4.16. This parameters also varies with what the tyre is subjected to in terms of temperature, pressure and load as well as where the slope is being computed based on which side of the peak the tyre lies in 2.1a. For this work, this parameter is considered to be constant throughout.

Tyre Radius

The radius here is the static loaded radius of the wheel and remains constant throughout. The radius however, changes dynamically based on temperature pressure, load and other parameters however for the scope of the thesis, this radius is considered to be constant.

Wheel Inertia

The wheel inertia is based on the mass of the whole wheel assembly and loaded tyre radius. The rotational inertia basically defines how much the wheel can be accelerated based on the torque applied to it.

4.3.5 Constant Gain Parameter

The term varying with slip ratio E_{Sx} from the equation 4.16 is derived from the previous slip and tyre parameters while the term varying with torque E_{Tq} is derived from the torque applied on the tyre along with the tyre radius and wheel inertia. Both the components play a role in calculating slip ratio, however, they are not very accurate in the high slip slip region since the tyre radius and the longitudinal stiffness will vary at every time instant. Also, the torque estimations are not accurate, giving high values of slip, especially when the velocity is really low. This, however is very difficult to pinpoint and determine as well as lies outside the scope of this work. Hence a constant linear factor is used to make the estimate follow the true slip ratio of the tyre.

The linear factor W decides how much to trust the dynamic evolution of previous slip with tyre parameters and torque applied to the wheels.

4.3.6 What The Equation Is Doing

Each elemental term in this equation i.e. E_{Sx} and E_{Tq} is effectively comparing the wheel accelerations with car accelerations.

From the first term in E_{Sx}, $\frac{C_x \cdot R_e^2}{I_w}$ part gives the rotational acceleration of the wheel and compares it with the vehicle acceleration a_x. This difference between wheel acceleration and vehicle acceleration evolves non-linearly with the tangential speed of the vehicle V_x and the previous slip ratio. So the term E_{Sx} gives how the evolution of the difference between wheel and vehicle acceleration determines the slip ratio.

The second element of the equation E_{tq}, begins with the term $\frac{T_{q,k} \cdot R_e}{V_{x,k} \cdot I_w}$ where $\frac{T_{q,k} \cdot R_e}{I_w}$ is the wheel acceleration based on the torque applied, while a_x is the car's acceleration. These accelerations are compared again, this time evolving with V_x as well as the torque applied T_q.

The difference between wheel acceleration and car acceleration is one of the slip indicator used in concept 1 [1]. However, concept 1 uses a static deterministic threshold. A triggering of this threshold would tell if the wheels are slipping or not without considering how the wheel slip probability evolves around dynamic parameters like torque, speed, accelerations as well as tyre parameters. It would lock the slip flag between two events. Here, the actual value of slip is calculated at each time instant using dynamic relations.

4.3.7 The Speed Estimation Process

The overview of the estimation process using a standard sensor suite and the dynamic slip detection concept 3 is shown in figure 4.10.

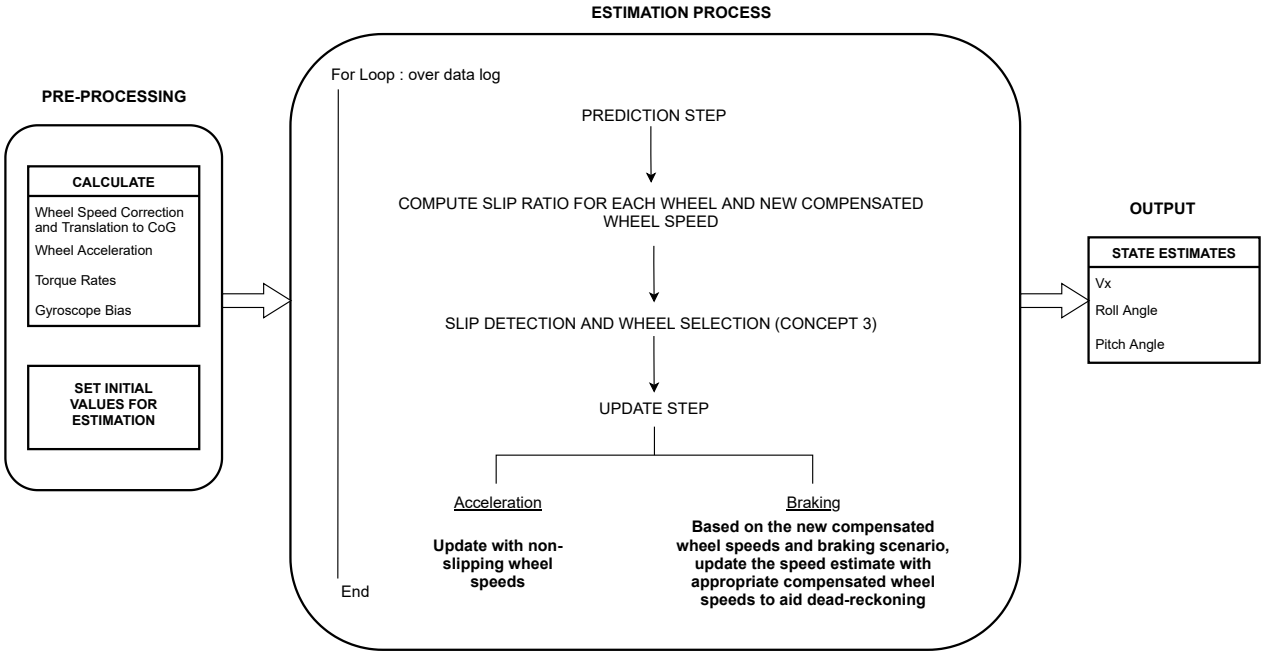

Figure 4.10: *Effect of accelerations, deceleration and speed on GPS speed error*

Pre-Processing

This step is similar to the pre-processing of different variable and parameters as explained in 4.2.5 except that the GPS speed signal is not modelled.

Estimation Process

The prediction step is the same as seen in the GPS approach as well as the precursor thesis. The process model is a kinematic vehicle model input to an EKF. In this case, the V_xRP filter from the precursor thesis work is used because it was the best performing filter among the ones developed. The next steps are what define this new approach.

Computing Slip Ratio

Slip Ratio calculated by the equation 4.18 is based on dynamics and static parameters. The way the equation estimates slip ratio introduces noisy estimates at lower speeds, especially when the vehicle is just starting, due to the high torque applied, as well as the extremely low speed of the vehicle. To tackle this, the slip ratio equation 4.18 is adopted based on the speed of the vehicle. This speed is the predicted speed of the vehicle. Since it is only used as a threshold to decide how the equation is adapted, it's accuracy is of little importance.

If the vehicle is moving at speeds greater than 15 km/h, equation 4.18 is used to calculate slip. If the vehicle

speed is between 5 km/h and 15 km/h, the slip ratio is calculated using the equation

$$S_{x,k+1} = (E_{Sx} + 1) \cdot S_x \cdot T_s \tag{4.19}$$

At speeds below 5 km/h, the new slip ratio is given by

$$S_{x,k+1} = S_{x,k} \tag{4.20}$$

This is to avoid high peaks and exponentially rising estimates due to low velocity in the denominator. This also avoids any noisy slip ratio calculations due to noisy torque data in the early stages of the data log when the car just starts moving. This can be observed in figure 4.11.

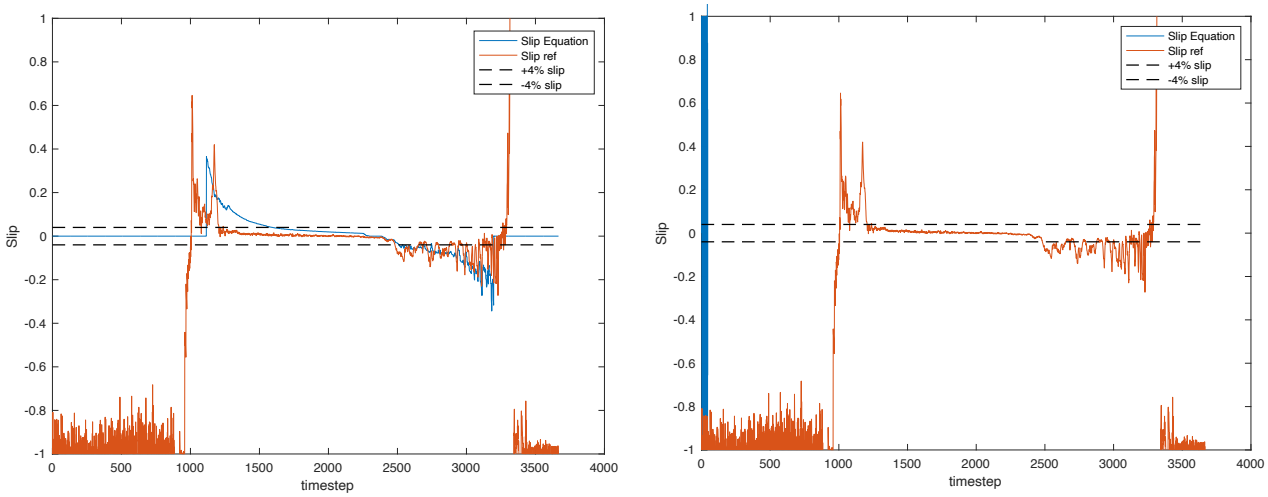

(a) *Slip Equation output based on velocity thresholds*

(b) *Slip Equation output without adapting to velocity*

Figure 4.11: *Slip Equation Outputs with and without speed thresholds plotted against reference slip ratio, calculated from the OxTS ground truth speed*

Compensated Wheel Speeds

Since the equation gives a slip ratio estimate for each wheel, the wheel speeds from the sensors can be compensated with this slip ratio to use as measurements that are more closer to the true speed of the car and can aid the speed estimate. A comparison between compensated and true wheel speeds can be seen in 4.12. The compensated wheel speeds are closer to the reference speed in yellow when the wheels are slipping more than 4% or are outside the 4% error limit. This helps the slip detection to not only trigger the slip flag, but also use these wheel speed measurements to aid dead-reckoning, especially in braking.

Slip Activation

Since this equation estimates the actual value of slip ratio rather than just triggering a flag based on events, the slip flag is activated if the slip ratio calculated is greater than 4% or if concept 1 detects slip or the engine Traction Control System (TCS) flag is active. A slip ratio of 4% is set as the threshold for slip flag activation due to the error limit set during this work. The error limit for the speed estimate is set at 4% of the reference speed signal from the OxTS. Thus 4% is taken as an acceptable amount of slip since the wheels within this slip ratio, once can argue that it those wheels could be trusted since they are still within the error limit.

Slip Deactivation

Similarly, the slip flag is deactivated if the slip ratio calculated is less than or equal to 4%, the Engine TCS flag is off and there is no other active slip indicator flag from concept 1.

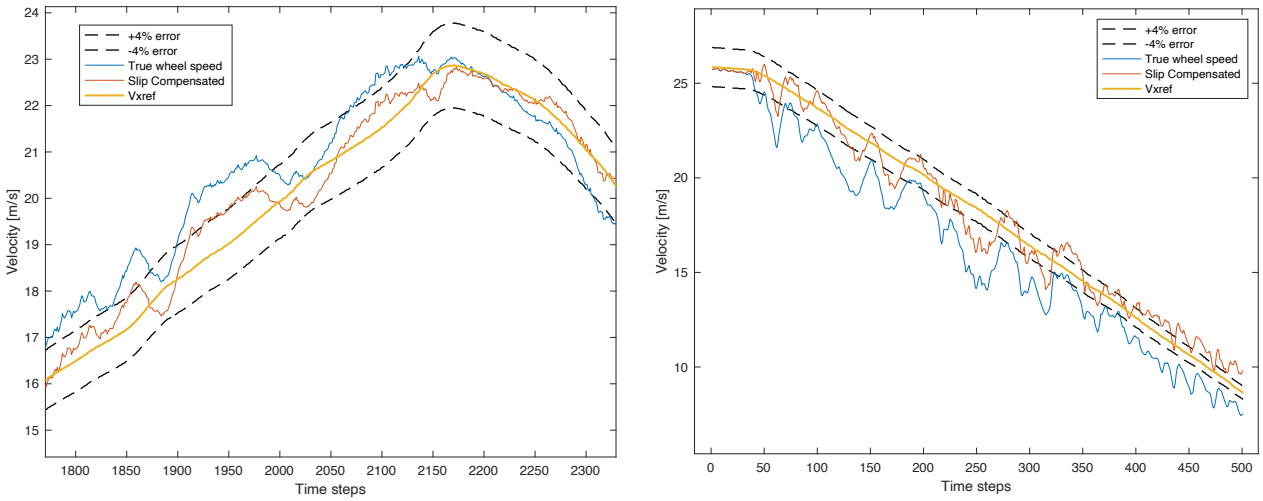

(a) *Compensated wheel speeds during acceleration*

(b) *Compensated wheel speeds during braking*

Figure 4.12: *Compensated wheel speeds compared with the true wheel speeds and reference speed signal from OxTS*

A Side Case

In cases where there is a wheel speed that is slower than the predicted speed of the vehicle, then that wheel speed is fed to the EKF as a measurement. The wheel speed threshold is defined by the predicted speed at which the vehicle is moving. If the speed of the vehicle is greater than or equal to 100 km/h, then a wheel speed that is slower than the predicted speed by 4 km/h is trusted. For speeds less than 100 km/h, a wheel speed slower than the predicted speed by 2 km/h is trusted.

Why Concept 1 Is Combined

This concept uses the previously developed Concept 1 for slip flag activation to determine whether the torque thresholds and acceleration thresholds can be trusted to detect slip. Trusting an estimated slip ratio can back-fire due to the static parameters, the equation's low pass filtering nature that could lead to wheel slip being missed completely. The thresholds in concept 1 also make up for activation of slip flags at lower speeds when the slip ratio equation may not be accurate because of using limited parameters to avoid noisy estimates. Thus, the "OR" condition is used to help to detect slip in case the slip equation fails to trigger the slip flag correctly during initial slip at slow speed.

This can be seen in figure 4.13. The slip ratio estimate in acceleration is late to rise due to the speed thresholds. At speeds lower than 5 km/h, just when the vehicle begins to move, the slip estimation is noisy and rises exponentially as seen in figure 4.11b. Thus the slip ratio is held constant at the previous value, which in the initial case is 1e-3. It is almost as if the slip ratio equation only works beyond 5 km/h which then leads to a slower slip ratio rise.

In deactivation, it is used to make sure that there is no slip flag active due to the torque thresholds or acceleration thresholds. As for braking, the slip ratio estimate is closer to the reference, more so than in acceleration. This could be because of the accurate brake torque measurements. This allows for using these speeds in the kalman filter as a measurement in braking and remove the burden from pure-dead reckoning, which was the case previously. This is used in the braking strategy explained next.

Braking Strategy

The braking logic for this concept includes strategically trusting appropriate wheel speeds, whether they be the true wheel speeds or the compensated wheel speeds, to aid dead-reckoning. This helps to trust a wheel speed that is closer to the true speed of the car and reduce reliance on pure dead-reckoning. The braking strategy has a 0.25s delay to trust that the vehicle is braking is similar to the earlier strategy [1]. Then, depending on if

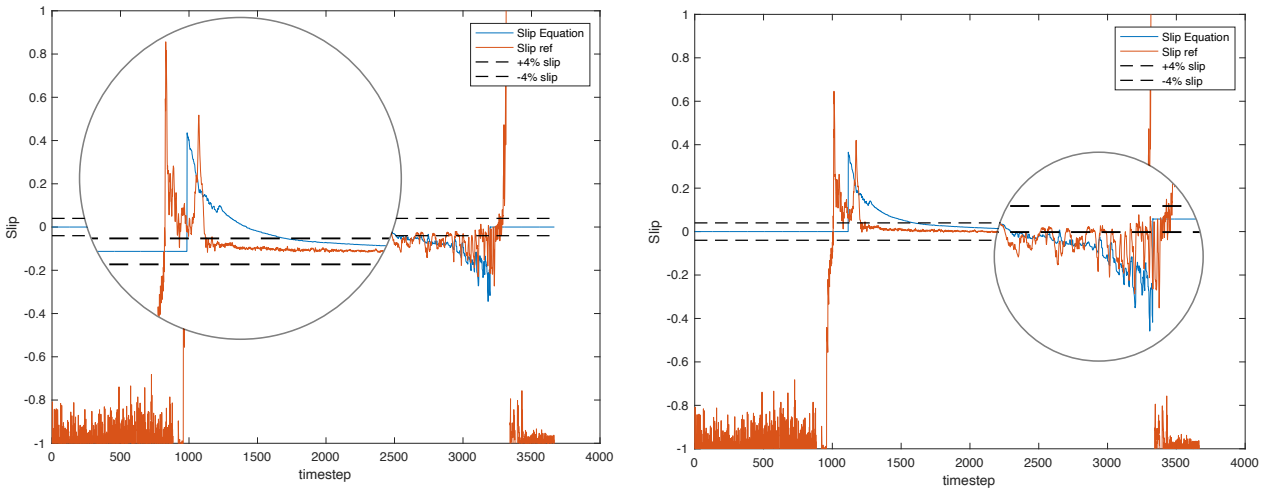

(a) *Late rise of slip ratio estimation*

(b) *Fairly accurate slip ratio estimate during braking*

Figure 4.13: *Slip Ratio estimations during braking and acceleration*

any wheel is faster than the speed estimate or no, the compensated wheel speeds are fed as a measurement based on the predicted speed.

The decision between which wheel speed to trust is based on the predicted speed of the vehicle or if any wheels are faster than the predicted speed. If the predicted speed is between 25 km/h and 50 km/h, then the fastest true wheel speed from the sensor is trusted. At speeds faster than 50 km/h, the slowest compensated front wheel speed is trusted while, at speeds slower than 25 km/h, the slowest compensated rear wheel speed is trusted. The reason why the slowest compensated wheel is trusted is to avoid some of the over-estimated slip ratios calculated in braking conditions due to static parameters of the tyres as well as errors in the torque values in the data log. The over-estimation can be observed in figure 4.13b where at the end, the slip ratios are higher and which will lead to the compensated wheel speeds being higher than the reference.

Limitations

The tyre parameters are limitation of this method as the equation fails to detect slip early enough due to the low pass nature of the equation, missing pronounced peaks in the beginning of slip increase. At higher speeds, once the torque is introduced in the equation, it becomes susceptible to torque sensor measurements. The torque sensor is affected by a lot of parameters that could lead to errors which in turn could lead to an incorrect slip ratio calculation in some cases. Another limitation is the unknown road-tyre friction coefficient, which is assumed to be constant throughout all data logs which in reality, is not the case.

This 4% limit on slip ratio is decided based on the error limit set in the vision of the thesis [1] and section 1.2. This means that if the wheels are slipping more that 4%, they shouldn't be trusted to estimate the speed of the vehicle.

5 Results

This chapters talks about the results of the two new methods for speed estimation in excessive wheel slip conditions. The chapter begins with listing the evaluation parameters and numbers. Next, the results of the three segments of data logs are shown and some examples are used to compare GPS speed and concept 3 against concept 2. A few examples for the two methods and how they perform are listed next. A short explanation of how the methods perform better or or worse as compared to the previous work is then given at the end of the chapter. For ease of reference, the approaches will now be referred to as GPS and C3 for GPS speed and slip detection concept 3 respectively. The brake manufacturer and Volvo's simple estimate will be referred to as OEM methods.

5.1 Process of Evaluation

Here is a brief overview of the evaluation process that is followed for the methods developed in this thesis work. The evaluation is divided into three major sections i.e. one for each segment in which the data log is divided - Complete data, slipping during acceleration, braking. This segmentation of data into three sections is explained in precursor thesis work [1]. Then, for each segment, the performance numbers and statistical parameters are tabulated for overview.

Performance evaluation is divided into two parts. First, the GPS method is compared with concept 2. Then, it is compared to Volvo's simple estimate as well as the brake manufacturer's estimate. Similarly, C3 is compared in two parts. All this is done for each segment of data log. Basically, both approaches are compared to V_xRP with concept 2, Volvo's simple estimate and the brake manufacturer's estimate. Then some examples are picked out to showcase the good and limitations of the these two approaches along with an explanation.

The evaluation is done for 15 data logs from the AWD large hybrid vehicle, thus named HY-1 to HY-15. These data logs contain various different maneuvers, speeds, environment conditions and wheel slip scenarios with long and short durations. These log files are described in 4.1.

Filter V_xRP with Concept 2 is the only method from previous work against which the new methods are compared because this was found to be the best performing from precursor thesis work. The objective of this work is to improve upon the previous methods, trying to make better estimation methods than the previously developed best one.

5.1.1 Data segmentation

Data logs are segmented into three different sections to analyse the performance of the estimation methods in specific cases. The sections are made on a high level. The first section is the complete data. The second section is the cases where the wheels are slipping over 4% while the car is accelerating. The third section contains cases where the vehicle is braking, irrespective of whether the wheels lock or no. In depth explanations of they are defined in each data log on a low-level is explained in the precursor thesis work section 4.2.2 [1]

5.1.2 Statistical Parameters for Evaluation

The parameters used for evaluation of the thesis work are the same as used in the precursor thesis work. They are percentage of data solved (i.e. the amount of time the estimate is within the 4% throughout the whole data log / section), RMSE, Peak minimum and maximum errors and the standard deviation. To understand the theory and the significance of these parameters in detail, the reader is guided towards it's explanation in precursor thesis work Section 4.3 [1].

It is important to note that the performance of these methods the consolidated table under the parameter "solved" is based on if the estimated speed is within $\pm 4\%$. Even the smallest deviation from that limit tells the diagnostic script that the method has failed. This check is done at each time step.

5.2 Performance : Complete Data

The table here shows a performance overview for the two methods over complete data logs. The column "Solved [%]" indicates the share (in %) of log data for which the estimated speed of the vehicle is within ±4% of the reference speed; an error limit set during the thesis work. This can also be seen as the amount of data for which the method accurately estimates speed i.e. the amount of time the speed estimate is within the aforementioned error limit. The cell colours indicate how good or bad the method performs for each data log. The green regions are where the method solves more share of data logs, while the red region means that it solves a lesser share of the data logs. This on its own does not represent how good the estimate is, but it gives an idea of how well the method performs on average.

A complementary consolidated table of averaged statistic parameters for each estimation method can be seen in 4.2. Here, the five estimation methods are compared among each other with green being the best and red being the worst performing. The main purpose of these parameters is to give some insight on the accuracy of each method. It is important to note that this are average errors over fifteen data logs which might be skewed by some outliers in the estimate in some data log. [1]

Table 5.1: Performance of different estimation methods over Complete data logs

COMPLETE DATA					
	Vx-R-P with CONCEPT 2	Vx-R-P GPS with CONCEPT 2	Vx-R-P with CONCEPT 3	VOLVO'S SIMPLE ESTMATE	BRAKE MANUFACTURER
Data Logs	Solved [%]	Solved [%]	Solved [%]	Solved [%]	Solved [%]
HY - 1	89.58	95.65	96.62	60.84	74.63
HY - 2	92.77	93.93	99.81	74.45	71.78
HY - 3	97.13	98.86	98.89	86.57	84.42
HY - 4	97.99	99.83	97.95	71.99	75.58
HY - 5	97.13	96.77	100.00	51.79	43.01
HY - 6	66.16	60.42	64.82	14.53	19.50
HY - 7	95.91	96.12	96.33	95.54	94.75
HY - 8	94.16	96.52	99.70	19.26	46.26
HY - 9	87.59	96.87	91.49	35.21	66.95
HY - 10	84.45	89.81	92.32	40.82	60.92
HY - 11	87.80	88.84	96.31	47.59	65.15
HY - 12	99.08	99.80	98.39	54.21	77.10
HY - 13	99.79	99.94	99.46	94.24	98.05
HY - 14	100.00	100.00	100.00	81.49	99.63
HY - 15	99.94	99.86	99.93	95.89	99.79
Average	**92.63**	**94.22**	**95.47**	**61.63**	**71.83**

Table 5.2: Average statistic parameters : Complete Data

COMPLETE DATA : Average of each statistic parameter						
Stat Parameters	Unit	Vx-R-P with CONCEPT 2	Vx-R-P GPS with CONCEPT 2	Vx-R-P with CONCEPT 3	VOLVO'S SIMPLE ESTMATE	BRAKE MANUFACTURER
Solved	[%]	**92.63**	**94.22**	**95.47**	**61.63**	**71.83**
Absolute RMSE	[m/s]	0.28	0.28	0.26	1.15	0.86
Max Absolute Error	[m/s]	0.44	0.40	0.51	2.82	2.46
Min Absolute Error	[m/s]	-1.11	-3.03	-2.23	-3.97	-1.73
Relative RMSE	[%]	2.06	2.14	2.04	14.87	9.80
Max Relative Error	[%]	4.02	4.37	4.39	79.57	36.92
Min Relative Error	[%]	-6.67	-24.51	-18.71	-21.15	-10.78
Standard Deviation	[m/s]	0.25	0.26	0.25	1.08	0.74

5.2.1 GPS vs Concept 2

Looking at table 5.1, it is clear that on average, over 15 data logs, GPS approach is better than Concept 2. V_xRP, GPS is also better than concept 2 over each data log as well bar a few exceptions. Data log HY-6 for example trusts the GPS speed update while the wheels are coming back to rolling from a locking state. This is happening at very low speed, less than 5 m/s during braking and the GPS speed signal has higher errors in that driving scenario.

From the statistical parameters table 5.2, it is observed that the GPS method on average is not as accurate as concept 2. The staircase type signal of the GPS accounts much of the higher errors, especially in the Minimum Relative Error parameter where it is the worst performing out of all methods. This result however as mentioned before, could be skewed by extreme outliers in one data log. Also, since it is relative, it is highly sensitive at lower speeds, meaning that a small absolute error at lower speed could correspond to an extremely large relative error.

GPS method however has the lowest average peak absolute error at 0.40 m/s.

5.2.2 GPS vs OEMs

From table 5.1 it is clear that GPS method performs better than both the OEM methods - Volvo's simple estimate and brake manufacturer both on average as well as individually over 15 data logs. The GPS method is also more accurate than OEM methods except in Minimum Absolute and Relative Error. The explanation for reduced accuracy in these cases is that the estimation trusts the GPS speed that lags behind and outputs a much slower speed measurement, especially in acceleration. In such cases , a trust on the GPS speed in all wheel slip cases is not ideal. Also, relative errors can be sensitive at lower speeds

5.2.3 Concept 3 vs Concept 2

From table 5.1, it can be seen that on average over 15 logs, C3 is the best performing method than C2. It is also better than C2 individually over each log except for HY-6 which in this case performs slightly worse during the braking case, where the compensated wheel speeds are not as accurate as expected.

As for statistical parameters in table 5.2, C3 shows the lowest average RMSE, relative RMSE and standard deviation among all methods making it slightly better than C2. Lower RMSE is credited to accurate slip detection dynamically at each time step, allowing dead-reckoning to be done without the onset of drift in most cases. However, the peak and relative errors when the estimate is slower than the true speed is very large, pointing towards extreme outliers during braking conditions. This can be attributed to incorrect wheel speeds being trusted in braking.

5.2.4 Concept 3 vs OEM

As compared to OEM estimations, C3 outperforms them on average as well as individually over 15 data logs. It is important to note that the OEM methods are simple and based on wheel speeds as mentioned earlier.

A similar trend can be observed in statistical parameters where C3 has better accuracy except in cases when the estimate is slower than the true speed, which could be attributed to trusting inaccurate wheel speeds either true or compensated, in braking strategy or an estimation with large outliers.

5.3 Performance : Slipping while Accelerating

In the tables 5.3 and 5.4, the performance of the two methods compared to previous methods during scenarios of slipping during acceleration are presented.

Table 5.3: Performance of different estimation methods over parts of the logged data where wheels are slipping during acceleration

SLIPPING IN ACCELERATION SCENARIOS					
	Vx-R-P with CONCEPT 2	Vx-R-P GPS with CONCEPT 2	Vx-R-P with CONCEPT 3	VOLVO'S SIMPLE ESTMATE	BRAKE MANUFACTURER
Data Logs	Solved [%]	Solved [%]	Solved [%]	Solved [%]	Solved [%]
HY - 1	100.00	100.00	100.00	86.79	76.32
HY - 2	87.54	89.22	99.66	56.14	48.26
HY - 3	93.26	99.59	97.16	68.69	59.63
HY - 4	100.00	100.00	100.00	80.79	65.75
HY - 5	96.57	95.35	100.00	30.49	26.15
HY - 6	99.20	99.17	100.00	27.39	13.43
HY - 7	91.35	91.35	89.81	89.88	85.41
HY - 8	100.00	100.00	100.00	21.51	31.88
HY - 9	79.29	98.26	87.05	14.37	34.93
HY - 10	94.43	95.09	100.00	59.34	65.66
HY - 11	100.00	100.00	100.00	64.22	72.86
HY - 12	100.00	100.00	100.00	68.73	71.35
HY - 13	100.00	100.00	100.00	81.25	93.34
HY - 14	100.00	100.00	100.00	78.31	95.33
HY - 15	100.00	100.00	100.00	81.85	96.34
Average	96.11	97.87	98.25	60.65	62.44

Table 5.4: Average statistic parameters : Slipping in Acceleration Data

ACCELERATION DATA : Average of each statistic parameter						
Stat Parameters	Unit	Vx-R-P with CONCEPT 2	Vx-R-P GPS with CONCEPT 2	Vx-R-P with CONCEPT 3	VOLVO'S SIMPLE ESTMATE	BRAKE MANUFACTURER
Solved	[%]	96.11	97.87	98.25	60.65	62.44
Absolute RMSE	[m/s]	0.19	0.16	0.19	1.24	0.91
Max Absolute Error	[m/s]	0.44	0.39	0.46	0.42	2.50
Min Absolute Error	[m/s]	-0.47	-0.33	-0.35	-3.92	-0.14
Relative RMSE	[%]	1.50	1.41	1.36	17.32	11.03
Max Relative Error	[%]	3.23	2.86	3.48	72.50	35.80
Min Relative Error	[%]	-3.90	-3.43	-2.49	-3.82	-0.48
Standard Deviation	[m/s]	0.16	0.13	0.16	0.87	0.61

5.3.1 GPS vs Concept 2

GPS method in segments of the data logs where wheels are slipping during acceleration outperforms C2 on average as well as individually over all 15 data logs. Higher solved % can be seen especially in HY-9 where the GPS speed update really helps to guide dead-reckoned speed estimate and keep it within ±4% of the reference speed. The performance numbers can be observed in table 5.3.

For all the average statistical performance parameters from table 5.4, the GPS method outperforms C2. The GPS method has the lower RMSE, lower maximum and minimum absolute errors, relative errors and standard deviation. It has also has the lowest RMSE, min and max absolute errors as well as standard deviation, showing

good accuracy as compared to other methods. The errors are lower for the GPS speed in acceleration as it stops the drift error onset from occurring too early, reducing the chances of the speed estimate drifting away, beyond the 4% error limit. This is especially prominent in the acceleration and slip cases where, when all wheels are detected to slip, the GPS speed signal pulls the estimate "down" towards the true speed of the vehicle in case, the estimate starts to drift.

5.3.2 GPS vs OEMs

As seen in table 5.3, GPS method performs better on average as well as individually over 15 data logs than the OEM methods based on wheel speeds.

In terms of accuracy, the GPS method is better than the OEM methods except in two cases - peak error when the estimated speed is lower than the true speed of the car. From table 5.4 it is observed that the minimum absolute error for GPS method is -0.33 m/s which is very small, however the relative error at that point is 3.43%, because the relative error is sensitive at lower speeds. Since the speed estimate updated from the GPS has a higher average peak error at lower speeds suggests that the error occurs when the vehicle starts accelerating from a standstill while the GPS update lags behind the true speed in such cases.

5.3.3 Concept 3 vs Concept 2

It is clear from table 5.3 that C3 is better that C2 on average as well as individually over 15 log files in segments of the data logs where wheels are slipping during acceleration. The only file where the performance numbers suggest otherwise is HY-7, due to the tuning parameters set for the V_xRP filter used along with C3.

The RMSE, maximum absolute error and standard deviation of errors are very similar for both C3 and C2. C3 has the best average relative RMSE, suggesting that the average RMSE close to 0.19 m/s have occurred at slightly higher speeds.

5.3.4 Concept 3 vs OEMs

C3 outperforms the OEMs simple wheel speed based methods of estimation over all data logs as seen in table 5.3. HY-7 is where C3 every so slightly keeps the speed estimate within the error limit for a lesser time than Volvo's simple estimate, which is because of the tuning parameters set for the filter and speed measurements.

C3 has an average peak absolute error of only 0.04 m/s higher than Volvo's simple estimate and 0.21 m/s higher average absolute error than the brake manufacturer when the speed estimate is slower than the true speed. In these situations, C3 also has a higher relative error, suggesting that the peak minimum absolute error occurs at low speeds.

5.4 Braking Scenarios

In the tables 5.3 and 5.4, the performance of the two methods compared to previous methods during braking scenarios are presented.

Table 5.5: Performance of different estimation methods over parts of the logged data where the vehicle is braking

ALL BRAKING SCENARIOS WITH AND WITHOUT LOCKING					
	Vx-R-P with CONCEPT 2	Vx-R-P GPS with CONCEPT 2	Vx-R-P with CONCEPT 3	VOLVO'S SIMPLE ESTMATE	BRAKE MANUFACTURER
Data Logs	Solved [%]	Solved [%]	Solved [%]	Solved [%]	Solved [%]
HY - 1	73.47	88.92	91.39	20.28	62.15
HY - 2	97.83	100.00	100.00	96.66	100.00
HY - 3	96.97	94.08	100.00	92.60	99.04
HY - 4	92.31	99.35	92.14	21.44	46.97
HY - 5	100.00	100.00	100.00	100.00	82.50
HY - 6	39.24	28.82	36.11	5.56	24.31
HY - 7	94.23	95.48	100.00	94.07	100.00
HY - 8	84.55	90.80	99.20	15.98	68.48
HY - 9	95.38	95.11	95.44	46.82	97.08
HY - 10	63.99	78.98	76.51	2.95	44.04
HY - 11	65.90	69.68	92.07	19.63	58.16
HY - 12	96.85	99.32	94.47	17.53	84.34
HY - 13	97.79	99.37	94.33	52.06	80.12
HY - 14	100.00	100.00	100.00	62.70	97.92
HY - 15	99.36	98.45	99.21	78.19	99.56
Average	86.52	89.22	91.39	48.43	76.31

Table 5.6: Average statistic parameters : Braking Data

BRAKE DATA : Average of each statistic parameter						
Stat Parameters	Unit	Vx-R-P with CONCEPT 2	Vx-R-P GPS with CONCEPT 2	Vx-R-P with CONCEPT 3	VOLVO'S SIMPLE ESTMATE	BRAKE MANUFACTURER
Solved	[%]	86.52	89.22	91.39	48.43	76.31
Absolute RMSE	[m/s]	0.38	0.34	0.32	1.03	0.58
Max Absolute Error	[m/s]	0.08	0.10	0.24	2.82	0.48
Min Absolute Error	[m/s]	-1.02	-2.15	-2.22	-0.04	-1.73
Relative RMSE	[%]	2.65	2.58	2.59	7.32	4.34
Max Relative Error	[%]	2.75	3.41	2.90	0.72	4.24
Min Relative Error	[%]	-6.18	-17.85	-18.57	-21.14	-10.78
Standard Deviation	[m/s]	0.25	0.23	0.24	0.59	0.43

5.4.1 GPS vs Concept 2

Segments of the data log where the vehicle is braking is a challenging scenario given that the wheel speeds are noisy and wheels almost always lock up, resulting in dead-reckoning to be relied upon, introducing drift errors. The performance of the GPS method over C2 as seen in 5.5 is better on average over 15 data logs. However, the method struggles in HY-6 at low speeds close to 4 m/s where the GPS update fails to set an accurate start point close to the true speed for dead-reckoning. This results in the dead-reckoned speed estimate to drift almost as soon as it starts and goes outside the 4% error limit.

The errors generated on average over 15 data logs by the GPS method are on the higher side, with the minimum

absolute error on average being 2.15 m/s and minimum relative error being 17.85%. This also hints at some extreme outliers that bias these averages.

5.4.2 GPS vs OEMs

GPS method performs better than OEM methods on average over 15 logs however, it doesn't match up to the solved % for logs HY-3, HY-7 especially. This is because the GPS method during braking is using the GPS speed rather than the wheel speeds which are not slipping, to update the estimate. The wheel speed based methods perform better for these data logs.

As for accuracy, the GPS method is better than the OEM methods except when it comes to minimum absolute error, minimum relative error and max relative error (suggesting that the error occurs at a low speed that significantly skews the relative error measurement). Most errors in the GPS method in braking are due to the trust put in the GPS speed during braking while the wheel speeds might have been accurate, especially at lower speeds as seen in HY-6.

5.4.3 Concept 3 vs Concept 2

Concept 3 is the best performing method on average over 15 data logs as seen in table 5.5, solving 91.39% on average. It is also individually better for each data log compared to C2 except in data logs HY-6, HY-12 and HY-13. In all these files, the fastest compensated wheel speeds are highly accurate and would boost the solved % for these files if trusted. However, while developing this method, it was observed that during braking, there were cases of over-estimation of slip ratios, thus leading to a brake strategy that trusted slowest compensated wheel speed.

As for accuracy, C3 has the lowest RMSE and low relative RMSE along with fairly low standard deviation. This method as mentioned above, struggles as it tries to avoid the over-estimation issue, generating large average minimum absolute and relative errors, biased by a couple of extreme outlier data logs. This also shows that the errors in the estimate are lowest on average but have spikes of high errors.

5.4.4 Concept 3 vs OEMs

When compared to OEMs estimation methods, C3 outperforms the OEMs simple wheel speed based methods on average as well as individually, barring HY-9 data log, where the difference in solved % is barely 1.6%.

Similar as compared to C2, the C3 method has very low RMSE but high peaks during braking when the estimate either jumps to trust a slipping / locking wheel, leading to high peak errors.

5.5 Examples

In this section some examples of each method are shown with sections where they are better than the previous method C2, sections where they struggle and what are the possible reasons for both.

5.5.1 Approach 1 : GPS speed as measurement

Better than C2 in slipping while acceleration scenarios

This approach outperforms each data log in terms of % solved or the amount of time over the logged data that the estimate is within the error limit. The most notable increase comes in data log HY-9 in segments of the data log where the wheel is slipping during acceleration seen in table 5.3. Here, the GPS approach keeps the speed estimate within the ±4% error limit for 98.26%, besting C2's solved% by 9%.

This improvement comes in a section where the vehicle is accelerated from a speed close to 8 m/s right after hard braking. On a slippery surface, this sudden increase of acceleration makes all the wheels slip. This can be observed in figure 5.1. All-wheel slip is correctly detected by the slip detection concept. Now, previous methods rely on the slip detection concept to accurately detect slip, providing a good starting point for dead-reckoning. In this case, C2 correctly detects slip and starts dead-reckoning at an accurate point. However, over the 8 seconds that the dead-reckoning goes on for, the speed estimate drifts considerably 5.1a. The problems with

dead-reckoning for this log can be read in [1]. In this situation, just guiding the dead-reckoning with a new GPS speed measurement every 1 second such that it starts over at a new and more accurate speed improves the estimate accuracy and keeps it within the desired error limits. As can be seen in figure 5.1b, the estimate is pushed "up" by the trust in the GPS speed, saving it from crossing the error limit. It is important to note that the GPS speed in this case was accurate and close to the error limit, which pushes the drifted speed estimate "up" towards the true speed. A GPS speed that was slower than the drifted estimate would not have helped in this case.

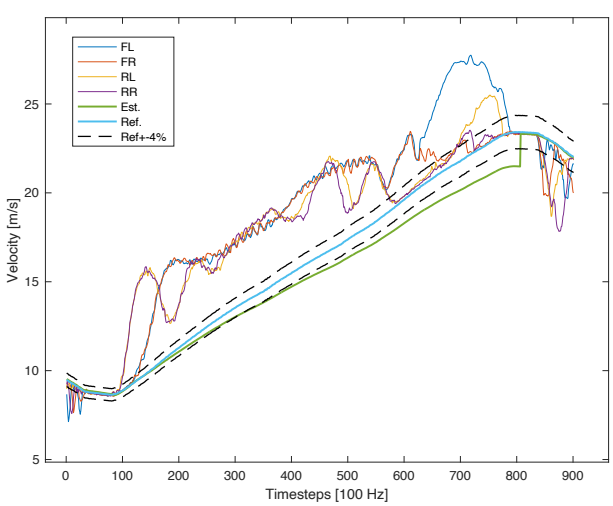

(a) *Speed Estimation using C2 and dead-reckoning*

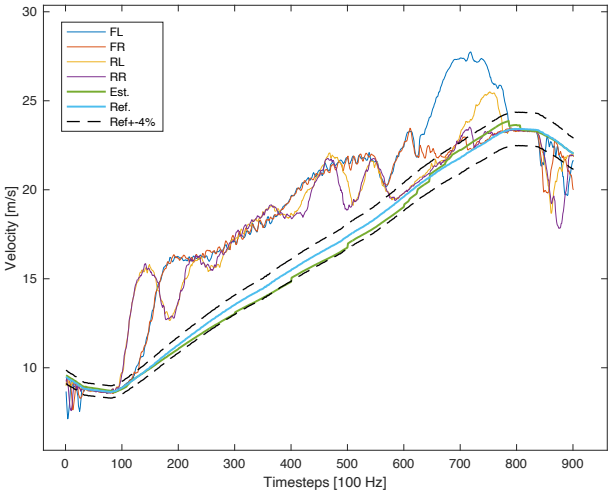

(b) *Speed estimation using C2 and dead-reckoning with GPS speed signal*

Figure 5.1: *Estimated speeds, wheel speeds and reference vehicle speed measurements*

The errors of the two estimation methods can be seen in 5.2a. The updates with GPS speed affecting the speed estimate and thus the error can be observed clearly in figure 5.2b at time steps around 300, 400, 500 and 600, saving the estimate from crossing the error threshold. As for C2 and pure dead-reckoning, the drift and consequent error in the estimate can be seen in figure 5.2a.

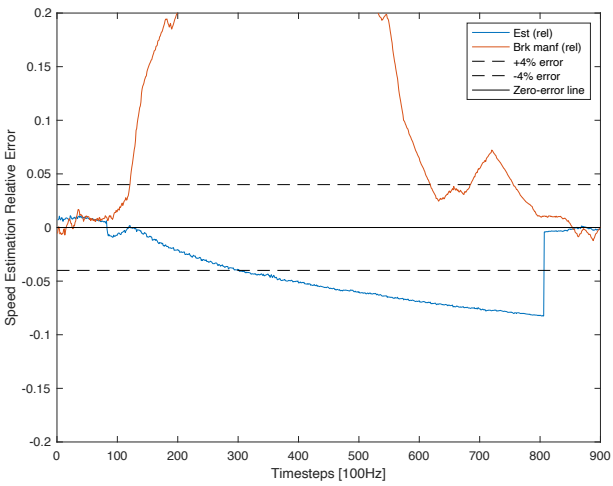

(a) *Pure dead-reckoning drifts away, causing errors greater than 4%*

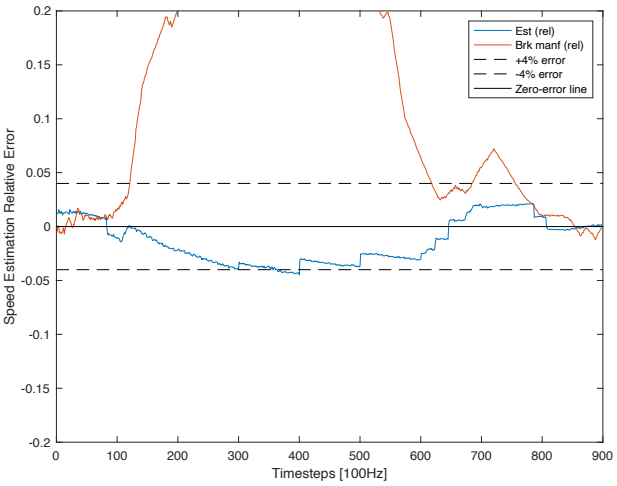

(b) *GPS update every second save the dead-reckoned speed estimate and keeps it within the 4% error limit*

Figure 5.2: *Relative error between speed estimations from pure dead-reckoning and GPS against the reference speed*

Where this method struggles

Data log HY-6 is where the GPS method struggles especially in braking conditions. A closer look at the nature of wheel speeds and the estimate in this condition is show in figure 5.3. The wheel speed measurements are extremely noisy due to ABS braking while driving on snowy roads. The wheel speeds drop as they start locking on low friction surfaces. The wheel speeds are slower than the reference speed of the car for 150 timesteps or 1.5 seconds. During this time, the GPS speed update is given a lower covariance and thus trusted. The point where the system trusts the GPS speed can be seen as a "spike" in the estimated speed at timestep 100. However, the update in the GPS speed measurement is not trusted enough and the dead-reckoning in this case starts to drift due to a poor starting point. By the time the GPS speed signal updates again i.e. at timestep 200 or after 1 second, the estimate has already drifted way beyond the error limit. Once it drifts away this far, the GPS speed update is not able to pull it back up to the true speed of the vehicle. Then, once the estimate drifts so far away that the wheel speeds rise above it, the faster wheel speeds are trusted more and more that bring the estimate back up within the error limits. It is however important to not that the speed errors in the GPS method in this case are lower than the errors in the brake manufacturer's speed estimate as seen in figure 5.3b.

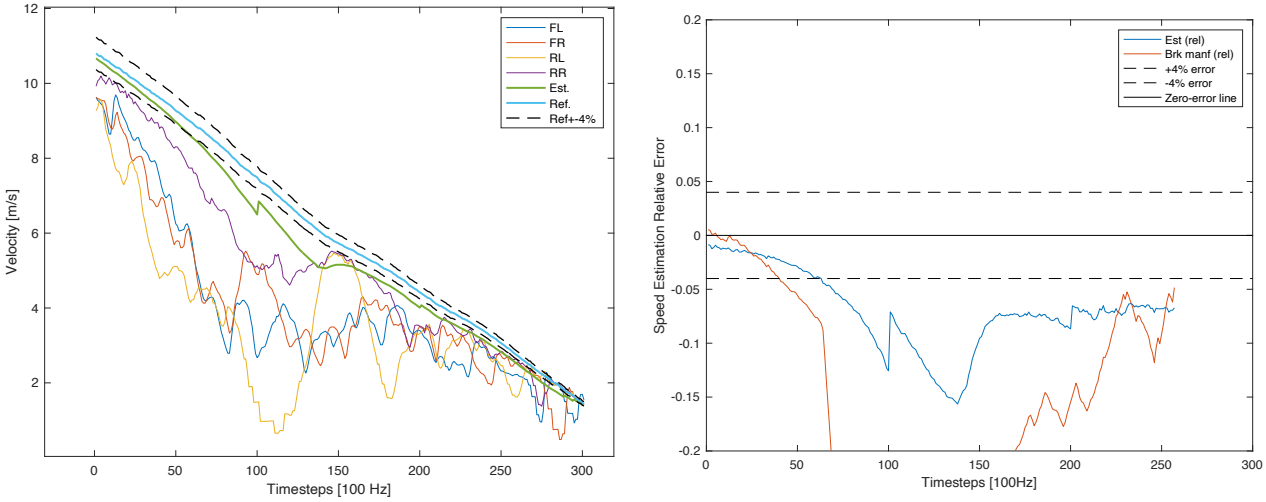

(a) *Estimated speed from C2, dead-reckoning with GPS speed updates*

(b) *GPS update every second but is not enough to save the dead-reckoned speed estimate as it drifts*

Figure 5.3: *GPS method struggles in HY-6 due to trust divided between the wheels and dead-reckoning between two GPS measurements which are 1 second apart.*

However, as mentioned in 4.2 and as seen in figure 4.6a, the GPS speed signal must be faster than the actual speed of the vehicle due to it's low update frequency. This is also the case in the modelled GPS speed signal used the GPS method. This can be seen in figure 5.4.

A good amount of trust in this speed saves the estimate in that it pulls the estimated speed up towards the true speed, and avoids an early onset of drift errors. Even still, it can't avoid an early onset of drift errors in dead-reckoning. This can be seen in figure 5.5. This discrepancy then is based purely on the fact that when the vehicle is braking, the GPS speed is trusted with a covariance that is tuned for all the files. This is done to avoid over-trusting the GPS speed and pulling the estimate up and above the error limit. For this particular file, a lower covariance suitable for the GPS speed signal to trust it helps the estimate pull up towards the true speed of the vehicle just enough to stay within the error limits. This solves the drift errors upto an extent. Further research and tuning based on more data can help to understand when to trust the GPS speed.

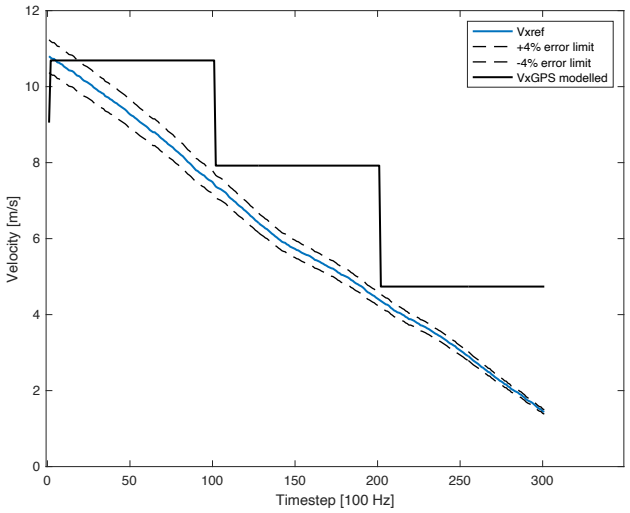

Figure 5.4: *modelled GPS speed signal with reference speed from OxTS*

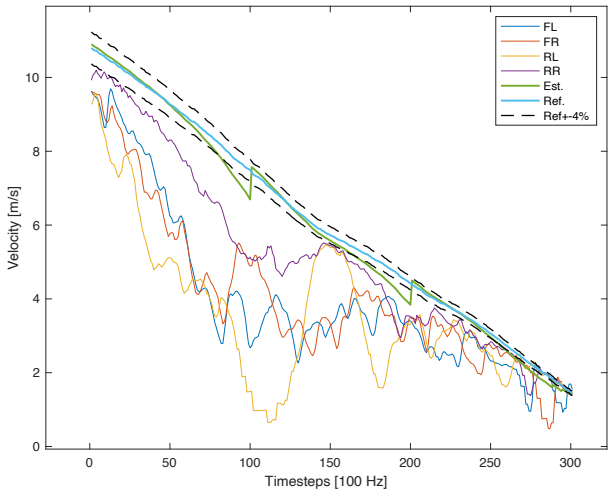

(a) *Estimated speed from C2, dead-reckoning with GPS speed updates with lower covariance on GPS speed*

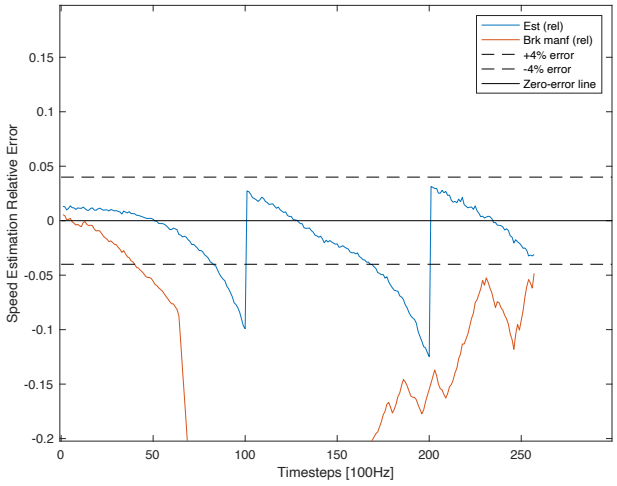

(b) *Relative errors in speed estimate when GPS speed signal is given lower covariance.*

Figure 5.5: *GPS method struggles in HY-10 due to trust divided between the wheels and dead-reckoning between two GPS measurements which are 1 second apart.*

5.5.2 Approach 2 : Slip Detection Concept 3

Where Concept 3 is better performing than C2

Concept 3 dynamically estimates the slip ratio of each tyre to activate and deactivate the slip flag. It's improvement over the estimation method developed previously using C2 is most noticeable in data log HY-2 from table 5.3. It estimates the speed within the error limit for 12% higher share of data log where the wheels are slipping during accelerations, as compared to C2.

This improvement comes in a part of the data log where the vehicle is accelerating and the wheels slowly start slipping and then increase the slip ratio gradually. This can be observed in figure 5.6. This case, when wheels slip slowly is one of the limitations or "grey zones" of C2 slip detection, mentioned in the precursor thesis work [1]. In figure 5.6a, the estimation of speed from previous method based on C2 is shown. Here, C2 first detects slip at correctly on three wheels - Front Left (Fl),Front Right(FR) and Rear Left (RL). Rear Right (RR) wheel is not slipping at that instant. Thus, RR wheel speed measurement is trusted during the estimation process. However, the RR wheel is also about to cross the threshold as it is slowly but surely slipping more and more.

The wheel speed residual variances do not trigger the slip flag immediately and the RR wheel speed is trusted during majority the acceleration phase. The RR wheel is then detected to slip around time step 150, at which point dead-reckoning begins. But, since the start point of dead-reckoning is already outside the error limit, the estimate drifts even further, producing larger errors until all wheels represent true speed at the instant the brakes are applied on the vehicle. C3 on the other hand maintains that all wheels are slipping throughout the acceleration phase. It starts dead-reckoning at the beginning of acceleration. Then as the estimate starts to drift, it trusts the wheel speeds that are slower than the estimate, always trusting the slowest wheel from there on along with dead-reckoning. This can be seen in figure 5.6b. The accurate detection of wheel slip and trusting the wheels at the right time proves to be an improved strategy to estimate vehicle speed. The relative errors in the speed estimate can be observed in figure 5.7.

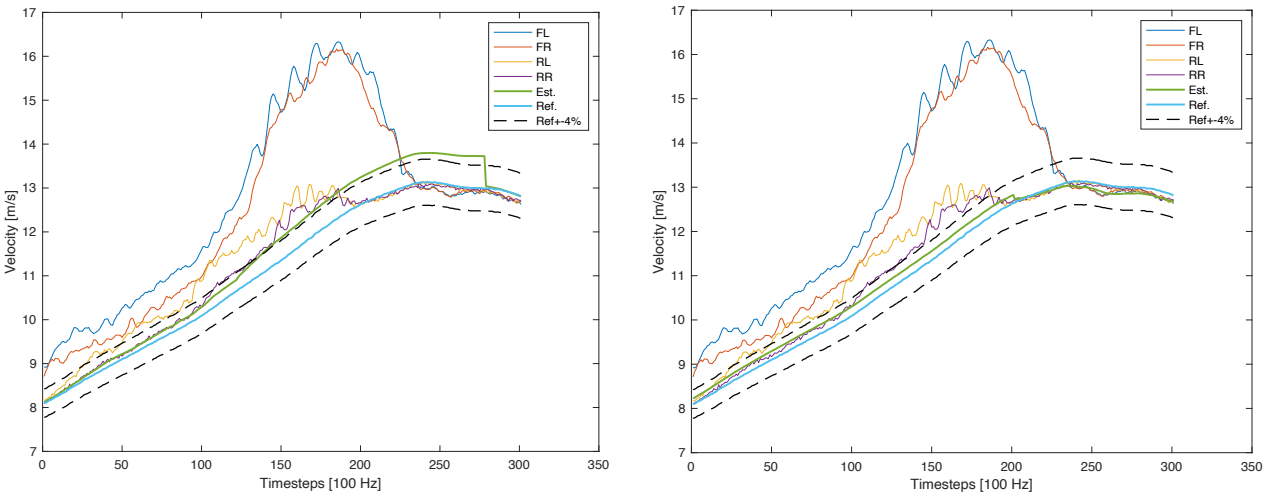

(a) *Estimated speed from C2*

(b) *Estimated speed from C3*

Figure 5.6: *Estimated speed from concepts 2 and 3 in scenarios where wheel slips during acceleration*

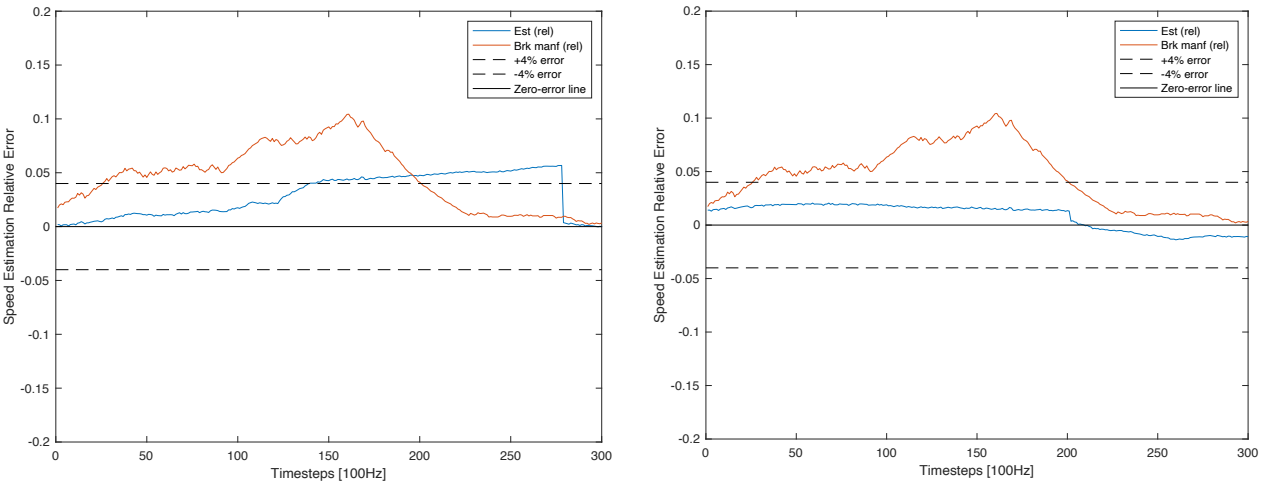

(a) *Relative error of estimated speed from C2 and brake manufacturer*

(b) *Relative error of estimated speed from C3 and brake manufacturer*

Figure 5.7: *Relative error of estimated speed from concepts 2, 3 and brake manufacturer in scenarios where wheel slips during acceleration*

Another improvement comes during the braking scenario in the data logs, noticeably in log HY-1 and HY-11 from table 5.5. For HY-11, the estimated speed signals for C2 with the old braking strategy and C3 with the

new braking strategy can be seen in figure 5.8. C3 with the new braking strategy solves almost 26% more share of braking scenario than C2. This is because during braking, the wheel speeds compensated by the slip ratio estimate is used as a measurement to aid dead-reckoning. In this case, the slowest of the compensated front wheel speeds is chosen to be trusted. The slip ratio estimation for the wheels can be seen in figure 5.9a and the compensated wheel speed can be seen in figure 5.9b. The compensated wheel speeds are closer to the true speed of the vehicle than the wheel speed sensor measurement. Thus, when predicted speed is updated with compensated wheel speeds that are accurate, the estimated speed is also accurate within the error limits. The relative errors of the two methods compared to the brake manufacturer's estimate can be seen in figure 5.10.

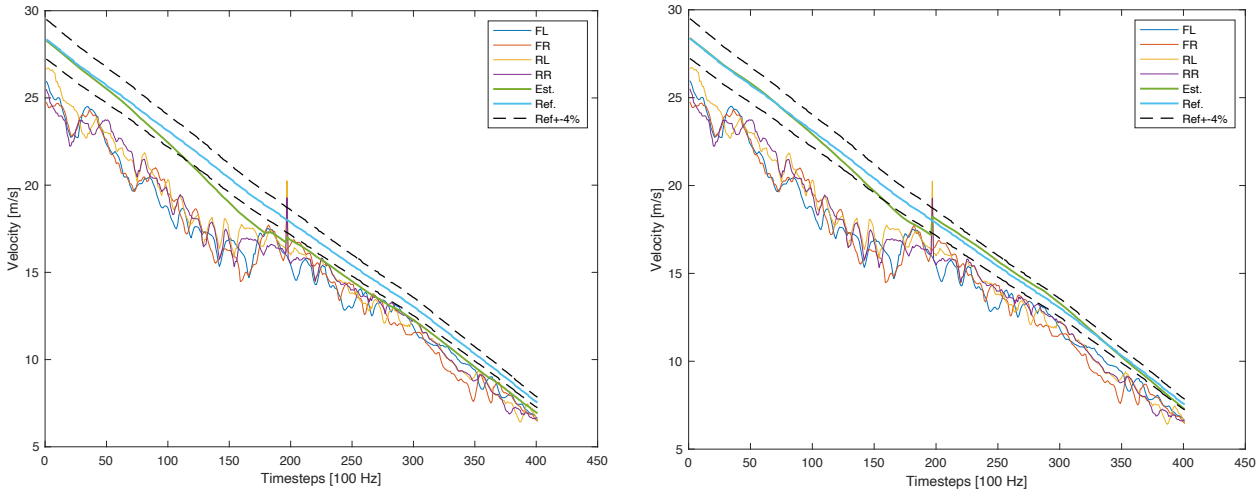

(a) *Estimated speed from C2*

(b) *Estimated speed from C3*

Figure 5.8: *Estimated speed from concepts 2 and 3 in braking scenario*

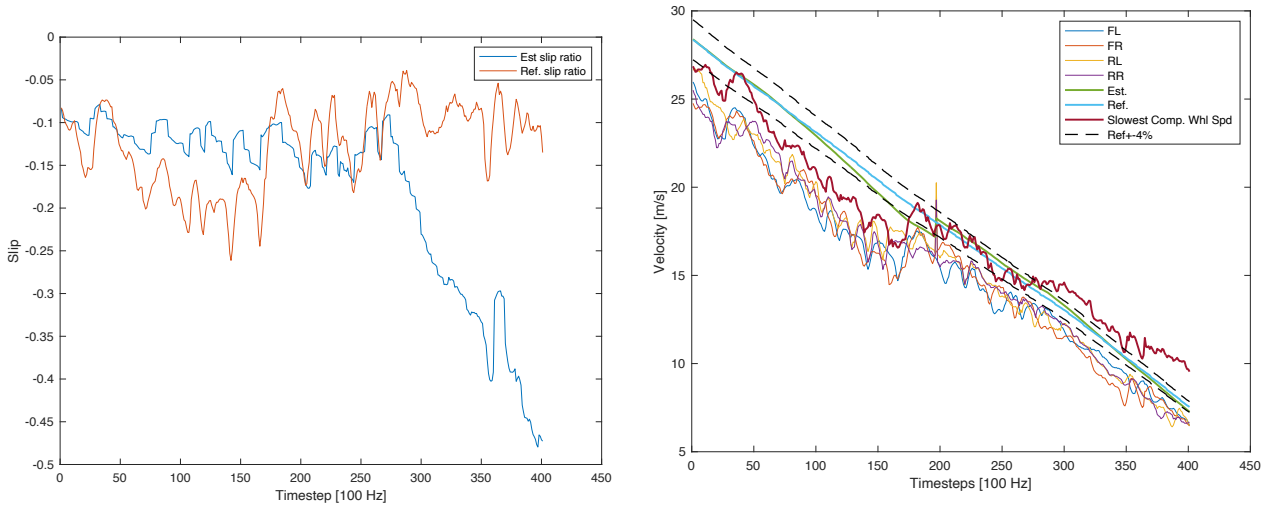

(a) *Slip Ratio estimation for the front left wheel*

(b) *Compensated wheel speed that is trusted for speed estimation in C3*

Figure 5.9: *Slip ratio estimate compared to reference slip ratio calculated from OxTS. Figure 5.9b shows the compensated wheel speed that is used to estimate the speed along with the true wheel speed measurements.*

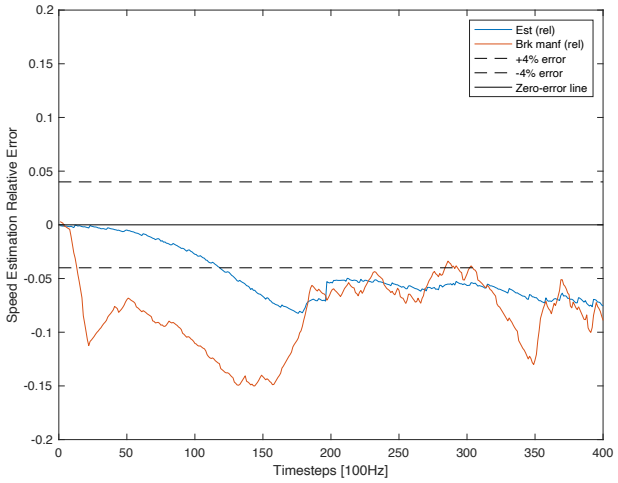

(a) *Relative error of estimated speed from C2 and brake manufacturer*

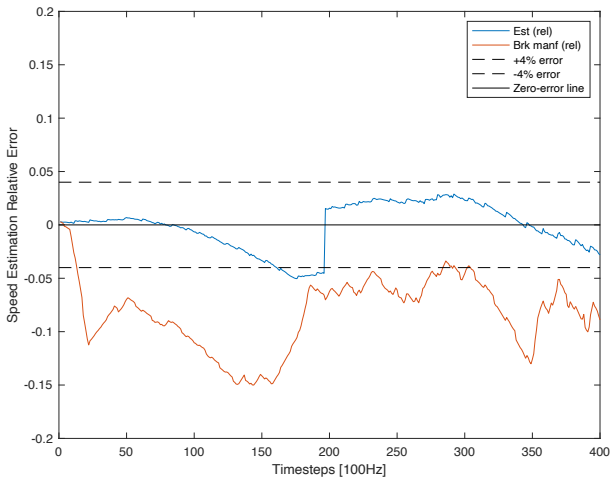

(b) *Relative error of estimated speed from C3 and brake manufacturer*

Figure 5.10: *Relative error of estimated speed from concepts 2, 3 and brake manufacturer during braking scenarios*

Similarly in HY-1, the new braking strategy trusts the slowest compensated front wheel at higher predicted speeds of the vehicle initially. The spikes coincide with the point where the compensated wheel speed is faster than the estimate, that helps to drag the estimate "up" and stops it from crossing the 4% limit. The slip ratio estimation, compensated wheel speeds can be seen in figure 5.11. The final estimated speed and the relative speed error can be seen in figure 5.12.

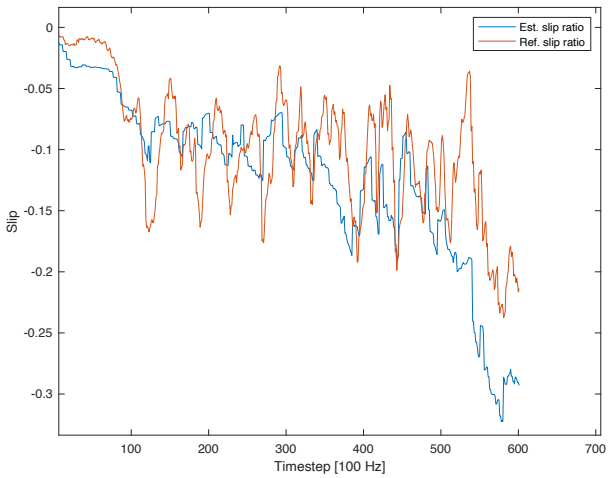

(a) *Slip Ratio estimation for the front left wheel*

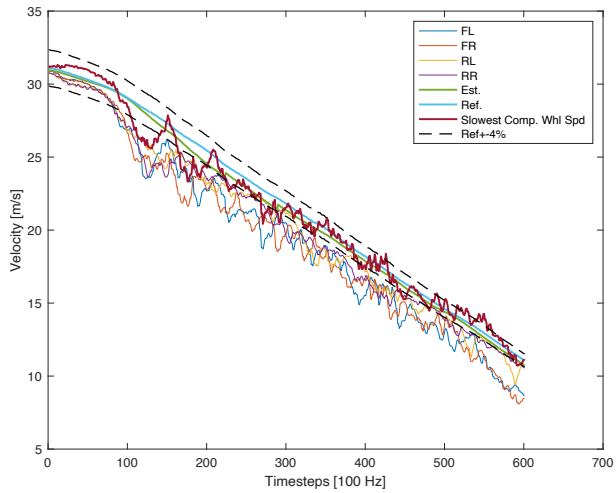

(b) *Compensated wheel speed that is trusted for speed estimation in C3*

Figure 5.11: *Slip ratio estimate compared to reference slip ratio calculated from OxTS. Figure 5.11b shows the compensated wheel speed that is used to estimate the speed along with the true wheel speed measurements.*

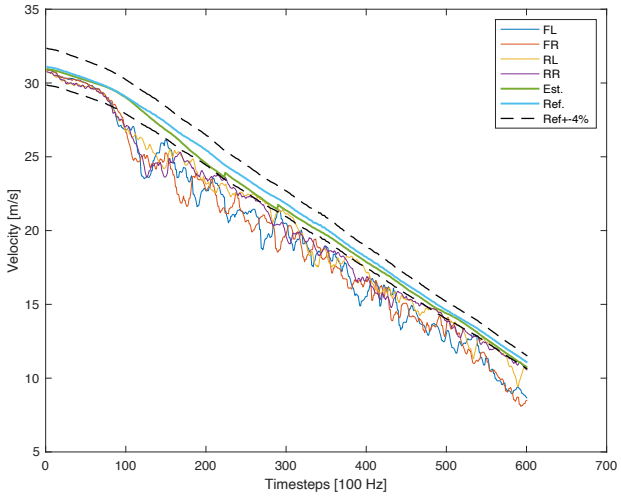

(a) *Estimated speed from C3*

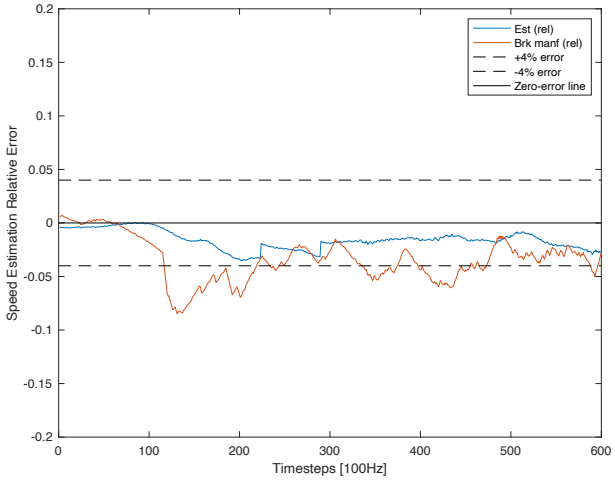

(b) *Relative error of estimated speed from C3 and brake manufacturer*

Figure 5.12: *Estimated speed and relative error from concepts 2 and 3 in braking scenario*

Where Concept 3 struggles

Concept 3 solves almost all the data files during segments of wheel slip while accelerating. However this method like all other methods struggles sometimes during braking. This can be noticed in table 5.5 for data log HY-6. HY-6 is a problematic data log to solve for most methods developed due to aggressive ABS braking and extreme wheel lock cases. For C3, estimating speed during braking involves deciding whether to trust the compensated or true wheel speeds as well as decide the correct wheel to trust. The estimated speed using C3 can be seen in figure 5.13a. the estimated speed drifts away as it dead-reckons while trusting the fastest true wheel speed here. As mentioned in section 4.3.7, the strategy to decide which wheel speeds to trust is based on the predicted speed of the vehicle. At speeds between 7.5 and 14 m/s, the fastest true wheel speeds is trusted along with dead-reckoning. In this case, the fastest true wheel speed is still way for off from the true speed of the vehicle and thus a huge drift in the estimate.

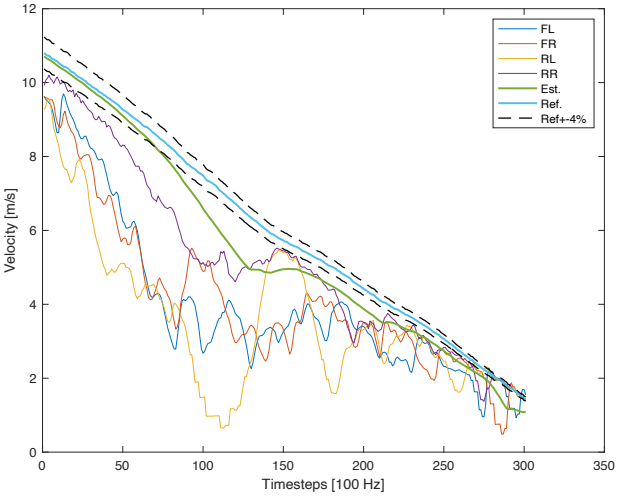

(a) *Estimated speed from C3 while trusting the true wheel speeds*

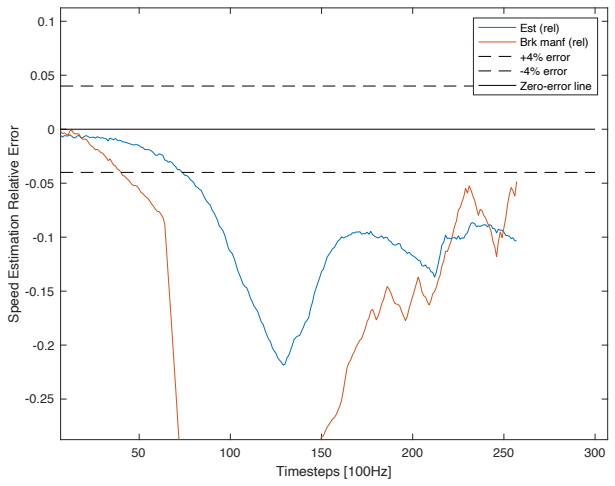

(b) *Relative error of estimated speed from C3 and brake manufacturer while trusting the true wheel speeds*

Figure 5.13: *C3 braking strategy struggles because it trusts the true wheel speeds*

The slip ratio estimates for the front and rear wheel are shown in figure 5.14. The slip ratio estimation looks good enough to correct the wheels speeds and trust it, which would solve the problem. Also, as discussed in

section 4.3.7, the slowest of the compensated wheel speed is trusted to avoid the over-estimation errors and thus over-estimated wheel speed for updating the speed estimate. This can be seen in 5.15a. However here it is seen that the fastest compensated wheel speed is actually closer to the true speed of the vehicle. The fastest corrected wheel speed can be seen in figure 5.15b.

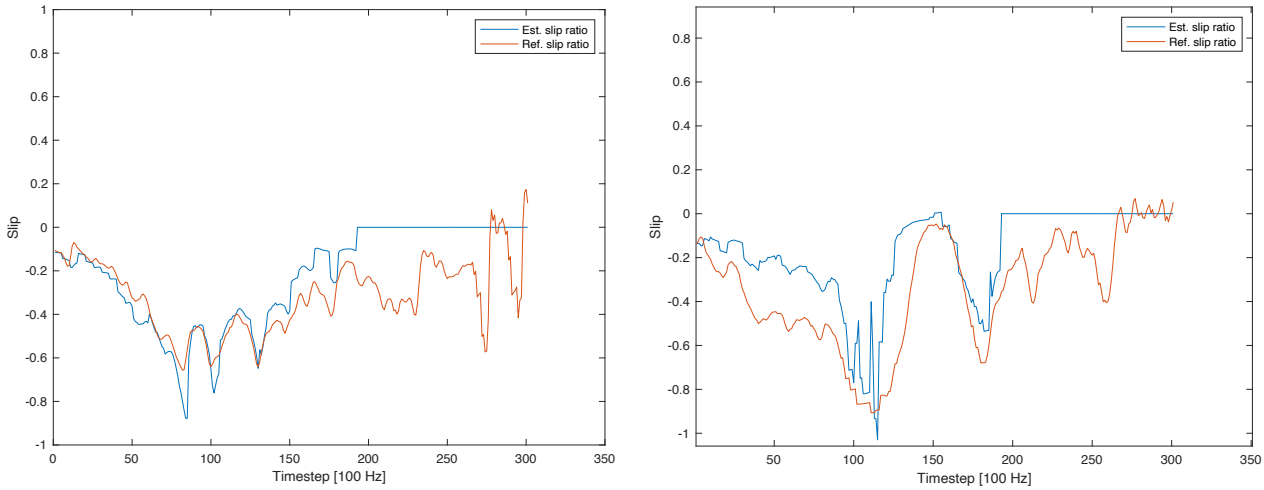

(a) *Estimated slip ratio vs ground truth for Front Left wheel* (b) *Estimated slip ratio vs ground truth for Rear Left wheel*

Figure 5.14: *The slip ratio estimates seem good enough to be used to correct the wheel speed measurements and use for speed estimation*

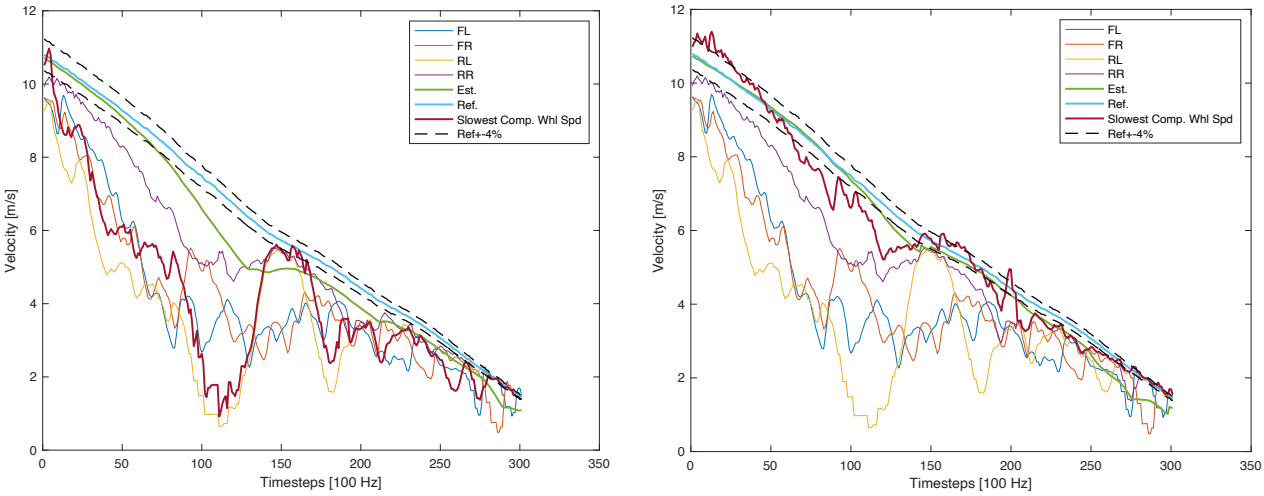

(a) *Slowest corrected wheel speed* (b) *Fastest corrected wheel speed*

Figure 5.15: *The slowest corrected wheel speed is very far away from the true speed of the vehicle however the fastest speed is fairly accurate and could be trusted*

The speed estimations if the fastest corrected wheel speed was trusted in the strategy can be seen in figure 5.15b and 5.16a. The result in performance would double, solving almost 70% share of the data log during braking as compared to 36% previously as seen in table 5.5.

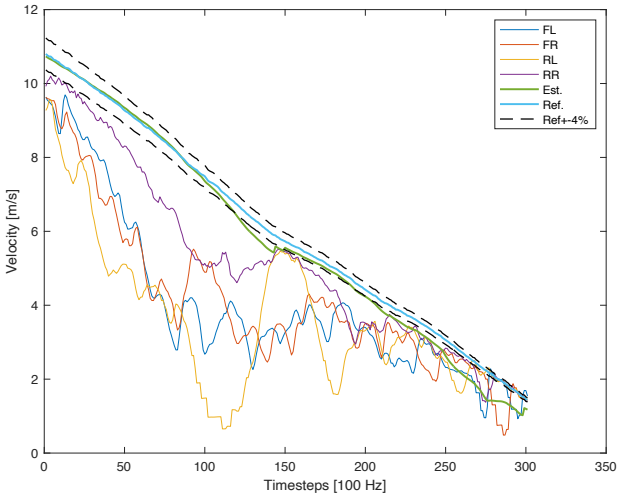

(a) *Estimated speed from C3 while trusting the fastest corrected wheel speed*

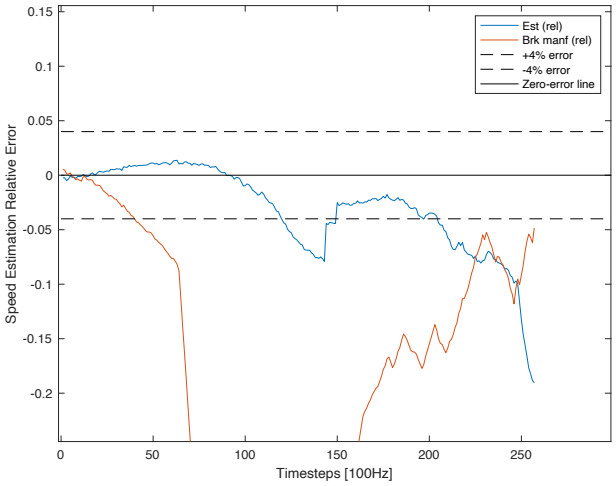

(b) *Relative error of estimated speed from C3 and brake manufacturer while trusting the fastest corrected wheel speed*

Figure 5.16: *Trusting the fastest corrected wheel speeds improves speed estimation during braking in this data log*

This file is an exception where the slip ratio estimate is highly accurate most likely due to accurate brake torque data. The estimation method in braking is developed for a universal approach and thus struggles to estimate the speed in this exception data log. This data also has extreme lock and ABS braking, where the wheel speeds are not even close to the true speed of the vehicle. So even though the performance numbers say the estimate is bad, the fact that the slip ratio estimation is accurate is a big positive.

6 Discussion

Estimating vehicle speed when wheels slip excessively on low friction surfaces is extremely challenging. It is especially so with a limited sensors or measurements; just an IMU that can be dead-reckoned, and wheel speed sensors, which are the only direct measurement of speed but, are not representative of true vehicle speed when slipping. Previously [1], a kinematics model based EKF with two slip detection systems was developed to estimate speed, and it's limitations and possible improvements analyzed. In this work, two approaches that improve the previous estimation method are developed. First is to model a GPS speed signal and introduce it as a secondary measurement of speed, when the wheel speeds cannot be used. Second, a new and dynamic slip detection concept is developed using limited sensors 4.1 to complement the kinematics model and EKF. A discussion about why these methods are chosen, it's characteristics, results and limitations follows.

6.1 Why these approaches are chosen

In the methods developed previously, a lot of burden was put on dead-reckoning to be accurate when all wheels are slipping since the only other sensor that could measure the speed - the wheel speed sensor, could not be trusted. Dead-reckoning of the accelerometer suffers from integration drift errors which lead to bad speed estimates. If the wheel speeds can't be trusted during excessive slip and dead-reckoning is prone to drift, an obvious solution is to introduce a secondary measurement of speed that is not affected by wheel slip. During research study in previous work [1], it was also found that a secondary speed measurements from GPS, cameras, Radar and others can be used with dead-reckoning the accelerometer and wheel speeds. The GPS module outputs a direct speed measurement while the other sensors need to be calibrated and speed needs to be estimated from their output, which brings in further challenges and complexity. Thus, a GPS speed signal is an ideal secondary measurement of speed. It also helps that most modern cars now come equipped with GPS modules, which makes it even more applicable to the speed estimation methods. So, the first approach introduces a GPS speed signal as a secondary measurement to aid speed estimation during excessive all-wheel slip conditions.

To address early onset of drift errors and unnecessary reliance on dead-reckoning, two slip detection concepts were developed previously. The task of these concepts was to identify which wheels were slipping, so the non-slipping wheel speeds could be fed to the EKF in the measurement update. This would help provide accurate measurements of speed from the wheel speed sensors, meaning that dead-reckoning would only begin if all-wheels are detected to be slipping. Also, if the concepts detected all-wheel slip at the right time, the dead-reckoning process would also start at a speed that is accurate, thus avoiding an early onset of drift errors. The challenge was to develop these concepts with the limited sensors available. One concept was based on static thresholds of torque rate and accelerations, while the other was based on wheel speed residual variances. However, both had limitations since the thresholds set to detect slip were static and did not rely on the speed of the vehicle, yaw, road-tyre friction and other dynamic parameters that affect vehicle motion. Also, the slip detection would only identify if a wheel is slipping but not by how much i.e. the slip ratio. A more dynamic slip detection strategy that could not just detect slip, but do so by estimating the slip ratio itself would be an ideal solution to this problem. This reduces the reliance on dead-reckoning since the slip detection would be even more accurate and in some cases, the slip ratio estimate can compensate the wheel speed measurements meaning that even during all-wheel slip, corrected wheel speeds can be fed to the EKF.

Even though other methods can be used to improve the estimation methods, given the time constraints as well as background of the author, these two approaches are found to be suitable to develop methods to improve speed estimation in excessive wheel slip conditions. These approaches also solve the most obvious limitations of the previous methods while also helping to understand how much they improve upon the previous methods. It also does so via two completely different ideas where one adds an absolutely new measurement of speed, while the other utilizes a new slip detection concept. The reason to do this is also provide substantial examples and possible routes of development in vehicle speed estimation.

6.2 The idea behind developing these approaches

Adding a secondary measurement of speed serves two purposes. One is improving the estimation of speed itself, providing another direct measurement of speed when the wheel speeds cannot be trusted during all-wheel slip. The second purpose it to help analyze how much of an impact just adding a secondary measurement of speed makes to an already developed, limited sensor based approach from previous work [1]. This also makes for validation of the analysis and limitations discussed in the previous methods, as well as justify further development of the approach of adding a secondary measurement. Thus, the best speed estimation developed in the previous work - EKF with slip detection Concept 2 is used as the base. A GPS speed signal is then added as a measurement when the slip detection concept detects all-wheel slip. Keeping the previous method untouched but rather just adding a secondary measurement helps to understand performance gain in a controlled way. The GPS speed signal is used only when all-wheel slip is detected so that, the wheel speed measurements which are very accurate when wheels are not slipping, are trusted to estimate vehicle speed without a lagging and slow update frequency speed signal from the GPS in the mix.

A new dynamic slip detection system helps to estimate vehicle speed using the limited sensor suite and an EKF, while also avoiding any other secondary measurement requirements. The kinematics based model used in the EKF has limitations as mentioned in the previous work, however for the purpose of this work, using the same EKF makes it easy to compare the improvements and performance of the new slip detection system. The V_xRP filter is chosen to evaluate the performance of this new slip detection concept. The idea of this concept is to make it more dynamic and such that a slip ratio for each wheel can be estimated. The previous concepts set up static thresholds for slip indicators to detect slip. However, the idea here is to use the estimated slip ratio itself to decide if the wheels should be trusted or no. Since the error limit in the speed estimate is set as $\pm 4\%$, a wheel slipping less than 4% can ideally be trusted. So, a wheel is detected to slip if the slip ratio is higher than 4%. The slip ratio estimation encompasses dynamic, static and tuning parameters, solving the static threshold only problem. The slip detection concept based on this slip ratio estimation now depends on velocity of the wheels, tyre parameters and applied torque at each time instant. This detection concept uses slip indicators such as torque rate and difference for wheel-car acceleration with static thresholds to complement the slip ratio estimate. Estimated slip ratio is also used to correct the wheel speeds to represent the true speed of the vehicle.

The common idea for both these methods is simple - improve the previous estimation method with two approaches suggested by analysis in the previous work while keeping the base similar to previous method which makes comparison of the performance gains much easier.

6.3 Some challenges and limitations

The data logs from real-world driving with excessive wheel slip are described in 4.1. In these logs, GPS speed signal is not recorded. Thus an artificial GPS signal is modelled from the reference / ground truth speed measurement signal from the OxTS. To make the modelled GPS signal representative of true GPS signal, it's signal and error characteristics are studied from two additional data logs 4.1 that include true GPS speed measurement for a vehicle drive on a highway, passing through two tunnels. This poses the first limitation - the signal and error characteristics that are used to model GPS speed signal are based on very less data, data that does not include excessive wheel slip conditions, does not include variations in environmental factors like weather, road, surrounding trees, cities and high rise buildings and overpasses as well as very high acceleration and braking scenarios. This makes the study of signal and error characteristics very limited and thus the modelled GPS speed signal highly biased by this specific data log and the driving maneuvers performed while logging it. The second limitation is the modelled GPS speed signal itself. Since the GPS speed signal is modelled and not the true signal, there is always bound to be some discrepancy had there been a comparison between the two.

For the slip detection concept approach the main limitations arise from how the equation is used to estimate slip ratio. The equation currently has a low-pass filter characteristic using a gain factor / tuning factor. This causes the slip ratio estimate to be too low pass filtered sometimes, causing it to sometimes miss the threshold or even estimate an extremely low slip ratio. Another limitation of this concept is that the parameters used in the equation are one too many and their lumped errors could cause outliers in the slip ratio estimate. The higher the number of variables that slip detection depends on, the higher the chances that one wrong value in

any one variable would lead to incorrect slip ratio and thus incorrect speed estimate. From the variables used in the equation for slip estimation, the powertrain torque data is an estimated quantity with high errors, the tyre radius is considered to be static and so is the longitudinal stiffness of the tyre which in reality are dynamic and dependent on a lot of external and internal factors.

6.4 The performance of these approaches

A consolidated table of performance numbers of these approaches compared to previous method and OEMs simple estimation methods can be seen in chapter 5. From the results, it is clear that the two new approaches developed in this work are better than the previous methods and OEMs' estimation. This is on average over 15 logs files. The approaches outperform the other methods in all three segments of the data logs i.e. complete data, slipping in acceleration and braking scenarios. The approaches keep the speed estimate within the $\pm 4\%$ error limit for larger share of data logs than other methods. The RMSE as well as standard deviation of errors is also very low for the two approaches on average.

On average for complete data, the GPS approach keeps the estimated speed within the error limit for 94% of the time over the data logs. The new slip detection concept keeps the estimate within the desired error limit for 95% of the time over the data logs. This is a 2 and 3 % improvement respectively from the previous method. The improvements for slipping in acceleration segment is 1% and 2 % respectively. The major improvements come in the braking section of the data, where the GPS approaches keeps the speed estimate within error limits 3% higher share of data while the slip detection concept improves over the previous method by 5%. The new approaches improve over the previous for all individual files barring a one or two which are explained in the results chapter 5. The new slip detection method also has the lowest RMSE and standard deviation of all the methods on average. From this, it is also found that from the two approaches, the new slip detection concept helps to get a better speed estimate.

The bigger picture however is that the two approaches make for viable options for speed estimation and also improve upon the previous methods. The results also show the performance gained by adding a secondary measurement of speed, as well as a dynamic slip detection strategy.

However, it is important to note that the statistical parameters might not be indicative of the true performance of the methods. This is specially in low speeds where the error limit is too narrow and relative error gets too high. It is also prone to extreme outliers such that even one outlier could skew the statistical parameter. Similar explanation can be applied to the solved% numbers in the results table, where an extreme outlier could sway the average solved% of the method.

6.5 Future Work

In this section, future work than can be done to improve the proposed methods is discussed.

6.5.1 More GPS data in different conditions

The improvements gained from utilizing GPS speed signals showcase a way in which speed estimation can benefit with a secondary measurement. A modern car equipped with a GPS module can surely take advantage of the speed signal from the GPS. Data logs from real-world driving on icy and snowy roads similar to the logs received during this work that have the true GPS speed signals would be a great starting point to test out this method. GPS data in different weather conditions, environment and maneuvers would help create a stronger argument on if the GPS speed signal can benefit the speed estimation process in excessive wheel slip conditions.

6.5.2 GPS speed to estimate radius and slip ratio

Having a measurement that does not get affected by wheel slip is advantageous for speed estimation. A logic to utilize GPS speed to estimate wheel slip and compensate it, a logic to utilize the vehicle speed from the GPS and estimated wheel slip to estimate the tyre radius would help in providing another measurement upon which a strategy to trust either the wheel speeds or GPS speed can be put together.

6.5.3 Slip ratio as a state

The slip ratio estimation equation can be used as a state in an EKF similar to the one developed during the thesis work. However, the non-linearity of the equation might require an Unscented or Cubature kalman filter. These filters will also need better measurement models that have accurate torque data. The current torque data is estimated, which is prone to high errors. The process and measurement model from [15] is a good starting point if the torque data can be accurate.

6.5.4 Dynamic tyre parameters

Currently, all tyre parameters used in the slip ratio equation are static. The tyre radius is the static loaded radius, the longitudinal stiffness is from the linear region of the force-slip curve and the inertia is assumed constant throughout. However, these parameters change constantly and utilizing dynamic values of these parameters would make the slip ratio equation even more accurate.

6.5.5 Estimating road-tyre friction

An online estimation of road-tyre friction would help calculate the maximum torque that can be applied to each wheel. This can be used as a threshold to determine if the wheels are likely to slip when this max torque limit is crossed.

6.5.6 Testing the methods on IPG Carmaker

It is a good idea to test these methods in a virtual environment since it is easy to create different scenarios of wheel slip and also understand if the estimation method works online without delays. Testing the methods on different road conditions would also facilitate studying different slip indicators, and the limitations of the current method in terms of robustness.

6.5.7 Machine Learning to further understand slip detection criteria

Currently the slip detection equation is based on the predicted speed of the vehicle. Machine learning is a technique that can be used to find more of these dynamic parameters that affect the slip ratio estimation.

7 Conclusion

Speed estimation with a limited amount of sensors and excessive all-wheel slip is a challenging task. The two approaches developed in this work present different ways of improving a kinematics based speed estimation process. One approach being to add a secondary measurement altogether to aid with the dead-reckoning of IMU, while the other method being a slip detection system to accurately detect speed and estimate the slip ratio of each wheel. Both these approaches showed improvements in speed estimation over the 15 log files from real-world driving. Both approaches were able to improve upon the previous methods over all three segments of the data logs - complete data log, slipping while accelerating and braking scenarios.

The GPS approach, using a secondary speed signal improved upon the previous method. The advantages of using a secondary measurement are big especially when all wheels are slipping since they are not affected by the wheels speeds. This helps reduce the burden on dead reckoning when all-wheel slip is detected. The GPS approach outperforms the simple OEM estimations as well on average as well as individually over 15 files. Performance gained by just adding a secondary speed signal validates further development into this method, gathering of more data and incorporating if not GPS, then any other sensor like a camera or radar. Even though it doesn't solve all files over 99% of the time as was the vision, it makes a solid case for using a secondary measurement of speed. One of the biggest challenges especially while using a GPS is that it is sensitive to the environment meaning that it's accuracy is dependent on the environment such as the weather, surrounding buildings, tree density, tunnels , over and underpasses and the likes. the GPS speed is also prone to errors during acceleration and braking, which is when majority of the slipping occurs. Even though an improvement is made in this work on speed estimation, further development and testing could validate it's use even more.

The new slip detection concept on average outperformed even the GPS approach, over all three segments of data. It also had the highest share of the speed estimate kept within the error limit with the lowest RMSE. The benefit of having a dynamic slip detection and estimation as well proved to be vital in the braking cases especially, when correct wheel speeds from slip ratio estimate are used as measurements. The performance of this method also warrants further study and development, especially using dynamic tyre parameters rather than static. It also validates the use of a stand-alone slip detection system with limited sensors and without secondary measurement to estimate the vehicle speed in excessive all wheel conditions. This approach also leaves some scope for improvement where more dynamic parameters that have and effect on slip could be combined, the slip ratio can be made a state in a non-linear filter such as UKF or CKF. Even testing this method for robustness on different surfaces on IPG carmaker could help.

Overall, these methods achieve the purpose of this project work, develop methods to improve the kinematics based speed estimation and analyse it's performance gains to validate it's use in the future. The methods developed have been kept as un-tuned for the data logs as possible for robustness checks or further testing on different data.

References

[1] C. Storckenfeldt and D. Ganatra, Vehicle Speed Estimation During Excessive Tyre Slip Conditions 2021, 2021.

[2] K. Tin Leung, J. F. Whidborne, D. Purdy, and A. Dunoyer, A review of ground vehicle dynamic state estimations utilising GPS/INS, *Vehicle System Dynamics* **49**, no. 1-2 2011, 29–58, 2011, ISSN: 00423114. DOI: 10.1080/00423110903406649.

[3] D. M. Bevly, J. C. Gerdes, and C. Wilson, The Use of GPS Based Velocity Measurements for Measurement of Sideslip and Wheel Slip, *Vehicle System Dynamics* **38**, no. 2 2002, 127–147, 2002, ISSN: 00423114. DOI: 10.1076/vesd.38.2.127.5619.

[4] S. L. Miller, B. Youngberg, A. Millie, P. Schweizer, and C. Gerdes, Calculating longitudinal wheel slip and tire parameters using GPS velocity, *Proceedings of the American Control Conference* **3** 2001, 1800–1805, 2001, ISSN: 07431619. DOI: 10.1109/acc.2001.945995.

[5] E. Bakker, L. Nyborg, and H. B. Pacejka, Tyre modelling for use in vehicle dynamics studies, *SAE Technical Papers* **96** 1987, 190–204, 1987, ISSN: 26883627. DOI: 10.4271/870421.

[6] X. Ding, Z. Wang, L. Zhang, and C. Wang, Longitudinal Vehicle Speed Estimation for Four-Wheel-Independently-Actuated Electric Vehicles Based on Multi-Sensor Fusion, *IEEE Transactions on Vehicular Technology* **69**, no. 11 2020, 12797–12806, 2020, ISSN: 19399359. DOI: 10.1109/TVT.2020.3026106.

[7] E. Stenborg and L. Hammarstrand, Using a single band GNSS receiver to improve relative positioning in autonomous cars, *IEEE Intelligent Vehicles Symposium, Proceedings* **2016-Augus**, no. Iv 2016, 921–926, 2016. DOI: 10.1109/IVS.2016.7535498.

[8] D. Sathyamorthy, S. Shafii, Z. F. M. Amin, A. Jusoh, and S. Z. Ali, Evaluation of the accuracy of global positioning system (GPS) speed measurement via GPS simulation, *Defence S and T Technical Bulletin* **8** 2015, 121–128, 2015, ISSN: 19856571.

[9] R. Vishwanathan, P. Weckler, J. Solie, and M. Stone, "Evaluation of ground speed sensing devices under varying ground surface conditions," 2005.

[10] M. Supej and I. Čuk, Comparison of global navigation satellite system devices on speed tracking in road (tran)SPORT applications, *Sensors (Switzerland)* **14** 2014, 23490–23508, 2014, ISSN: 14248220. DOI: 10.3390/s141223490.

[11] A. Dyukov, S. Choy, and D. Silcock, Accuracy of Speed Measurements using GNSS in Challenging Environments Accuracy of Speed Measurements using GNSS in Challenging Environments, **03**, no. June 2016, 794–811, 2016.

[12] M. Akkamis, M. Keskin, and Y. E. Sekerli, Comparative Appraisal of Three Low-Cost GPS Speed Sensors with Different Data Update Frequencies, *AgriEngineering* **3**, no. 2 2021, 423–437, 2021. DOI: 10.3390/agriengineering3020028.

[13] A novel longitudinal speed estimator for four-wheel slip in snowy conditions, *Applied Sciences (Switzerland)* **11**, no. 6 2021, 2021, ISSN: 20763417. DOI: 10.3390/app11062809.

[14] K. Nam, Y. Hori, and C. Lee, Wheel slip control for improving traction-ability and energy efficiency of a personal electric vehicle, *Energies* **8**, no. 7 2015, 6820–6840, 2015, ISSN: 19961073. DOI: 10.3390/en8076820.

[15] N. Gosala, A. Buhler, M. Prajapat, C. Ehmke, M. Gupta, R. Sivanesan, A. Gawel, M. Pfeiffer, M. Burki, I. Sa, R. Dube, and R. Siegwart, Redundant perception and state estimation for reliable autonomous racing, *Proceedings - IEEE International Conference on Robotics and Automation* **2019-May** 2019, 6561–6567, 2019, ISSN: 10504729. DOI: 10.1109/ICRA.2019.8794155. eprint: 1809.10099.

[16] S. Särkka, *Bayesian Filtering and Smoothing*. Cambridge: Cambridge University Press, 2013.

[17] R. E. Kalman, A New Approach to Linear Filtering and Prediction Problems. *Transactions of the ASME, Journal of Basic Engineering* **82(1)** 1960, 35–45, 1960. DOI: https://doi.org/10.1115/1.3662552.

[18] P. Zarchan and H. Musoff, *Fundamentals of kalman filtering : A practical approach*. American Institute of Aeronautics and Astronautics, 2000, ISBN: 9781600867187.

[19] K. Kobayashi, K. Watanabe, and C. Science, Estimation of Absolute Vehicle Speed using Fuzzy Logic Rule-Based Kalman Filter, *Proceedings of the American Control Conference Seattle, Washington, USA*, no. June 1995, 3086–3090, 1995.

[20] H. B. Pacejka, *Tyre and Vehicle Dynamics*. 2012. DOI: 10.1016/B978-0-08-097016-5.00002-4.

[21] R. Rajamani, *Lateral Vehicle Dynamics and Control*. 2016, pp. 135–181, ISBN: 9781461414322. DOI: 10.1002/9781118380000.ch5.

[22] H. B. Pacejka, *Tyre and Vehicle Dynamics*. 2012. DOI: 10.1016/B978-0-08-097016-5.00002-4.

[23] U. Kiencke and L. Nielsen, *Automotive Control Systems For Engine, Driveline, and Vehicle*. Berlin Heidelberg: Springer, 2005.

[24] R. Rajamani, *Lateral Vehicle Dynamics and Control*. 2016, pp. 135–181, ISBN: 9781461414322. DOI: 10.1002/9781118380000.ch5.

DEPARTMENT OF MECHANICS AND
MARITIME SCIENCES
CHALMERS UNIVERSITY OF TECHNOLOGY
Gothenburg, Sweden 2021
www.chalmers.se

CHALMERS
UNIVERSITY OF TECHNOLOGY